Ghent University

Faculty of Sciences

Department of Plant Biotechnology and Bioinformatics

Chromatin modification complexes link transcript elongation to RNA processing in the regulation of plant growth and development

Sabine Le Gall

Promoter

Prof. Dr. Mieke Van Lijsebettens

Thesis submitted in partial fulfilment of the requirements to obtain the degree of Doctor in Philosophy (Ph.D.) in Sciences: Biochemistry and Biotechnology

Academic year 2017-2018

Examination committee

Chair

Prof. Dr. Lieven De Veylder

Center for Plant Systems Biology, VIB

Department of Plant Biotechnology and Bioinformatics, Ghent University

Secretary

Prof. Dr. Ann Depicker

Center for Plant Systems Biology, VIB

Department of Plant Biotechnology and Bioinformatics, Ghent University

Members

Prof. Dr. Mieke Van Lijsebettens (Promoter)

Center for Plant Systems Biology, VIB

Department of Plant Biotechnology and Bioinformatics, Ghent University

Prof. Dr. Frank Van Breusegem

Center for Plant Systems Biology, VIB

Department of Plant Biotechnology and Bioinformatics, Ghent University

Dr. Hilde Nelissen

Center for Plant Systems Biology, VIB

Department of Plant Biotechnology and Bioinformatics, Ghent University

Prof. Dr. Klaus Grasser

Department of Cell Biology and Plant Biochemistry, University of Regensburg

Prof. Dr. Koen Geuten

Department of Molecular Biotechnology of Plants and Micro-organisms, KU Leuven

"Sans la curiosité de l'esprit, que serions-nous? Telle est bien la beauté et la noblesse de la science: désir sans fin de repousser les frontières du savoir, de traquer les secrets de la matière et de la vie sans idée préconçue des conséquences éventuelles. "

Marie Skłodowska-*Curie*

Table of Contents

Chapter 2 RNA binding proteins link H2B monoubiquitination with m-RNA processing through interaction with the HUB1 and HUB2 E3 ubiquitin ligases 65

Summary

In eukaryotes, mRNA levels are precisely controlled in space and time. RNA polymerase II (RNA pol II) transcript synthesis and mRNA processing are at the basis of this control and are therefore regulated at several stages. In the past, transcription initiation was considered the crucial step in controlling transcription. But recently the elongation phase of RNA polymerase II transcription has proven to be also dynamic and highly regulated. Indeed, transcript elongation is at the cross-road of transcription and pre-mRNA processing.

Today, chromatin is today seen as a major player of transcriptional gene regulation notably via histone modification. In this thesis, we discuss two complexes responsible for histone modification, Elongator with a histone acetylation activity and HUB1/2 with histone H2B monoubiquitination (H2Bub) activity. Their activities promote RNA pol II during transcript elongation. The Elongator complex regulates transcription by its inherent histone acetyl transferase activity, interestingly, the complex does not seem to act in a general fashion to aid the transcription of all genes but shows specificity to certain genes and processes via an unknown mechanism. H2Bub is a key histone modification that has significant effects on gene transcription, mainly associated with transcriptional activation and transcript elongation. The reversible monoubiquitination of histone H2B in chromatin is an important biochemical event in the regulation of important cellular and developmental processes in plants. H2Bub levels are dynamically regulated via deposition and removal of ubiquitin by specific enzymes. However, like Elongator, HUB1/2 targets specific genes and pathways for its H2Bub activity via an unknown mechanism.

The aim of this dissertation was to investigate the mechanisms of specificity and targeting of genes of the two activating histone modifiers, HUB1/2 and Elongator, during transcript elongation. This thesis is divided into three parts. The first part exposes the general context of transcription, RNA binding proteins and histone modifiers and continues with the functional study of HUB1/2 interactors. The second part is dedicated to Elongator with a general review and two studies that present different aspects of

Elongator activity. Finally, the third part that consist of a general discussion and perspectives.

The **first chapter** is an introduction to the dynamic and complex processes of transcription with a focus on transcript elongation, on histone modifiers and their respective histone modifications with a focus on activation of transcription and histone H2B monoubiquitination and finally a review on RNA binding proteins. An overview of the different steps of transcription shows the major components of RNA pol II transcription. Transcript elongation is detailed with the co-transcriptional processing of pre-mRNA. The current knowledge on the role of histone modifications in transcription activation is reviewed. The H2Bub is introduced across species, with a special emphasis on its role in plants. Finally, because our research shows that the HUB1/2 interactors obtained are RNA binding proteins, an overview of RNA binding proteins and their role in RNA biology is included.

The aim of the **second chapter** was to investigate how the specificity of the HUB1/2 complex is directed. Tandem affinity purification with HUB1/2 identified two RNA binding proteins, SPEN and KHD, for which RNA binding activity was demonstrated. Phenotypic and molecular analyses suggested shared and specific functions between KHD, SPEN and HUB1. HUB1-mediated H2Bub is important in the regulation of the *CCA1* and *FLC* genes, regulating the clock and flowering time, respectively, and they were analysed in the *spen* and *khd* mutants. Strikingly, in *spen* mutants, splicing of *CCA1* and H2Bub were reduced and showed a role for SPEN in linking H2Bub with the spliceosome activity. The analysis of FLC and its long non-coding antisense *COOLAIR* showed a role for SPEN in COOLAIR splicing or poly-adenylation with no effect on the H2Bub level of FLC. The function of SPEN on specific genes at coding RNA and long non-coding RNA links the RNA pol II elongation complex to mRNA processing but also to long non-coding RNA processing and represents an additional level of transcriptional regulation.

The **third chapter** is a review paper that was published in the BBA-Gene Regulatory Mechanisms in 2016. The role of plant Elongator-mediated transcriptional control in a chromatin and epigenetics context are described with the phenotypes of Elongator mutants in plants, meta-analysis of plant Elongator subunit gene expression, plant

Elongator complex composition, interactors and nuclear functions, molecular pathways and genes targeted by Elongator activities in plants.

The **fourth chapter** is adapted from a research paper published in the Journal of Cell Science in 2017. The hypocotyl phenotypes in darkness and light of Elongator mutants were studied, the pathways affected and the genes targeted for Elongator HAT activity identified. This study showed that Elongator plays a role in early seedling growth and development in darkness and light. A model is proposed in which Elongator represses the plant immune response and promotes hypocotyl elongation and photomorphogenesis via transcriptional control of positive photomorphogenesis regulators and a growth-regulatory network that converges on genes involved in cell wall biogenesis and hormone signalling.

The **fifth chapter** is adapted from a research paper published in Plant Physiology in 2016. The aim was to identify the target genes/pathways of the tRNA modification function of Elongator via comparison between the Elongator mutant, *elo3-6*, and the *grxs17* mutant with a function in tRNA modification. Common phenotypes between *elo3-6* and *grxs17* in primary root size reduction and reduction of leaf size and changes in leaf shape suggested that the tRNA modification activity of Elongator contributed to these phenotypes. Distinct phenotypes between elo3-6 and grxs17, such as altered hypocotyl growth in light and darkness, suggested that the HAT activity of Elongator causes these phenotypes.

The **sixth chapter** discusses the results presented in this thesis and places them in the general context of RNA pol II transcript elongation. The model on pathways targeted by the different Elongator activities presented in Chapter 3 was extended and refined in Chapter 6 as a result of our research (Chapter 4 and 5). The future perspectives for uncovering more on the specificity of histone modification in gene targeting are debated.

Objectives

In plants, the histone modification complexes HUB and Elongator play an important role in the regulation of transcript elongation, steering several biological processes. Their chromatin modification activity and some of their targets have been identified, however, the mechanisms behind their specificity and target choice are still unknown. Indeed, it is unclear how they interact with the RNA pol II transcript elongation complex; proteins that are part of their interaction network are unknown; the effect of upstream regulation on their activity and target gene selection is unexplored. In addition, several phenotypes and thus downstream target pathways regulated by HUB1 and Elongator have not been analysed so far.

An interactome approach was taken in part 1 of this thesis to get more insight into the molecular mechanism of target gene selection by HUB1. In the second part, Elongator mutant phenotypes were the starting point to identify novel downstream pathways and target genes and to distinguish which activities of the Elongator complex contribute to which phenotypes.

H2B monoubiquitination by HUB1 typically occurs in the coding region of genes of actively transcribed regions and is supposed to facilitate RNAPII transcript elongation. To better understand how the specificity of the HUB1 complex is directed towards target genes, we searched for HUB1 interacting proteins by tandem affinity purification, KHD and SPEN, predicted as RNA binding were further analysed. A phylogenic tree positioned them together with proteins carrying the same domain structure, RNA binding was demonstrated by EMSA, their mutant phenotypes were compared to those of HUB1 to find commonly affected pathways both at the physiological and molecular level. The expression, splicing and H2Bub level of two known targets of HUB1, the circadian clock regulator CCA1 and the flowering time repressor FLC, correlated with phenotypes observed in the interactor mutants and were analysed in the *spen* and *khd* mutants. A link between HUB1-mediated H2Bub and mRNA processing through the action of the RNA binding SPEN protein was revealed. Our data are in line with the published RNA pol II transcript elongation complex and advance the functional and mechanistic insight of the different molecular processes that are at work at this platform.

The main activities of the Elongator complex are in histone H3K14 acetylation and in tRNA modification. In order to identify targets and downstream pathways involved in these two activities, two approaches were taken. In a first study, mutants of the Elongator complex were investigated for their peculiar hypocotyl phenotype in light and darkness. Transcriptome of the *elo3-6* mutant was analysed in darkness and different light qualities to unravel how Elongator affects the transcriptional regulation of different pathways that result in the hypocotyl phenotype. Physiological phenotypic comparison of *elo* to other mutants presenting similar phenotypes was used as a basis for molecular phenotyping. The H3K14 acetylation levels of several candidate genes were tested to identify target genes for histone acetylation activity of Elongator. Our data allowed to generate a model to explain the Elongator-mediated transcriptional regulation of hypocotyl growth in light and darkness. In a second study, a comparison between an Elongator mutant and a mutant of GRXS17, a thiol oxidoreductase associated with tRNA thiolation was performed. The aim was to identify common phenotypes that might be due to the tRNA modification activity of Elongator and divergent phenotypes that might be due to the other activities of Elongator. Leaves, roots, transcriptome and pathogen and DNA damage sensitivities were compared. Some of the observed phenotypes could confirm the already described link between pathways and activities and new ones were also identified. These two approaches complete the description of the Elongator activities that grant the complex a role in several levels of regulation.

Abbreviations

ABA: Abscisic Acid

BR: Brassinosteroid

CCA1: Circadian Clock Associated 1

cDNA: complementary DNA

ChIP: Chromatin Immunoprecipitation

Col-0: Colombia 0

DAG: Days After Germination

DAS: Days After Sowing

DNA: Deoxyribonucleic acid

ELP/ELO: Elongator

FACT: FAcilitate Chromatin Transcription

FLC: Flowering Locus C

GFP: Green Fluorescent Protein

H2Bub: histone H2B monoubiquitination

HAT: histone acetyltransferase

HFR1: Long Hypocotyl in Far-Red 1

HUB: Histone monoubiquitination

HY5: Elongated Hypocotyl 5

HYH: homolog of HY5

IAA: Indole-3-acetic acid

JA: jasmonic acid

miRNA: micro RNA

miRNA: microRNA

mRNA: Messenger RNA

PCR: Polymerase Chain Reaction

pre-mRNA: precursor mRNA

pri-miRNA: primary miRNA

PTM: Post-Translational Modifications

qPCR: Quantitative PCR

RBP: RNA-binding proteins

RNA pol II: RNA Polymerase II

RNA: Ribonucleic acid

RNAi: RNA interference

RT-PCR: Reverse transcription-polymerase chain reaction

SAM: S-adenosylmethionine

T-DNA: Transfer DNA

TEF: transcript elongation factors

TF: transcription factors

tRNA: transfer RNA

Ws: Wassilewskija

Y2H: Yeast 2 Hybrid

Part I. HUB1/2 INTERACTORS

Chapter 1 Relation between histone modification, transcript elongation and RNA binding proteins

1   Introduction

The structure of an organism is defined by the complete genetic information contained in the DNA. Eukaryotic cells compact DNA via a nucleoprotein complex, known as chromatin. Chromatin performs functions in fitting DNA in a small volume but also strengthening it to allow mitosis and meiosis, and as a mechanism to control expression and DNA replication. This genetic information is transcribed by the cell in the nucleus into a messenger RNA (mRNA) which is itself translated into a protein. Transcriptional regulation is one of the major molecular mechanisms that controls the organism structure and response to the environment. The transcription machinery in Eukaryotes is much more complex than in Prokaryotes or Archaea (which have only one polymerase, while Eukaryotes use two nuclear enzymes, RNA polymerase I and II, and additionally three polymerases, III IV and V to synthesize different classes of RNA, such as ribosomal RNA, pre-messenger RNA, small RNA and siRNA). However, the general mechanism of transcription and its regulation are conserved (Thomas and Chiang, 2006; Zhou and Law, 2015). In eukaryotic cells, RNA Polymerase II (RNA pol II) catalyzes the transcription of protein-encoding genes and the chromatin state determines transcriptional activity, which is either repressed or active and might be especially important in the regulation of developmental transitions (Andrews and Luger, 2011). Chromatin might act as an interface between environmental/developmental stimuli and the RNA pol II transcriptional machinery. The fundamental repeating unit of the chromatin is the nucleosome, in which histones play a pivotal role. The nucleosome consists of 146 base pairs of DNA, wrapped around an octamer composed of dimers of the "core" histones H2A, H2B, H3 and H4, the linker DNA between two adjacent histone octamers, and histone H1, which is involved in the further DNA packaging that leads to the final chromatin structure (Kornberg and Lorch, 1999). Chromatin is a highly dynamic structure that shows different levels of condensation and is commonly divided into euchromatin and heterochromatin. In euchromatic regions, genes are actively transcribed, whereas heterochromatic regions are transcriptionally inactive. The accessibility of the genome can be changed by covalent, post-translational modifications of the N-terminal tails of histones, including acetylation, methylation and ubiquitination (Tse *et al.*, 1998; Nelissen *et al.*, 2007). These distinct histone

modifications can generate synergistic or antagonistic interaction affinities for chromatin-associated proteins, which in turn dictate the dynamic transitions between active and silent chromatin states. Histone modifying multi-subunit complexes alter the chromatin structure by changing the conformational state or the mobilization of the nucleosomes. Chromatin modifications act in concert to regulate, for instance, gene transcription from initiation to elongation.

2   Transcription is a dynamic process

Transcription by RNA pol II is a complex process organized in different steps that starts with the need for a transcript and ends with a complete transcript (Cheung and Cramer, 2012). Each step requires a number of protein factors. During transcription RNA is synthesized from a complementary strand of DNA, read in 3'→5' direction, but synthesized in 5'→3'direction. In eukaryotes, transcription takes place in the nucleus of the cell while in prokaryotes it takes place in the cytoplasm or nucleoid. The five eukaryotic RNA polymerases are similar in structure and subunit configuration, RNA pol II only possesses an extra C-terminal domain (CTD) in its largest subunit Rpb1. The CTD serves as a binding platform for other proteins involved in transcription, mRNA processing and histone modification. Transcription can be divided into three steps: initiation, elongation and termination (Figure 1).

The pre-initiation complex is formed by RNA pol II recruitment and an open complex formation at the promoter that allows access to the DNA for the RNA pol II complex through the transcription bubble. Transcription initiation and its related factors are well described while later stages are less well understood. At this stage, the transcription can still be aborted by release of the nascent transcript from the advancing transcription complex due to the unstable nature of the DNA-RNA hybrid (Luse, 2013). The most common promoter is a sequence called TATA box, found -30 base pairs from the start site. This sequence is recognized by the TATA Binding Protein (TBP), a subunit of the general transcription factor TFIIB (Figure 2). TFIIB makes the contact between DNA and the TBP and stabilizes the association. This allows the recruitment of the TFIIF-RNA pol II complex followed by TFIIE and TFIIH. TFIIA can join the association at any time and, like TFIIB, stabilizes the DNA/TBP association. All these complexes play specific roles in the processes of transcription initiation such as promoter melting, promoter

clearance and inhibiting nonspecific promoter binding. These different general transcription factors, together with RNA pol II, form the pre-initiation complex (PIC) (Figure 2).
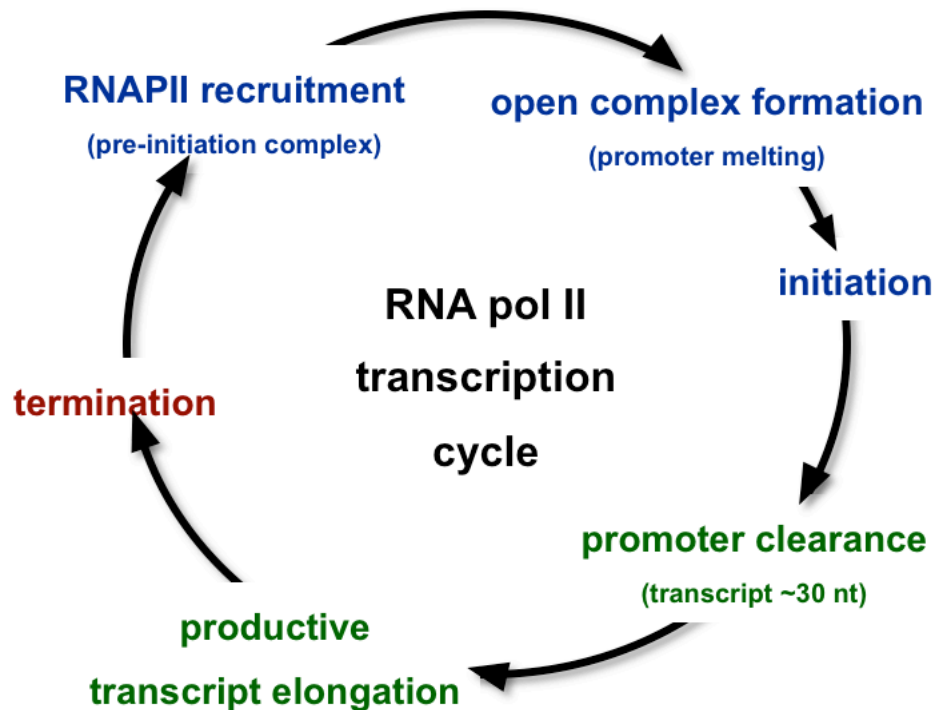
Figure 1: RNA pol II transcription cycle (from Van Lijsebettens & Grasser, 2014). Transcription by RNA pol II is characterized by a cycle of events, starting with polymerase recruitment and open complex formation, which are prerequisites for the initiation step. As the RNA pol II complex makes the transition from initiation to transcript elongation, various changes occur during promoter clearance, including the loss of contact with initiation factors and the establishment of a stable association with the nascent transcript. Because initially the DNA–RNA hybrid is rather short and unstable, the nascent transcript may be released from the RNA pol II complex, resulting in abortive transcription. Approximately 30 nucleotides downstream of the transcription start-site, promoter clearance is complete and RNA pol II becomes engaged in productive elongation. There are also impediments during elongation, such as the chromatinized DNA template; however, elongation continues until transcriptional termination occurs.

After formation of the PIC, RNA pol II uses base pairing complementarity with the DNA template to create an RNA copy in a step called elongation. When the complex formed by the nascent transcript and the RNA pol II reaches around 30 nucleotides downstream of the transcription start site it loses contact with the promoter. When this promoter clearance is complete the elongation starts. Elongation continues along the DNA

template and can also be regulated by the state of the DNA sequence (damage, mismatch). Elongation can also undergo pausing as a regulatory mechanism. During the different steps in the transcription process, the phosphorylation of RNA pol II changes. Specific subunits of a complex, called Mediator, make a molecular bridge in the contact between RNA pol II and the general transcription factors resulting in the start of transcription initiation or elongation after pausing (Allen and Taatjes, 2015). The Mediator complex stimulates the kinase activity of TFIIH which phosphorylates the CTD of RNA pol II on Ser5 and Ser7. The phosphorylation results in the dissociation of Mediator (Max *et al.*, 2007). The RNA pol II then proceeds to elongation, while Mediator may remain attached to the promoter as part of the scaffold complex, which can facilitate the next rounds of polymerase recruitment.
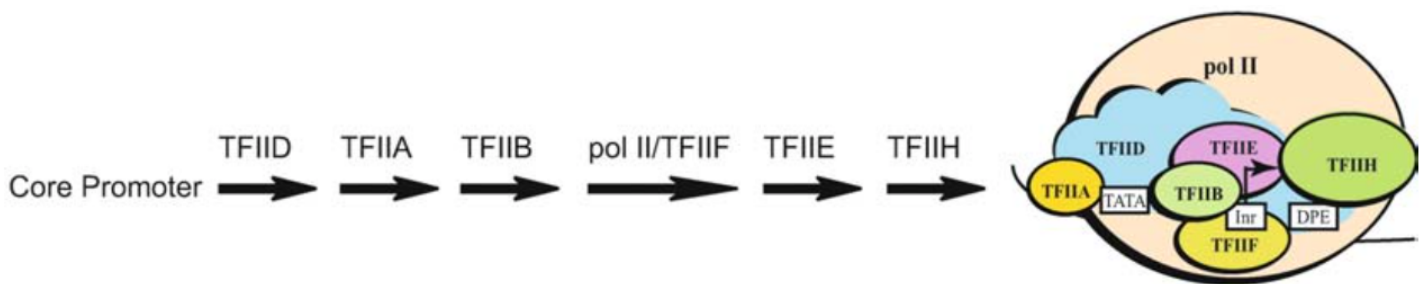
Figure 2: Preinitiation complex (PIC) formation modified from Thomas and Chiang, 2006. PIC formation may occur by stepwise recruitment of the general transcription machinery (sequential assembly pathway). TFIID first binds to the promoter region, followed by the entry of TFIIA and TFIIB that help stabilize promoter-bound TFIID, and then the recruitment of pol II/TFIIF. After formation of a stable TFIID-TFIIA-TFIIB-pol II/TFIIF-promoter complex, TFIIE is then recruited, with the subsequent entry of TFIIH.

Transcription finishes with the termination, an essential step in generating pre-mRNA. It occurs only after the polymerase has transcribed after the poly(A) site that indicates the end of the transcription. The 3'end of the pre-mRNA and the polymerase dissociate from the DNA template, when the RNA forms a hairpin due to a region rich in G and C. The stable hairpin causes the polymerase to stall and the weak interaction of A-U in the DNA-RNA sequence causes the RNA and DNA to dissociate. The mRNA is cleaved, polyadenylated and transported to the cytoplasm, where it will be translated.

3   Transcript elongation and RNA biology

RNA pol II requires additional factors for transcription initiation, elongation and termination. Transcript elongation is highly regulated both by protein factors that bind to a DNA template, the RNA transcript or the transcription complex as it moves along the template. Elongation is a repetitive but temporally discontinuous formation of phosphodiester bonds. Important components which bind with RNA pol II during elongation consist of SAGA, FACT, Paf1c, TFIIS, RAD6/Bre1, COMPASS, Elongator and others. These transcript elongation factors (TEFs) have been shown to serve diverse functions such as facilitating the processivity of RNA pol II, assisting in the progression through repressive chromatin and modifying histones within transcribed regions. In plants, TEFs play crucial roles in development and certain stress responses indicating their importance in establishing proper gene expression (Table 1). TEFs are often conserved among eukaryotes. In plants, their interplay with environmental and developmental stimuli has diverged, as have target genes and upstream signals. Therefore, plants serve as a great model to understand the influence of TEFs on transcriptome modulation and their influence on development. Most of the TEFs play a role in relaxing the chromatin state to allow RNA pol II passage.

A major regulator of elongation is sequence-dependent pausing (Kwak and Lis, 2013; Jonkers and Lis, 2015). In the initial steps of elongation, RNA pol II can pause and accumulate at very high levels in the promoter-proximal region, 30-60 nucleotides downstream of the transcription start site. This can act as a quality check point for RNA 5'end capping and RNA pol II modification, before continuing the elongation. The pausing mechanism also allows for shorter response time in active transcription to external stimuli. At the pausing site, RNA pol II is stabilized by pausing factors such as NELF (negative elongation factor) and DSIF (DRB sensitivity inducing factor, SPT4/5) (Figure 3). Release of the paused RNA pol II is regulated by the P-TEFb complex. This complex is recruited to the promoter by direct or indirect interaction to specific transcription factors (TFs) and cofactors. Recruitment of other co-activators and elongation factors such as Mediator or SEC (super elongation complex) that make the contact between enhancer and promoter and activates P-TEFb. This complex

phosphorylates the CTD of RNA pol II at the Ser2, as well as NELF, which is then evicted from RNA pol II and DSIF, which becomes a positive elongation factor.

Table 1: Transcript elongation factors characterized in *Arabidopsis* (modified from Van Lijsebettens & Grasser, 2014).

Factor	Subunits	Molecular function	Mutant phenotype
TFIIS	TFIIS	Modulates RNAPII properties	Seed dormancy
SPT4–SPT5	SPT4, SPT5	Modulates RNAPII properties	Growth and development, auxin response
P-TEFb	CDKC;2, CYCT1;5 (CYCT1;4)	Modulates RNAPII properties	Flowering time, growth, reproductive development
FACT	SSRP1, SPT16	Histone chaperone	Vegetative, reproductive development
SPT6	SPT6L	Histone chaperone	Embryo basal–apical polarity
IWS1	IWS1	Modulates histone modifications	Growth, brassinosteroid-dependent or nitrogen-responsive gene expression
PAF1C	VIP3, VIP4, VIP5, ELF7, ELF8/VIP6, CDC73/PHP	Modulates histone modifications	Vegetative, reproductive development
SWI/SNF	Multiple subunits, including BRM, SYD, MINU1/2, PKL	Nucleosome remodeling	Growth and development, hormone signaling
HUB1	HUB1, HUB2	Histone H2B monoubiquitination	Growth, seed dormancy, flowering time, circadian clock, photomorphogenesis, cutin and wax composition, pathogen susceptibility
UBC1	UBC1, UBC2	Histone H2B monoubiquitination	Flowering time
SUP32/UBP26	SUP32/UBP26	Histone H2B deubiquitination	Flowering time
ATXR3/SDG2	ATXR3/SDG2	Histone H3K4 methylation	Flowering time, reproductive development
ASHH2/SDG8	ASHH2/SDG8	Histone H3K36 methylation	Flowering time, branching, reproductive organ development, pathogen defense
LSD1	LSD1	Histone H3K4 Demethylation	Flowering time
JMJ14	JMJ14	Histone H3K4 demethylation	Flowering time
IBM1	IBM1	Histone H3K9 demethylation	Vegetative, reproductive development
REF6/JMJ12	REF6/JMJ12	Histone H3K27 demethylation	Developmental patterning, responses to various stimuli
Elongator	ELP1/ELO2/ABO1, ELP2, ELP3HAG3/ELO3, ELP4/ELO1, ELP5, ELP6	Histone H3K14 acetylation	Growth, auxin, abscisic acid, and immune response
HDA19	HD1/HDA19/RPD3A	Histone H3K9/K14 deacetylation	Light response
SWR1C	PIE1, ARP6, SWC6	H2A.Z deposition	Growth, flowering time, flower morphology, temperature response

[a]Abbreviations: BRM, BRAHMA; CDKC, cyclin-dependent kinase C; CYCT, cyclin T; MINU1/2, MINUSCULE 1/2; PKL, PICKLE; SYD, SPLAYED.

a Pol II after recruitment   **Paused Pol II after entry**   **Pol II after release**
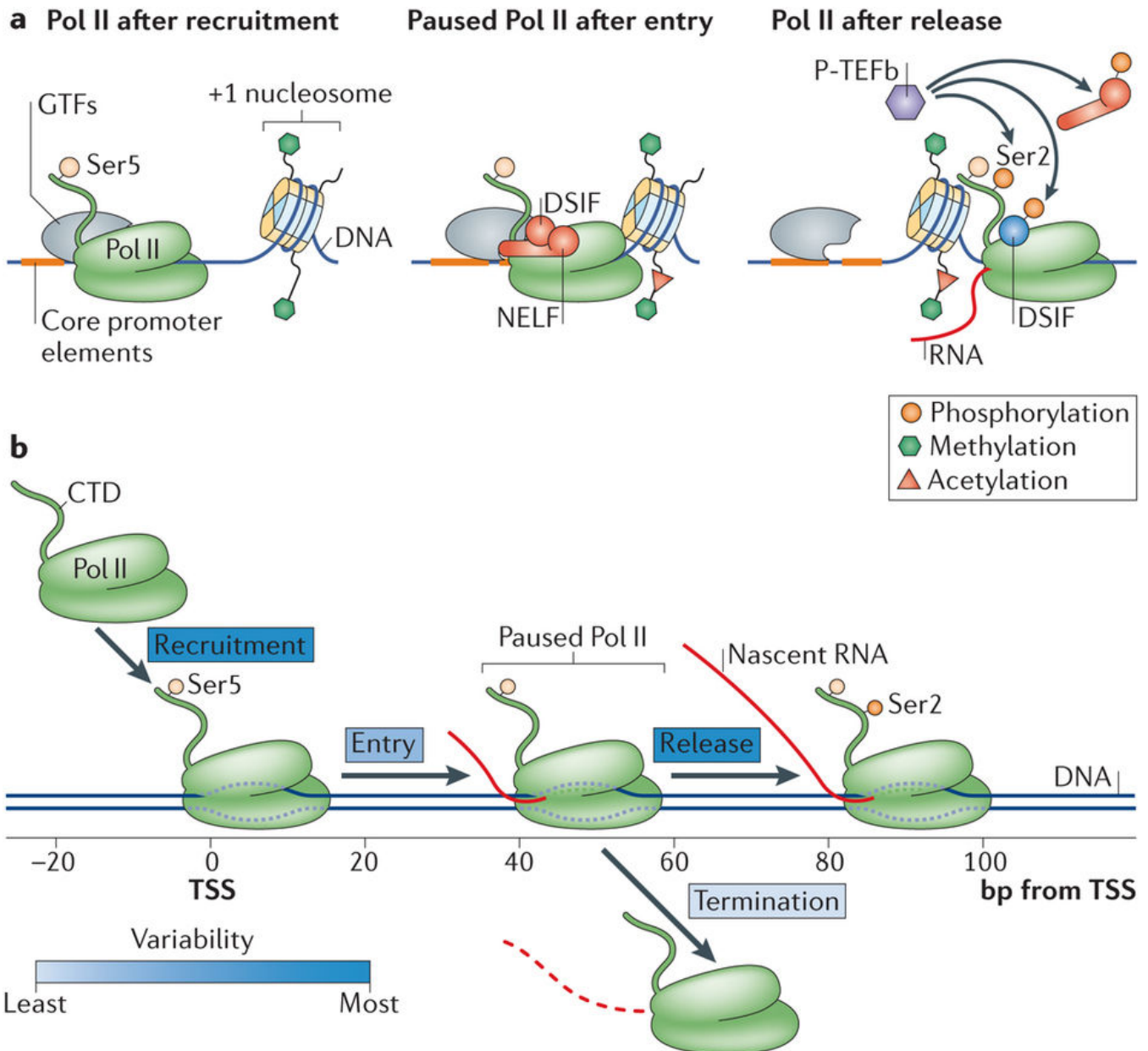
Figure 3: Model of promoter-proximal RNA pol II pausing (from Jonkers and Lis, 2015)

A. RNA polymerase II (Pol II) is associated with promoters and just downstream of, the transcription start site (TSS). The transcriptional state, position and composition of Pol II are variable and depend on factors that contribute to recruitment, initiation, pausing and release of Pol II. Recruitment of Pol II by general transcription factors (GTFs) results in the formation of a pre-initiation complex (PIC). After rapid Pol II initiation and entry into the pause site, Pol II pausing by negative elongation factor (NELF) and DRB-sensitivity-inducing factor (DSIF) occurs, facilitated by the core promoter elements and the +1 nucleosome. Positive transcript elongation factor-b (P-TEFb) mediates the release of paused Pol II by phosphorylating NELF, DSIF and the carboxy-terminal domain (CTD) of Pol II. DSIF becomes a positive elongation factor after phosphorylation. B. The transcription cycle is predominantly regulated near the TSS, at the steps of recruitment of Pol II to promoters, and release from the promoter-proximal pause site. These steps

are most variable in terms of rate (as indicated by the dark blue shading of the boxes defining the steps). Other steps, such as transcription initiation and entry to the pause site, as well as transcription termination from the pause site, seem not to be as variable in rate and less subject to regulation (as indicated by the lighter blue shading of the boxes).

Elongation rates can vary between genes and play a role in co-transcriptional processes such as splicing and termination. The elongation rate can be modified by gene features like number of exons and DNA sequence, but also histone marks or histone content and nucleosome occupancy. RNA pol II is slowest at the promoter-proximal pause site and speeds up after release over 15kb. RNA pol II mediated transcription also slows down around exons and at the termination site. TEFs such as SEC, PAF, FACT and Spt6 facilitate elongation (Table 1). Nucleosomes can create a physical barrier causing RNA pol II to pause or reduce the elongation rate.

Elongation is the step that forms the pre-mRNA and where co-transcriptional modification happens, changing the pre-mRNA into a mature mRNA. Therefore, processing and synthesis are tightly linked and there is an interplay between the processing and transcription machinery. The three major steps of mRNA maturation (Figure 4) are 5'end capping, addition of polyadenylation tail at the 3'end (polyA tail) and splicing. An additional packaging step of the mRNA with chaperones and export factors is sometimes also distinguished after the 3'end processing, for correct export.
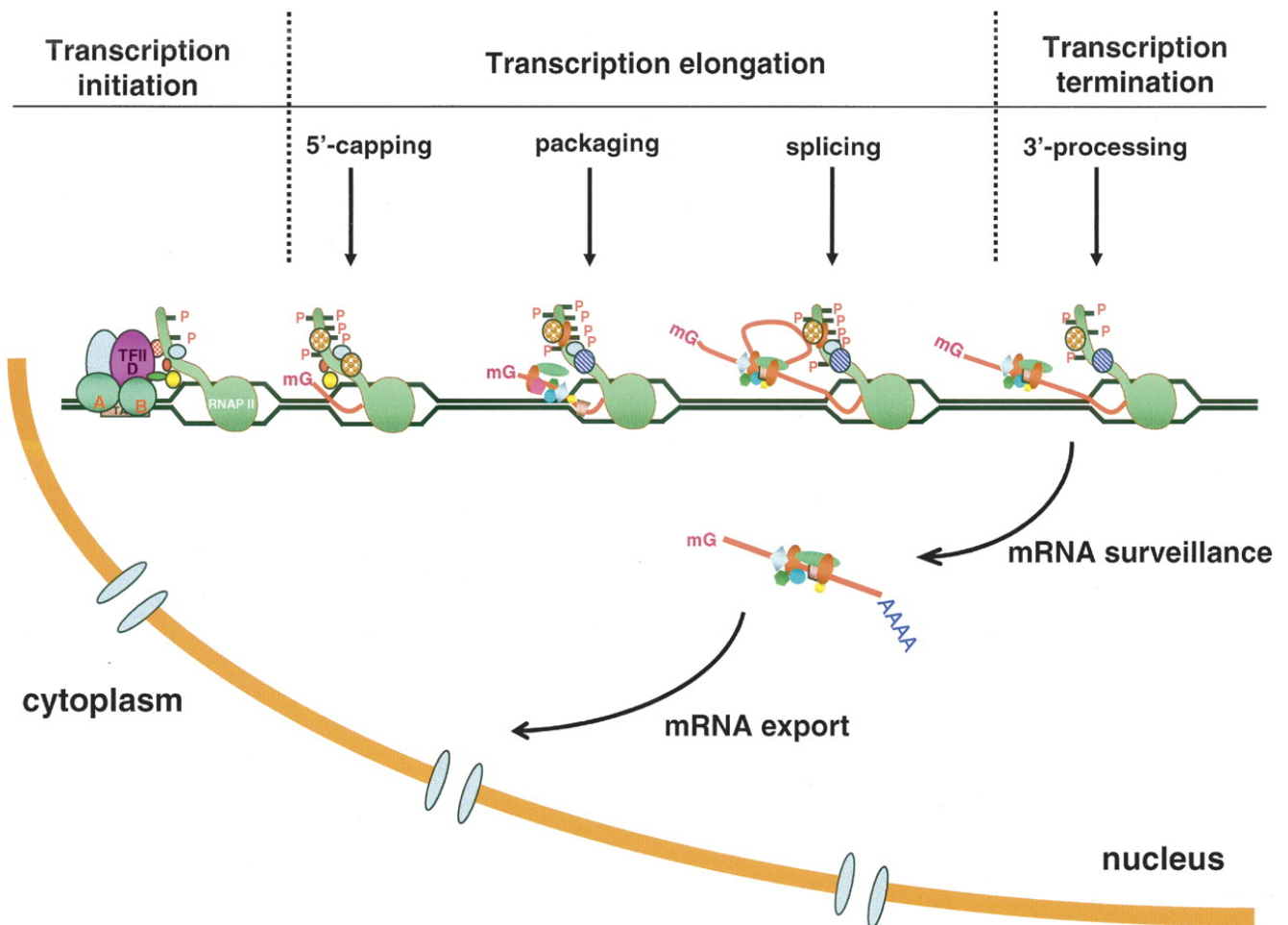
Figure 4: Processes involved in the synthesis of mature mRNA by RNA pol II (from Li and Manley, 2006). In eukaryotic cells, the generation of a translatable mRNA is a highly coordinated, multiple-step process that occurs in the nucleus. RNA pol II, and specifically the C-terminal domain (CTD) of its largest subunit (indicated by "tail" on the RNAP), orchestrates these processes in a manner that involves changes in CTD phosphorylation status and corresponding changes in associated factors. These proteins in turn effect the subsequent processing reactions and/or help to recruit processing/packaging factors to the nascent transcript. In the process of maturation, the nascent RNA is capped at its 5' end, introns are removed by splicing, and its 3' end is cleaved and polyadenylated. After going through the mRNA surveillance system, the matured mRNA is exported to the cytoplasm for translation. Each stage in RNA pol II transcription and the steps of co-transcriptional processing are indicated at the top.

3.1 5'end capping

Capping occurs when the pre-mRNA is 20-35 nucleotides long and is carried out by the CEC (capping enzyme complex) (Bentley, 2014) (Figure 4). A 7-methylguanosine (m^7G) is formed at the 5'end, by removal of the terminal 5'phosphate by a phosphatase, leaving a diphosphate group. This is followed by the addition of a GTP by a guanosyl transferase,

and transfer of a methyl group from S-adenosyl methionine. Phosphorylation of the Ser5 of the CTP plays a crucial role by interacting directly with the guanine-7-methyltransferase and the mRNA-capping enzyme. Capping of the nascent transcript coincides often with the promoter-proximal pausing. The mRNA-capping complex interacts with SPT4/5 (DSIF), therefore the related pausing might be a checkpoint for correct capping before the elongation continues.

The capping has several functions, such as regulation of the nuclear export, prevention of degradation by exonucleases, promotion of translation and 5'proximal intron excision. De-capping has been shown to happen in vivo, mostly in the cytoplasm, but can also occur in the nucleus and lead to premature degradation.

3.2   Splicing

Splicing is the process by which introns, non-coding RNA regions, are removed from the pre-mRNA (Figure 4). The process connects retained exons, the coding part of the RNA sequence, to form a continuous sequence. It can take place during transcription or directly after. Delayed splicing is another way to regulate the timing of gene activation (Bentley, 2014). Most eukaryotic introns are spliced through the action of the spliceosome, a complex of small nuclear ribonucleoprotein (snRNPs). However, some introns are self-splicing. The spliceosome is made of five small nuclear RNAs (snRNA) associated with protein factors, together forming the snRNPs. They are in the major spliceosome and named U1, U2, U4, U5 and U6.

Splicing, like elongation, takes several minutes and the elongation rate can affect splicing efficiency (Luco *et al.*, 2011). The degree of co-transcriptional splicing for each intron depends on the time difference between splicing and elongation/termination. Relative rates of splicing, transcript elongation and poly(A) site cleavage can all affect the extent of co-transcriptional splicing. Therefore, the position of the intron can influence the co- or post-transcriptional splicing.

Alternative splicing is the process by which a range of proteins can be created by variation of the exon composition of the same mRNA. Exons can be extended or skipped and introns can be retained to create alternative splicing. This process can be tissue-and/or cell-specific or in response to external stimuli and is highly regulated (Figure 5).

Creation of the isoforms is regulated through trans-acting proteins binding to cis-acting sites on the pre-mRNA transcript and secondary structure of the pre-mRNA. Splicing that skips an alternative exon is slower than splicing including that exon. The elongation rate can influence the alternative splicing decision by determining the window of opportunity for the co-transcriptional process to happen by influencing where the spliceosome assembles and where splicing regulators bind (Bentley, 2014). Control of splice site choice is very complex and RNA-binding proteins and elongation rate alone are not enough to explain the complete regulation process. Chromatin structure and epigenetic histone modification are key regulators of splicing (Figure 5). It has been shown that some acetyltransferases and methyltransferase interact with U2snRNP and U1snRNP, as well as chromatin remodellers SW1/SNF with U1 and U5, suggesting a role for chromatin complexes and remodellers in assembly of the spliceosome (Luco *et al.*, 2011). Nucleosome density varies more in alternatively spliced exons and nucleosome occupancy might also regulate splicing through regulation of RNA pol II pausing (Figure 3 and 5).
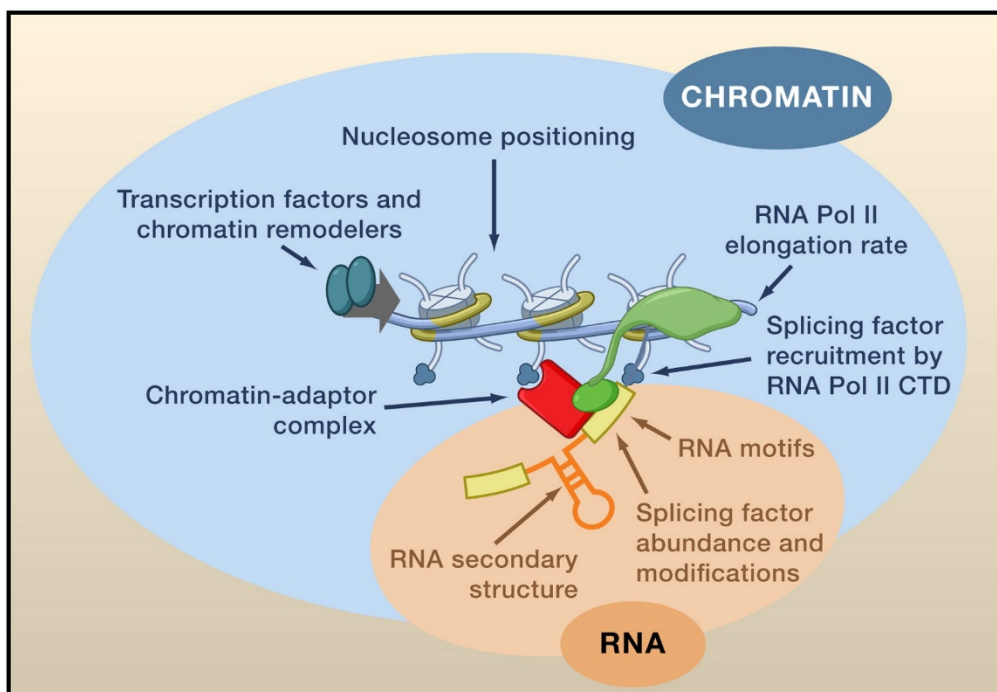
Figure 5: An Integrated Model for the Regulation of Alternative Splicing (from Luco *et al.*, 2011). Alternative splicing patterns are determined by a combination of parameters including *cis*-acting RNA regulatory elements and RNA secondary structures (highlighted in orange) together with transcriptional and chromatin properties (highlighted in blue) that modulate the recruitment of splicing factors to the pre-mRNA.

3.3   Cleavage and polyadenylation

Processing of the 3'end of the pre-mRNA is complete when a polyadenylation signal sequence is present near the 3'end of the pre-mRNA followed by a cleavage site and a GU-rich sequence (Figure 4). The multi-subunit proteins, cleavage and polyadenylation specificity factor (CPSF) and cleavage stimulation factor (CStF) transfer from the RNA pol II to the polyadenylation signal sequence and form with other proteins a complex that cleaves the pre-mRNA at the cleavage site. The poly(A) polymerase present in the complex adds adenosine monophosphate units from an adenosine triphosphate producing pyrophosphate. When the tail reaches around 250 nucleotides the poly(A) polymerase loses contact with the CPSF and polyadenylation stops. CPSF is still in contact with the RNA pol II and can transmit the signal to stop transcription. The polyadenylation machinery is physically linked to the spliceosome (Millevoi *et al.*, 2006).

Like for alternative splicing, alternative polyadenylation allows one gene to code for different mRNAs by changing the 3'end. The choice of the poly(A) site is regulated by extracellular stimuli and expression of polyadenylation proteins. Alternative polyadenylation can be influenced by many factors such as the promoter at the transcription start site, recruitment of polyadenylation factors directly or other proteins that influence alternative polyadenylation, nucleosome density at the site of alternative polyadenylation, the factors associated with RNA pol II, various RNA binding proteins associated with the nascent transcript, inhibition by the U1 snRNP and presence of N6-methyladenosine (Tian and Manley, 2017).

The poly(A) tail inhibits degradation and helps export and translation through poly(A) binding proteins (Figure 4). Through time and different processes such as action of miRNA, the tails get shorter, which reduces their translation and promotes degradation.

4   Activating histone modifiers

To hold a great amount of information in the space of the nucleus, the eukaryotic cell compacts the DNA into a nucleo-protein complex: the chromatin. The nucleosome makes the fundamental unit of the chromatin, it consists of 146 base pairs of DNA wrapped around an octamer composed by dimers of the "core" histones (Figure 6).

Histones are constitutive proteins classified into 5 types: the linker histone, H1, and the core histones, H2A, H2B, H3 and H4 (Kornberg and Lorch, 1999), and their variants (Ausió, 2006).

The chromatin structure is highly dynamic that presents itself in different levels of condensation: euchromatin and heterochromatin. The euchromatin corresponds to open regions that are actively transcribed whereas heterochromatin regions are transcriptionally inactive. In the euchromatin the nucleosome assembly is in a more relaxed state that allows for flexible transcriptional states. Heterochromatin is constituted of DNA in highly compacted nucleosome assembly that makes it inaccessible to transcription factors or chromatin-associated proteins. Two forms of heterochromatin can be distinguished (Quina *et al.*, 2006). Constitutive heterochromatin found around the centromeres and telomeres made of repetitive sequence such as satellite repeats and transposon repeats. Facultative heterochromatin can vary depending on cell types and is related to the differentiation mechanisms. Therefore, the function of chromatin extends beyond packaging of DNA but instead the dynamic state of chromatin structure dictates the activation and function of the genome.
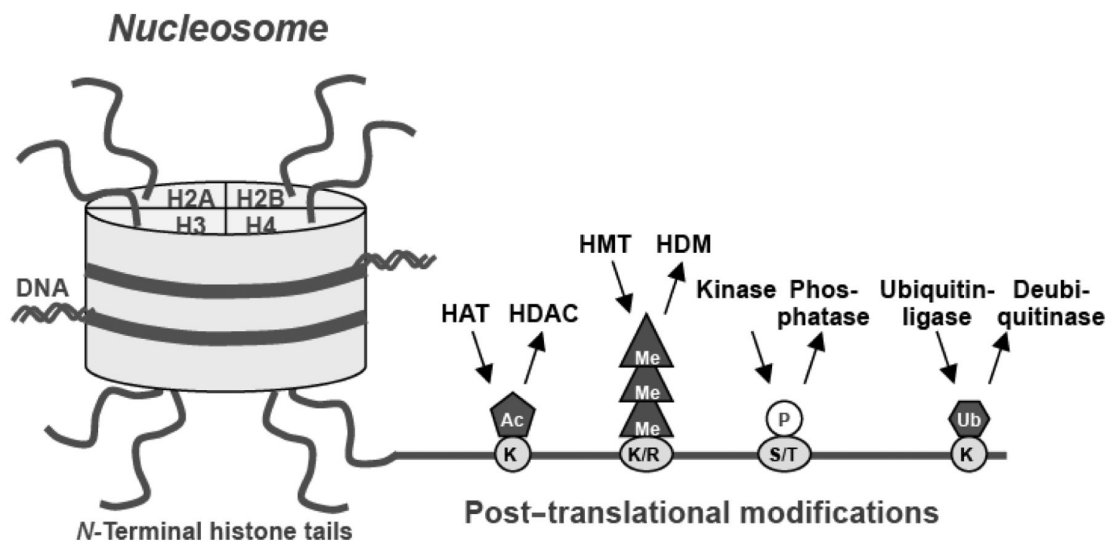
Figure 6: Nucleosome and covalent post-translational histone modifications (from Gezer and Holdenrieder, 2014). Chromatin is formed by nucleosomal units consisting of a central histone octamer with double-represented histones H2A, H2B, H3 and H4 and 147 bp double-stranded DNA. N-Terminal histone tails protruding from the nucleosomes can be post-translationally modified by acetyl (Ac), methyl (Me), phosphate (P), ubiquitin (Ub) and other groups at the basic amino acids lysine (K) and arginine (R), as well as at serine (S) and threonine (T). Various enzymes are involved in

these processes, such as histone acetyltransferases (HAT) and deacetylases (HDAC), histone methyltransferases (HMT) and demethylases (HDM).

4.1 Histone modifications

Histones are the most abundant proteins in eukaryotic cells. These basic proteins contain high amounts of arginines and lysines, positively charged amino acids. Histone types can be distinguished by their size, net charge, relative content of lysine and arginine, and solubility properties (Nelissen *et al.*, 2007). Histones form heterodimers such as H3-H4 and H2A-H2B, fundamental for the formation of the core histone octamer (Figure 6). Like the histone proteins, the various histone modifications and the enzymatic machinery are conserved through evolution (Strahl and Allis, 2000).

Histone modifications are critical to regulate chromatin structure and function. They can affect many functions related to DNA, such as transcription, recombination, DNA repair, replication and chromosomal organization. The unstructured 15-30 residues of the N-termini of the histones, histone tails (Kornberg and Lorch, 1999), can be modified by acetylation, methylation, ubiquitination, phosphorylation, sumoylation and poly(ADP)ribosylation through a wide range of enzymes that determine their abundance and genome wide distribution (Pikaard and Mittelsten Scheid, 2014) (Figure 6). These histone modifications are qualified as Post-Translational Modifications (PTMs) and provide a signal for other proteins such as RNA pol II to access the DNA (Table 2). Enzymes that mediate histone modification include acetyltransferases, methyltransferases, kinases, and ubiquitinases. The enzymes that remove these modifications include deacetylases, phosphatases, demethylases, and de-ubiquitinases. These histone modifications act sequentially or in combination to form a histone code that is read by other proteins (Strahl and Allis, 2000). The dynamic processes of modification and repositioning work together to establish or alter regional chromatin properties, the importance of these processes varies when looking at individual loci.

Table 2: Types of covalent histone post-translational modification and their enzymes.

	Role in transcription	Sites of histone modification	Writer	Eraser
Group 1: small chemical modification				
Acetylation	activation	H3 K9, K14, K18, K56	HAT	HDAC
		H4 K5, K8, K12, K16		
		H2A		
		H2B K6, K7, K16, K17		
Phosphorylation	activation	H3 S10	kinase	phosphatase
Methylation	activation	H3 K4, K36, K79	KMT (SET domain)	LDL JmjC
	repression	H3 K9, K27		
		H4 K20		
Group 2: large chemical modification				
Ubiquitylation	activation	H2B K123	ubiquitin ligase	DUB
	repression	H2A K119		
Sumoylation	repression	H3?	ubiquitin ligase (STUbLs)	SUMO protease
		H4 K5, K8, K12, K16		
		H2A K126		
		H2B K6, K7, K16, K17		
ADP-ribosylation			PARP	PARG

4.1.1 Acetylation

Histone acetylation is an epigenetic mark associated with active chromatin and transcription (Marmorstein and Zhou, 2014). Histone acetyltransferases (HAT) are responsible for adding an acetyl group to conserved lysine amino acids while histone deacetylases (HDAC) can remove these, creating a dynamic equilibrium affecting chromatin structure and transcriptional activity (Table 2 and Figure 6). Understanding the functions of HATs and HDACs is complicated by their redundancy and their participation in multiprotein complexes. Transcriptional activity is correlated with hyper-acetylation of the promoter and with a smaller effect also in the coding region. Acetylation of histones H3 and H4 counteracts the tendency of nucleosomal fibers to fold into highly compact structures *in vitro* (Tse *et al.,* 1998) and acetylated chromatin is more accessible in vivo as seen by its increased sensitivity to DNase I (Hebbes *et al.*, 1994). In yeast, the chromatin base state is characterized by intermediate levels of H3 and H4 acetylation, due to a mix of untargeted HAT and HDAC activities, activation and repression being local acetylation/deacetylation events (Vogelauer *et al.*, 2000). Site-specific acetylation or deacetylation leads to locally restricted activation or repression of transcription, respectively. In differentiated, higher eukaryotic cells, most of the genome consists of hypoacetylated, inactive chromatin while the yeast genome is more highly acetylated and more active. Histone acetylation usually accumulates at the promoter upon gene activation and deacetylation of the promoter is associated with repression. However, broad acetylation patterns on chromosomal domains were also described for more stable gene expression such as the β-globulin gene locus or the HOX gene cluster (Forsberg and Bresnick, 2001; Fukuda *et al.*, 2006). Deacetylation of histone 3 is guided by H3K36 methylation by Set2 in coding regions thus suppressing intragenic transcription initiation (Carrozza *et al.*, 2005). The promoter regions of actively transcribed genes are highly acetylated, the coding regions of genes contain a lower level of acetylation which is important to facilitate RNAPII transcript elongation that also regulates gene expression levels (Van Lijsebettens and Grasser, 2014). Interestingly, active transcription also correlates with histone acetylation in the coding region of genes, but here the observed increases are often surprisingly modest (Kouskouti *et al.,* 2005). This might argue that histone acetylation does not play an important role in RNAPII transcript elongation through chromatin. However, HATs and HDACs are

enriched in the coding region of genes (Govind *et al.,* 2007) indicating substantial turnover of acetylation.

The addition of the acetyl group from acetyl-Coenzyme A neutralizes the positive charge of the lysines and therefore modifies interaction between DNA and histones and other proteins, decondensing the chromatin. It is believed that neutralization of the positively charged lysine by acetylation reduces the strength of binding of the strongly basic histones or histone tails to the negatively charged DNA thus opening DNA binding sites (Vettese-Dadey *et al.,* 1996). It also has a role in the decompaction of the nucleosomes (Shogren-Knaak *et al.,* 2006). Acetylation could also provide a binding surface for proteins with a bromodomain that could then associate with the chromatin and regulate DNA-templated processes such as chromatin remodelling, acetylation, phosphorylation.

Substrates of HATs and HDACs consist of a wide range of proteins in addition to histones, such as cytoskeletal proteins, molecular chaperones and nuclear import factors giving them roles independent of transcription (Glozak *et al.,* 2005). The acetylation status is believed to regulate stability of the protein. Deacetylation by HDACs in many cases is a prerequisite for subsequent ubiquitination. Therefore, acetylation may protect a protein from ubiquitination and degradation.

There are five major HAT families: the Gcn5-related N-terminal acetyltransferases (GNAT), the MYST family, the CBP/p300 family, the family related to mammalian TAF250, and nuclear receptor co-activators (Pandey *et al.,*2002; Nelissen *et al.,* 2007). Each family has substrates of choice, GNAT targets histone 3, MYST histone 4 and CBP/p300 both histone 3 and 4. GNAT family members regulate the recruitment of transcription factors to their target promoters. MYST family members are involved in the regulation of a variety of DNA-mediated reactions, such as promoter-driven transcriptional regulation, long-range/chromosome-wide gene regulation, double-stranded DNA break repair and licensing of DNA replication. Involvement of HAT in transcript regulation was first described in *Tetrahymena* HAT A, a homolog of the yeast Gnc5 (Brownell *et al.,* 1996). Since then, Gnc5 homologs have been found in numerous eukaryotes. GNAT and MYST have domains found in enzymes that acetylate non-histone proteins. The HAT families conserve a similar structure with a central region for binding acetyl-CoA and catalysis, flanked by divergent amino- and carboxy- terminal

segments, both likely playing a role in histone substrate binding (Marmorstein and Zhou, 2014; Fukuda *et al.*, 2006). In plants, homologs are known for four families: CBP, MYST, GNAT and TAF250. The plant CBP family has a different structure than in other kingdoms with no bromodomain recognizing acetylated histone. It also contains more members as compared to animals (1) or fungi (0). In histone deacetylation, the acetyl group can be transferred back to Coenzyme A or to ADP-ribose by the NAD-dependent deacetylases (Denu, 2003). In plants, HDAC are classified in three families: the RPD3/HDA1 superfamily, the SIR2 family and the HD2-like family (Pandey *et al.*, 2002). The HD2/HDT family is specific to plants and implicated in gene silencing, but no HDAC activity has been shown yet (Pikaard and Mittelsten Scheid, 2014).

4.1.2   Methylation

Like acetylation, histone methylation is well documented and a potentially reversible mark (Pikaard and Mittelsten Scheid, 2014, Berr *et al.*, 2011). Arginine and lysine residues can receive a methyl group from the donor S-adenosylmethionine (SAM) by enzymatic reaction performed by a histone methyltransferase (HMTs) (Table 2 and Figure 6). HMTs have a SET domain conserved throughout evolution. In *Arabidopsis* 47 genes contain a SET domain. An amino acid residue can carry several methylation marks, one to three for lysine and one or two for arginine. The reaction is performed by distinct enzymes, histone lysine methyltransferases (HKMTs) or protein arginine methyltransferases (PRMTs). Methylation is mainly associated with transcriptional repression and silent heterochromatin initiation and maintenance. But some methylation marks have been associated with activation of transcription. The different methylation states have different functions and these differs between eukaryotes. Histone methylation can be considered as a biological language with different dialects.

Methylation of lysine increases the hydrophobicity and therefore can alter intra- and intermolecular reactions and create new binding surfaces for regulatory factors. Histone H3K9 and H3K27 methylation are associated with silenced regions, whereas H3K4 and H3K36 methylation are associated with active genes. The degree of methylation adds another level of complexity, i.e. H3K9 mono and dimethylation are typical for silenced chromatin where trimethylation is found in euchromatin. Arginine methylation mainly occurs at Arg2, Arg8, Arg17, Arg26 of histone H3 and Arg3 of histone H4 (Bedford and

Richard, 2005). It is involved in many processes such as transcription regulation, RNA processing, nuclear transport, DNA-damage repair and signal transduction. Compared to other post translational modifications of histones, methylation is relatively stable, but can be removed by histone demethylases. In *Arabidopsis*, there are 4 specific lysine histone demethylases (LDL) and 21 JUMONJI-C-DOMAIN (JmjC).

4.1.3   Ubiquitination and Sumoylation

Ubiquitin is a highly conserved protein of 76 amino acids, associated with proteolysis by its role in labelling proteins for degradation. These proteins are polyubiquitinated by the action of a ubiquitin-activating enzyme E1 and a ubiquitin-conjugating enzyme E2 that usually work with ubiquitin ligase E3 (Conaway *et al.*, 2002). 90% of the E3 ubiquitin ligases are part of the ubiquitin-proteasome pathway and are part of a large and diverse family of proteins.

Ubiquitination at lysine residues occurs mainly at histones H2A and H2B. H2A ubiquitination is more frequently correlated with gene silencing (Cao and Yan, 2012), while H2B ubiquitination induces transcriptional activation by promoting other epigenetic marks related to histone methylation (Shukla *et al.*, 2006). De-ubiquitination is made by cleavage of the bond between the ubiquitin and the substrate. There are two types of de-ubiquitination (DUB) enzymes: the ubiquitin C-terminal hydrolases (UCHs) and the ubiquitin-specific processing proteases (UBPs), with 27 putative UBPs in *Arabidopsis* (Table 2 and Figure 6). Histone ubiquitination and de-ubiquitination are dynamic processes and important for deposition of other activating or repressing marks (Weake and Workman, 2008).

Another process competing with ubiquitin modifications on histones is sumoylation (Table 2 and Figure 6). Sumoylation of target proteins is mediated by similar enzymes as those for ubiquitination, called small-ubiquitin-like-modifier (SUMO) proteins, with 8 members in *Arabidopsis* (Nelissen *et al.*, 2007). Histone sumoylation appears to act antagonistically to the activating lysine modifications of histones, such as acetylation and ubiquitination. Sumoylation has been shown for all core histones H2A, H2B, H3 and H4 with site specificity. Protein sumoylation also affects subcellular localization, protein stability, and interactions with proteins or DNA. Like some ubiquitination, sumoylation is labile in native conditions.

4.1.4 Phosphorylation and ribosylation

Phosphorylation is present at all core histones on serine and threonine residues (Nelissen *et al.*, 2007) (Figure 6). It is involved in DNA repair and regulation of chromosome segregation and cell division (Houben *et al.,* 2007). Phosphorylation of histones can be influenced by other post translational modifications of histones. H3S10Ph is linked with transcriptional activation and acetylation of H3K9 and H3K14 as they target the same H3 tail (Table 2).

Ribosylation is known for its involvement in DNA repair. It is also a reversible histone modification catalysed by Poly(ADP-ribose) polymerase (PARP) that attaches poly(ADP)-ribose from NAD+. Reversibility is carried out by poly(ADP)-ribose glycohydrolase (PARG) (Table 2). Depending on the chromatin environment, ADP-ribosylation plays a role in both transcriptional activation and repression (Nelissen *et al*., 2007). PARP-1 can act on the nucleosome by ribosylation but also directly on transcription by altering the activity of promoters. It is involved in chromatin decondensation and keeping some repetitive elements condensed.

4.2 Histone modifiers for transcription activation

Covalent post-translational modifications of histones are finely regulating transcription, some are marks of transcription activation (Berr *et al*., 2011). Transcription of some genes is more sensitive to the absence or deficiency of some histone modifiers (Table 1). For example, in plants, the expression of genes responsive to auxin, abscisic acid, pathogen infection, and flowering-time regulators and, thus, reactive to internal and external stimuli, is frequently affected in mutants with defective histone modifying genes.

Activating histone marks (H2Bub, H3K4me3, H3K36me3, H3K9ac) are found in the gene bodies (Figure 7). Some like H3K9ac are abundant at the beginning of the gene body and found in the promoter region. Therefore, they are related to the initiation of transcription, while others like H2Bub are facilitators of transcript elongation by their absence from the promoter and abundance in the middle part of the gene body (Figure 7) (Van Lijsebettens & Grasser, 2014).
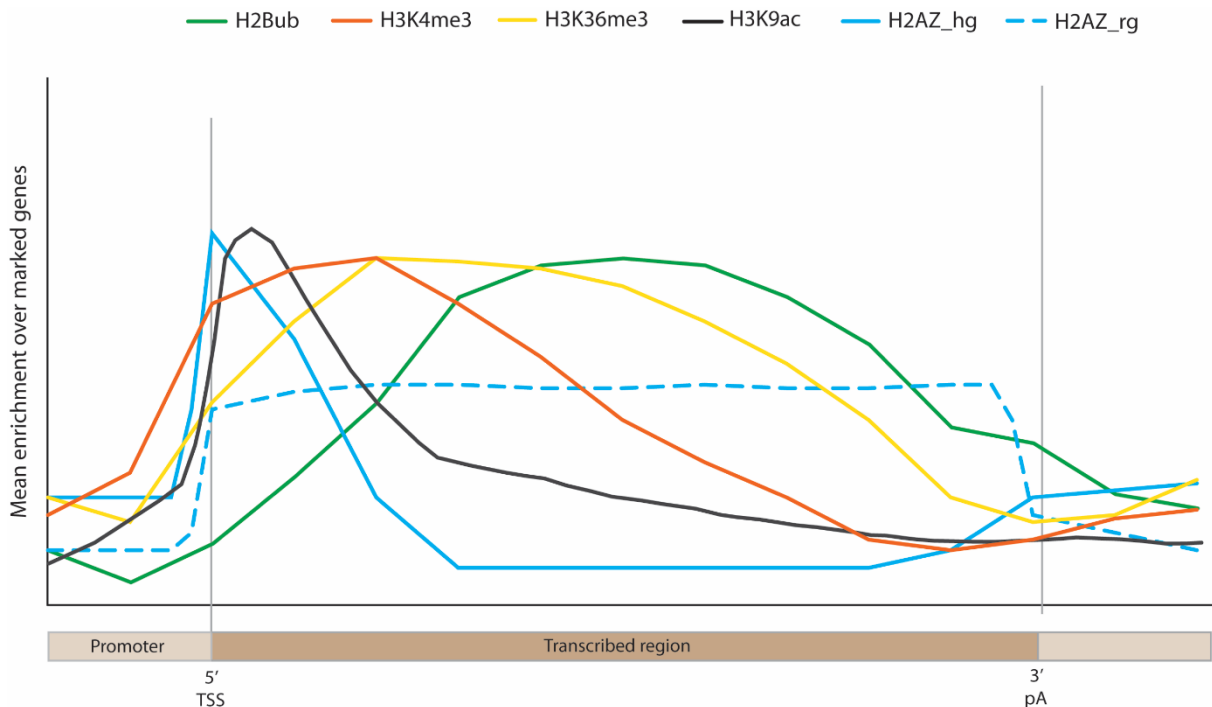
Figure 7: Distribution of histone marks and the histone variant H2A.Z over active gene bodies in *Arabidopsis* (from Van Lijsebettens & Grasser, 2014). Compiled data showing mean enrichment of the gene expression activating histone marks H2Bub, H3K4me3, H3K36me3, H3K9ac, and the histone variant H2A.Z_hg (hg, housekeeping genes), and H2A.Z_rg (rg, responsive genes) on marked genes from ChIP-chip experiments represented on a schematized gene scaled to accommodate different transcribed region lengths. Below, scheme of a gene with a promoter, transcription start-site (TSS), transcribed region, and polyadenylation site (pA).

Histone H2B monoubiquitination at lysine 143 is present in highly expressed genes together with histone acetylation and methylation (H3K56ac, H3K4me3, H3K4me2, H3K9me3, and H3K36me3). These marks define active chromatin. Rad6/Bre1-mediated H2B ubiquitination is required for Lysine 4 Histone 3 and Lysine 79 Histone 3 methylation in both yeast and higher eukaryotes (Osley, 2006). H2Bub is required to reach the maximal gene expression level and is linked to transcript elongation. De-ubiquitination might be as important for transcript elongation. H2B de-ubiquitination, mediated by Ubp8 within SAGA, is necessary for the recruitment of the Ctk1 kinase, which phosphorylates Ser-2 of the CTD of RNA polymerase II. The phosphorylation provides a binding site for the H3K36 methyltransferase Set2, required for transcript elongation. H2Bub might act as a check point for RNA pol II pausing during early transcript elongation and might proceed with several rounds of H2B ubiquitination and

de-ubiquitination, allowing several pausing and checkpoints during elongation (Weake and Workman, 2008). [see paragraph 5]

While DNA methylation is mainly linked to gene silencing, histone methylation represents a mark for transcription activation (Kouzarides, 2002) (Table 2). H3K4me3, H3K36me3, and, to a lesser extent, H3K4me2, H3K9me3, and H3K36me2, mark active genes in euchromatin (Van Lijsebettens & Grasser, 2014). H3K4me3 around the transcription start-sites is highly correlated with gene activity (Figure 7). In plants, ASH1 HOMOLOG 2 (ASHH2)/SDG8 is the main HMT for H3K36me2/H3K36me3 and has an impact on flowering time, branching, reproductive organ development, and pathogen defense. SDG2/ATXR3 is the major responsible for H3K4me3 and is broadly expressed during development and acts on a high number of genes (Berr *et al.*, 2011). ATX1/SDG27 is also involved in H3K4me3 and impacts flowering time, root and leaf growth, ABA-dependent genes and ABA-independent genes under drought stress response and pathogens resistance. Activities of ATX1 and ATX2 seem to overlap in the flowering time control (Saleh *et al.*, 2008). SDG25/ATXR7 is also involved in flowering time control by activation of *FLC* and affects methylation of both H3K4 and H3K36. H3K4me2 and H3K36me3 are involved in pollen and stamen development through SDG4/ASHR3. The major methyltransferase for H3K36me2 and me3 is SDG8/ASHH2/EFS/CCR1, which activates *FLC* and *MAF* genes. SDG26/ASHH1 is also involved in flowering time control. *Arabidopsis* has 4 lysine-specific demethylase (LSD1) homologs: LDL1, LDL2, LDL3 and FLD. FLD, LDL1 and LDL2 affect H3K4 methylation levels at the *FLC* gene in *Arabidopsis*. Four of the 21 proteins containing the demethylation domain jumonji have been characterized in *Arabidopsis*. ELF6/JMJ11 and its homolog REF6/JMJ12 are involved in flowering time regulation and brassinosteroid regulated genes and demethylate H3K9me3. The demethylation activity of IBM1/JMJ25 protects active genes from heterochromatinization. JMJ15/MEE27 and JMJ14 demethylate H3K4 and JMJ14 is also involved in flowering time control independent of FLC.

Acetylation of core histones have been shown to positively affect gene transcription (Nelissen *et al.*, 2007). The new conformation facilitates the access of transcriptional regulatory proteins to the chromatin resulting in an increased transcriptional activity (Nelissen *et al.*, 2010). Acetylation of lysines at the promoter is associated with

transcription initiation (Figure 7). External stimuli such as light show the dynamics of histone acetylation-deacetylation. De-etiolation increases the levels of H3K9ac at the positive regulators of photomorphogenesis *HYH* and *HY5* as well as some downstream targets. In the dark, *PHYA* has high levels of H3K9/K14ac that are reduced when the plants are placed in light. Circadian clock regulators *CCA1, LHY* and *TOC1* show an enrichment of H3K4me3 and acetylation, corresponding to their mRNA oscillations (Hemmes *et al*., 2012). AtELP3/ELO3/HAG3 as part of the Elongator complex is reported to interact via MINIYO (IYO) with RNAPII to promote transcriptional elongation activity (Sanmartin *et al.,* 2011). ELO3-mediated H3K14ac has target genes in auxin response and pathogen defense. It colocalizes with euchromatin and active RNA pol II. Elongator is part of the GNAT family and is conserved from Archeae to Eukaryotes (Pandey *et al.,* 2002; Woloszynska *et al.,* 2016; Chapter 4). In yeast, its function is redundant to the one of Gcn5 (Kristjuhan *et al*., 2002). In human, C. elegans and drosophila Elongator has an acetylation activity in α-Tubulin (Creppe *et al*., 2009), this has not been studied in plants. Elongator was the first HAT shown to assist transcription elongation (Wittschieben *et al.,* 1999), it performs acetylation of H3K14 of gene bodies and surprisingly although it has remained highly conserved through evolution, it is not essential. The ELO3 subunit has many other activities such as in DNA methylation, tRNA modification and pri-miRNA processing (Woloszynska *et al*., 2016; Chapter 4). The ELO3/ELP3 contains a HAT and a SAM domain which is unusual as HAT domains are rather associated with PHD domains or Bromodomains (Glatt and Müller, 2013). While the ELP4/5/6 form a subcomplex with a hexameric ring-like structure similar as observed for the homo-hexameric members of the RecA-like NTPase family. This subcomplex was shown to specifically bind the anticodon loop of tRNA in the central cavity of its hexameric ring. ELP4/5/6 represents the first hetero-hexameric assembly of hexameric ATPases.

All histone proteins of the core in the nucleosome are phosphorylated at specific serine and threonine residues. The phosphorylated histones are correlated with transcriptional activation and often linked to acetylation of H3K9 and H3K14 (Turner, 2000).

5   Histone H2B monoubiquitination

Histone H2B is ubiquitinated at the C-terminal tail in most organisms. 1-5% of H2B are monoubiquitinated and this mark is associated with active transcription. It is performed in yeast by Bre1, in human by RNF20/RNF40 and in plants by HUB1/HUB2. H2Bub has been shown to associate with transcript elongation factors such as FACT which correlates with the position of the mark along the gene downstream of the promoter (Figure 7 and paragraph 3.1.3 and 3.4) In plants, it has key roles in major switches of the plant life cycles such as seed germination, initiation of flowering and circadian clock regulation. *hub1* and *hub2* mutants are characterized by very reduced fitness that shows the importance of this histone monoubiquitinase for plant transcription regulation in several key pathways.

5.1   Identification

The enzymes responsible for H2Bub were first identified in *S. cerevisiae* as the E2, Rad6 (Robzyk *et al.*, 2000), and the E3, Bre1 (Wood *et al.*, 2003a). In *Arabidopsis,* the RING-type E3 ligases, HUB1 and its homolog HUB2, were identified as functional orthologs of the human and yeast RNF20 and Bre1 proteins, respectively, that monoubiquitinate histone H2B (Fleury *et al.*, 2007, Liu *et al.*, 2007b; Figure 8). *HUB2* is 57% identical with *HUB1* at the nucleic acid level and 30% at the amino acid level. HUB1 and HUB2 share 13 and 12.5% identity and 31 and 29% similarity with yeast BRE1, respectively (Liu *et al.*, 2007b).   *HUB2* has the same number of exons as *HUB1*, and the protein contains the same two domains (Chromosome segregation ATPase domain and RING-finger). There is a lack of a strong additive effect in the double mutant of *hub1* and *hub2,* both show reduced level of H2Bub and similar defect in organ growth (Fleury *et al.,* 2007). H2Bub activity is shown for HUB1 in vitro (Fleury *et al.,* 2007) and in vivo for HUB1 and HUB2 (Liu *et al.,* 2007b).

 There are two functional E2 Rad6 homologs in *Arabidopsis*, UBC1 and UBC2 (Cao *et al.*, 2008, Xu *et al.,* 2009). For the ubiquitination, an E2 and an E3 ligase are necessary, while de-ubiquitination is performed by a de-ubiquitinase, which are also conserved (Table 3).
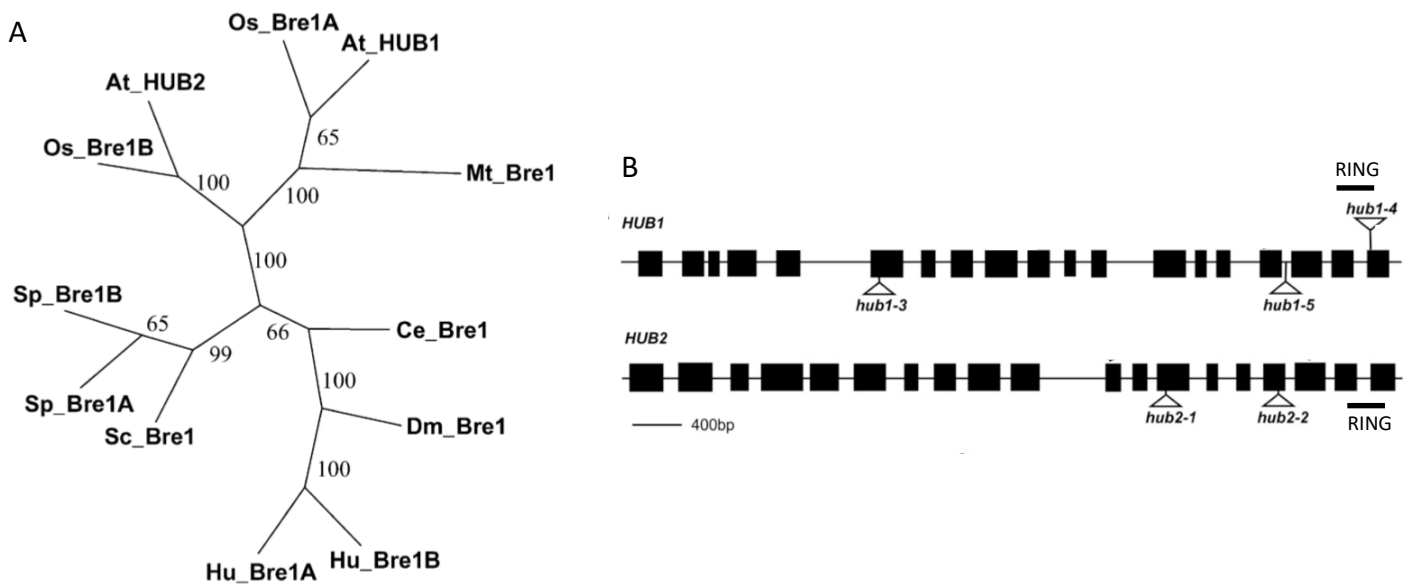
Figure 8: HUB1 and HUB2 are homologs (modified from Liu *et al.*, 2007b). A. Phylogenetic Tree of HUB1 Homologs. B. Schematic illustration of the gene structure of *HUB1* and *HUB2* with the positions of the T-DNA insertions and RING domains.

Table 3: Enzymes involved in H2B ubiquitination/de-ubiquitination in yeast, humans and *Arabidopsis* (modified from Cao and Ma, 2011).

	H2B ubiquitination		H2B de-ubiquitination
	E2	E3	
S. cerevisiae	Rad6	Bre1	Ubp8/Ubp10
S. pombe	Rhp6	Brl1, Brl2	
Human	hRad6A, hRad6B	RNF20/hBre1A, RNF40/hBre1B	Usp22
Arabidopsis	UBC1, UBC2	HUB1, HUB2	SUP32/UBP26

5.2   Mechanisms

In H2B monoubiquitination, a single ubiquitin is conjugated to a lysine (120 in human, 123 in *S. cerevisiae*, 119 in *S. pombe*, 143/146 in *Arabidopsis*) (Osley, 2006; Cao *et al.,* 2008). The essential 76 amino acid protein ubiquitin (Ub) is attached to the ε- amino acid group of a lysine (K) residue. This reaction called ubiquitination or ubiquitinylation or ubiquitylation is catalysed by a sequential action of Ub-activating (E1), Ub-conjugating (E2), and Ub-ligating (E3) enzymes (Figure 9). HUB1 and HUB2 function in a similar way as their human homologs, RNF20 and RNF40 (hBre1A and hBre1B). There are indications that these proteins function as a tetramer, with two copies of each polypeptide (Zhu *et al.,* 2005; Cao *et al.,* 2008). In such a complex, the absence of a single protein would destroy the tetramer and result in a similar phenotype as absence of both proteins.
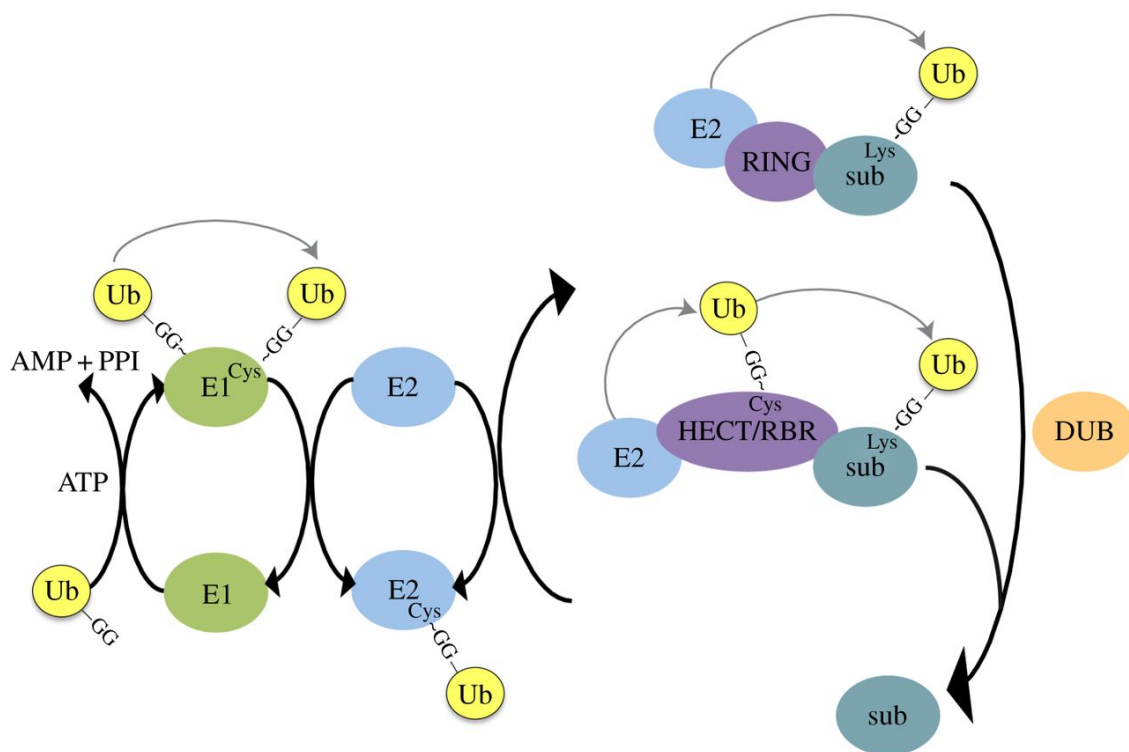
Figure 9: Illustration of the ubiquitination cascade (from Brown and Jackson, 2015). Ubiquitin is produced as a precursor polypeptide and cleaved to reveal a carboxyl-terminal GG- motif. In an ATP-dependent reaction, an E1 enzyme transforms this motif into a ubiquitin-adenylate intermediate, which reacts with a Cys in the catalytic domain of the E1 to form an E1~Ub, thioester linkage. At least for UBA1 (the best-characterized ubiquitin E1), a second ubiquitin molecule is adenylated and remains non-covalently linked to the E1 adenylation active site. Double loading of the E1 with ubiquitin is believed to potentiate transfer of ubiquitin from the E1 to the E2. The ubiquitin-charged E1 is recognized by an E2 conjugating enzyme and ubiquitin is transferred to the catalytic

cysteine of the E2 via a thioester linkage. Ubiquitin is subsequently conjugated to a substrate lysine, through E2 recognition of a substrate/E3 ligase complex. E1 and E3 binding sites to the E2 overlap, ensuring progression of the ubiquitination cascade. RING E3s facilitate transfer of ubiquitin from the E2 to substrate without binding ubiquitin directly. Alternatively, ubiquitin is transferred to an active site cysteine in HECT/RBR E3s before forming an isopeptide linkage with the substrate lysine. Multiple cycles of substrate binding to ubiquitin-charged E2s lead to ubiquitin chain formation. Ubiquitination can be reversed by de-ubiquitinating enzymes (DUBs).

Histone H2B monoubiquitination (H2Bub) is required for transmethylation of histone H3 and thereby plays a crucial role in the formation of transcriptionally active chromatin (Wood *et al.*, 2003b; Kim *et al.*, 2005a; Zhu *et al.*, 2005) (Figure 10). It is supposed that H2B monoubiquitination is part of a transcription-coupled, chromatin-based mechanism to rapidly modulate gene expression, for example in response to photomorphogenesis (Bourbousse *et al.*, 2012). H2Bub facilitates directly the processivity of RNA pol II through the nucleosomes during transcript elongation by affecting DNA accessibility to help recruit the histone chaperone FACT (FAcilitate Chromatin Transcription) (Pavri *et al.*, 2006). It interacts with the SPT16 of the FACT to regulate nucleosome dynamics, to reassemble nucleosomes and restore chromatin structure during elongation, therefore promoting accuracy of RNA pol II (Fleming *et al.*, 2008; Lolas *et al.*, 2010). In human, the RNF20/RNF40 E3 ligase complex catalyzes H2Bub formation and this activity requires WAC. WAC interacts through its C-terminal coiled-coil region with RNF20/40 and through the N-terminal WW domain with Pol II, thus directly linking H2B ubiquitination to the transcription machinery (Zhang and Yu, 2011).

H2Bub influences also indirectly transcription by regulating H3K4 methylation. In human and yeast, PAFc (Polymerase-associated factor 1 complex) serves as a platform during transcript elongation for H2Bub (Figure 10) (Cao and Ma, 2011), which induces the trimethylation on histone H3 K4 and K79 by COMPASS. In *Arabidopsis*, this mechanism is gene-dependent, only in a subset of genes the H3K4me3 is activated by H2Bub (Himanen *et al.*, 2012b; Schmitz *et al.*, 2009; Cao *et al.*, 2008; Gu *et al.*, 2009).
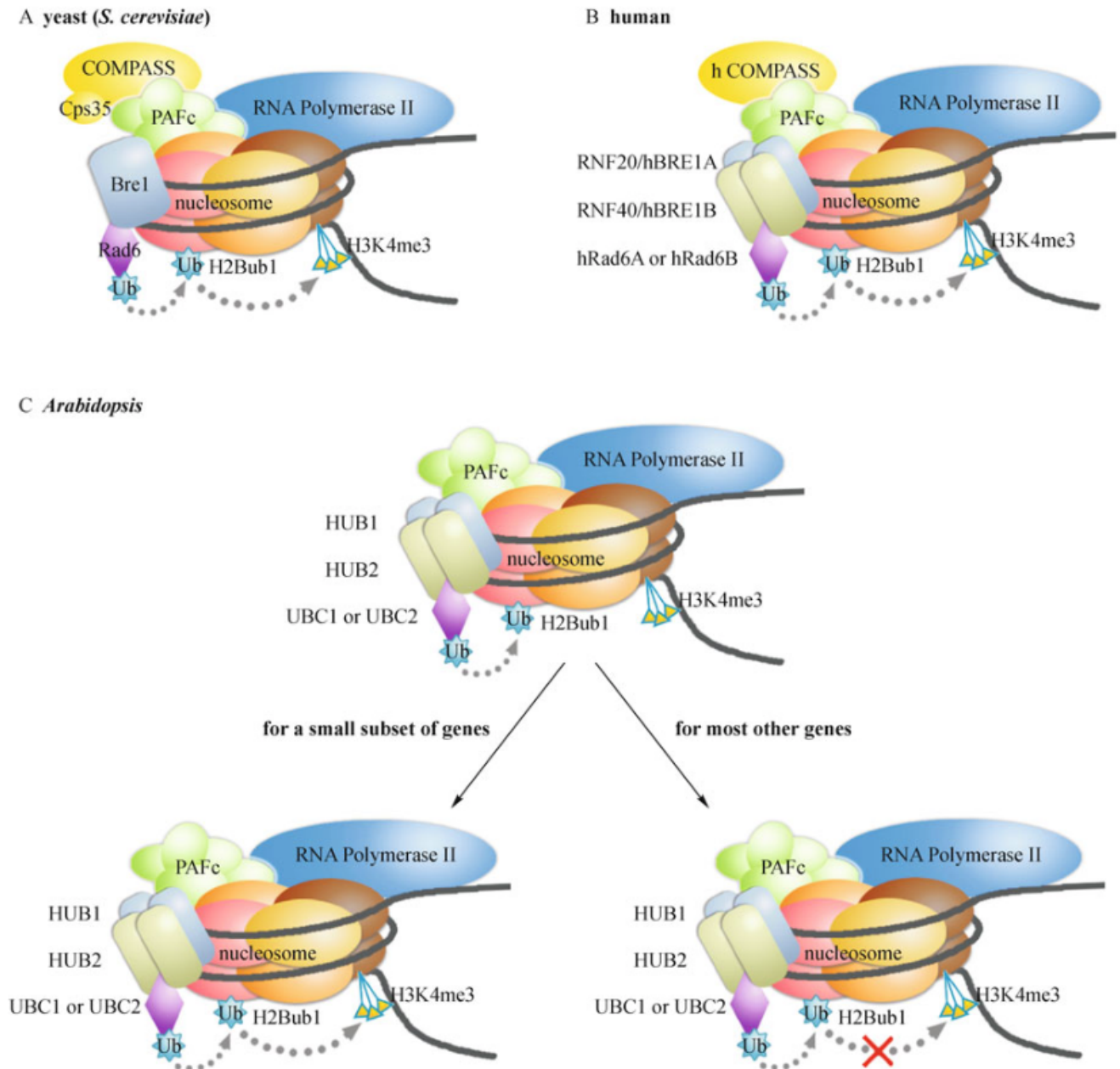
Figure 10: H2Bub1 regulates H3K4 methylation in yeast, humans, and Arabidopsis (from Cao and Ma, 2011). The production of H2Bub1 is conserved among yeast, humans, and Arabidopsis. Rad6-Bre1 and their homologs are responsible for H2B monoubiquitination; and the PAF complex is required for H2Bub1 formation. H2Bub1 activates gene expression by promoting H3K4 methylation in different organisms, but the dependency of H3K4 methylation on H2Bub1 is divergent. (A) Yeast H2Bub1 controls the binding of Cps35 (a subunit of the H3K4 methyltransferase COMPASS) to the target chromatin, which is essential for the catalytic activity of COMPASS; thus, H2B monoubiquitination is required for H3K4 methylation in yeast. (B) Human H2Bub1 is also necessary for H3K4 methylation, although the regulatory mechanism is unclear. (C) In Arabidopsis, H2B monoubiquitination is required for H3K4 tri-methylation for only a small subset of genes (e.g., *FLC*, *MAF4*, and *MAF5*).

Chromatin decompaction by H2Bub is created by features on the ubiquitin (Debelouchina *et al.,* 2017). A small acidic, negatively charged, patch comprised of Glu16 and Glu18, impacts the local and higher order of chromatin. Other surfaces of the ubiquitin like hydrophobic residues Ile44 and Phe45 have a supporting role. The decompaction mechanism is mediated by electrostatic interaction. Ubiquitins are also interacting with each other and proximities of other monoubiquitinated histones may act as a wedge to prevent the establishment of a closed interface between the nucleosomes. In this process, ubiquitin potentially utilizes its acidic patch as a 'hook' to form transient interactions with different basic residues such as lysine and arginine side chains from histone proteins or proximal ubiquitin moieties.

5.3 Role in plant development

In yeast, mutations in Bre1 generate an enlarged cell and in fruit flies, it causes defects in leg growth and wings. In plants, H2Bub is involved in a wide range of developmental processes such as the cell cycle during early organ growth, dormancy, and flowering time (Feng and Shen, 2014). Mutation in the *HUB1* gene disrupts cell division in vegetative meristems (Fleury *et al.,* 2007). *hub1-1* mutant has reduced leaf and root growth. These phenotypes correlate with downregulation of several cell cycle genes. Transcriptional programming by chromatin activation is an important part of the cell cycle regulation and HUB1 is one of the key factor of this regulation.

The *HUB1* and *HUB2* genes were also identified by seed dormancy phenotypes (Liu *et al.,* 2007b). *hub1-2* has a reduced dormancy phenotype, in addition to alterations in leaf colour, plant architecture, flower morphology and in seedling establishment. Histone H2B monoubiquitination plays an important role in the induction and/or maintenance of dormancy levels. In the *hub1-2* mutant, the expression of several dormancy-related genes, including *DOG1, ATS2, NCED9, PER1,* and *CYP707A2,* is reduced, demonstrating the involvement of chromatin modification in the seed dormancy mechanism.

In rice, HUB1/ HUB2 are involved in late anther development (Cao *et al.,* 2015). Mutations of OsHUB1 and OsHUB2 resulted in severe defects in anther development and pollen formation. Loss-of-function mutations of OsHUBs have altered stamen morphology with shorter anthers and abnormal wall layers and aborted pollen. Several genes involved in anther development have a reduced expression level in these mutants.

No anther defects were reported in Arabidopsis *hub1* and *hub2* mutants suggesting differences in the regulation of the male reproductive development in rice.

The early flowering of *hub* mutants correlates with downregulation of several flowering time regulatory genes such as *FKF1, FD, CDF3, CONSTANS, FLC, MAF3, MAF4* and *MAF5* (genes in italics) and reduced H2Bub in their coding regions (Cao *et al.*, 2008). In wild type, the H2Bub level in *FLC* is higher in the gene body than in the promoter region. The level of H3K4me3 and H2Bub is correlated for individual genes of the *FLC* clade. A defect in H2Bub significantly decreased the level of H3K4me3 and H3K36me2 in the chromatin of *FLC, MAF1, MAF4,* and *MAF5* and repressed the expression of those genes, suggesting that H2Bub is required for the enhancement of H3K4me3 and H3K36me2 and the increased expression of those genes. But after removal of H2Bub no changes in the expression or level of H3K4me3 or H3K36me2 in *MAF2* and *MAF3* were observed. There is uncoupling between H2Bub and H3 methylation in chromatin of some genes with high levels of H2Bub and H3K4me3. The transient and dynamic nature of H2Bub might be important for the regulation of transcription (Henry *et al.*, 2003). Both the monoubiquitination and de-ubiquitination of H2B are involved in transcriptional activation. The disruption of either process affects the transient dynamics of H2B ubiquitination, leading to alterations in the levels of H3K4me3 and H3K36me2. Accumulation of H2Bub1 at *FLC* chromatin affects H3K36 methylation but H3K4 methylation remains unchanged (Schmitz *et al.*, 2009). This is consistent with a model in which H3K4me3 occurs prior to H2B de-ubiquitination, whereas H3K36me3 occurs afterward.

5.4 Role in plant environmental response

H2Bub plays a role in transcription activation for a fast response of the plant to environmental stresses such as pathogen defense, changes in the cuticle and wax composition and photomorphogenesis. HUB1 is a regulatory component of plant defense against necrotrophic fungal pathogens (Dhawan *et al.*, 2009). Loss-of-function mutants of HUB1 have extreme susceptibility to *B. cinerea* and *A. brassicicola.* The *hub1* or *hub2* mutations lead to reduction of the cell wall thickness, increasing water permeability. Some genes of the cutin and wax biosynthesis pathway, *ATT1, LACS2, HTH* and *CER1* are direct targets of H2B monoubiquitination (Ménard *et al.*, 2014). HUB1

interacts specifically with the MED21 subunit of the middle module of Mediator, an evolutionarily conserved protein complex with a role in relaying signals from other regulators to RNA pol II that is like HUB1 transcriptionally induced by the elicitor chitin. Some necrotrophic pathogens produce toxins that can interfere with plant chromatin or the chromatin modification machinery as a virulence target to suppress expression of plant defense genes. The PAF complex is required for the function of HUB1 in the control of flowering time, whereas interaction of HUB1 with the Mediator complex is required for its disease resistance functions.

During photomorphogenesis, in response to light signals, plants undergo a rapid and extensive transcriptional reprogramming independent of cell division. In *Arabidopsis*, light perception induces a rapid redistribution of H2Bub and gene induction is associated with an H2Bub enrichment (Bourbousse *et al.*, 2012). H2Bub is not simultaneously removed when genes are down regulated, loss of H2Bub is mainly replication dependent. H3K4me3 induced by H2Bub create a temporally marking that allows the light-adapted expression response. Approximately 10% of the light-induced genes were affected by H2Bub, many of them encoding for regulatory components rather than being structural elements of the photosynthetic machinery.

HUB1 has also a function in regulation of circadian clock genes. The *hub1* mutant shows altered amplitudes of diurnal expression of clock genes that correlates with reduced H2Bubat the circadian clock oscillator, *CCA1*, and its downstream light-related genes (*ARR4, GIGANTEA, APRR5, FLC, ELF4* and *LHY*) (Himanen *et al.,* 2012b). Like other chromatin remodellers, HUB1/2 is involved in a wide range of biological processes and by its role in transcriptional control contributes to general plant fitness (Himanen *et al.,* 2012a).

6   RNA binding proteins, an overview

RNA-binding proteins (RBPs) are a heterogeneous class of proteins found in every organism. Most RBPs recognize specific cis-active motifs in mRNA and regulate the fate and processing of mRNA. As trans-acting regulatory factors, RBPs are essential for the post-transcriptional regulation in eukaryotes. In plants, knowledge of these proteins comes from targeted studies of specific RBPs or bioinformatics predictions based on

sequence homology with canonical domains found across the kingdoms of life (Silverman *et al.*, 2013). More than 300 RBPs were found in *Arabidopsis* (TAIR 10), which is similar to other plant species. However, these numbers are quite predictive as only a few have been functionally characterized in plants with roles in flowering time (FCA, FPA), hormonal responses (SR proteins and ABA response), pathogen defense (GRP7, FPA), circadian timekeeping (GRP7, GRP8), and abiotic stress responses (atRZ-1a, CSP3) (Köster *et al.*, 2017). Plant RBP mutants can suffer from severe phenotypes or lethality and several proteins have a demonstrated role in pre-mRNA processing including alternative splicing (SR45, PTB1, 2 and 3, RSZ33, GRP7, NSR), 3'-end formation (FPA, HLP1), pri-microRNA processing (TOUGH, GRP7, RS40, RS41, HOS5, HYL5, SE), and mRNA export (MOS11, UAP56).

Recent studies with new mRNA interactome capture methods using *in vivo* crosslinking with UV are providing experimental evidence for the RNA binding abilities of many candidate RBPs predicted *in silico* as well as identifying novel RBPs and domains (Köster *et al.*, 2017). These methods have been developed first in yeast and mammals (Castello *et al.*, 2012) and to date, only a few interactome studies have been reported on plants using UV crosslinking and oligo(dT) affinity capture using *Arabidopsis* leaves and cell cultures (Marondedze *et al.*, 2016), *Arabidopsis* etiolated seedlings (Reichel *et al.*, 2016) and *Arabidopsis* leaf mesophyll protoplasts (Zhang *et al.*, 2016). These three studies have identified 1816 potential RBPs and provide evidence for the RNA association of many predicted RBPs with canonical RNA binding domains with, for example, 157 of the 197 predicted RRM proteins. Strikingly, a large number of RBPs were identified without RNA binding domains. In addition, there is very little overlap between these studies with only 79 proteins detected in all three. A possible explanation might be by the different tissues in different physiological states underlying these studies, suggesting that these interactomes show only a snapshot of the RBPs linked to RNA at a given time and in a specific tissue, with only strong interactions detected.

The individual nucleotide resolution crosslinking and immunoprecipitation (iCLIP) was recently adapted with success for plants and tested with AtGRP7-GFP to identify genome-wide targets (Meyer *et al.*, 2017). The technique relies on UV-induced covalent bonds between RBPs and their target RNAs, followed by immunoprecipitation, which

provides information about the site of interaction. The study shows that exposure to the UV-C for crosslinking in seedling reaches the interior of leaves but not the meristems but that the timeframe did not enhance the UV stress response marker. Comparison with RIP-seq which uses formaldehyde crosslinking, shows complementary results with a 53% overlap. Overall iCLIP is a suitable method for identification of *in vivo* targets of plant RBPs and their binding landscape at a genome-wide scale.

6.1 Types of RNA binding domains

The most abundant domains are the RNA recognition motif (RRM), pentatricopeptide repeat (PPR) and the K homology (KH) motif (Table 4). Other domains include Cold Shock domain, dsRNA-binding domains, several types of zinc finger domains (the most abundant being C-x8-X-x5-X-x3-H), DEAD/DEAH box, Pumilio and PIWI/Argonaute/Zwille. These domains may be present in an RBP in single copies, multiple copies or associated with other functional domains.

Table 4: The total number of putative RNA-binding proteins containing each specified RNA-binding domain in four different eukaryotes (from Silverman *et al.*, 2013).

Domain	*Arabidopsis*	Rice	Maize	Human
RRM	197 (601)	22/180 (95/570)	285 (447)	597 (1012)
KH	28 (69)	3/26 (13/70)	53 (78)	113 (183)
CSD	5 (4)	2/3 (1/7)	4 (10)	18 (33)
DS-RBD	5 (30)	0/22 (0/42)	6 (19)	50 (114)
ZnF (C-x8-C-x5-C-x3-H)	5 (97)	0/40 (14/150)	60 (106)	64 (179)
DEAD/DEAH box	9 (150)	3/65 (81/211)	94 (70)	200 (409)
PPR	450	1/477	303	8
RGG box	56	17/170	86	152
PUF	25 (25)	0/15 (0/40)	22 (16)	8 (23)

PAZ	6 (20)	4/25 (37/48)	3 (6)	12 (27)
LSM	36 (75)	7/22 (9/52)	36 (55)	35 (64)

Numbers are provided from various annotation databases as described below, as well as (in parentheses) from the InterPro database, using the following domains: RNA recognition motif domain (IPR000504), K homology domain (IPR004087), Cold shock protein (IPR011129), Double-stranded RNA binding (IPR001159), Zinc finger, CCCH-type (IPR000571), DNA/RNA helicase, DEAD/DEAH box type, N-terminal (IPR011545), Pumilio RNA-binding repeat (IPR001313), Argonaute/Dicer protein, PAZ (IPR003100), Like-Sm (LSM) domain (IPR010920). *Arabidopsis:* Proteins from TAIR10 ('functional annotations' table) with the specified domain and RNA-binding function. Rice: Proteins from RGAP7 ('locus info' and 'Pfam' tables) with the specified domain. The numbers of proteins that are found in the RiceRBP database by blastp search with an e-value cutoff of 1e-50 are also given (e.g. 22/180 means 22 of the 180 RRM domain-containing proteins are found in RiceRBP). Maize: Proteins from Phytozome v8.0 ('annotation info' table) with the specified domain. Human: Proteins from Pfam (Homo sapiens proteome file) with the specified domain.

6.2 Roles in RNA biology

RBPs play a major role in post-transcriptional control of mRNA (splicing, polyadenylation, mRNA stabilization, mRNA localization and translation). The potential number of active RBPs in plants may be high and approach the complexity seen in mammals (>1000 RBP, Silverman *et al.*, 2013). As the RNA emerges from the RNA polymerase it is immediately bound by/to RBPs. They regulate seemingly every aspect of RNA metabolism and function including RNA biogenesis, maturation, transport, cellular localization and stability. Therefore, they are supposedly as diverse as their targets, whether being mRNA or non-coding RNA (lncRNA, miRNA, siRNA, scRNA). Characterized RBPs have roles in flowering time (FPA and FCA) (Schomburg *et al.*, 2001; Liu *et al.*, 2007a), hormonal responses (Cruz *et al.*, 2014), pathogen defense (Woloshen *et al.*, 2011), circadian timekeeping (Schmal *et al.*, 2013), and abiotic stress responses (Kim *et al.*, 2005b; Kim *et al.*, 2009).

In plants, regulation of transcript level, stability and translation are essential mechanisms for a fast reprogramming of their transcriptome and proteome in response to hormonal cues and environmental stresses like temperature, light or salt stresses. RNA binding proteins are essential participants in these post-transcriptional changes in response to internal or external conditions and signals and their expression and/or

activity is regulated accordingly (Lorkovic, 2009). Many of these stresses activate a chaperone function of RBPs and help regulate the stability and translation of the bound RNA. For example, UAB proteins target mRNA stability and translation after ABA-induced phosphorylation that is necessary for these RNA binding kinases to bind their target mRNA. An RNA chaperone, the Cold Shock Protein B (cspB) from *Bacillus subtilus*, has been overexpressed in maize to enhance drought stress tolerance, in the so-called Droughtgard® technology from Monsanto. Indeed, cspB helps to maintain normal physiological performance during mild drought stress by binding and unfolding tangled RNA molecules so that they can function normally (Castiglioni et al., 2008; Adee *et al.*, 2016). Thus, basic research on RBPs can result in interesting biotechnological applications.

RBPs have also a key role in plant defense such as a range of RRM containing RBPs are modified by ADP-ribosylation during infection by the HopU1 effector protein of *Pseudomonas syringae* (Jeong *et al.*, 2011). The modification reduces the binding abilities of the RRM proteins and plants become susceptible to the pathogen.

Other RBPs serve as regulators involved in major developmental transitions such as flowering (Lorkovic, 2009). Both RRM domain RBPs, FCA and FPA promote flowering by inhibiting FLOWERING LOCUS C (FLC) expression. FCA negatively regulates its own expression through a mechanism that involves alternative splicing and polyadenylation. FCA and FPA promote the use of proximal polyadenylation and 3′ processing sites, and in their absence, general intergenic transcription increases (Sonmez *et al.*, 2011). The autonomous pathway of flowering involves other RBPs such as HEN4, a KH domain protein that regulates AGAMOUS pre-mRNA, PEP, also a KH domain protein involved in vegetative and reproductive development, or FLK, a KH domain protein antagonist of PEP in FLC regulation.

6.3 RRM domain

The most frequent RNA-binding domain is the 80 amino acid long RNA Recognition Motif (RRM), which forms a well-conserved structure of four antiparallel β-strands and two α-helices (Maris *et al.*, 2005). In *Arabidopsis*, this domain is found in 197 proteins according to TAIR10 and 601 according to InterPro. 50% do not have obvious homologs in metazoan (Lorković and Barta, 2002). RRM-containing RNA binding proteins can be

divided into several groups according to their structure (Figure 10).
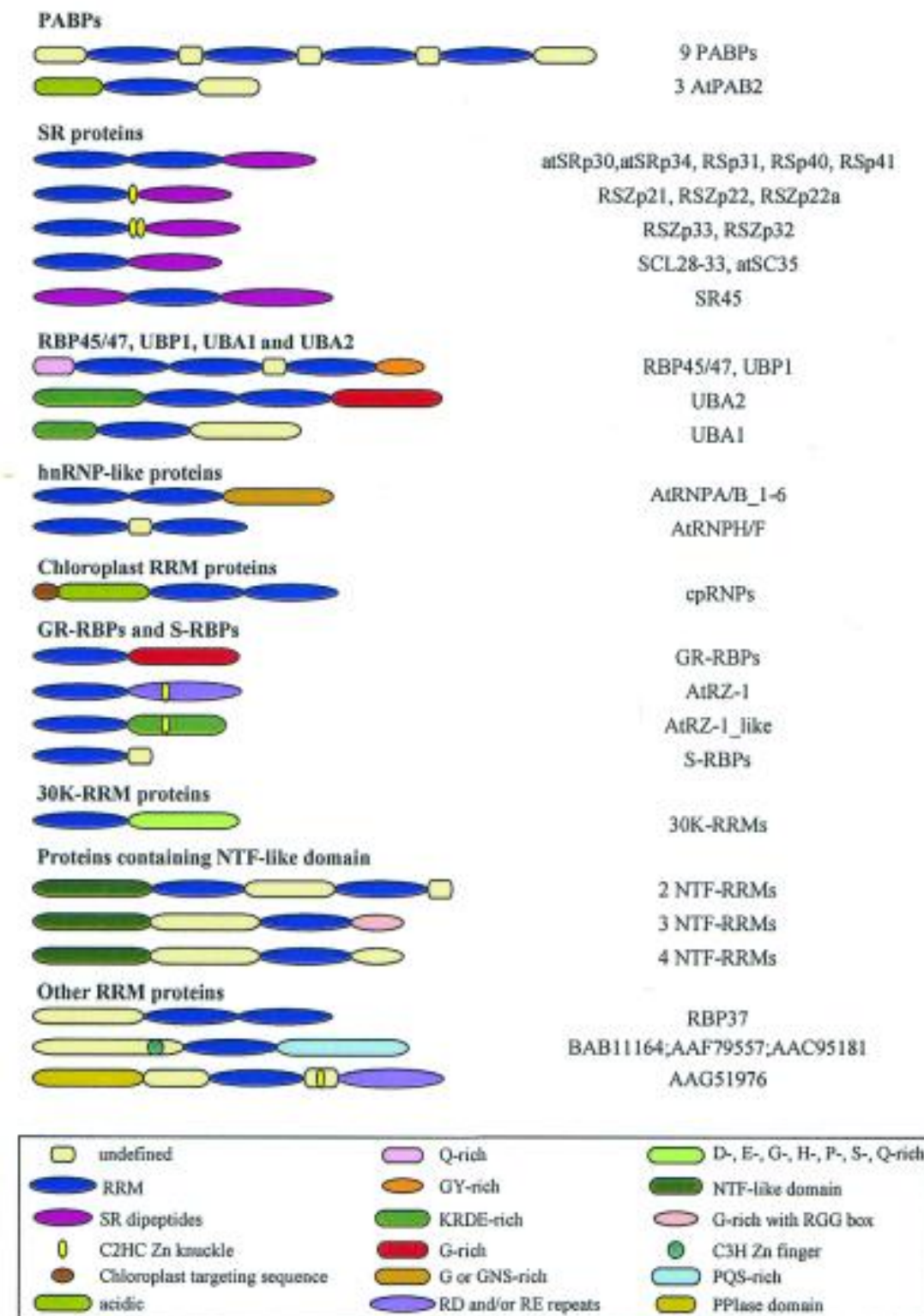
Figure 11: **Schematic representation of the modular structure of Arabidopsis RRM-containing proteins** (from Lorković and Barta, 2002). Only major types of domain combinations are shown. Individual modules are identified by different shapes

and colours. Different types of domains (RNA-binding, auxiliary domains and other distinctive regions of proteins) are listed at the bottom.

One group of RRM proteins is poly(A) binding (PABP, Figure 11). This interaction between mRNA and RBP is essential for polyadenylation, control of the poly(A) tail length, translation initiation and degradation of the mRNA. Another group of RRM proteins is SR proteins, which are essential splicing factors (Figure 11). They consist of one or two N-terminal RRM and a C-terminal domain, rich in SR (Ser/Arg) dipeptides. In this group are also found other spliceosome associated proteins and finally CstF-64 (cleavage factor stimulation factor of 64kDa, a protein involved in polyadenylation), nucleolin, S19 ribosomal protein and translation initiation factor 3 (TIF3). The group of UBP1, RBP45 and RBP47 consists of structurally related proteins of three RRMs and a glutamine-rich N-terminus (Figure 11). They are involved in splicing efficiency. Metazoan hnRNP A/B proteins are composed of two adjacent N-terminal positioned RRMs and a glycine-rich C-terminal auxiliary domain (Figure 11). hnRNP A/B are involved in alternative splicing by promoting usage of a distal 5'spliced site. In Arabidopsis, there are 6 of these proteins and only two possess the glycine-rich C-terminal domain, the other four have a domain equally enriched in glycine, asparagine and serine. In the chloroplast of higher plants, there is a group of nuclei encoded RRM RBPs (Figure 11). They possess an acidic domain at the N-termini and two consecutive RRM domain at the C-termini. They are involved in chloroplast RNA editing and mRNA 3'end formation. The group of glycine-rich and small RRM-containing proteins consist in *Arabidopsis* of 27 members divided into two sub categories, all possessing a N-terminal RRM domain (Figure 11). They are a homogenous group of eight glycine-rich RNA binding proteins, implicated in responses to environmental stresses and rRNA processing and some are regulated by the circadian clock; and a heterogeneous group of fifteen small RRM- containing protein grouped by their low molecular weight. The 30K-RRM proteins are a homogenous group of eight proteins with one RRM domain and a molecular weight of ~ 30kDa (Figure 11). The C-terminal extension of these proteins is rich in proline, glutamine, histidine, glycine, serine and acidic amino acids and could be used for protein-protein interactions. In *Arabidopsis,* there are nine RRM proteins containing an NTF-like domain (Figure 11). The NTF-like domain is involved in nuclear

protein import/export. Three have an N-terminal NTF domain followed by one RRM and an RGG box at the C-termini. Furthermore, there are 69 RRM proteins in *Arabidopsis* that do not belong to any of these groups (Figure 11).

Some of these RBPs belong to the Split ends (Spen) family of large proteins characterized by N-terminal RNA recognition motifs (RRMs) and a conserved SPOC (Spen paralog and ortholog C-terminal) domain. The SPOC domain is believed to mediate protein-protein interaction and has diverse functions among the family. They have been identified as RNA binding proteins that regulate alternative 3'-end cleavage and polyadenylation (Sanchez-Pulido *et al.*, 2004; Arieti *et al.*, 2014).

6.4   KH domain

Another frequently occurring RNA binding domain is the K Homology domain (KH). In metazoan, KH proteins have been implicated in transcription, mRNA stability, translational silencing and mRNA localization (Valverde *et al.,* 2008). In *Arabidopsis*, this domain is found in 28 proteins according to TAIR10 and 69 according to InterPro. They contain 1 to 5 KH domains. KH domains are found unaccompanied in proteins containing 3 or more KH, while proteins containing one or two KH frequently combine up to eight different domains.

KH domains are known to bind ssRNA and ssDNA with more affinity for ssRNA. One domain recognizes 4 nucleic acid bases and the clustering of the motives in a protein serves to increase specificity. As seen for other RNA binding domains, combinatorial binding of multiple KH domains within the same protein is often key to high affinity and high specificity interaction with the RNA target. In proteins where the structures of both nucleic acid-KH complex and free KH have been uncovered, the binding produces little to no changes in the protein conformation. For example, in the AU-rich element RNA-binding protein KSRP (K-homology splicing regulator protein), that contain 4 KH domains, KH domains 3 and 4 behave as independent binding modules to interact with different regions of the AU-rich RNA targets and promotes the degradation of specific mRNAs that encode proteins with functions in cellular proliferation and inflammatory response (Garcia-Mayoral *et al.*, 2007). KHDRBS1 (KH domain containing, RNA binding, signal transduction associated 1) also called Sam68 is a human KH protein with two KH domain member of the Signal Transduction and Activation of RNA (STAR) family and

responsible for forming an inducible bridge between the pre-mRNA and the splicing machinery (Batsché *et al.*, 2006).

7   References

Adee, E., Roozeboom, K., Balboa, G.R., Schlegel, A., Ciampitti, I.A., 2016. Drought-Tolerant Corn Hybrids Yield More in Drought-Stressed Environments with No Penalty in Non-stressed Environments. Frontiers in Plant Science 7. https://doi.org/10.3389/fpls.2016.01534

Allen, B.L., Taatjes, D.J., 2015. The Mediator complex: a central integrator of transcription. Nature Reviews Molecular Cell Biology 16, 155–166. https://doi.org/10.1038/nrm3951

Andrews, A.J., Luger, K., 2011. Nucleosome Structure(s) and Stability: Variations on a Theme. Annual Review of Biophysics 40, 99–117. https://doi.org/10.1146/annurev-biophys-042910-155329

Arieti, F., Gabus, C., Tambalo, M., Huet, T., Round, A., Thore, S., 2014. The crystal structure of the Split End protein SHARP adds a new layer of complexity to proteins containing RNA recognition motifs. Nucleic Acids Research 42, 6742–6752. https://doi.org/10.1093/nar/gku277

Ausio, J., 2006. Histone variants--the structure behind the function. Briefings in Functional Genomics and Proteomics 5, 228–243. https://doi.org/10.1093/bfgp/ell020

Batsché, E., Yaniv, M., Muchardt, C., 2006. The human SWI/SNF subunit Brm is a regulator of alternative splicing. Nature structural and molecular biology 13, 22–29. https://doi.org/10.1038/nsmb1030

Bedford, M.T., Richard, S., 2005. Arginine Methylation. Molecular Cell 18, 263–272. https://doi.org/10.1016/j.molcel.2005.04.003

Bentley, D.L., 2014. Coupling mRNA processing with transcription in time and space. Nature Reviews Genetics 15, 163–175. https://doi.org/10.1038/nrg3662

Berr, A., Shafiq, S., Shen, W.-H., 2011. Histone modifications in transcriptional activation during plant development. Biochimica et Biophysica Acta (BBA) - Gene Regulatory Mechanisms 1809, 567–576. https://doi.org/10.1016/j.bbagrm.2011.07.001

Bourbousse, C., Ahmed, I., Roudier, F., Zabulon, G., Blondet, E., Balzergue, S., Colot, V., Bowler, C., Barneche, F., 2012. Histone H2B Monoubiquitination Facilitates the Rapid Modulation of Gene Expression during Arabidopsis Photomorphogenesis. PLoS Genetics 8, e1002825. https://doi.org/10.1371/journal.pgen.1002825

Brown, J.S., Jackson, S.P., 2015. Ubiquitylation, neddylation and the DNA damage response. Open Biology 5, 150018–150018. https://doi.org/10.1098/rsob.150018

Brownell, J.E., Zhou, J., Ranalli, T., Kobayashi, R., Edmondson, D.G., Roth, S.Y., Allis, C.D., 1996. Tetrahymena histone acetyltransferase A: a homolog to yeast Gcn5p linking histone acetylation to gene activation. Cell 84, 843–851. https://doi.org/10.1016/S0092-8674(00)81063-6

Cao, H., Li, X., Wang, Z., Ding, M., Sun, Y., Dong, F., Chen, F., Liu, L., Doughty, J., Li, Y., Liu, Y.-X., 2015. Histone H2B Monoubiquitination Mediated by HISTONE MONOUBIQUITINATION1 and HISTONE MONOUBIQUITINATION2 Is Involved in Anther Development by Regulating

Tapetum Degradation-Related Genes in Rice. Plant Physiology 168, 1389–1405. https://doi.org/10.1104/pp.114.256578

Cao, J., Yan, Q., 2012. Histone Ubiquitination and Deubiquitination in Transcription, DNA Damage Response, and Cancer. Frontiers in Oncology 2. https://doi.org/10.3389/fonc.2012.00026

Cao, Y., Dai, Y., Cui, S., Ma, L., 2008. Histone H2B Monoubiquitination in the Chromatin of FLOWERING LOCUS C Regulates Flowering Time in Arabidopsis. THE PLANT CELL ONLINE 20, 2586–2602. https://doi.org/10.1105/tpc.108.062760

Cao, Y., Ma, L., 2011. Conservation and divergence of the histone H2B monoubiquitination pathway from yeast to humans and plants. Frontiers in Biology 6, 109–117. https://doi.org/10.1007/s11515-011-1000-6

Carrozza, M.J., Li, B., Florens, L., Suganuma, T., Swanson, S.K., Lee, K.K., Shia, W.-J., Anderson, S., Yates, J., Washburn, M.P., Workman, J.L., 2005. Histone H3 Methylation by Set2 Directs Deacetylation of Coding Regions by Rpd3S to Suppress Spurious Intragenic Transcription. Cell 123, 581–592. https://doi.org/10.1016/j.cell.2005.10.023

Castello, A., Fischer, B., Eichelbaum, K., Horos, R., Beckmann, B.M., Strein, C., Davey, N.E., Humphreys, D.T., Preiss, T., Steinmetz, L.M., Krijgsveld, J., Hentze, M.W., 2012. Insights into RNA Biology from an Atlas of Mammalian mRNA-Binding Proteins. Cell 149, 1393–1406. https://doi.org/10.1016/j.cell.2012.04.031

Castiglioni, P., Warner, D., Bensen, R.J., Anstrom, D.C., Harrison, J., Stoecker, M., Abad, M., Kumar, G., Salvador, S., D'Ordine, R., Navarro, S., Back, S., Fernandes, M., Targolli, J., Dasgupta, S., Bonin, C., Luethy, M.H., Heard, J.E., 2008. Bacterial RNA Chaperones Confer Abiotic Stress Tolerance in Plants and Improved Grain Yield in Maize under Water-Limited Conditions. PLANT PHYSIOLOGY 147, 446–455. https://doi.org/10.1104/pp.108.118828

Cheung, A.C.M., Cramer, P., 2012. A Movie of RNA Polymerase II Transcription. Cell 149, 1431–1437. https://doi.org/10.1016/j.cell.2012.06.006

Conaway, R.C., Brower, C.S., Conaway, J.W., 2002. Emerging roles of ubiquitin in transcription regulation. Science 296, 1254–1258. https://doi.org/10.1126/science.1067466

Creppe, C., Malinouskaya, L., Volvert, M.-L., Gillard, M., Close, P., Malaise, O., Laguesse, S., Cornez, I., Rahmouni, S., Ormenese, S., Belachew, S., Malgrange, B., Chapelle, J.-P., Siebenlist, U., Moonen, G., Chariot, A., Nguyen, L., 2009. Elongator Controls the Migration and Differentiation of Cortical Neurons through Acetylation of α-Tubulin. Cell 136, 551–564. https://doi.org/10.1016/j.cell.2008.11.043

Cruz, T., Carvalho, R., Richardson, D., Duque, P., 2014. Abscisic Acid (ABA) Regulation of Arabidopsis SR Protein Gene Expression. International Journal of Molecular Sciences 15, 17541–17564. https://doi.org/10.3390/ijms151017541

Debelouchina, G.T., Gerecht, K., Muir, T.W., 2016. Ubiquitin utilizes an acidic surface patch to alter chromatin structure. Nature Chemical Biology 13, 105–110. https://doi.org/10.1038/nchembio.2235

Denu, J.M., 2003. Linking chromatin function with metabolic networks: Sir2 family of NAD 1 - dependent deacetylases. TRENDS in Biochemical Sciences 28, 41–48. https://doi.org/10.1016/S0968-0004(02)00005-1

Dhawan, R., Luo, H., Foerster, A.M., AbuQamar, S., Du, H.-N., Briggs, S.D., Scheid, O.M., Mengiste, T., 2009. HISTONE MONOUBIQUITINATION1 Interacts with a Subunit of the Mediator Complex and Regulates Defense against Necrotrophic Fungal Pathogens in Arabidopsis. THE PLANT CELL ONLINE 21, 1000–1019. https://doi.org/10.1105/tpc.108.062364

Feng, J., Shen, W.-H., 2014. Dynamic regulation and function of histone monoubiquitination in plants. Frontiers in Plant Science 5. https://doi.org/10.3389/fpls.2014.00083

Fleming, A.B., Kao, C.-F., Hillyer, C., Pikaart, M., Osley, M.A., 2008. H2B Ubiquitylation Plays a Role in Nucleosome Dynamics during Transcription Elongation. Molecular Cell 31, 57–66. https://doi.org/10.1016/j.molcel.2008.04.025

Fleury, D., Himanen, K., Cnops, G., Nelissen, H., Boccardi, T.M., Maere, S., Beemster, G.T.S., Neyt, P., Anami, S., Robles, P., Micol, J.L., Inze, D., Van Lijsebettens, M., 2007. The Arabidopsis thaliana Homolog of Yeast BRE1 Has a Function in Cell Cycle Regulation during Early Leaf and Root Growth. THE PLANT CELL ONLINE 19, 417–432. https://doi.org/10.1105/tpc.106.041319

Forsberg, C.E., Bresnick, E.H., 2001. Histone acetylation beyond promoters: long-range acetylation patterns in the chromatin world. Bioessays 23, 820–830. https://doi.org/10.1002/bies.1117/pdf

Fukuda, H., Sano, N., Muto, S., Horikoshi, M., 2006. Simple histone acetylation plays a complex role in the regulation of gene expression. Briefings in Functional Genomics and Proteomics 5, 190–208. https://doi.org/10.1093/bfgp/ell032

García-Mayoral, M.F., Hollingworth, D., Masino, L., Díaz-Moreno, I., Kelly, G., Gherzi, R., Chou, C.-F., Chen, C.-Y., Ramos, A., 2007. The Structure of the C-Terminal KH Domains of KSRP Reveals a Noncanonical Motif Important for mRNA Degradation. Structure 15, 485–498. https://doi.org/10.1016/j.str.2007.03.006

Gezer, U., Holdenrieder, S., 2014. Post-translational histone modifications in circulating nucleosomes as new biomarkers in colorectal cancer. in vivo 28, 287–292.

Glatt, S., Müller, C.W., 2013. Structural insights into Elongator function. Current Opinion in Structural Biology 23, 235–242. https://doi.org/10.1016/j.sbi.2013.02.009

Glozak, M.A., Sengupta, N., Zhang, X., Seto, E., 2005. Acetylation and deacetylation of non-histone proteins. Gene 363, 15–23. https://doi.org/10.1016/j.gene.2005.09.010

Govind, C.K., Zhang, F., Qiu, H., Hofmeyer, K., Hinnebusch, A.G., 2007. Gcn5 Promotes Acetylation, Eviction, and Methylation of Nucleosomes in Transcribed Coding Regions. Molecular Cell 25, 31–42. https://doi.org/10.1016/j.molcel.2006.11.020

Gu, X., Jiang, D., Wang, Y., Bachmair, A., He, Y., 2009. Repression of the floral transition via histone H2B monoubiquitination. The Plant Journal 57, 522–533. https://doi.org/10.1111/j.1365-313X.2008.03709.x

Hebbes, T.R., Clayton, A.L., Thorne, A.W., Crane-Robinson, C., 1994. Core histone hyperacetylation co-maps with generalized DNase I sensitivity in the chicken beta-globin chromosomal domain. The EMBO journal 13, 1823. https://doi.org/PMC395022

Hemmes, H., Henriques, R., Jang, I.-C., Kim, S., Chua, N.-H., 2012. Circadian Clock Regulates Dynamic Chromatin Modifications Associated with Arabidopsis CCA1/LHY and TOC1 Transcriptional Rhythms. Plant and Cell Physiology 53, 2016–2029. https://doi.org/10.1093/pcp/pcs148

Henry, K.W., 2003. Transcriptional activation via sequential histone H2B ubiquitylation and deubiquitylation, mediated by SAGA-associated Ubp8. Genes & Development 17, 2648–2663. https://doi.org/10.1101/gad.1144003

Himanen, K., Boccardi, T.M., De Rycke, R., Odeny, O.P., Van Lijsebettens, M., 2012a. Is HUB1 a hub for plant fitness? Plant Signaling & Behavior 7, 1537–1540. https://doi.org/10.4161/psb.22326

Himanen, K., Woloszynska, M., Boccardi, T.M., De Groeve, S., Nelissen, H., Bruno, L., Vuylsteke, M., Van Lijsebettens, M., 2012b. Histone H2B monoubiquitination is required to reach maximal transcript levels of circadian clock genes in Arabidopsis: *HUB1 regulates transcript levels*. The Plant Journal 72, 249–260. https://doi.org/10.1111/j.1365-313X.2012.05071.x

Houben, A., Demidov, D., Caperta, A.D., Karimi, R., Agueci, F., Vlasenko, L., 2007. Phosphorylation of histone H3 in plants—A dynamic affair. Biochimica et Biophysica Acta (BBA) - Gene Structure and Expression 1769, 308–315. https://doi.org/10.1016/j.bbaexp.2007.01.002

Jonkers, I., Lis, J.T., 2015. Getting up to speed with transcription elongation by RNA polymerase II. Nature Reviews Molecular Cell Biology 16, 167–177. https://doi.org/10.1038/nrm3953

Kim, J., Hake, S.B., Roeder, R.G., 2005. The Human Homolog of Yeast BRE1 Functions as a Transcriptional Coactivator through Direct Activator Interactions. Molecular Cell 20, 759–770. https://doi.org/10.1016/j.molcel.2005.11.012

Kim, M.-H., Sasaki, K., Imai, R., 2009. Cold Shock Domain Protein 3 Regulates Freezing Tolerance in Arabidopsis thaliana. Journal of Biological Chemistry 284, 23454–23460. https://doi.org/10.1074/jbc.M109.025791

Kim, Y.-O., Kim, J.S., Kang, H., 2005. Cold-inducible zinc finger-containing glycine-rich RNA-binding protein contributes to the enhancement of freezing tolerance in Arabidopsis thaliana: Function of an RNA-binding protein. The Plant Journal 42, 890–900. https://doi.org/10.1111/j.1365-313X.2005.02420.x

Kornberg, R.D., Lorch, Y., 1999. Twenty-five years of the nucleosome, fundamental particle of the eukaryote chromosome. Cell 98, 285–294. https://doi.org/10.1016/S0092-8674(00)81958-3

Köster, T., Marondedze, C., Meyer, K., Staiger, D., 2017. RNA-Binding Proteins Revisited – The Emerging Arabidopsis mRNA Interactome. Trends in Plant Science. https://doi.org/10.1016/j.tplants.2017.03.009

Kouskouti, A., Talianidis, I., 2005. Histone modifications defining active genes persist after transcriptional and mitotic inactivation. The EMBO journal 24, 347–357. https://doi.org/10.1038/sj.emboj.7600516

Kouzarides, T., 2002. Histone methylation in transcriptional control. Current opinion in genetics & development 12, 198–209. https://doi.org/10.1016/S0959-437X(02)00287-3

Kristjuhan, A., Walker, J., Suka, N., Grunstein, M., Roberts, D., Cairns, B.R., Svejstrup, J.Q., 2002. Transcriptional inhibition of genes with severe histone h3 hypoacetylation in the coding region. Molecular cell 10, 925–933. https://doi.org/10.1016/S1097-2765(02)00647-0

Kwak, H., Lis, J.T., 2013. Control of Transcriptional Elongation. Annual Review of Genetics 47, 483–508. https://doi.org/10.1146/annurev-genet-110711-155440

Li, X., Manley, J.L., 2006. Cotranscriptional processes and their influence on genome stability. Genes & Development 20, 1838–1847. https://doi.org/10.1101/gad.1438306

Liu, F., Quesada, V., Crevillén, P., Bäurle, I., Swiezewski, S., Dean, C., 2007. The Arabidopsis RNA-Binding Protein FCA Requires a Lysine-Specific Demethylase 1 Homolog to Downregulate FLC. Molecular Cell 28, 398–407. https://doi.org/10.1016/j.molcel.2007.10.018

Liu, Y., Koornneef, M., Soppe, W.J.J., 2007. The Absence of Histone H2B Monoubiquitination in the Arabidopsis hub1 (rdo4) Mutant Reveals a Role for Chromatin Remodeling in Seed Dormancy. THE PLANT CELL ONLINE 19, 433–444. https://doi.org/10.1105/tpc.106.049221

Lolas, I.B., Himanen, K., Grønlund, J.T., Lynggaard, C., Houben, A., Melzer, M., Van Lijsebettens, M., Grasser, K.D., 2010. The transcript elongation factor FACT affects Arabidopsis vegetative and reproductive development and genetically interacts with HUB1/2. The Plant Journal 61, 686–697. https://doi.org/10.1111/j.1365-313X.2009.04096.x

Lorković, Z.J., 2009. Role of plant RNA-binding proteins in development, stress response and genome organization. Trends in Plant Science 14, 229–236. https://doi.org/10.1016/j.tplants.2009.01.007

Lorkovic, Z.J., Barta, A., 2002. Genome analysis: RNA recognition motif (RRM) and K homology (KH) domain RNA-binding proteins from the flowering plant Arabidopsis thaliana. Nucleic Acids Research 20, 623–635. https://doi.org/10.1093/nar/30.3.623

Luco, R.F., Allo, M., Schor, I.E., Kornblihtt, A.R., Misteli, T., 2011. Epigenetics in Alternative Pre-mRNA Splicing. Cell 144, 16–26. https://doi.org/10.1016/j.cell.2010.11.056

Luse, D.S., 2013. Promoter clearance by RNA polymerase II. Biochimica et Biophysica Acta (BBA) - Gene Regulatory Mechanisms 1829, 63–68. https://doi.org/10.1016/j.bbagrm.2012.08.010

Maris, C., Dominguez, C., Allain, F.H.-T., 2005. The RNA recognition motif, a plastic RNA-binding platform to regulate post-transcriptional gene expression: The RRM domain, a plastic RNA-binding platform. FEBS Journal 272, 2118–2131. https://doi.org/10.1111/j.1742-4658.2005.04653.x

Marmorstein, R., Zhou, M.-M., 2014. Writers and Readers of Histone Acetylation: Structure, Mechanism, and Inhibition. Cold Spring Harbor Perspectives in Biology 6, a018762–a018762. https://doi.org/10.1101/cshperspect.a018762

Marondedze, C., Thomas, L., Serrano, N.L., Lilley, K.S., Gehring, C., 2016. The RNA-binding protein repertoire of Arabidopsis thaliana. Scientific Reports 6. https://doi.org/10.1038/srep29766

Max, T., Søgaard, M., Svejstrup, J.Q., 2007. Hyperphosphorylation of the C-terminal Repeat Domain of RNA Polymerase II Facilitates Dissociation of Its Complex with Mediator. Journal of Biological Chemistry 282, 14113–14120. https://doi.org/10.1074/jbc.M701345200

Ménard, R., Verdier, G., Ors, M., Erhardt, M., Beisson, F., Shen, W.-H., 2014. Histone H2B Monoubiquitination is Involved in the Regulation of Cutin and Wax Composition in Arabidopsis thaliana. Plant and Cell Physiology 55, 455–466. https://doi.org/10.1093/pcp/pct182

Meyer, K., Köster, T., Nolte, C., Weinholdt, C., Lewinski, M., Grosse, I., Staiger, D., 2017. Adaptation of iCLIP to plants determines the binding landscape of the clock-regulated RNA-binding protein AtGRP7. Genome Biology 18. https://doi.org/10.1186/s13059-017-1332-x

Millevoi, S., Loulergue, C., Dettwiler, S., Karaa, S.Z., Keller, W., Antoniou, M., Vagner, S., 2006. An interaction between U2AF 65 and CF I m links the splicing and 3′ end processing machineries. The EMBO journal 25, 4854–4864. https://doi.org/10.1038/sj.emboj.7601331

Nelissen, H., Boccardi, T.M., Himanen, K., Van Lijsebettens, M., 2007. Impact of Core Histone Modifications on Transcriptional Regulation and Plant Growth. Critical Reviews in Plant Sciences 26, 243–263. https://doi.org/10.1080/07352680701612820

Nelissen, H., De Groeve, S., Fleury, D., Neyt, P., Bruno, L., Bitonti, M.B., Vandenbussche, F., Van Der Straeten, D., Yamaguchi, T., Tsukaya, H., Witters, E., De Jaeger, G., Houben, A., Van Lijsebettens, M., 2010. Plant Elongator regulates auxin-related genes during RNA polymerase II transcription elongation. Proceedings of the National Academy of Sciences 107, 1678–1683. https://doi.org/10.1073/pnas.0913559107

Osley, M.A., 2006. Regulation of histone H2A and H2B ubiquitylation. Briefings in Functional Genomics and Proteomics 5, 179–189. https://doi.org/10.1093/bfgp/ell022

Pandey, R., Muller, A., Napoli, C.A., Selinger, D.A., Pikaard, C.S., Richards, E.J., Bender, J., Mount, D.W., Jorgensen, R.A., 2002. Analysis of histone acetyltransferase and histone deacetylase families of Arabidopsis thaliana suggests functional diversification of chromatin modification among multicellular eukaryotes. Nucleic acids research 30, 5036–5055. https://doi.org/10.1093/nar/gkf660

Pavri, R., Zhu, B., Li, G., Trojer, P., Mandal, S., Shilatifard, A., Reinberg, D., 2006. Histone H2B Monoubiquitination Functions Cooperatively with FACT to Regulate Elongation by RNA Polymerase II. Cell 125, 703–717. https://doi.org/10.1016/j.cell.2006.04.029

Pikaard, C.S., Mittelsten Scheid, O., 2014. Epigenetic Regulation in Plants. Cold Spring Harbor Perspectives in Biology 6, a019315–a019315. https://doi.org/10.1101/cshperspect.a019315

Quina, A.S., Buschbeck, M., Di Croce, L., 2006. Chromatin structure and epigenetics. Biochemical Pharmacology 72, 1563–1569. https://doi.org/10.1016/j.bcp.2006.06.016

Reichel, M., Liao, Y., Rettel, M., Ragan, C., Evers, M., Alleaume, A.-M., Horos, R., Hentze, M.W., Preiss, T., Millar, A.A., 2016. In Planta Determination of the mRNA-Binding Proteome of Arabidopsis Etiolated Seedlings. The Plant Cell 28, 2435–2452. https://doi.org/10.1105/tpc.16.00562

Robzyk, K., Recht, J., Osley, M.A., 2000. Rad6-Dependent Ubiquitination of Histone H2B in Yeast. Science 287, 501–504. https://doi.org/10.1126/science.287.5452.501

Saleh, A., Alvarez-Venegas, R., Yilmaz, M., Le, O., Hou, G., Sadder, M., Al-Abdallat, A., Xia, Y., Lu, G., Ladunga, I., Avramova, Z., 2008. The Highly Similar Arabidopsis Homologs of Trithorax ATX1 and ATX2 Encode Proteins with Divergent Biochemical Functions. THE PLANT CELL ONLINE 20, 568–579. https://doi.org/10.1105/tpc.107.056614

Sánchez-Pulido, L., Rojas, A.M., Van Wely, K.H., Martinez-A, C., Valencia, A., 2004. SPOC: a widely distributed domain associated with cancer, apoptosis and transcription. BMC bioinformatics 5, 91. https://doi.org/10.1186/1471-2105-5-91

Sanmartín, M., Sauer, M., Muñoz, A., Zouhar, J., Ordóñez, A., van de Ven, W.T.G., Caro, E., de la Paz Sánchez, M., Raikhel, N.V., Gutiérrez, C., Sánchez-Serrano, J.J., Rojo, E., 2011. A Molecular Switch for Initiating Cell Differentiation in Arabidopsis. Current Biology 21, 999–1008. https://doi.org/10.1016/j.cub.2011.04.041

Schmal, C., Reimann, P., Staiger, D., 2013. A Circadian Clock-Regulated Toggle Switch Explains AtGRP7 and AtGRP8 Oscillations in Arabidopsis thaliana. PLoS Computational Biology 9, e1002986. https://doi.org/10.1371/journal.pcbi.1002986

Schmitz, R.J., Tamada, Y., Doyle, M.R., Zhang, X., Amasino, R.M., 2009. Histone H2B Deubiquitination Is Required for Transcriptional Activation of FLOWERING LOCUS C and for Proper Control of Flowering in Arabidopsis. PLANT PHYSIOLOGY 149, 1196–1204. https://doi.org/10.1104/pp.108.131508

Schomburg, F.M., Patton, D.A., Meinke, D.W., Amasino, R.M., 2001. FPA, a gene involved in floral induction in Arabidopsis, encodes a protein containing RNA-recognition motifs. The Plant Cell 13, 1427–1436. https://doi.org/10.1105/TPC.010017

Shogren-Knaak, M., Ishii, H., Sun, J.-M., Pazin, M.J., Davie, J.R., Peterson, C.L., 2006. Histone H4-K16 Acetylation Controls Chromatin Structure and Protein Interactions. Science 311, 844–847. https://doi.org/10.1126/science.1124000

Shukla, A., Stanojevic, N., Duan, Z., Shadle, T., Bhaumik, S.R., 2006. Functional Analysis of H2B-Lys-123 Ubiquitination in Regulation of H3-Lys-4 Methylation and Recruitment of RNA Polymerase II at the Coding Sequences of Several Active Genes *in Vivo*. Journal of Biological Chemistry 281, 19045–19054. https://doi.org/10.1074/jbc.M513533200

Silverman, I.M., Li, F., Gregory, B.D., 2013. Genomic era analyses of RNA secondary structure and RNA-binding proteins reveal their significance to post-transcriptional regulation in plants. Plant Science 205–206, 55–62. https://doi.org/10.1016/j.plantsci.2013.01.009

Sonmez, C., Baurle, I., Magusin, A., Dreos, R., Laubinger, S., Weigel, D., Dean, C., 2011. RNA 3' processing functions of Arabidopsis FCA and FPA limit intergenic transcription. Proceedings of the National Academy of Sciences 108, 8508–8513. https://doi.org/10.1073/pnas.1105334108

Strahl, B.D., Allis, C.D., 2000. The language of covalent histone modifications. Nature 403, 41. https://doi.org/10.1038/47412

Thomas, M.C., Chiang, C.-M., 2006. The General Transcription Machinery and General Cofactors. Critical Reviews in Biochemistry and Molecular Biology 41, 105–178. https://doi.org/10.1080/10409230600648736

Tian, B., Manley, J.L., 2016. Alternative polyadenylation of mRNA precursors. Nature Reviews Molecular Cell Biology 18, 18–30. https://doi.org/10.1038/nrm.2016.116

Tse, C., Sera, T., Wolffe, A.P., Hansen, J.C., 1998. Disruption of higher-order folding by core histone acetylation dramatically enhances transcription of nucleosomal arrays by RNA polymerase III. Molecular and cellular biology 18, 4629–4638. https://doi.org/10.1128/MCB.18.8.4629

Turner, B.M., 2000. Histone acetylation and an epigenetic code. Bioessays 22, 836–845.
Valverde, R., Edwards, L., Regan, L., 2008. Structure and function of KH domains: Structure and function of KH domains. FEBS Journal 275, 2712–2726. https://doi.org/10.1111/j.1742-4658.2008.06411.x

Van Lijsebettens, M., Grasser, K.D., 2014. Transcript elongation factors: shaping transcriptomes after transcript initiation. Trends in Plant Science 19, 717–726. https://doi.org/10.1016/j.tplants.2014.07.002

Vettese-Dadey, M., Grant, P.A., Hebbes, T.R., Crane-Robinson, C., Allis, C.D., Workman, J.L., 1996. Acetylation of histone H4 plays a primary role in enhancing transcription factor binding to nucleosomal DNA in vitro. The EMBO journal 15, 2508. https://doi.org/10.1002/j.1460-2075.1996.tb00608.x

Vogelauer, M., Wu, J., Suka, N., Grunstein, M., 2000. Global histone acetylation and deacetylation in yeast. Nature 408, 495–498. https://doi.org/10.1038/35044127

Weake, V.M., Workman, J.L., 2008. Histone Ubiquitination: Triggering Gene Activity. Molecular Cell 29, 653–663. https://doi.org/10.1016/j.molcel.2008.02.014

Wittschieben, B.Ø., Otero, G., de Bizemont, T., Fellows, J., Erdjument-Bromage, H., Ohba, R., Li, Y., Allis, C.D., Tempst, P., Svejstrup, J.Q., 1999. A novel histone acetyltransferase is an integral subunit of elongating RNA polymerase II holoenzyme. Molecular cell 4, 123–128.

Woloshen, V., Huang, S., Li, X., 2011. RNA-Binding Proteins in Plant Immunity. Journal of Pathogens 2011, 1–11. https://doi.org/10.4061/2011/278697

Woloszynska, M., Le Gall, S., Van Lijsebettens, M., 2016. Plant Elongator-mediated transcriptional control in a chromatin and epigenetic context. Biochimica et Biophysica Acta (BBA) - Gene Regulatory Mechanisms 1859, 1025–1033. https://doi.org/10.1016/j.bbagrm.2016.06.008

Wood, A., Krogan, N.J., Dover, J., Schneider, J., Heidt, J., Boateng, M.A., Dean, K., Golshani, A., Zhang, Y., Greenblatt, J.F., others, 2003a. Bre1, an E3 ubiquitin ligase required for recruitment and substrate selection of Rad6 at a promoter. Molecular cell 11, 267–274. https://doi.org/10.1016/S1097-2765(02)00802-X

Wood, A., Schneider, J., Dover, J., Johnston, M., Shilatifard, A., 2003b. The Paf1 Complex Is Essential for Histone Monoubiquitination by the Rad6-Bre1 Complex, Which Signals for Histone Methylation by COMPASS and Dot1p. Journal of Biological Chemistry 278, 34739–34742. https://doi.org/10.1074/jbc.C300269200

Xu, L., Ménard, R., Berr, A., Fuchs, J., Cognat, V., Meyer, D., Shen, W.-H., 2009. The E2 ubiquitin-conjugating enzymes, AtUBC1 and AtUBC2, play redundant roles and are involved in activation of *FLC* expression and repression of flowering in *Arabidopsis thaliana*. The Plant Journal 57, 279–288. https://doi.org/10.1111/j.1365-313X.2008.03684.x

Zhang, F., Yu, X., 2011. WAC, a Functional Partner of RNF20/40, Regulates Histone H2B Ubiquitination and Gene Transcription. Molecular Cell 41, 384–397. https://doi.org/10.1016/j.molcel.2011.01.024

Zhang, Z., Boonen, K., Ferrari, P., Schoofs, L., Janssens, E., van Noort, V., Rolland, F., Geuten, K., 2016. UV crosslinked mRNA-binding proteins captured from leaf mesophyll protoplasts. Plant Methods 12. https://doi.org/10.1186/s13007-016-0142-6

Zhou, M., Law, J.A., 2015. RNA Pol IV and V in gene silencing: Rebel polymerases evolving away from Pol II's rules. Current Opinion in Plant Biology 27, 154–164. https://doi.org/10.1016/j.pbi.2015.07.005

Zhu, B., Zheng, Y., Pham, A.-D., Mandal, S.S., Erdjument-Bromage, H., Tempst, P., Reinberg, D., 2005. Monoubiquitination of Human Histone H2B: The Factors Involved and Their Roles in HOX Gene Regulation. Molecular Cell 20, 601–611. https://doi.org/10.1016/j.molcel.2005.09.025

Chapter 2 RNA binding proteins link H2B monoubiquitination with m-RNA processing through interaction with the HUB1 and HUB2 E3 ubiquitin ligases

Magdalena Woloszynska[a,b,1,2], Sabine Le Gall[a,b,1], Pia Neyt[a,b], Tommaso M. Boccardi[a,b],

Marion Grasser[c], Stijn Aesaert[a,b], Stijn Dhondt[a,b], Leonardo Bruno[d], Jorge Fung[e], Paloma

Mas[e], Marc Van Montagu[a,b], Dirk Inzé[a,b], Geert De Jaeger[a,b], Klaus Grasser[c], Kristiina

Himanen[a,b,3], and Mieke Van Lijsebettens[a,b,3]

[a]Department of Plant Biotechnology and Bioinformatics, Gent University, 9052 Ghent, Belgium; [b]Center for Plant Systems Biology, VIB, 9052 Gent, Belgium; [c]Cell Biology and Plant Biochemistry Group, Institute of Plant Sciences, University of Regensburg, 93053 Regensburg, Germany; [d]Dipartimento di Biologia, Ecologia e Scienze della Terra, Università della Calabria, 87036 Arcavacata di Rende, Italy; [e]Center for Research in AgriGenomics (CRAG), Consortium Consejo Superior de Investigaciones Científicas-Instituto Recerca i Tecnologia Agroalimentaries-Universidad Autonoma de Barcelona-Universidad de Barcelona (CSIC-IRTA-UAB-UB), 08193 Barcelona, Spain

[1] These authors contributed equally to this work.

[2] Present address: Department of Genetics, Faculty of Biology and Animal Sciences, Wroclaw University of Environmental and Life Sciences, ul. Kozuchowska 7, 51-631 Wroclaw, Poland.
[3] Present address: Department of Agricultural Sciences, University of Helsinki, 00790 Helsinki, and Department of Biosciences, Viikki Plant Science Centre (ViPS), 00014 University of Helsinki, Finland

Author contribution

This chapter was adapted from the manuscript in preparation for PNAS.

S.L.G. made the recombinant protein cloning, purification and EMSA, crosses and partially the genotyping of the luciferase reporter lines, phenotyping for flowering time and root, CCA1 alternative splicing analysis, COOLAIR analysis and helped with leaf phenotyping, RNAseq and ChIP. SLG participated in the writing of the manuscript.

1 Abstract

In *Arabidopsis*, HISTONE MONOUBIQUITINATION1 (HUB1) and its ortholog, HUB2, act in heterotetramers in modulating developmental programs, such as flowering time, dormancy, and circadian clock. HUB1 interacting proteins, KHD and SPEN, were identified by means of Tandem Affinity Purification, that showed RNA binding activity in an electrophoretic mobility shift assay. The knock-down *khd-1*, knock-out *spen-1* and knock-out *hub* mutants all had reduced rosette and leaf area; in *hub1-4* leaf number was also reduced which coincided with early flowering; strikingly, in *spen-1*, flowering was slightly but significantly delayed. The *khd* and *spen* mutants had respectively a large and small set of differentially expressed genes in common with *hub1*, interestingly, *spen* mutants had also a large set of specific differentially-expressed genes, suggesting shared and specific functions between KHD, SPEN and HUB1. HUB1-mediated histone H2B monoubiquitination (H2Bub) is important in the regulation of the *CCA1* and *FLC* genes, regulating the clock and flowering time, respectively, and was analysed in *spen* and *khd* mutants. In *spen* mutants, a defective clock period was measured by luciferase reporter activity, that correlated with reduced α and β forms of CCA1, and reduced H2Bub, suggesting a role for SPEN in spliceosome activity and a link between splicing and HUB1 activity in histone monoubiquitination. In *spen* mutants, H2Bub at *FLC* was normal, its increased expression correlated with an increased distal versus proximal ratio of its long non-coding antisense *COOLAIR*, indicating a role for SPEN in *COOLAIR* splicing and a link to non-coding RNA activity.

2 Introduction

In eukaryotic cells, the genomic DNA is organized in nucleosomes that consist of 146 bp DNA wrapped around an octamer of "core" histone dimers of H2A, H2B, H3 and H4 (Luger *et al.*, 1997); linker DNA and histone H1 connect adjacent nucleosomes. The chromatin structure is highly dynamic, with nucleosomal histone tail modifications such as methylation, acetylation and ubiquitination determining the availability of the DNA to RNA polymerase II (RNAPII) transcription; a major chromatin state for active genes in *Arabidopsis* is determined by histone H2B monoubiquitination (H2Bub), histone H3 acetylation and methylation (Roudier *et al.*, 2011). H2Bub is absent from the *Arabidopsis* promoter regions, peaks at the gene bodies and is required to reach maximal gene

expression levels, indicating that this histone modification is specifically linked with transcript elongation (Bourbousse *et al.*, 2012; Himanen *et al.*, 2012; Feng and Shen, 2014; Van Lijsebettens and Grasser, 2014). In *Arabidopsis*, the conserved E3 ubiquitin ligase, HUB1, and its homolog, HUB2, function in H2Bub together with E1 activating and E2 conjugating enzymes during transcriptional activation of numerous genes and pathways (Fleury *et al.*, 2007; Liu et al., 2007; Cao *et al.*, 2008; Xu et *al.*, 2009; Bourbousse *et al.*, 2012; Himanen *et al.*, 2012). The steady state between H2B monoubiquitination and de-ubiquitylation by ubiquitin proteases (UBPs) determines the deposition of other activating marks to histones at transcript elongation and is required for proper gene activation. Indeed, the *Arabidopsis sup32/ubp26* de-ubiquitination mutants had reduced expression of the floral repressor *FLC* and flowered early as a consequence of H2Bub accumulation, depletion in the activating H3K36me3 and increase in the repressive H3K27me3 mark (Schmitz *et al.*, 2009).

Proteins interacting with the H2Bub machinery might represent regulators of H2Bub dynamics, transcript elongation efficiency, specificity of target genes, a link to pre-mRNA processing or upstream signalling. We identified the KHD and SPEN proteins in tandem affinity purification using HUB1 and HUB2 as baits, with in vitro RNA binding activity and affecting splicing at the CCA1 gene and the FLC-derived long non-coding antisense RNA, COOLAIR. We hypothesize that SPEN function in splicing is linked to HUB1/HUB2-mediated H2Bub and non-coding RNA activity.

3   Results and Discussion

3.1   SPEN and KHD identified as core components of the HUB1/HUB2 complex

To identify HUB1 associated proteins that may represent upstream regulators, cofactors or components of the core complex, we performed several Tandem Affinity Purifications (TAP) using Arabidopsis cell cultures overexpressing tagged full length and modified HUB1 and HUB2 proteins. Using HUB1 as bait, HUB2 and the RNA-binding proteins SPEN and KHD were purified in several TAPs (Table 1, Table S1). Reverse TAP with either HUB2 or SPEN as bait purified respectively HUB1, KHD and SPEN, or HUB1, HUB2 and KHD proteins. Hence, the SPEN and KHD proteins are part of a larger protein complex

including the HUB1/ HUB2 dimer. HUB2 has been implicated as a non-redundant component in the H2B monoubiquitination reaction and we could confirm it as interacting with HUB1. However, when point mutations were introduced to the RING domain of HUB1 (HUB1pm), no HUB2, SPEN and KHD interactions could be detected, suggesting that the RING domain could be essential for the heterodimerization and formation of the complex with other interactors. Some other interactors that were detected only one time using the original TAP tag might represent transient or weak interactors with HUB1 (Table S2). Several ubiquitin related proteins, transcription factors, RNA binding proteins, RNA helicases, and nucleolar proteins were detected with low protein score. Amongst these, Spt16, a component of the FACT complex that genetically interacts with HUB1 (Lolas et al., 2010). The ubiquitin related proteins (Ulp1 protase family proteins, Ubiquitin-specific protease-related, U-box domain containing protein), that are likely to act in HUB1 mediated ubiquitination and or degradation processes were interacting only with the full length HUB1 suggesting functional interaction with the RING domain. The HUB1pm interacted with putative DEAD-box helicases and non-repetitive/WGA-negative nucleoporin family protein.

Pairwise yeast two-hybrid system (Y2H) confirmed strong HUB1/HUB1 and HUB1/HUB2 but not HUB2/HUB2 interactions as already reported by Cao *et al.*, 2008. The interaction of HUB1 with SPEN was very strong (Fig. S1 *A* and *B*) and required both N- and C-termini of SPEN (Fig. S1 *A, C,* and *D*) although the interaction of HUB1 with the N-terminus of SPEN was stronger (Fig. S1 *A, C,* and *D*). The full length SPEN and both N and C fragments of SPEN also showed weak dimerization activity (Fig. S1 *B-D*). No direct interaction was seen between SPEN and HUB2, or between KHD and HUB1, HUB2 or SPEN. Therefore, one or more additional proteins might mediate the interaction of KHD with HUB1, HUB2 and SPEN. In conclusion, two RNA domain proteins, SPEN and KHD, were identified by TAP as integral part of the HUB1/HUB2 core complex and for SPEN a strong and direct interaction with HUB1 was confirmed by Y2H.

GFP-SPEN and GFP-KHD fusion constructs were transiently expressed upon infiltration of *Nicotiana benthamina* leaves with agrobacteria, and stably expressed in *Arabidopsis* lines obtained by floral dip. The GFP-SPEN fluorescence was exclusively located in the nucleus, excluding nucleolus, in leaf (Fig. 1A) or primary root (Fig. 1*B*) epidermis cells.

GFP-KHD fluorescence was located in the nucleus, excluding nucleolus, in leaf (Fig. 1 *C*) and root (Fig. 1 *D*) epidermis, in cytoplasm around the nucleus and near the plasmalemma, which was comparable to the GFP-HUB1 and GFP-HUB2 localization (Liu *et al.*, 2007).

Table 1: Copurified proteins identified by MS in TAP eluates of *Arabidopsis* cell cultures using HUB1, HUB2, SPEN and HUB1pm (with mutated RING domain) as a bait

Bait	Tag	TAP	TAPs with identified protein			
			HUB1	HUB2	KHD	SPEN
			At2G44950	At1G55250	At1G51580	At1G27750
HUB1	N-TAP	2	2	2	2	2
HUB1	N-GS	4	4	4	3	2
HUB1pm	N-TAP	3	3	0	0	0
HUB2	N-GS	2	2	2	2	2
SPEN	C-GS	4	2	2	3	4
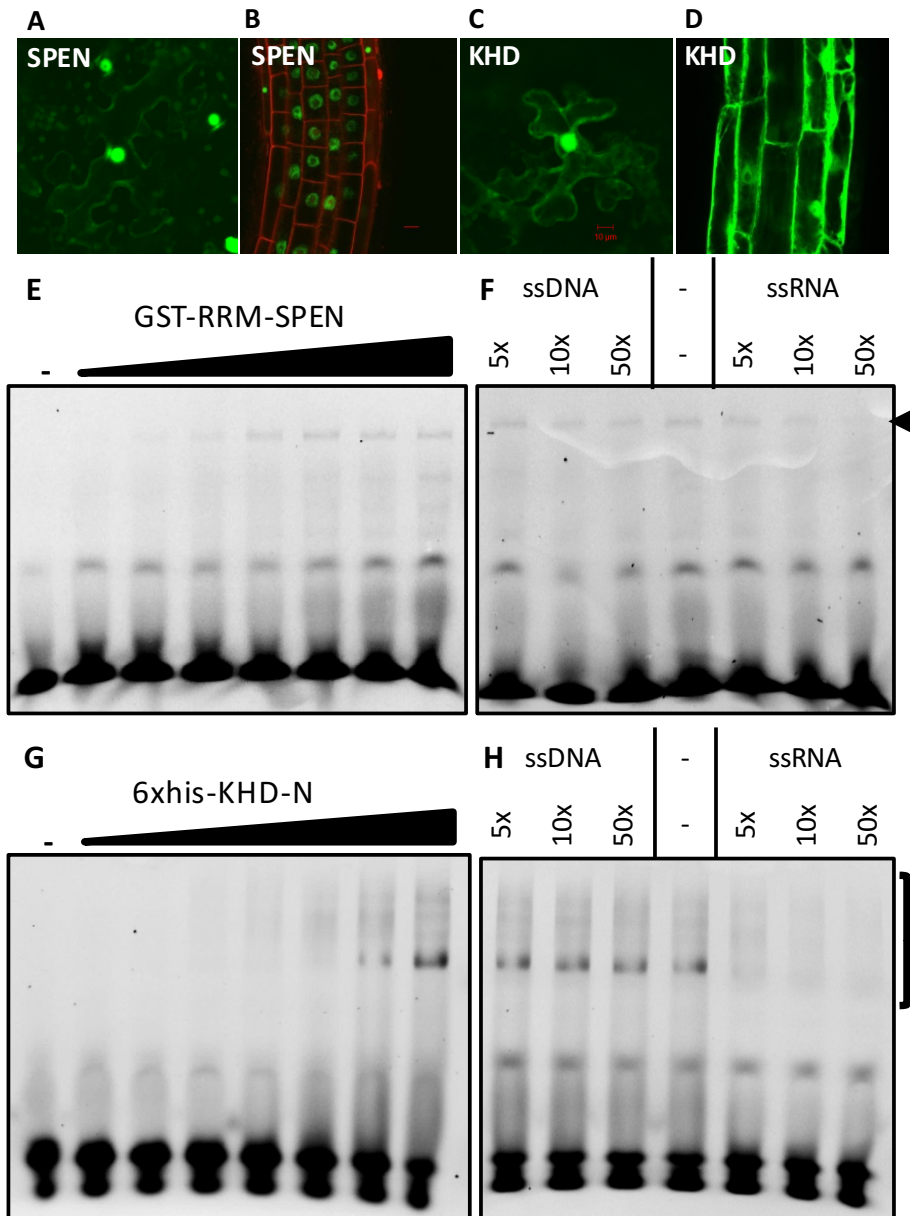
Figure 1: SPEN and KHD localization and RNA-DNA binding.
(*A-D*). 35S::GFP::SPEN and 35S::GFP::KHD detection in infiltration of (A-C) *N. benthamiana* leaves and transformant (*B* and *D*) *A. thaliana* roots. Scale bars = 10 μm. (*E-H*). Comparison of binding affinity of GST-RRM-SPEN (*E*) or 6× His-KHD-N (*G*) to ssRNA (repetition ≥ 10) and competition-assay between labelled ssRNA and unlabelled ssRNA or ssDNA (repetition ≥ 8) with GST-RRM-SPEN (*F*) or 6× His-KHD-N (*H*). For the EMSA the Cy3-labeled 25 bp nucleotide fragment was incubated either in the absence (lanes 1) or in the presence of increasing concentrations of the protein (0.1 μM, 0.2 μM, 0.5 μM, 1 μM, 2 μM, 3 μM, 5 μM; lanes 2–8, respectively) and run on a 5% (*E* and *F*) or 7% (*G* and *H*) native acrylamide gel. For the competition-assay the Cy3-ssRNA 25-bp nucleotide fragment was incubated with 3 μM of protein (control lane 4) and increasing concentration of 25-bp ssDNA (5×, 10× and 50× the concentration of Cy3-ssRNA, lane 1-3, respectively) or 25-bp ssRNA (5×, 10× and 50× the concentration of Cy3-ssRNA, lane 5-7, respectively). The lower band corresponds to the free RNA and the arrow or brackets indicate the protein-RNA complex.

3.2 The SPEN and KHD domain proteins contain RNA binding domains

The SPEN gene (AT1G27750) is 4326 nucleotides long and contains eight exons, it encodes a 117.47 kDa protein, and contains a conserved RRM RNA-binding domain and a spen paralog and ortholog C-terminal (SPOC) protein-binding domain (Fig. S2*A&B*), like in animal Split Ends (Spen) proteins, that function in transcriptional repression (Ariyoshi and Schwabe, 2003). In the *Arabidopsis* genome, the RRM domain retrieved 273 unique AGI codes, while the SPOC domain retrieved only 6 proteins, only three of those are Spen proteins combining SPOC with one or more RRM motif, i.e. SPEN, Q0WPC2 AT4G12640 and the flowering time regulator, FPA (with three RRMs), that controls alternative splicing and polyadenylation of antisense transcripts of the floral repressor *FLC* (Hornyik *et al.*, 2010) with three RRMs. Two cladograms illustrates the phylogeny of SPEN proteins in eudicots (Fig. S2*A&B*).

The KHD (At1g51580) genomic sequence is 2491 nucleotides long and composed of 7 exons, it encodes a 67.12-kDa protein with 5 conserved K homology domains (KH) ranging from 70 to 77 amino acids (Fig. S2*C&D*). In *Arabidopsis thaliana,* 37 unique AGI codes of proteins containing 1 to 5 KH domains were present. All proteins with three or more K homology motifs (including KHD) have no other domains, proteins containing only one or two KH motifs frequently combine up to eight different domains. Two cladograms of 12 proteins with 3, 4 or 5 KH domains (Fig. S2*C&D*) grouped KHD with HUA ENHANCER4 (HEN4, At5g64390) that facilitates the processing of *AGAMOUS* pre-mRNA (Cheng *et al.*, 2003), and REGULATOR OF CBF GENE EXPRESSION 3/SHINY1/HIGH OSMOTIC STRESS GENE EXPRESSION 5 (RCF3/SHI1/HOS5, At5G53060), that is involved in pre-mRNA processing (Chen *et al.,* 2013). KH proteins with 3 KH motifs clustered together, amongst which FLOWERING LOCUS KH DOMAIN (FLK) and PEPPER (PEP), a *FLC* repressor and activator, respectively (Mockler *et al.*, 2004; Ripoll *et al.*, 2009).

3.3 SPEN and KHD bind RNA

To test the *in vitro* RNA binding capabilities of the SPEN protein, its RRM domain was selected because the production of the full length protein in *E. coli* proved unsuccessful.

A GST-RRM-SPEN fusion was expressed and purified by affinity chromatography (Fig. S3A and B). Two products can be observed in the purification corresponding to the GST-RRM-SPEN for the highest molecular weight and to free GST for the lowest. The RNA-binding of the purified GST-RRM-SPEN was examined using Electromobility Shift Assays (EMSA). Incubating increasing concentrations of the recombinant protein with the fluorescently labelled ssRNA followed by EMSA analysis demonstrated a dose-dependent interaction of GST-RRM-SPEN with the RNA probe starting from a protein concentration of 0.2 µM (Fig. 1*E*). While incubation of increasing amount of the protein with the fluorescently labelled dsRNA followed by EMSA analysis shows an interaction of GST-RRM-SPEN with the dsRNA probe from a protein concentration of 1µM (Fig. S3C). Therefore GST-RRM-SPEN displays a greater affinity to ssRNA than dsRNA. To test the selectivity of the protein for RNA, competition experiments with increasing amounts of unlabelled ssRNA or ssDNA were performed (Fig. 1*F*). The protein-RNA complex formed by a fixed concentration of GST-RRM-SPEN (3 µM) and a constant amount of labelled RNA probe is efficiently competed by the addition of a 10-fold excess of unlabelled ssRNA and the complex is barely detectable in the presence of a 50-fold excess of unlabelled ssRNA. In contrast, the complex is hardly affected by the addition of a 50-fold excess of unlabelled ssDNA, demonstrating that the GST-RRM-SPEN displays a clear preference for ssRNA over ssDNA.

KHD is predicted as an RNA binding protein because it contains 5 KH domains (UniProt database, Chen *et al.*, 2017). To test the RNA-binding properties of KHD, we expressed the region comprising the two N-terminal KH domains, as hexa-His-tagged fusion protein named 6xHis-KHD-N, in *E. coli*, because the production of the full length protein was unsuccessful. The recombinant protein was purified by metal-chelate affinity chromatography (Fig. 1*G,* Fig. S3A and B). In EMSAs, a dose-dependent interaction with ssRNA was observed starting from a protein concentration of 0.5 µM (Fig. 1*G*). While incubation of increasing amount of the protein with the fluorescently labelled dsRNA followed by EMSA analysis shows an interaction of 6xhis-KHD-N with the dsRNA probe from a protein concentration of 1µM (Fig. S3D). Therefore 6xhis-KHD-displays a greater affinity to ssRNA than dsRNA. In a competition assay (Fig. 1H), the complex formed by a fixed amount of 6xHis-KHD-N (3 µM) and the labelled ssRNA probe was efficiently competed by the addition of excess amounts of unlabelled ssRNA,

whereas the addition of ssDNA did not affect the detected protein-RNA complex. Therefore, 6xHis-KHD-N selectively interacts with the ssRNA probe, but apparently not with the ssDNA.

Thus, we demonstrated *in vitro* RNA binding for both SPEN and KHD by EMSA; furthermore, KHD is present, and SPEN absent in the *in planta* mRNA binding proteome datasets (Reichel *et al.,* 2016; Köster *et al.,* 2017) supporting a role for KHD in mRNA-related processes and for SPEN rather in pre-mRNA processing or non-coding RNA-related biology.

3.4   Growth and flowering time in spen, khd and hub mutants

The expression of *HUB1, KHD, SPEN* in the shoot apex and the root apical meristem was analysed with whole mount, multi-probe in situ hybridization of 4-day-old seedlings grown *in vitro* with sequence specific probes for *SPEN, KHD* and *HUB1* genes. A red fluorochrome label was used for *SPEN*, a green one for *KHD* and a blue one for *HUB1*. Interestingly, a strong coexpression of *HUB1, SPEN* and *KHD* was observed in the shoot apical meristem, visible as the white-pink complementary colour of green, red and blue (Fig. 2*A*). The *SPEN* and *HUB1* genes were coexpressed in expanding leaves and *KHD* and *HUB1* were coexpressed in leaf primordia and vascular tissue. In primary roots, no coexpression of the three genes was observed, however, *SPEN* and *KHD* were coexpressed in the cortex, stele and root apical meristem, *SPEN* was coexpressed with HUB1 in the epidermal cell layer (Fig. S4A). The whole mount *in situ* expression patterns of *HUB1* correlated with previously described phenotypes in *hub1* leaf, root and flowering time (Fleury *et al.,* 2007; Cao *et al.,* 2008). Hence, flowering time, leaf and root growth were compared between *spen-1* and *khd-1* and *hub2-1* and *hub1-4*, and analysed in the overexpression lines 35S::GFP::HUB1, 35S::GFP::HUB2, 35S::GFP::SPEN and 35S::GFP::KHD. The *spen-1* (SALK_025388) has a T-DNA insertion in exon 2 (Fig. 2B) that severely reduced the *SPEN* transcript levels and thus is a knock-out mutant (Fig. 2C). The *khd-1* (SALK_046957) has a T-DNA insertion in the promoter, next to the 5'UTR region of *KHD* (Fig. 2*B*) that reduced *KHD* transcript levels and is a knock-down mutant (Fig. 2C). Although it is a weak allele some significant phenotypes can be observed such as reduction in growth and notable number of differentially expressed genes, 2351 (Fig.

3A; Table S3). Contrarily to animals where mutations in chromatin remodellers are mostly lethal, their impact on survival is limited in plants (Nelissen *et al.*, 2007). In plants chromatin states are established and modified throughout the development and in response to the environment making them more dynamic and with more targeted systems than seen in animals allowing plants to react upon unfavourable conditions by changing growth.

Flowering time in days after germination (DAG) and the number of rosette leaves at bolting were determined in a randomization experiment *in soil* (Fig. 2D,E and S4B). In wild type, flowering time was 21 ± 1.7 DAG with rosette leaf number of 7.5 ± 0.7 and was similar in *khd-1, 35S::GFP::HUB1, 35S::GFP::SPEN* and *35S::GFP::KHD* plants (21.1±1.8, 20.9±1.8, 21.6±1.6 and 21.1±1.9 DAG, and 7.4±0.5, 7.5±0.7, 7.3±0.8and 7.3±0.6 leaves, respectively). In *spen-1* plants, flowering was significantly delayed by two days (23.4 ± 2.4 DAG) with an increased leaf number (8.1 ± 0.9). On the contrary, *hub1-4, hub2-1, hub1-3hub2-1* and *35S::GFP::HUB2* plants were early flowering (15.1±1.1, 16.9±1.6, 15.9±1.2, 19.4±1.9 DAG, respectively) with reduced or wild type rosette leaf number (6.1±0.4, 6.7±0.5, 6.4±0.5, 7.5±0.6 respectively). In conclusion, HUB1/HUB2 and SPEN both regulate flowering time, but in an opposite way, suggesting SPEN might also act on the flowering time regulator, FLC, as HUB1/HUB2 (Cao *et al.*, 2008) but not necessarily via H2Bub.

Seedling growth of the mutant lines and overexpression lines was monitored *in soil* using the automated weighing, imaging and watering high-throughput phenotyping platform WIWAM (Skirycz *et al.*, 2011; Clauw *et al.*, 2015). At 23 DAS the projected rosette area was measured, stockiness (indicator of leaf shape) and compactness were calculated (Fig. 2F; Fig. S4C,D). Projected rosette area was reduced for *spen-1* and *khd-1* by respectively 16 and 17% while increased for *hub1-4* and *hub1-2* by respectively 11 and 7% (Fig. 2F). In hub1-4 and hub2-1 stockiness was reduced (Fig. S4C), and in *spen-1* compactness was reduced (Fig. S4D). In 21 day-olds *in vitro* grown plants, the individual leaf area was reduced in all mutants (Fig. S4E). The leaf number in *hub1-4, hub2-1,* was reduced as compared to wild type, but was similar to wild type in *spen-1* and *khd-1*. Primary root length was reduced in all genotypes except for *hub1-4* at 10 DAG (Fig. S4*F*) which correlated for spen-1, 35S::GFP::HUB1, 35S::GFP::KHD and 35S::GFP::SPEN with a

reduced primary root meristem size at 5 DAG (Fig. S4 *G,H*), indicating that mutation and overexpression of *SPEN* and *KHD* affect cell proliferation. For *hub1-4* the reduction in meristem size may not affect primary root size due to a delay in development. At 5 DAG the meristem has reached its maximal number of cortex cell in wild type (Dello Ioio *et al.*, 2007) but maybe not in *hub1-4*. It could be that *hub1-4* meristem reaches its maximum size with a delay thus creating a delay in root development. In the *khd-1* mutant, the reduced primary root length is probably due to reduced cell elongation because there is no reduction in cortex cell number of the meristem.
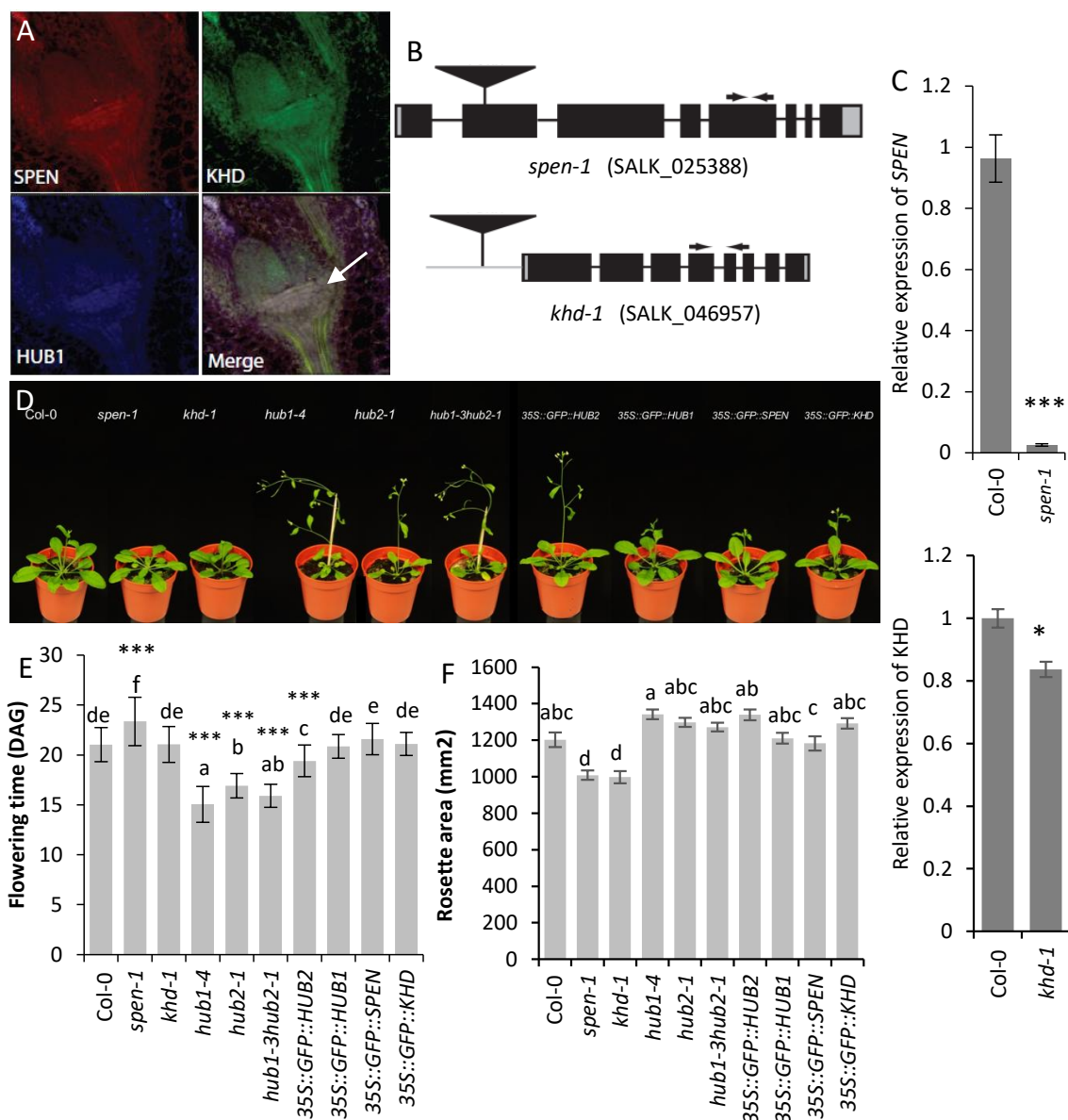
Figure 2: Expression patterns and phenotypes in the shoot.
(*A*). Whole mount, multi-probe in situ hybridization of the shoot apex. Superposition of *HUB1, SPEN* and *KHD* expression pattern shows a strong coexpression in the shoot

apical meristem, in white-pink. (*B*). Schematic view of the *spen* and *khd* T-DNA insertion lines. (*C*). Relative expression of *KHD* and *SPEN* in Col-0 and mutant lines. (*D*). Representative plants at 26 DAG. (*E*). Flowering time of perturbed lines in DAG ($n \geq 28$). Ordinary one-way ANOVA with 95% confidence shows a significant difference between the genotypes (***P < 0.001), represented by the letters. Three biological repeats were performed. (*D* and *E*) Error bars represent standard errors. Asterisks indicate statistically significant differences to Col-0 (*P < 0.05, **P < 0.01, ***P < 0.001). (F). Projected rosette area of perturbed lines in mm² at 23 DAS. Significance at 95% confidence was shown by ordinary one-way ANOVA. Three biological repeats were performed.

3.5 Transcriptomes of spen, khd and hub1 mutants

RNA deep sequencing was done on *hub1-4*, *khd-1*, *spen-1* and Col-0 total RNA prepared from shoot apices and data were analysed for differentially expressed genes (DEG, down-regulated with $\log_2$ FC $\leq$ -0.5 and up-regulated with $\log_2$ FC $\geq$ 0.5; *P* < 0.05, Fig. 3A). More than 40% and almost 50% of differentially expressed genes in *hub1-4* and *khd-1* respectively, were in common which suggests that KHD might act together with HUB1 in the transcriptional regulation of a large number of genes. In contrast, only around 5,5% and 16% of DEG in *hub1-4* and *spen-1* were common, indicating that SPEN might have a more specialized function unrelated to HUB-mediated H2Bub. Very few DEG were common in all three mutants suggesting limited combined activity of KHD, SPEN and HUB1 in transcriptional regulation (Table S4). Substantial portions of the DEG were unique to each mutant, i.e. 44% of DEG in *khd-1*, 52% in *hub1-4* and 63% in *spen-1* suggesting additional specific roles for HUB1, KHD and SPEN.

Next, pathways were identified, called gene ontology classes (GO), based on differentially expressed genes - common and specific GOs were identified amongst the three mutants. Genes commonly down-regulated in all three mutants and in the *hub1-4* and *spen-1* genotypes fall into the same ontology classes coding for cell cycle proteins, histone kinases and ribosomal proteins. Genes down-regulated in *hub1-4* and *khd-1* encode proteins related to cell cycle, chromatin, ribosomes or involved in secondary metabolism. The *hub1-4* specific down-regulated genes grouped mainly into ontology classes related to defense and stress response, cell wall organization or biosynthesis and flower development containing the flowering repressors *FLC*, *FLM*, *SMZ* and *BOP2*. Many *khd-1* unique down-regulated genes clustered into organ morphogenesis, growth,

leaf and flower development classes (*GRF9* growth regulator, *SPL15* phase transition regulator, *RBR1* and *VIM3* repressors of flowering activator *FWA*), or were involved in cell cycle or nucleic acid metabolism. The *spen-1*-uniquely down-regulated genes related to the circadian clock and flowering time (*PRR5*, *ELF3*, *FKF1* and *SRR1*) and signal transmission. In summary, analysis of down-regulated genes showed that HUB1, KHD and SPEN are involved in common pathways but probably only sporadically regulate the same target genes working as a complex.

Number of genes upregulated commonly in all three mutants was too low (38) for reliable clustering analysis, therefore we compared the *hub1-4* mutant individually to *khd-1* or *spen-1* (Table S3). Both comparisons identified genes involved mainly in programmed cell death, regulatory processes and response to different stimuli. Among the *hub1-4/khd-1* overlapping genes additional categories of upregulated genes were detected like tropism, cell wall, transmembrane transport and response to hormones. Genes upregulated only in individual mutants, also clustered predominantly to response to stimulus class.

QQS, *PCNA2*, *AT1G18990*, *AT1G66650*, and *AT5G56370* showing low expression in *hub1-4*, *khd-1* and/or *spen-1* (Fig. S5A; Table S4) were selected for chromatin immunoprecipitation with H2Bub antibodies followed by a qPCR (ChIP-qPCR) with primers annealing to their promoters and coding regions (Fig. S5B). The H2Bub at the *QQS* gene was significantly lower in the central part of the gene in all three mutants (Fig. S5B), but H2Bub was normal at *PCNA2, AT1G18990, AT1G66650*, and *AT5G56370* in *khd-1* and *spen-1*. The RNA-binding capacity of KHD and SPEN might link the complicated siRNA-mediated regulation of the *QQS* gene (Bortolini Silveira *et al.*, 2013) with HUB1-mediated H2Bub during transcript elongation.
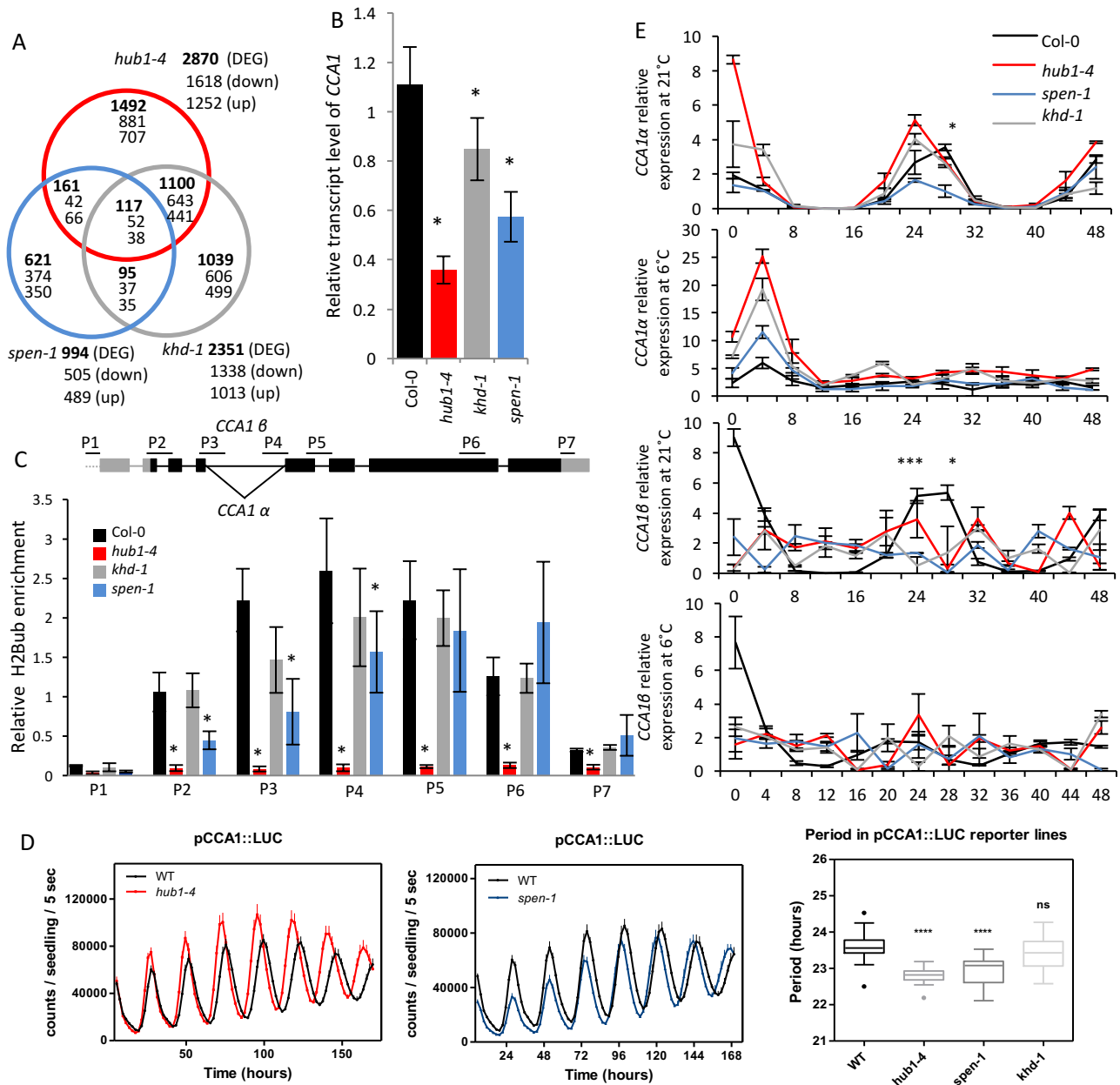
Figure 3: Mutant transcriptome and *CCA1* analysis.
(*A*). Venn diagram of transcriptome of *hub1-4, spen-1* and *khd-1* expression profile compare to Col-0. (*B*). Relative expression of *CCA1* by qPCR in Col-0 and mutants. (*C*). Relative enrichment of H2Bub measured by ChIP assay with H2Bub antibodies on the *CCA1* gene. Five biological repeats were performed. (*D*). Bioluminescence analysis of *pCCA1::LUC, hub1-4, spen-1* and *khd-1* mutants. Period estimates of *hub1-4, spen-1* and *khd-1* in *pCCA1::LUC* (*B-D*) Error bars represent standard errors. (*E*). Circadian traces of *CCA1α* and *CCA1β* transcript accumulation at 21°C and 6°C. Asterisks indicate statistically significant differences from *spen-1* to Col-0 using Student's t-test (*$P < 0.05$, ***$P < 0.01$, ****$P < 0.001$). (*B* and *C*) Asterisks indicate statistically significant differences to Col-0 using Student's t-test (*$P < 0.05$).

3.6 SPEN and HUB1 regulate CCA1 gene expression through H2Bub and pre-mRNA splicing

The H2Bub of the clock regulator CCA1, a known target of HUB1 (Himanen *et al.*, 2012), was determined in *khd-1* and *spen-1* mutants in order to investigate whether it was correlated with its reduced expression in *khd-1* and *spen-1* seedlings, and whether KHD and SPEN act together with HUB1/2 histone monoubiquitylase during transcription activation. Chromatin immunoprecipitation with H2Bub antibodies followed by a qPCR with primers annealing to promoter and coding regions of the *CCA1* gene (Fig. 3 *B* and *C*) showed that H2Bub peaked centrally in the gene body in wild type while absent from the promoter region (Fig. 3 *B* and *C*, black bars), but was very low over the whole gene in the *hub1-4* mutant (Fig. 3 *B* and *C*, red bars) which is characteristic of HUB1/2 target genes. In the *spen-1* mutant, reduced gene expression correlated with a significant reduction of H2Bub at the 5' and central part of the *CCA1* gene suggesting that SPEN affects HUB1-mediated H2Bub activity at CCA1. In the knock-down allele, *khd-1*, the H2Bub at *CCA1* is reduced but not significantly, hence it is not clear whether KHD functions in HUB1-mediated H2Bub at CCA1.

The downregulation of the *CCA1* gene expression in *spen-1* and *khd-1* as well as in *hub1-4* prompted us to investigate circadian rhythms by means of reporter lines expressing the LUCIFERASE (LUC) fused to the *CCA1* and *TOC1* promoters (*pCCA1::LUC* and *pTOC1::LUC*) that were introgressed into the *spen-1, khd-1 and hub1-4* mutants. Bioluminescence analysis showed that compared to WT, circadian rhythms were clearly sustained in the mutants but the circadian period was significantly shortened for both reporters in *hub1-4* and *spen-1* (Fig. 3D and S4*H*). The amplitude was not significantly affected in those mutants except for the promoter activity of *TOC1* in *hub1-4* mutant plants and a lower amplitude was observed in *khd-1* (Fig. S4*H*). The changes in circadian period suggest that the loss of HUB1 and SPEN function makes the clock run faster than in WT.

Subsequently, alternative splicing of *CCA1* was analysed in the *hub1-4, spen-1* and *khd-1* mutants measuring the relative expression of the *CCA1α* and *CCA1β* transcript level by qPCR over a time course of 48h in continuous light, in normal temperature (21°C) and cold condition (6°C) (Fig. 3E) (Seo *et al.*, 2012; Cui *et al.*, 2014). In *CCA1α* the fourth intron

is spliced while in *CCA1β* the fourth intron is retained (Fig. 3C). The Col-o wild type showed rhythmic patterns for both transcripts in normal temperature condition with a peak at time point, ZT28. Col-o in the cold loses the ZT28 peak and the relative expression of *CCA1α* and *CCA1β* is reduced. The *hub1*, *khd-1* and *spen-1* mutants showed a peak at time point, ZT24 at 21°C for the *CCA1α* splice variant, confirming the shorter clock period as shown by the LUC reporter lines. In these conditions only *spen-1* has a reduced expression level of *CCA1α* suggesting a positive role for SPEN in splicing of the *CCA1* gene at the fourth intron. In *hub1-4* the *CCA1α* peaks at ZT24 at 21°C and is higher in level as compared to wild type suggesting a regulatory effect of H2Bub on alternative splicing. Strikingly, at 21°C, *hub1-4, spen-1* and *khd-1* showed no peak for the *CCA1β* splice variant indicating that the intron retention mechanism necessary for the formation of this transcript is affected. In cold condition, there is no distinction between Col-o and the three mutants as the rhythmic pattern of the *CCA1α* and *β* transcript levels were absent and all peaks were lost. Alternative splicing is regulated by RNA-binding proteins, chromatin structure, histone modifications and RNA pol II elongation rate (Luco *et al.*, 2011). Slow elongation expands and fast elongation compresses the "window of opportunity" for recognition of upstream splice sites, thereby decreasing or increasing intron retention (Fong *et al.*, 2014). Moreover, alternatively spliced introns are removed more slowly than constitutive introns and therefore their splicing requires a longer transcript elongation time. In summary, at normal temperature, the general *CCA1* transcript level is reduced in *hub1* but there is increased *CCA1α* and reduced *CCA1β*, indicating that slow transcript elongation rate might result from decreased H2Bub that would enhance splicing of intron 4 and shift the *CCA1α*/*CCA1β* balance towards *CCA1α*. In spen-1, the H2Bub at *CCA1* is reduced in the first part of the coding region until intron 4, where the intron retention/splicing is established suggesting that SPEN plays a role to recruit HUB1/2 at the splice site for maximum H2Bub which might function as a signal for splice site selection. Consequently, in *spen-1*, decrease of H2Bub might result not only in slower transcript elongation rate but also in reduced splicing, therefore the total *CCA1* transcript level is downregulated and *CCA1α*/*CCA1β* balance is not shifted.

In yeast, H2Bub facilitates the early spliceosome assembly at certain genes (Hérissant *et al.*, 2014). Our data suggest that SPEN might provide an important link between the splicing machinery and HUB1-mediated H2Bub, possibly SPEN might be an

adaptor protein between the histone mark H2Bub and the splicing factors. Our data suggest that the RRM domain of SPEN would bind the nascent ssRNA and its SPOC domain would bind proteins of the spliceosome or the transcript elongation complex. Indeed, the RNA polymerase II transcript elongation complex interact with mRNA splicing factors (Antosz *et al.*, 2017). Coupling the role of H2Bub in transcript elongation to the interaction between the transcript elongation complex and the splicing machinery might be done by SPEN for specific genes. Hence, our data show a new function for histone modifications in regulating transcription through alternative splicing.

3.7   SPEN regulates FLC expression via COOLAIR splicing, independent of H2Bub

The flowering time repressor gene, *FLC* (Fig. 4A), is also a known target of HUB1-mediated H2bub (Cao *et al.*, 2008). Strikingly, the H2Bub level at the *FLC* gene was normal in both *khd-1* and *spen-1* (Fig. 4C) showing a lack of correlation with its down-regulation in *khd-1* and up-regulation in *spen-1* (Fig. 4B). In *hub1-4*, downregulation of the *FLC* gene expression correlated with reduced H2Bub levels. Thus, SPEN inhibits and KHD promotes *FLC* gene expression irrespective of their H2Bub state indicating that SPEN and KHD do not contribute to HUB1-mediated H2Bub regulation of *FLC*, we investigated whether they are involved in the non-coding RNA-mediated regulation of *FLC* expression.

FLC encodes a transcriptional repressor that prevents the activation of genes required for floral transition; its antisense, *COOLAIR*, fully encompasses the *FLC* gene and its transcription is independent of the sense transcript (Swiezewski *et al.*, 2009). In the autonomous pathway, alternative splicing and polyadenylation of *COOLAIR* result either in a proximal or a distal antisense transcript (Fig. 4E) that function in *FLC* gene expression regulation. Moreover, splicing of intron 1 of *COOLAIR* by the essential PRP8 spliceosomal subunit promotes the proximal poly(A) site (Marquardt *et al.*, 2014). FCA (RRM domain) and FY promote the use of the proximal poly(A) site, and FPA triggers the demethylation of dimethylated histone H3 lysine 4 by FLD in the gene body of *FLC* leading to a repressed state and reduced expression of sense and via the feedback loop of antisense transcripts. The *COOLAIR* transcripts function antagonistically with the proximal antisense functioning as a repressor and the distal antisense as an activator of

FLC (Ietswaart *et al.*, 2012). During a short cold treatment, the proximal antisense stabilization and production is increased compared to the distal one (Csorba *et al.*, 2014) which correlates with a reduction in sense *FLC* transcription.

We investigated whether HUB1, SPEN or KHD play a role in the regulation of the *FLC* antisense *COOLAIR* alternative polyadenylation and splicing using qPCR on total RNA of their respective mutants (Fig. 4D). Strikingly, in normal conditions, distal *COOLAIR* transcript was increased in *spen-1* which corresponds to an increase in the *FLC* sense transcript and a delay in flowering (Fig. 2E), suggesting a role for SPEN in either repressing the distal or promoting the proximal antisense transcript and thus the splicing of *COOLAIR*. Upon vernalisation, distal *COOLAIR* is not increased anymore in *spen-1*, the ratio proximal/distal is reverted to wild type but the *FLC* sense transcript is still significantly higher than in Col-0 although lower than without vernalisation. This effect may be due to the high expression before vernalisation and the slow degradation of spliced *FLC* transcript (Swiezeski *et al.*, 2009). In both conditions, the reduced *FLC* sense transcript level and unchanged proximal/distal *COOLAIR* ratio in *hub1-4*, confirmed that reduced *FLC* sense transcript and early flowering are due to the reduced H2Bub at the *FLC* gene body. In normal conditions, there is no significant change in *COOLAIR* transcript levels or proximal/distal ratio in *khd-1*, which fits its normal flowering time (Fig. 2E). In conclusion, our data link the *FLC* sense transcript increase in *spen-1* to its long-non-coding-RNA (lncRNA) *COOLAIR* metabolism and not to H2Bub at *FLC*, while the decrease in *FLC* sense transcript in *hub1-4* and *khd-1* is not linked to the lncRNA metabolism but to H2Bub at *FLC*.

Delayed flowering time in *spen* and earlier flowering in the *hub1* mutants was correlated with respectively increased and decreased *FLC* expression levels. In the *spen* mutant, increased distal antisense *COOLAIR* transcript and distal/proximal *COOLAIR* ratio indicate that SPEN plays a role in *COOLAIR* polyadenylation or splicing to control the level of the sense *FLC* transcript and acts antagonistically to HUB1 in *FLC* regulation. A number of flowering time regulators with RNA-binding capacity such as FPA and FCA (RRM-domain), and FLK and PEP (KHD-domain) have been identified and are part of a regulatory loop in which FCA and FPA independently regulate 3'end formation of antisense RNA (*COOLAIR*) at the *FLC* locus that triggers FLD demethylation of

H3K4me2 leading to a repressed chromatin state (Ietswaart *et al.*, 2012). FLK and PEP have antagonistic effect on *FLC* expression but their mechanisms of actions are not known (Ripoll *et al.*, 2009). They interact with other KH proteins HEN4 and HUA1 to form a complex that assists transcript elongation and facilitate correct splicing (Rodriguez-Cazorla *et al.,* 2015). The SPOC domain in SPEN is important for its copurification with HUB1 and KHD, hence it suggests that SPEN works together with those proteins in the RNA-mediated control of FLC and might represent an antagonistic regulatory loop to HUB1-mediated histone H2Bub, both activities might be cross-talking to environmental and developmental cues. Our data link HUB1-mediated H2Bub at a specific gene (FLC) with its RNA-mediated regulation (COOLAIR) through the HUB1- and RNA-binding activity of the SPEN protein in plants, which has not been reported in other organisms so far.
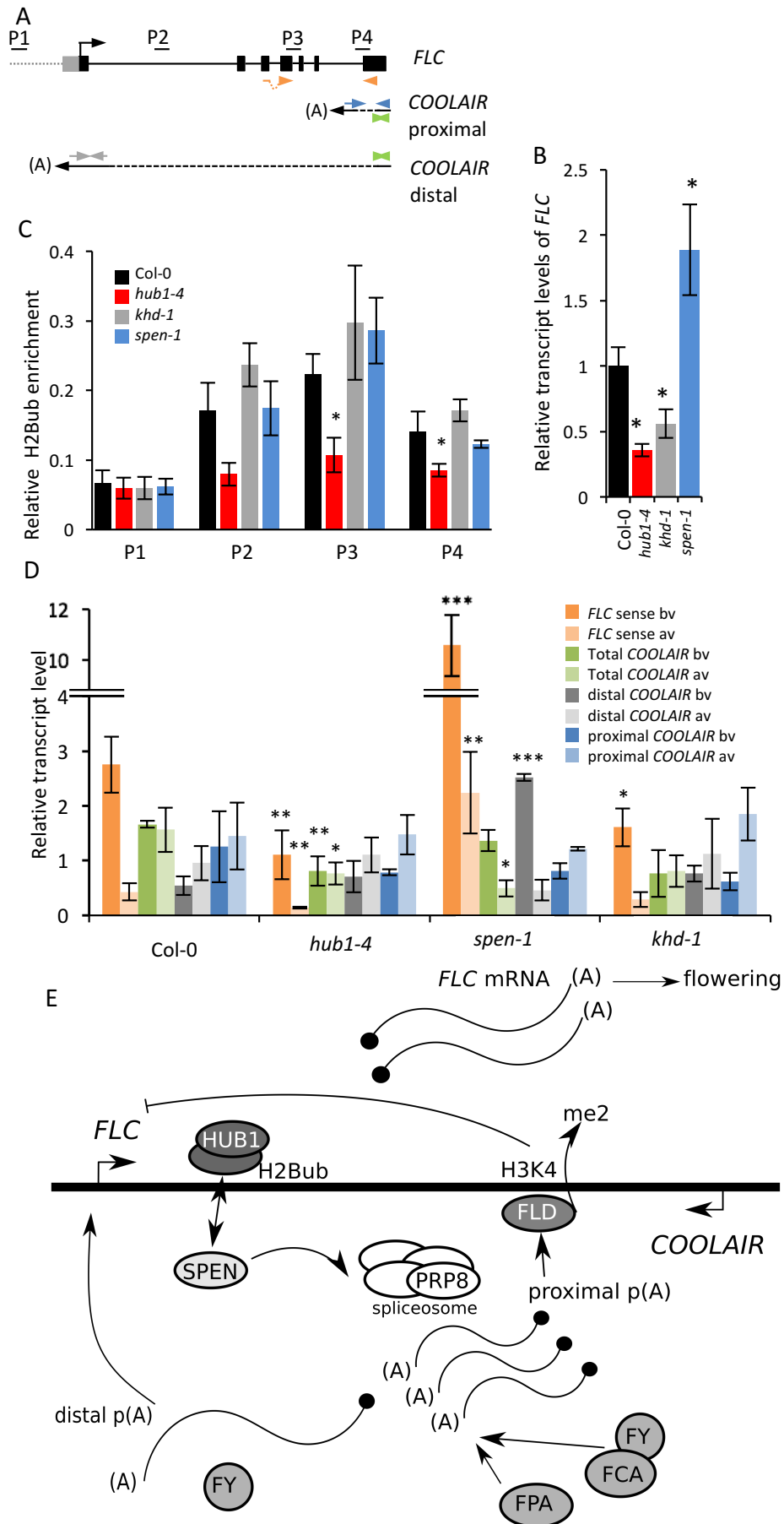
Figure 4: FLC analysis
(*A*). Schematic representation of *FLC* sense and antisense, showing the position of the primers used for (D): spliced *FLC* in orange, total *COOLAIR* in green, distal *COOLAIR* in grey and proximal *COOLAIR* in blue. (*B*). Relative expression of *FLC* by qPCR in Col-o and mutants. (*C*). Relative enrichment of H2Bub measured by ChIP assay with H2Bub antibodies on the *FLC* gene. Five biological repeats were performed. (*D*). qRT-PCR showing *FLC* and *COOLAIR* forms relative expression in after-vernalisation (av) and before-vernalisation (bv) material. Asterisks indicate statistically significant differences to Col-o using Student's t-test (*P < 0.05, **P < 0.01, ***P < 0.001). (*E*). Model of *FLC/COOLAIR* regulation in normal conditions modified from Ietswaart *et al*. (2012) and Marquardt *et al*. (2014). (*B-D*) Error bars represent standard errors. (*B* and *C*) Asterisks indicate statistically significant differences to Col-o using Student's t-test (*P < 0.05, **P < 0.01, ***P < 0.001).

4   Conclusion

We demonstrated that SPEN is a positive regulator of the splicing of the FLC antisense COOLAIR, indeed, in spen mutants, increased FLC expression and delay in flowering time correlated with increased distal FLC antisense COOLAIR splice form, which is in agreement with the absence of SPEN in mRNA-binding proteome datasets (reviewed by Köster et al., 2017) and in support for a role of SPEN in non-coding RNA-related processes – without a link to H2Bub. However, both HUB1 and SPEN are required for correct α and β splice form levels of the circadian oscillator gene CCA1, and for H2Bub at the first half of its coding region, explaining reduced CCA1 expression, reduced growth in roots and leaves, and shorter diurnal period in the respective mutants. SPEN might have a role in recruitment of HUB1/2 and establishing the maximum H2Bub at the splice site, that would increase the transcript elongation rate and splicing efficiency. Physical interaction between several chromatin-associated proteins and splicing components has been reported (Sims *et al*., 2007). In humans, an adaptor complex was described between H3-K36me3, its binding protein MRG15, and the splicing regulator PTB, (Luco *et al*., 2010). This adaptor system consists of a chromatin-binding protein that reads specific histone marks, and an interacting splicing regulator. SPEN might be part of a such complex as a splicing regulator in addition to an activity in directing H2Bub. SPEN would make the link between the nascent RNA via its RRM domain and the H2Bub via

interaction with HUB1/2 by its SPOC domain, thus bridging the H2Bub to the pre-mRNA.

The SPEN function in FLC expression via antisense COOLAIR splicing or polyadenylation is independent of H2Bub, but its function in CCA1 splicing or polyadenylation determines H2Bub level in a linear way indicating that defective spliceosome recruitment and/or activity affect levels of H2Bub in plants. The data are in line with abundant specific and limited common transcripts between *spen* and *hub1* transcriptomes. The low number of DEG in *spen-1* compared with *hub1-4* argues for a more specialized activity on some genes and pathways. We see a small overlap of 278 DEG between the two transcriptomes. A large portion of those DEG may be due to the deregulation of *CCA1* expression seen in both mutants, notably genes implicated in sugar metabolism and cell wall production (Schaffer *et al.*, 2001; Nagel *et al.*, 2015). A large portion of DEG found in *spen-1* are not overlapping with *hub1-4* (716 DEG) including flowering time regulation genes and can therefore be linked to an HUB1 independent activity of SPEN such as seen in FLC.

In yeast, Npl3 is a SR-like protein with 2 RRM and a Ser-Arg rich domain interacting with Bre1 (homolog of HUB1) and necessary for correct splicing (Moehle *et al.,* 2012). BRE1 is also reported to have an independent effect on splicing of some genes but not linked to spliceosome recruitment. Npl3 has multiple roles in the regulation of gene expression, including in pre-mRNA splicing, 3'end processing, and mRNA export. Npl3 and SPEN are not homologs and Npl3 has role in splicing regulation of a large subset of genes mainly ribosomal protein genes, contrary to SPEN that targets antisense lncRNA for splicing in addition to coding sense RNA at specific genes. In humans, the splicing factor SART3 binds histones H2A, H2B, H3 and H4 and enhance deubiquitination of H2B (Long *et al.*, 2014). So far, a few reports in yeast and human documented a link between the H2B monoubiquitination and deubiquitination dynamics and splicing. Here, the functional analysis of SPEN showed such link in plants, identified the CCA1 as a target gene for such activity, moreover a role for SPEN in antisense lncRNA COOLAIR splicing was uncovered that was independent of the H2Bub at the coding region of FLC suggesting that the SPEN role in splicing depends on other proteins that guide it to its target.

In *khd-1*, *FLC* and *CCA1* expression are reduced, but H2Bub and antisense COOLAIR were normal. Interestingly, KHD was identified in an mRNA binding interactome (Reichel *et al.*, 2016), and it localized in the nucleus and cytoplasm suggesting a role for KHD in mRNA stability, export or translation.

5   Materials and Methods

5.1   Plant material and growth conditions.

The mutants *hub1-4* (SALK_122512), *spen-1* (SALK_025388), *khd-1* (SALK_046957) (Alonso et al., 2003), *hub1-3* (GABI_276D08), *hub2-1* (GABI_634H04), *khd-2* (GABI-164F03) (Rosso et al., 2003), are in Col-0 background and were obtained from the Nottingham Arabidopsis Stock Centre and T-DNA insertions were confirmed by PCR. The clock reporter lines expressing *pCCA1::LUC* (Salome and McClung, 2005) and *pTOC1::LUC* (Portoles and Mas, 2007) were crossed into the *hub1-4, spen-1* and *khd-1* mutants and homozygous lines analysed by in vivo luminescence assays.

The p35S::GFP::SPEN and p35S::GFP::KHD constructs were obtained by Gateway recombination and were transformed into *Agrobacterium tumefaciens* cells, which were used for tobacco leaf infiltration and stable transformation into *Arabidopsis thaliana*, Col-0 by floral dip (Zhang *et al., 2006*).

Seedlings were grown on half-strength (0.5×) Murashige and Skoog (MS) medium and unless differently indicated the growth chamber conditions were 16 h day/8 h night with white light and 20°C. Seeds for *in-vitro* time-lapse analysis were sterilized in 3% bleach for 15 min and sown on medium containing 0.5× MS medium (Duchefa) solidified with 0.9 g L^{-1} plant tissue culture agar (Lab M) on round Petri dishes. After a stratification period of 2 days, the plates were placed on the IGIS platform (Dhondt *et al.*, 2014) in a growth chamber under long-day conditions (16 h light, 8 h darkness) at 21°C. Average light intensity, supplied by cool-white fluorescent tubes (Spectralux Plus 36W/840; Radium), was around 60 mE m^{-2} s^{-1}. For bioluminescence assays, plants were stratified for 2 days at 4ºC on Murashige and Skoog (MS) agar medium plates and grown for 7 days under LD cycles (12 h light, 12 h dark) with 60 µmol.m^{-2}-.s^{-1} white light at constant 22ºC. Seedlings were transferred to 96-well plates containing MS-agar and 3 mM luciferine

(Promega). Luminescence rhythms were monitored under constant white light conditions (60 $\mu mol.m^{-2}.s^{-1}$) using a luminometer LB-960 (Berthold Technologies) and the software MikroWin 2000, version 4.34 (Mikrotek Laborsysteme) for the analysis.

5.2 Tandem Affinity Purification.

TAP (Rigaut *et al.*, 1999) or GS (Bürckstümmer *et al.*, 2006) tags were fused N-terminally to full length cDNAs of HUB1, HUB1pm and HUB2 as the RING domain is in the C-terminal part of the HUB1/2, and tag was fused C-terminally to SPEN. In the HUB1pm, two cysteines of the RING domain (positions 826 and 829) were altered into serines. The TAP-tagged HUB1 proteins complemented partially the *hub1-1* mutation (Fleury *et al.*, 2007). Tagged transgenes were expressed under the control of the constitutive cauliflower tobacco mosaic virus 35S promoter and transformed in *Arabidopsis* cell suspension cultures (Van Leene *et al.*, 2007). Protocols of proteolysis, benzonase treatement (cleaves RNA and DNA) and peptide isolation, acquisition of mass spectra by a 4800 Proteomics Analyzer (Applied Biosystems), and MS-based protein homology identification based on the TAIR genomic database, were according to Van Leene *et al.* (2010). Experimental background proteins were subtracted based on approximately 40 TAP experiments on wild type cultures and cultures expressing TAP-tagged mock proteins GUS, RFP and GFP (Van Leene *et al.*, 2010).

5.3 Bioinformatic analysis

With the PLAZA 2.5 bioinformatic tool, common down- or up-regulated genes were classified into significantly overrepresented (>2 fold, *P* < 0.05) gene ontology (GO) classes, only non-redundant classes are presented (Table S3) (Van Bel *et al.*, 2012).

5.4 RNA binding assays.

The coding sequence (CDS) of SPEN and KHD were amplified by PCR with HiFi DNA polymerase (KAPA Biosystems) and iProof high fidelidy PCR kit (Biorad), respectively, using an *Arabidopsis thaliana* cDNA library as template and the primers (providing also the required restriction enzyme cleavage sites) (Table S5).

The amplified PCR fragment of SPEN was digested with BamHI/SalI and cloned into the BamHI/SalI-digested *E. coli* expression plasmid pGEX-5X-1 (Amersham) providing an N-terminal glutathione S transferase (GST) resulting in the pGEX-5X-1-RRM-SPEN plasmid

for the RRM domain of SPEN. The obtained PCR fragment of KHD was digested with BamHI/SalI and cloned into the BamHI/SalI-digested *E. coli* expression plasmid pQE9 (Qiagen) providing an N-terminal 6×His-tag resulting in the pQE9-KHD-N plasmid for the N-end part of KHD containing 2 KH domains. All plasmid constructions were checked by DNA sequencing. For production of proteins the pGEX-5X-1-RRM-SPEN expression vector was transformed in *E. coli* BL21+pRARE cells. After induction by [1 mM] IPTG, the GST-tagged RRM-SPEN was purified by glutathione-sepharose affinity chromatography as previously described (Krohn *et al,* 2002). *E. coli* M15 cells were transformed with the pQE9-KHD-N expression vector. After induction by [1 mM] IPTG, the 6× His-tagged KHD-N was purified by metal-chelate chromatography using Ni-NTA agarose (Qiagen) from *E. coli* lysates essentially as described previously (Kammel *et al,* 2013). Using PD10 columns (Pharmacia) the purified proteins were collected in buffer (10 mM phosphate buffer, pH 7.0. 1 mM EDTA, 1 mM DTT, 0.5 mM PMSF) and the recombinant proteins were analysed by SDS-PAGE and mass spectrometry confirming their identity. RNA binding of the recombinant proteins was examined by electrophoretic mobility shift assays (EMSAs) using fluorescently-labelled RNA or unlabelled RNA and DNA oligonucleotides (Table S5) (Kammel *et al,* 2013). Different protein concentrations were incubated for 15 min with the Cy3-labeled ssRNA (25 nM) probe in a binding buffer (10 mM Hepes pH7.9, 3% Ficoll, 10 mM $MgCl_2$, 5 mM KCl, 200 mM NaCl, 1 mM EDTA, 0.5 mM DTT, 1 mM Spermidine, 0.1 mg/ml BSA). Binding reactions were analysed in 5% gels for GST-RRM-SPEN in 1× TBE and 7% (w/v) polyacrylamide gels for 6× His-KHD-N and the RNA was visualized by imaging using a Typhoon 8600 instrument (Amersham Biosciences). Competition-assays were done using constant concentration of protein (3 μM) and labelled ssRNA-probe and increasing concentrations of unlabelled ssRNA or ssDNA. dsRNA and dsDNA probe were obtained by hybridization of the single strand probe with their complement.

5.5   Confocal Microscopy and Multiprobe in situ Hybridization.

The localization of the fusion proteins 35S::GFP::SPEN and 35S::GFP::KHD were analysed by confocal microscope (Olympus, FV10 ASW) on primary roots of 5 day-old transgenic Arabidopsis seedlings grown in vertical position under continuous light. Multiprobes of *HUB1*, *SPEN* and *KHD* riboprobes were hybridized *in situ* on fixed 4 day-old Arabidopsis seedlings according to (Bruno *et al.*, 2011) with minor modifications, i.e.

the hybridization step was performed overnight at 55°C, and the mixture of primary and secondary antibodies was diluted 1:500.

5.6 Growth analysis and flowering time determination

Flowering time was determined *in vivo* as the number of days between germination and the initiation of floral stem elongation at 0.1cm height. The number of rosette leaves produced by the apical meristem was recorded at that time (n≥28). Leaf series were prepared from *in vitro* grown plants aligning all the rosette leaves on 1% agar plates (n=10) at 18 days. Leaves were photographed and scanned to measure leaf area by ImageJ 1.41.

5.7 Image acquisition, image processing and data analysis.

The image acquisition, image processing and data analysis procedures for the *in-vitro* growth analysis have been described elsewhere (Dhondt *et al.*,2014). For the *in-vivo* growth analysis, image acquisition was performed using a Canon EOS 550D slr cameras equipped with a Canon EF 35mm f/2 objective. Pictures were automatically captured daily by a Perl script (www.perl.org) using the gPhoto2 library (www.gphoto.org). Image preprocessing and segmentation for the seedling selection and growth analysis was performed with C++ scripts using the OpenCV image analysis library (www.opencv.org). Parsing of quantitative measurements and further data analysis was performed with Perl scripts (www.perl.org). Graphs of the calculated data were automatically plotted making use of the graphing utility gnuplot (www.gnuplot.info). Further details of the analysis will be published elsewhere.

5.8 Root growth analysis.

Seeds were germinated on ½ Murashige and Skoog medium supplemented with 1% (w/v) sucrose, 0.8% (w/v) agarose, pH 5.7. Seeds were surface sterilized and stratified at 4°C for two nights and moved to the growth chamber. Seedlings grown vertically at 21°C under 24-h light conditions (75 µmol m-2 s-1) were used for root analysis. The root meristem size was determined 5-days-after-germination as the number of cells in the cortex cell file from the QC to the first elongated cell (Casamitjana-Martínez *et al.*, 2003). The samples were mounted with clearing solution (80 g chloral hydrate, 30 ml glycerol and 10 ml dH2O) and observed immediately. Root length was marked at 10-days-after-germination and measured with the ImageJ software (http://rsbweb.nih.gov/ij/). Means

between samples were compared by a two-tailed Student's t-test, variances were compared using an ANOVA.

5.9 RNA methods.

RNA was isolated using RNeasy Plant Kit (Qiagen) with on-column DNase digestion, manufacturer's protocol was modified by two additional washes of RNeasy spin columns with the RPE buffer. cDNA was synthesised with iScript cDNA Synthesis Kit (BIO-RAD, 170-8891).

Real-time PCR was performed in technical triplicate using the LightCycler 480 SYBR Green I Master reagent and the Janus robot (PerkinElmer) for pipetting. The LightCycler 480 Real-Time PCR System was used for amplification (95°C for 10 min, 45 cycles of 95°C/10 s, 60°C/15 s, 72°C/30 s followed by melting curve analysis). The QPCR results were analysed using the qBase Plus software (Biogazelle). The PP2A (At1g13320) and UBC (At5g25760) genes were used as references for gene expression normalization, primer sequences are in Table S4. For transcriptome, RNA was extracted from shoot apices of 10-day-old seedlings. After library preparation by TruSeq, RNA was sequenced on Illumina HiSeq.

5.10 ChIP-qPCR.

ChIP was done according to the protocol of Bowler *et al.* (2004) using two week old seedlings. The isolated chromatin was sonicated in SONICS Vibra-cell sonicator with four 15 s pulses at 20% amplitude and immunoprecipitated using 5 µg of H2BUb antibodies (Medimabs, MM-029). Protein A Agarose (Millipore, 16-157) was used to collect immunoprecipitated chromatin. After reverse cross-linking and proteinase K digestion DNA was purified with MinElute PCR Purification Kit (Qiagen) and eluted with elution buffer supplemented with RNaseA (10 µg/ml). Samples were analysed by real-time qPCR with primers in the promoter and coding regions of the *FLC* (Cao *et al.*, 2008), *CCA1*, QQS and PCNA2 (Table S5) genes and the amount of the immunoprecipitated DNA was calculated relative to the input.

5.11 Detection and quantification of polyadenylated COOLAIR

For non-vernalized samples, seedlings were grown in long day conditions for 10 days at 21˚C. For vernalisation, seedlings were grown 10 DAG in normal conditions (long day,

21˚C), then transferred for 7 days to cold (short day 8h light, 16h darkness at 7˚C) and finally recovered for 7days in normal conditions. Primer pairs for spliced FLC (FLC2), total COOLAIR (COOLAIR), proximal poly(A) COOLAIR (proxCOOLAIR) and distal poly(A) COOLAIR (distCOOLAIR) are described in Table S4 (Marquadt *et al.*, 2014) (Fig. 4A).

5.12 Detection and quantification of alternatively spliced CCA1 over a 48h time course

Seedlings were grown in long day condition for 15 days at 21˚C then transferred at time point ZT0 in continuous light condition at 21˚C or 6˚C. Seedling pools were harvested in triplicate every 4h from time point ZT0 until ZT48. Primer pairs were used to identify the two splice variant CCA1α and CCA1β (Seo *et al.*, 2012) (Table S5 and Fig.3D).

5.13 Yeast Two-Hybrid Analysis.

Constructs used for Y2H were obtained by cloning cDNAs of HUB1, HUB2, SPEN, SPEN N-terminus (761 aa including RRM domain) and SPEN C-terminus (488 aa including SPOC domain) using Gateway Technology (Life Technologies). Constructs were introduced by an LR recombination into the pDEST^{tm}22 and pDEST^{tm}32 destination vectors resulting in fusions to the GAL4 activation domain (AD) and GAL4 binding domain (BD), respectively (ProQuest^{TM} Two-HybridSystem, Life Technologies). All plasmids were transformed into yeast strains with opposite mating types MaV203 MATa and MATα. Transformed yeast strains were selected for the presence of pDEST22 or pDEST32 vector, the abundance of the fusion proteins was assessed by Western-blot and the absence of the constructs self-activation was verified in a colony-lift filter assay using X-Gal as substrate. Diploid transformants were tested for positive interactions by growing the mating strains in SD-Leucine-Tryptophan-Histidine medium with increasing concentrations (3 mM and 10 mM) of 3-Amino-1,2,4-Triazole (3-AT) assessing the strength of interactions. The provided constructs of the interacting proteins DmDP and DmE2F were used as the positive control and the negative control consisted of a yeast strain containing an empty AD vector mated with the BD fusion of the protein of interest. For each interaction three independent biological repeats were performed.

6 References

Alonso, J.M., Stepanova, A.N., Leisse, T.J., Kim, C.J., Chen, H., Shinn, P., Stevenson, D.K., Zimmerman, J., Barajas, P., Cheuk, R., Gadrinab, C., others, 2003. Genome-Wide Insertional Mutagenesis of Arabidopsis thaliana. Science 301, 653–657. https://doi.org/10.1126/science.1086391

Antosz, W., Pfab, A., Ehrnsberger, H.F., Holzinger, P., Köllen, K., Mortensen, S.A., Bruckmann, A., Schubert, T., Längst, G., Griesenbeck, J., Schubert, V., Grasser, M., Grasser, K.D., 2017. The Composition of the Arabidopsis RNA Polymerase II Transcript Elongation Complex Reveals the Interplay between Elongation and mRNA Processing Factors. The Plant Cell 29, 854–870. https://doi.org/10.1105/tpc.16.00735

Ariyoshi, M., Schwabe, J.W., 2003. A conserved structural motif reveals the essential transcriptional repression function of Spen proteins and their role in developmental signalling. Genes & development 17, 1909–1920. https://doi.org/10.1101/gad.266203

Bortolini Silveira, A., Trontin, C., Cortijo, S., Barau, J., Del Bem, L.E.V., Loudet, O., Colot, V., Vincentz, M., 2013. Extensive Natural Epigenetic Variation at a De Novo Originated Gene. PLoS Genetics 9, e1003437. https://doi.org/10.1371/journal.pgen.1003437

Bourbousse, C., Ahmed, I., Roudier, F., Zabulon, G., Blondet, E., Balzergue, S., Colot, V., Bowler, C., Barneche, F., 2012. Histone H2B Monoubiquitination Facilitates the Rapid Modulation of Gene Expression during Arabidopsis Photomorphogenesis. PLoS Genetics 8, e1002825. https://doi.org/10.1371/journal.pgen.1002825

Bowler, C., Benvenuto, G., Laflamme, P., Molino, D., Probst, A.V., Tariq, M., Paszkowski, J., 2004. Chromatin techniques for plant cells. The Plant Journal 39, 776–789. https://doi.org/10.1111/j.1365-313X.2004.02169.x

Bruno, L., Muto, A., Spadafora, N.D., Iaria, D., Chiappetta, A., Van Lijsebettens, M., Bitonti, M.B., 2011. Multi-probe in situ hybridization to whole mount Arabidopsis seedlings. The International Journal of Developmental Biology 55, 197–203. https://doi.org/10.1387/ijdb.103132lb

Bürckstümmer, T., Bennett, K.L., Preradovic, A., Schütze, G., Hantschel, O., Superti-Furga, G., Bauch, A., 2006. An efficient tandem affinity purification procedure for interaction proteomics in mammalian cells. Nature Methods 3, 1013–1019. https://doi.org/10.1038/nmeth968

Cao, Y., Dai, Y., Cui, S., Ma, L., 2008. Histone H2B Monoubiquitination in the Chromatin of FLOWERING LOCUS C Regulates Flowering Time in Arabidopsis. THE PLANT CELL ONLINE 20, 2586–2602. https://doi.org/10.1105/tpc.108.062760

Casamitjana-Martınez, E., Hofhuis, H.F., Xu, J., Liu, C.-M., Heidstra, R., Scheres, B., 2003. Root-specific CLE19 overexpression and the sol1/2 suppressors implicate a CLV-like pathway in the control of Arabidopsis root meristem maintenance. Current Biology 13, 1435–1441.

Chen, C., Huang, H., Wu, C.H., 2017. Protein Bioinformatics Databases and Resources. Methods Molecular Biology 3–39. https://doi.org/10.1007/978-1-4939-6783-4_1.

Chen, T., Cui, P., Chen, H., Ali, S., Zhang, S., Xiong, L., 2013. A KH-Domain RNA-Binding Protein Interacts with FIERY2/CTD Phosphatase-Like 1 and Splicing Factors and Is Important for Pre-mRNA Splicing in Arabidopsis. PLoS Genetics 9, e1003875. https://doi.org/10.1371/journal.pgen.1003875

Clauw, P., Coppens, F., De Beuf, K., Dhondt, S., Van Daele, T., Maleux, K., Storme, V., Clement, L., Gonzalez, N., Inzé, D., 2015. Leaf Responses to Mild Drought Stress in Natural Variants of Arabidopsis. Plant Physiology 167, 800–816. https://doi.org/10.1104/pp.114.254284

Csorba, T., Questa, J.I., Sun, Q., Dean, C., 2014. Antisense *COOLAIR* mediates the coordinated switching of chromatin states at *FLC* during vernalisation. Proceedings of the National Academy of Sciences 111, 16160–16165. https://doi.org/10.1073/pnas.1419030111

Cui, Z., Xu, Q., Wang, X., 2014. Regulation of the circadian clock through pre-mRNA splicing in Arabidopsis. Journal of Experimental Botany 65, 1973–1980. https://doi.org/10.1093/jxb/eru085

Felsenstein, J., 1987. Estimation of hominoid phylogeny from a DNA hybridization data set. Journal of molecular evolution 26, 123–131.

Feng, J., Shen, W.-H., 2014. Dynamic regulation and function of histone monoubiquitination in plants. Frontiers in Plant Science 5. https://doi.org/10.3389/fpls.2014.00083

Fleury, D., Himanen, K., Cnops, G., Nelissen, H., Boccardi, T.M., Maere, S., Beemster, G.T.S., Neyt, P., Anami, S., Robles, P., Micol, J.L., Inze, D., Van Lijsebettens, M., 2007. The Arabidopsis thaliana Homolog of Yeast BRE1 Has a Function in Cell Cycle Regulation during Early Leaf and Root Growth. THE PLANT CELL ONLINE 19, 417–432. https://doi.org/10.1105/tpc.106.041319

Fong, N., Kim, H., Zhou, Y., Ji, X., Qiu, J., Saldi, T., Diener, K., Jones, K., Fu, X.-D., Bentley, D.L., 2014. Pre-mRNA splicing is facilitated by an optimal RNA polymerase II elongation rate. Genes & Development 28, 2663–2676. https://doi.org/10.1101/gad.252106.114

Hérissant, L., Moehle, E.A., Bertaccini, D., Van Dorsselaer, A., Schaeffer-Reiss, C., Guthrie, C., Dargemont, C., 2014. H2B ubiquitylation modulates spliceosome assembly and function in budding yeast: Histone marks and mRNA splicing. Biology of the Cell 106, 126–138. https://doi.org/10.1111/boc.201400003

Himanen, K., Woloszynska, M., Boccardi, T.M., De Groeve, S., Nelissen, H., Bruno, L., Vuylsteke, M., Van Lijsebettens, M., 2012. Histone H2B monoubiquitination is required to reach maximal transcript levels of circadian clock genes in Arabidopsis: *HUB1 regulates transcript levels*. The Plant Journal 72, 249–260. https://doi.org/10.1111/j.1365-313X.2012.05071.x

Hornyik, C., Terzi, L.C., Simpson, G.G., 2010. The Spen Family Protein FPA Controls Alternative Cleavage and Polyadenylation of RNA. Developmental Cell 18, 203–213. https://doi.org/10.1016/j.devcel.2009.12.009

Ietswaart, R., Wu, Z., Dean, C., 2012. Flowering time control: another window to the connection between antisense RNA and chromatin. Trends in Genetics 28, 445–453. https://doi.org/10.1016/j.tig.2012.06.002

Kammel, C., Thomaier, M., Sørensen, B.B., Schubert, T., Längst, G., Grasser, M., Grasser, K.D., 2013. Arabidopsis DEAD-Box RNA Helicase UAP56 Interacts with Both RNA and DNA as well as with mRNA Export Factors. PLoS ONE 8, e60644. https://doi.org/10.1371/journal.pone.0060644

Köster, T., Marondedze, C., Meyer, K., Staiger, D., 2017. RNA-Binding Proteins Revisited – The Emerging Arabidopsis mRNA Interactome. Trends in Plant Science. https://doi.org/10.1016/j.tplants.2017.03.009

Krohn, N.M., 2002. Specificity of the Stimulatory Interaction between Chromosomal HMGB Proteins and the Transcription Factor Dof2 and Its Negative Regulation by Protein Kinase CK2-mediated Phosphorylation. Journal of Biological Chemistry 277, 32438–32444. https://doi.org/10.1074/jbc.M203814200

Kumar, S., Stecher, G., Tamura, K., 2016. MEGA7: Molecular Evolutionary Genetics Analysis Version 7.0 for Bigger Datasets. Molecular Biology and Evolution 33, 1870–1874. https://doi.org/10.1093/molbev/msw054

Liu, Y., Koornneef, M., Soppe, W.J.J., 2007. The Absence of Histone H2B Monoubiquitination in the Arabidopsis hub1 (rdo4) Mutant Reveals a Role for Chromatin Remodeling in Seed Dormancy. THE PLANT CELL ONLINE 19, 433–444. https://doi.org/10.1105/tpc.106.049221

Lolas, I.B., Himanen, K., Grønlund, J.T., Lynggaard, C., Houben, A., Melzer, M., Van Lijsebettens, M., Grasser, K.D., 2010. The transcript elongation factor FACT affects Arabidopsis vegetative and reproductive development and genetically interacts with HUB1/2. The Plant Journal 61, 686–697. https://doi.org/10.1111/j.1365-313X.2009.04096.x

Long, L., Thelen, J.P., Furgason, M., Haj-Yahya, M., Brik, A., Cheng, D., Peng, J., Yao, T., 2014. The U4/U6 Recycling Factor SART3 Has Histone Chaperone Activity and Associates with USP15 to Regulate H2B Deubiquitination. Journal of Biological Chemistry 289, 8916–8930. https://doi.org/10.1074/jbc.M114.551754

Luco, R.F., Allo, M., Schor, I.E., Kornblihtt, A.R., Misteli, T., 2011. Epigenetics in Alternative Pre-mRNA Splicing. Cell 144, 16–26. https://doi.org/10.1016/j.cell.2010.11.056

Luger, K., Mäder, A.W., Richmond, R.K., Sargent, D.F., Richmond, T.J., 1997. Crystal structure of the nucleosome core particle at 2.8 A ̊ resolution. Nature 389, 18.

Marquardt, S., Raitskin, O., Wu, Z., Liu, F., Sun, Q., Dean, C., 2014. Functional Consequences of Splicing of the Antisense Transcript COOLAIR on FLC Transcription. Molecular Cell 54, 156–165. https://doi.org/10.1016/j.molcel.2014.03.026

Mockler, T.C., Yu, X., Shalitin, D., Parikh, D., Michael, T.P., Liou, J., Huang, J., Smith, Z., Alonso, J.M., Ecker, J.R., others, 2004. Regulation of flowering time in Arabidopsis by K homology domain proteins. Proceedings of the National Academy of Sciences of the United States of America 101, 12759–12764. https://doi.org/10.1073/pnas.0404552101

Moehle, E.A., Ryan, C.J., Krogan, N.J., Kress, T.L., Guthrie, C., 2012. The Yeast SR-Like Protein Npl3 Links Chromatin Modification to mRNA Processing. PLoS Genetics 8, e1003101. https://doi.org/10.1371/journal.pgen.1003101

Nagel, D.H., Doherty, C.J., Pruneda-Paz, J.L., Schmitz, R.J., Ecker, J.R., Kay, S.A., 2015. Genome-wide identification of CCA1 targets uncovers an expanded clock network in *Arabidopsis*. Proceedings of the National Academy of Sciences 112, E4802–E4810. https://doi.org/10.1073/pnas.1513609112

Nei, M., Kumar, S., 2000. Molecular Evolution and Phylogenetics. Oxford university press.
Portolés, S., Más, P., 2007. Altered oscillator function affects clock resonance and is responsible for the reduced day-length sensitivity of CKB4 overexpressing plants: CKB4 and clock resonance with the environment. The Plant Journal 51, 966–977. https://doi.org/10.1111/j.1365-313X.2007.03186.x

Reichel, M., Liao, Y., Rettel, M., Ragan, C., Evers, M., Alleaume, A.-M., Horos, R., Hentze, M.W., Preiss, T., Millar, A.A., 2016. In Planta Determination of the mRNA-Binding Proteome of Arabidopsis Etiolated Seedlings. The Plant Cell 28, 2435–2452. https://doi.org/10.1105/tpc.16.00562

Rigaut, G., Shevchenko, A., Rutz, B., Wilm, M., Mann, M., Séraphin, B., 1999. A generic protein purification method for protein complex characterization and proteome exploration. Nature biotechnology 17, 1030–1032. https://doi.org/10.1038/13732

Ripoll, J.J., Rodríguez-Cazorla, E., González-Reig, S., Andújar, A., Alonso-Cantabrana, H., Perez-Amador, M.A., Carbonell, J., Martínez-Laborda, A., Vera, A., 2009. Antagonistic interactions between Arabidopsis K-homology domain genes uncover PEPPER as a positive regulator of the central floral repressor FLOWERING LOCUS C. Developmental Biology 333, 251–262. https://doi.org/10.1016/j.ydbio.2009.06.035

Rodríguez-Cazorla, E., Ripoll, J.J., Andújar, A., Bailey, L.J., Martínez-Laborda, A., Yanofsky, M.F., Vera, A., 2015. K-homology Nuclear Ribonucleoproteins Regulate Floral Organ Identity and Determinacy in Arabidopsis. PLOS Genetics 11, e1004983. https://doi.org/10.1371/journal.pgen.1004983

Rosso, M.G., Li, Y., Strizhov, N., Reiss, B., Dekker, K., Weisshaar, B., 2003. An Arabidopsis thaliana T-DNA mutagenized population (GABI-Kat) for flanking sequence tag-based reverse genetics. Plant molecular biology 53, 247–259. https://doi.org/10.1023/B:PLAN.0000009297.37235.4a

Roudier, F., Ahmed, I., Bérard, C., Sarazin, A., Mary-Huard, T., Cortijo, S., Bouyer, D., Caillieux, E., Duvernois-Berthet, E., Al-Shikhley, L., others, 2011. Integrative epigenomic mapping defines four main chromatin states in Arabidopsis. The EMBO journal 30, 1928–1938. https://doi.org/10.1038/emboj.2011.103

Rzhetsky, A., Nei, M., 1992. A simple method for estimating and testing minimum-evolution trees. https://doi.org/no DOI

Saitou, N., Nei, M., 1987. The neighbor-joining method: a new method for reconstructing phylogenetic trees. Molecular biology and evolution 4, 406–425. https://doi.org/10.1093/oxfordjournals.molbev.a040454

Salome, P.A., McClung, C.R., 2005. PSEUDO-RESPONSE REGULATOR 7 and 9 Are Partially Redundant Genes Essential for the Temperature Responsiveness of the Arabidopsis Circadian Clock. THE PLANT CELL ONLINE 17, 791–803. https://doi.org/10.1105/tpc.104.029504

Schaffer, R., Landgraf, J., Accerbi, M., Simon, V., Larson, M., Wisman, E., 2001. Microarray analysis of diurnal and circadian-regulated genes in Arabidopsis. The Plant Cell 13, 113–123. https://doi.org/10.1105/tpc.13.1.113

Schmitz, R.J., Tamada, Y., Doyle, M.R., Zhang, X., Amasino, R.M., 2009. Histone H2B Deubiquitination Is Required for Transcriptional Activation of FLOWERING LOCUS C and for Proper Control of Flowering in Arabidopsis. PLANT PHYSIOLOGY 149, 1196–1204. https://doi.org/10.1104/pp.108.131508

Seo, P.J., Park, M.-J., Lim, M.-H., Kim, S.-G., Lee, M., Baldwin, I.T., Park, C.-M., 2012. A Self-Regulatory Circuit of CIRCADIAN CLOCK-ASSOCIATED1 Underlies the Circadian Clock

Regulation of Temperature Responses in *Arabidopsis*. The Plant Cell 24, 2427–2442. https://doi.org/10.1105/tpc.112.098723

Skirycz, A., Vandenbroucke, K., Clauw, P., Maleux, K., De Meyer, B., Dhondt, S., Pucci, A., Gonzalez, N., Hoeberichts, F., Tognetti, V.B., 2011. Survival and growth of Arabidopsis plants given limited water are not equal. Nature biotechnology 29, 212–214. https://doi.org/10.1038/nbt.1800

Swiezewski, S., Liu, F., Magusin, A., Dean, C., 2009. Cold-induced silencing by long antisense transcripts of an Arabidopsis Polycomb target. Nature 462, 799–802. https://doi.org/10.1038/nature08618

Tamura, K., Peterson, D., Peterson, N., Stecher, G., Nei, M., Kumar, S., 2011. MEGA5: Molecular Evolutionary Genetics Analysis Using Maximum Likelihood, Evolutionary Distance, and Maximum Parsimony Methods. Molecular Biology and Evolution 28, 2731–2739. https://doi.org/10.1093/molbev/msr121

Van Bel, M., Proost, S., Wischnitzki, E., Movahedi, S., Scheerlinck, C., Van de Peer, Y., Vandepoele, K., 2012. Dissecting plant genomes with the PLAZA comparative genomics platform. Plant Physiol 158, 590–600.

Van Leene, J., Eeckhout, D., Persiau, G., Van De Slijke, E., Geerinck, J., Van Isterdael, G., Witters, E., De Jaeger, G., 2011. Isolation of Transcription Factor Complexes from Arabidopsis Cell Suspension Cultures by Tandem Affinity Purification, in: Yuan, L., Perry, S.E. (Eds.), Plant Transcription Factors. Humana Press, Totowa, NJ, pp. 195–218. https://doi.org/10.1007/978-1-61779-154-3_11

Van Leene, J., Hollunder, J., Eeckhout, D., Persiau, G., Van De Slijke, E., Stals, H., Van Isterdael, G., Verkest, A., Neirynck, S., Buffel, Y., De Bodt, S., Maere, S., Laukens, K., Pharazyn, A., Ferreira, P.C.G., Eloy, N., Renne, C., Meyer, C., Faure, J.-D., Steinbrenner, J., Beynon, J., Larkin, J.C., Van de Peer, Y., Hilson, P., Kuiper, M., De Veylder, L., Van Onckelen, H., Inzé, D., Witters, E., De Jaeger, G., 2010. Targeted interactomics reveals a complex core cell cycle machinery in Arabidopsis thaliana. Molecular Systems Biology 6. https://doi.org/10.1038/msb.2010.53

Van Leene, J., Stals, H., Eeckhout, D., Persiau, G., Van De Slijke, E., Van Isterdael, G., De Clercq, A., Bonnet, E., Laukens, K., Remmerie, N., others, 2007. A tandem affinity purification-based technology platform to study the cell cycle interactome in Arabidopsis thaliana. Molecular & Cellular Proteomics 6, 1226–1238. https://doi.org/10.1074/mcp.M700078-MCP200

Van Lijsebettens, M., Grasser, K.D., 2014. Transcript elongation factors: shaping transcriptomes after transcript initiation. Trends in Plant Science 19, 717–726. https://doi.org/10.1016/j.tplants.2014.07.002

Xu, L., Ménard, R., Berr, A., Fuchs, J., Cognat, V., Meyer, D., Shen, W.-H., 2009. The E2 ubiquitin-conjugating enzymes, AtUBC1 and AtUBC2, play redundant roles and are involved in activation of *FLC* expression and repression of flowering in *Arabidopsis thaliana*. The Plant Journal 57, 279–288. https://doi.org/10.1111/j.1365-313X.2008.03684.x

Zhang, X., Henriques, R., Lin, S.-S., Niu, Q.-W., Chua, N.-H., 2006. Agrobacterium-mediated transformation of Arabidopsis thaliana using the floral dip method. Nature Protocols 1, 641–646. https://doi.org/10.1038/nprot.2006.97

Zuckerkandl, E., Pauling, L., 1965. Evolutionary divergence and convergence in proteins. Evolving genes and proteins 97, 97–166. https://doi.org/no DOI

7 Supplemental figures and tables
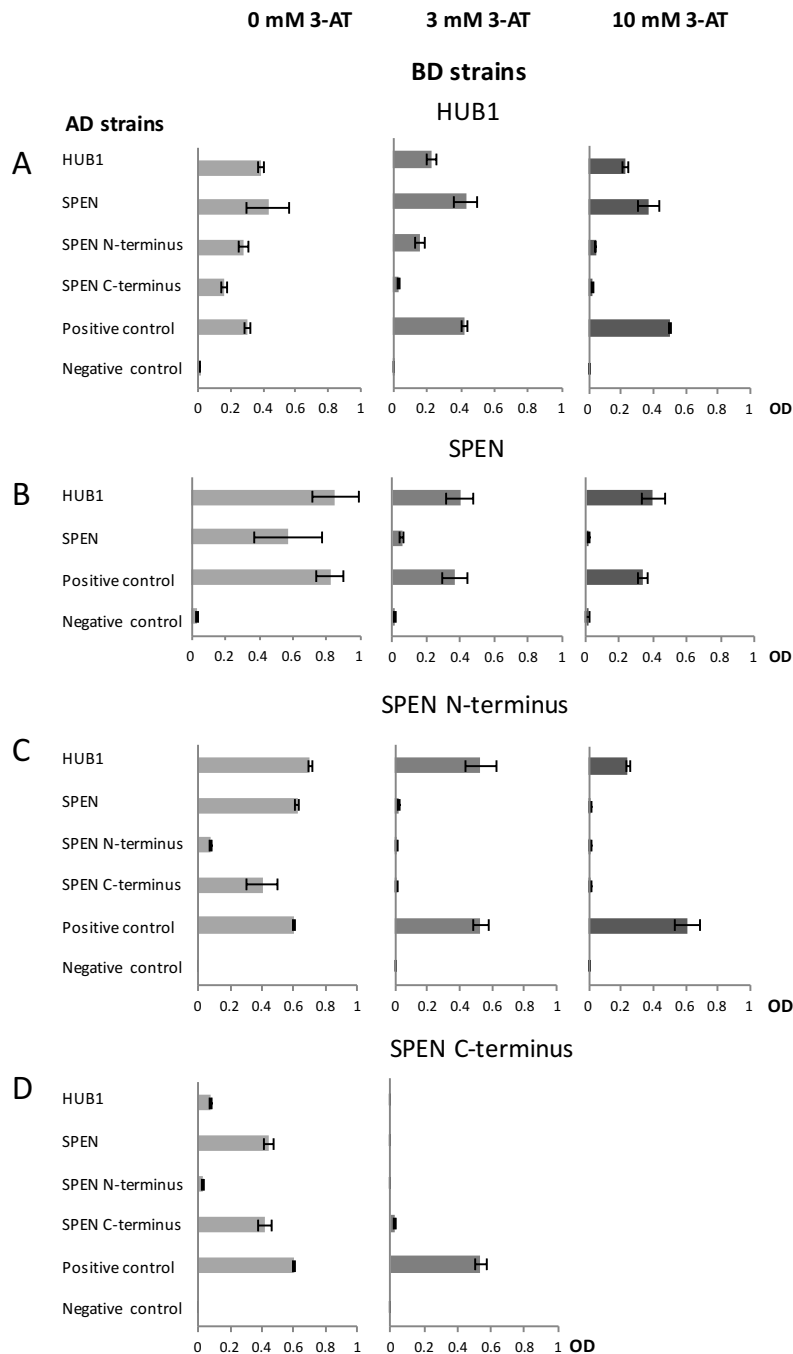
Fig. S1. Yeast two-hybrid interactions between HUB1, SPEN, SPEN N-terminus and SPEN C-terminus.

The yeast strains expressing the proteins fused to AD domain (AD strains, ordinate axis) or BD domain (BD strains, panels A-D) were mated pairwise to test for direct interaction between proteins which permits yeast growth on selective medium and was quantified as the optical density (OD_{600}) of the culture. Different concentrations of 3-Amino 1,2,4, Triaxole (AT) were applied to medium to detect the high-affinity binding between two interactors which allows yeast to survive increased concentrations of 3-AT. For each interaction three independent biological repeats were performed.
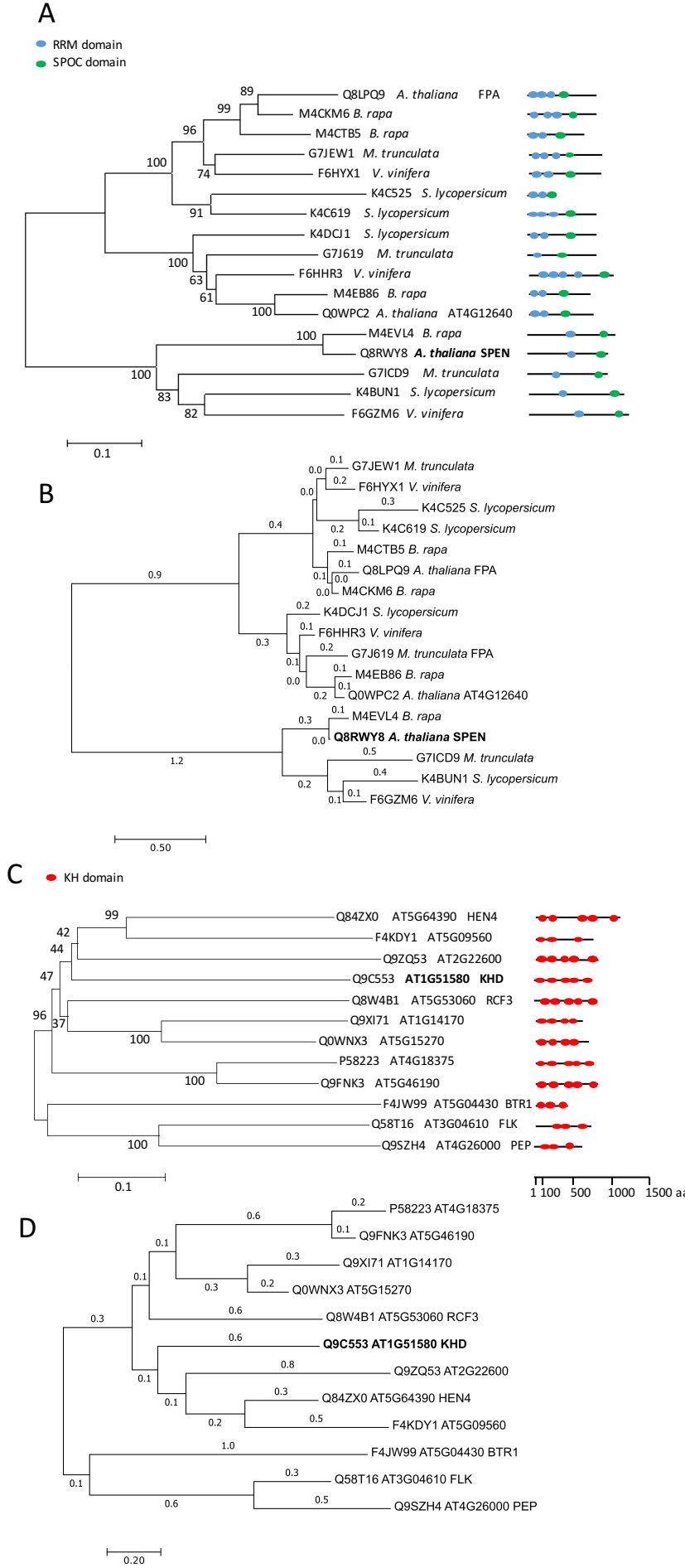
Fig. S2. Evolutionary relationships of taxa using two methods.
The evolutionary history was inferred using the Neighbor-Joining method (A&C) (Saitou and Nei, 1987) or the Minimum Evolution method (B &D) (Rzhetsky and Nei, 1992). Optimal tree with the sum of branch length = 3.18684050 (A), = 4.81273120 (B), = 3.59573317 (C) and = 5.86333275 (D) is shown. The analysis involved 17 (*A&B*) and 12 (*C&D*) amino acid sequences. All positions containing gaps and missing data were eliminated. There was a total of 154 (*A&B*) and 260 (*C&D*) positions in the final dataset. Evolutionary analyses were conducted in MEGA5 (A&C)(Tamura *et al.*, 2011) and in MEGA7 (B&D) (Kumar *et al.,* 2016).
(A&C) The percentage of replicate trees in which the associated taxa clustered together in the bootstrap test (500 replicates) are shown next to the branches (Felsenstein, 1987). The tree is drawn to scale, with branch lengths in the same units as those of the evolutionary distances used to infer the phylogenetic tree. The evolutionary distances were computed using the p-distance method (Nei and Kumar, 2000) and are in the units of the number of amino acid differences per site.
(B&D)The tree is drawn to scale, with branch lengths (next to the branches) in the same units as those of the evolutionary distances used to infer the phylogenetic tree. The evolutionary distances were computed using the Poisson correction method (Zuckerkandl and Pauling, 1965) and are in the units of the number of amino acid substitutions per site. The ME tree was searched using the Close-Neighbor-Interchange (CNI) algorithm (Nei and Kumar, 2000) at a search level of 1. The Neighbor-joining algorithm (Saitou and Nei, 1987) was used to generate the initial tree.
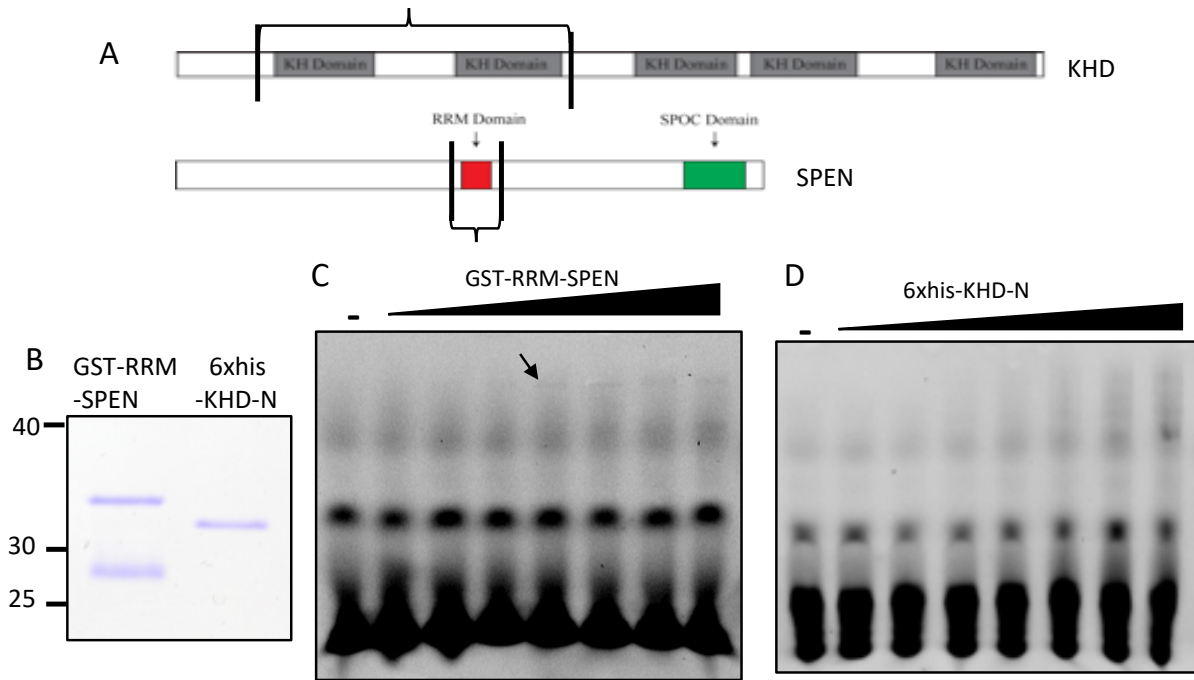
Fig. S3. Protein purification and dsRNA EMSA.
(A). Scheme of SPEN and KHD proteins with functional domains. Brace indicates the part that was overexpressed in *E.coli* and represented in the purified protein fraction used for EMSA. (B). 12% SDS acrylamide gel of 0.3μM of GST-RRM-SPEN and his-KHD-N purified protein, stained by Coomassie Brilliant Blue. Lane 1 upper band GST-RRM-SPEN 36kDa, lower band GST 27kDa; lane 2 6xhis-KHD-N 31kDa. (C-D). Comparison of binding affinity of GST-RRM-SPEN (C) or 6xhis-KHD-N (D) to dsRNA (repetition ≥ 6). For the EMSA the Cy3-labeled 25 bp nucleotide fragment was incubated either in the absence (lanes 1) or in the presence of increasing concentrations of the protein (0.1μM, 0.2 μM, 0.5 μM, 1μM, 2 μM, 3μM, 5 μM; lanes 2–8, respectively) and run on a 5% (C) or 7% (D) native acrylamide gel.
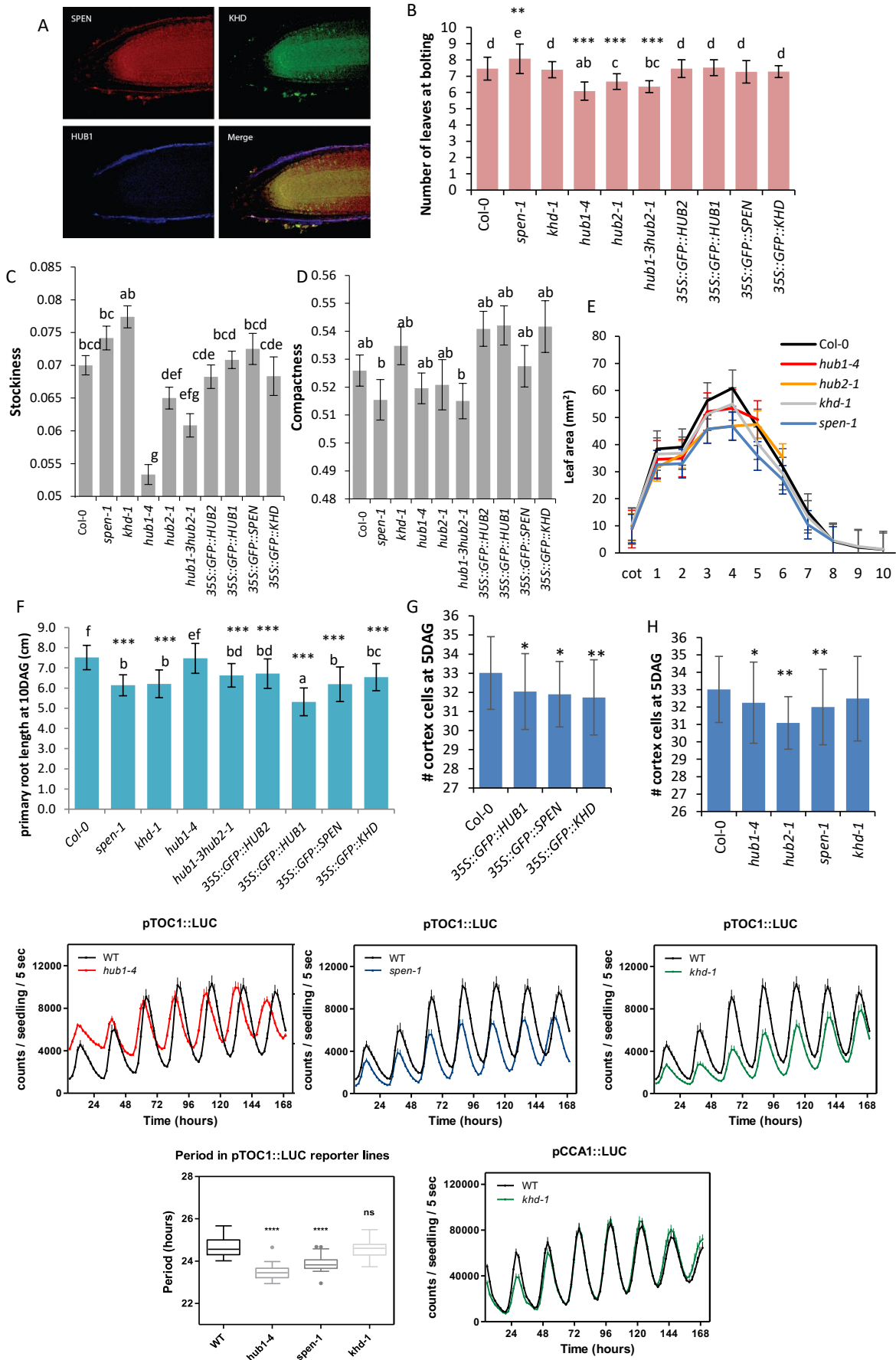
Fig. S4. Expression patterns in the root and phenotypes in leaf, root, diurnal clock

(A). Whole mount, multi-probe in situ hybridization of the root tip. Superposition of the expression patterns shows no coexpression for the three genes but *SPEN* and *KHD* are coexpressed in the cortex, stele and root apical meristem, *SPEN* is coexpressed with HUB1 in the epidermal cell layer. (B). Number of rosette leaves at bolting ($n \geq 28$). Ordinary one-way ANOVA with 95% confidence shows a significant difference between the genotypes (***P < 0.001), represented by the letters. Three biological repeats were performed. (C) Stockiness calculated at 23 DAS. (D) Compactness of the rosette calculated at 23 DAS. (E). Leaf series analysis of three biological repeats of *in vitro* grown transgenic lines at 21 DAS. (F) Primary root length at 10 days after germination ($n \geq 15$). Ordinary one-way ANOVA with 95% confidence shows a significant difference between the genotypes (***P < 0.001), represented by the letters. Three biological repeats were performed (G). Root meristem size measured by number of cortex cells at 5 DAG overexpression lines ($n > 15$). Three biological repeats were performed (H). Root meristem size measured by number of cortex cells at 5 DAG in mutants ($n \geq 10$). Three biological repeats were performed. (I). Bioluminescence analysis of *pCCA1::LUC* , *khd-1* and *pTOC1::LUC*, *hub1-4*, *spen-1* and *khd-1* mutants. Period estimates of *hub1-4*, *spen-1* and *khd-1* in *pTOC1::LUC*. Luminescence was recorded under constant white light conditions following synchronization under LD. Data are represented as the means +SEM of the luminescence of at least 12 individual seedlings. Ordinary one-way ANOVA with 95% confidence shows the relevance of the differences within periods (**** *P* < 0.0001). ns: not significant. (B and G) Error bars represent standard deviation. Asterisks indicate statistically significant differences (*P < 0.05, **P < 0.01, ***P < 0.001). (C-D) Error bars represent standard error. Ordinary one-way ANOVA with 95% confidence shows a significant difference between the genotypes.
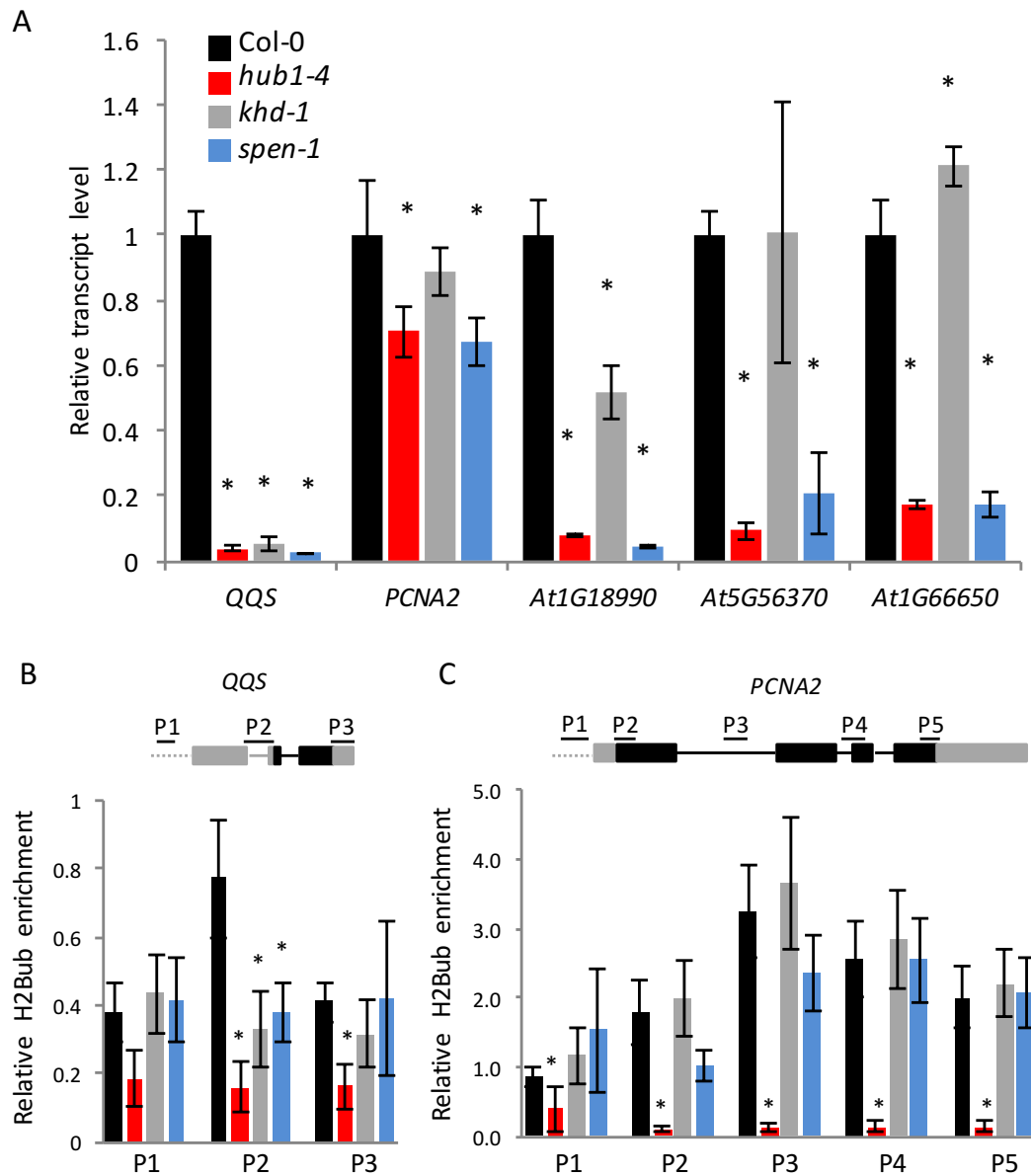
Fig. S5. Expression and H2Bub of selected genes
(A). Relative expression level of selected genes by qPCR. (B) and (C). Relative H2Bub enrichment measured by ChIP assay with H2Bub antibodies of selected genes. Two biological repeats were performed. The Col-0 line and *hub1-4, khd-1* and *spen-1* mutants from the SALK collection were used.

Table S1 – Protein Identification details obtained by tandem affinity purification with the 4800 MALDI TOF/TOF^{TM} Proteomics analyzer (AB SCIEX) and the GPS explorer v3.6 (AB SCIEX) software package combined with search engine Mascot version 2.1 (Matrix Science) and database TAIR8.
Column headers for Protein and Peptide data are explained below.

Protein score: The score calculated by the Mascot search engine for each protein. This score is based on the probability that peptide mass matches are non-random events. If the Protein Score is equal to or greater than the Mascot® Significance Level calculated for the database search, the protein match is considered to be statistically non-random at the 95% confidence interval. Protein score = -10*Log(P), where P is the probability that the observed match is a random event. **Expect**: Protein score expectation value. **RMS error (ppm):** RMS error of the set of matched mass values, in ppm. **Sequence coverage %:** Percentage of protein sequence covered by assigned peptide matches. **Unique peptides**: The number of peptides with unique sequences matching the selected protein. **Total Ion Score**: A score calculated by weighting Ion Scores for all individual peptides matched to a given protein. **Peptide Number:** Peptide index number within the list of peptides associated with a given protein. **Start**: The starting position of the peptide in the protein. **End:** The ending position of the peptide in the protein. **Observed**: The observed monoisotopic mass of the peptide in the spectrum (m/z). **Mr (Exp)**: The experimental mass of the peptide calculated from the observed m/z value. **Mr (Calc)**: The theoretical mass of the peptide based on its sequence. **Delta (Da)**: The difference between the theoretical (Mr (Calc)) and experimental (Mr (Exp)) masses, in Daltons. **Miss**: Number of missed Trypsin cleavage sites. **Ions score**: The Ions Score is calculated by the Mascot search engine for each peptide matched from MS/MS peak lists. This score is based on the probability that ion fragmentation matches are non-random events. If the Ion Score is equal to or greater than the Mascot® Significance Level calculated for the database search, the peptide match is considered to be statistically non-random at the 95% confidence interval. Ions score = -10*Log(P), where P is the probability that the observed match is a random event. **Peptide:** The amino acid sequence of the selected peptide. **Variable Modification**: Variable modification type on the peptide.

Id nr	Bait	Tag	Identified protein			PMF data					MSMS data												Variable Modification
			Locus	Name	# Found/ # exp	Protein Score	Expect	RMS error (ppm)	Sequence coverage %	Unique Peptides	Total Ion Score	Peptide Number	Start	End	Observed	Mr(Exp)	Mr(Calc)	Delta (Da)	Miss	Ions Score	Expect	Peptide	
1	HUB1pm	N-TAP	AT2G44950	HUB1	3/3	177	6.5E-14	12	8	7	165	1	40	51	1389.76	1388.75	1388.77	-0.02	0	53	9.4E-05	K.LDTAVLQFQNLK.L	
1												2	13	27	1501.75	1500.74	1500.76	-0.01	0	112	1.5E-10	R.HFSSISPSEAAAAVK.K	
2	HUB1	N-TAP	AT2G44950	HUB1	2/2	514	1.3E-47	7	37	29	332	1	312	320	945.53	944.52	944.53	-0.01	0	42	2.3E-03	K.ELTVLASGR.L	
2												2	667	675	1035.58	1034.58	1034.58	0.00	0	33	1.0E-02	K.LFLEGITSR.Q	
2												3	486	497	1304.66	1303.65	1303.66	0.00	0	41	2.4E-03	R.ADVQSLSGVLCR.K	
2												4	179	190	1506.79	1505.79	1505.79	0.00	1	66	5.8E-06	R.CLKDELYPTVLR.T	
2												5	455	468	1584.74	1583.73	1583.73	0.00	0	41	1.2E-03	K.ALISSFPEEMSSMR.S	
2												6	274	289	1607.85	1606.84	1606.84	0.00	0	71	1.8E-06	R.DATAGAFFPVLSLGNK.L	
2												7	767	780	1662.86	1661.85	1661.85	0.00	0	38	3.1E-03	R.LDYGALELELEIER.F	
3	HUB1	N-TAP	AT1G55250	HUB2	2/2	208	5.2E-17	2	22	10	166	1	379	386	993.54	992.53	992.53	0.00	0	64	1.0E-05	R.LYSLINDR.I	
3												2	173	181	1028.61	1027.60	1027.60	0.00	1	15	6.1E-01	R.KVEEALALR.H	
3												3	399	408	1143.63	1142.63	1142.63	0.00	0	27	5.0E-02	K.ILTEAIQAER.S	
3												4	387	396	1290.64	1289.63	1289.63	0.00	0	23	1.3E-01	R.IHHWNAELDR.Y	
3												5	497	508	1479.76	1478.75	1478.75	0.00	1	37	4.9E-03	R.WKDTAQDALYLR.E	
4	HUB1	N-TAP	AT1G51580	KH domain-containing protein	2/2	381	2.6E-34	5	34	17	263	1	378	386	999.51	998.50	998.50	0.01	0	17	3.4E-01	K.GGHLISEMR.R	
4												2	173	182	1115.62	1114.61	1114.61	0.00	1	5	7.5E+00	K.IREDSGAIVR.I	
4												3	364	373	1154.67	1153.66	1153.66	0.00	0	51	8.3E-05	R.LLVHSPYIGR.L	
4												4	54	65	1368.70	1367.70	1367.69	0.00	0	38	3.5E-03	R.VIDDIPVPSEER.V	
4												5	420	431	1463.77	1462.76	1462.76	0.00	0	53	1.4E-04	K.TVQDALFQILCR.L	
4												6	349	363	1557.86	1556.86	1556.86	0.00	0	88	1.9E-08	R.IVEIGFEPSAAVVAR.L	
4												7	8	22	1614.85	1613.84	1613.83	0.01	0	11	1.8E+00	K.RPATTATAAESVHFR.L	
5	HUB1	N-TAP	AT1G27750	SPEN-like	2/2	598	5.2E-56	4	34	35	298	1	110	117	882.54	881.53	881.53	0.00	0	42	4.3E-04	R.LVADLVPR.Y	
5												2	551	557	899.47	898.46	898.46	0.00	0	32	8.0E-03	R.FFFDPVK.G	
5												3	558	565	926.47	925.47	925.47	0.00	0	24	6.9E-02	K.GFALAEYR.S	
5												4	587	595	965.49	964.49	964.48	0.01	0	10	2.8E+00	K.FMDIGVGAR.G	
5												5	353	359	989.49	988.49	988.48	0.01	0	28	4.6E-02	R.WAFFQYK.K	
5												6	1027	1036	1115.57	1114.56	1114.56	0.00	0	7	3.6E+00	K.IPASSPMWAR.H	
5												7	1008	1017	1197.65	1196.64	1196.64	0.00	0	55	4.9E-05	K.GLQDFITYLK.Q	

No	Protein	Type	AGI	Description	Ratio	Score	E-value	a	b	c	d	#	Start	End	Obs	Mr(expt)	Mr(calc)	Delta	Miss	Ion Score	E-value	Sequence	Modification
5												8	983	993	1270.67	1269.66	1269.66	0.00	1	12	1.2E+00	K.ATFANTQPHKR.E	
5												9	937	948	1331.71	1330.70	1330.70	0.00	0	34	1.0E-02	K.SGVHYSTIIAQR.L	
5												10	456	468	1377.72	1376.71	1376.72	0.00	0	18	4.1E-01	R.GLLNQHTPSPSAR.G	
5												11	994	1006	1505.74	1504.73	1504.73	0.00	0	8	3.6E+00	R.EVCQLIPAAFSDR.K	
5												12	956	969	1612.87	1611.86	1611.87	0.00	0	24	6.4E-02	K.YIIGSPEPVQWPVK.L	
5												13	261	281	2254.01	2253.00	2253.00	0.00	0	4	4.4E+00	K.SIATCFGFFNSSSTEDVATGR.Y	
6	HUB1	N-GS	AT2G44950	HUB1	4/4	327	6.5E-29	7	28	18	240	1	667	675	1035.58	1034.58	1034.58	0.00	0	18	3.4E-01	K.LFLEGITSR.Q	
6												2	486	497	1304.66	1303.65	1303.66	0.00	0	20	2.6E-01	R.ADVQSLSGVLCR.K	
6												3	274	289	1607.84	1606.83	1606.84	0.00	0	61	1.8E-05	R.DATAGAFFPVLSLGNK.L	
6												4	767	780	1662.86	1661.85	1661.85	0.00	0	44	9.5E-04	R.LDYGALELELEIER.F	
6												5	686	704	2181.05	2180.05	2180.05	0.00	1	98	2.8E-09	K.YIMDKDIQQGSAYASFLSK.K	Oxidation (M)
7	HUB1	N-GS	AT1G55250	HUB2	4/4	235	1.0E-19	4	29	13	164	1	379	386	993.53	992.53	992.53	0.00	0	26	6.9E-02	R.LYSLINDR.I	
7												2	399	408	1143.63	1142.63	1142.63	0.00	0	23	1.1E-01	K.ILTEAIQAER.S	
7												3	387	396	1290.63	1289.62	1289.63	0.00	0	32	1.7E-02	R.IHHWNAELDR.Y	
7												4	125	140	1733.87	1732.86	1732.86	0.00	0	84	8.8E-08	R.AGANQEALNYLDIVDK.K	
8	HUB1	N-GS	AT1G51580	KH domain-containing protein	3/4	130	3.3E-09	7	16	8	100	1	364	373	1154.67	1153.66	1153.66	0.00	0	41	8.0E-04	R.LLVHSPYIGR.L	
8												2	420	431	1463.76	1462.75	1462.76	-0.01	0	34	1.0E-02	K.TVQDALFQILCR.L	
8												3	8	22	1614.83	1613.82	1613.83	0.00	0	24	9.0E-02	K.RPATTATAAESVHFR.L	
9	HUB1	N-GS	AT1G27750	SPEN-like	2/4	197	6.5E-16	8	22	20	83	1	558	565	926.48	925.47	925.47	0.00	0	26	4.8E-02	K.GFALAEYR.S	
9												2	937	948	1331.70	1330.69	1330.70	-0.01	0	57	5.4E-05	K.SGVHYSTIIAQR.L	
10	HUB2	N-GS	AT2G44950	HUB1	2/2	886	8.2E-85	4	37	27	703	1	535	541	945.49	944.48	944.47	0.01	0	28	4.0E-02	K.LFLDMYK.R	Oxidation (M)
10												2	667	675	1035.58	1034.58	1034.58	0.00	0	28	2.9E-02	K.LFLEGITSR.Q	
10												3	486	497	1304.66	1303.66	1303.66	0.00	0	56	6.4E-05	R.ADVQSLSGVLCR.K	
10												4	179	190	1506.80	1505.79	1505.79	0.00	1	33	1.2E-02	R.CLKDELYPTVLR.T	
10												5	274	289	1607.84	1606.83	1606.84	0.00	0	102	1.2E-09	R.DATAGAFFPVLSLGNK.L	
10												6	767	780	1662.86	1661.85	1661.85	0.00	0	80	2.0E-07	R.LDYGALELELEIER.F	
10												7	509	527	2040.96	2039.95	2039.95	0.00	0	121	1.1E-11	R.SADYASQLGDLNATVCDLK.N	
10												8	686	704	2181.05	2180.04	2180.05	0.00	1	118	2.9E-11	K.YIMDKDIQQGSAYASFLSK.K	Oxidation (M)
10												9	248	270	2643.30	2642.30	2642.30	0.00	1	136	4.3E-13	R.IRGELEDEVVELQQCNGDLSALR.A	
11	HUB2	N-GS	AT1G55250	HUB2	2/2	1030	3.3E-99	5	49	22	833	1	379	386	993.54	992.53	992.53	0.00	0	48	4.0E-04	R.LYSLINDR.I	
11												2	173	181	1028.61	1027.60	1027.60	0.00	1	45	4.8E-04	R.KVEEALALR.H	

No	Bait	Loc	AGI	Description	Cov	Score	E-value					Pep	Start	End	Calc	Obs	Match	Delta	Miss	PepScore	Pep E-value	Sequence	Mod
11												3	399	408	1143.64	1142.63	1142.63	0.00	0	61	2.0E-05	K.ILTEAIQAER.S	
11												4	387	396	1290.64	1289.63	1289.63	0.00	0	57	4.9E-05	R.IHHWNAELDR.Y	
11												5	497	508	1479.76	1478.75	1478.75	0.00	1	91	1.9E-08	R.WKDTAQDALYLR.E	
11												6	387	398	1581.79	1580.78	1580.78	0.00	1	36	5.6E-03	R.IHHWNAELDRYK.I	
11												7	125	140	1733.87	1732.86	1732.86	0.00	0	105	6.0E-10	R.AGANQEALNYLDIVDK.K	
11												8	125	141	1861.93	1860.93	1860.96	-0.03	1	76	5.2E-07	R.AGANQEALNYLDIVDKK.R	
11												9	182	200	2198.01	2197.00	2197.00	0.00	0	72	8.2E-07	R.HSSTMELMGLFENTIDTQK.T	Oxidation (M)
11												10	360	378	2404.08	2403.07	2403.06	0.01	1	98	1.3E-09	R.QCQDIENELKDDQYIYSSR.L	
11												11	248	270	2682.28	2681.27	2681.27	0.00	1	144	4.7E-14	R.HKEHSEQIQAYISSHSTDQSELK.H	
12	HUB2	N-GS	AT1G51580	KH domain-containing protein	2/2	133	1.6E-09	10	14	7	110	1	364	373	1154.67	1153.66	1153.66	0.00	0	38	1.5E-03	R.LLVHSPYIGR.L	
12												2	420	431	1463.77	1462.76	1462.76	0.00	0	47	4.8E-04	K.TVQDALFQILCR.L	
12												3	349	363	1557.83	1556.82	1556.86	-0.03	0	24	7.4E-02	R.IVEIGFEPSAAVVAR.L	
13	HUB2	N-GS	AT1G27750	SPEN-like	2/2	285	1.0E-24	6	19	18	197	1	558	565	926.47	925.47	925.47	0.00	0	32	1.2E-02	K.GFALAEYR.S	
13												2	353	359	989.49	988.48	988.48	0.00	0	23	1.2E-01	R.WAFFQYK.K	
13												3	1008	1017	1197.65	1196.64	1196.64	0.00	0	37	3.2E-03	K.GLQDFITYLK.Q	
13												4	937	948	1331.71	1330.70	1330.70	0.00	0	50	2.4E-04	K.SGVHYSTIIAQR.L	
13												5	261	281	2254.01	2253.01	2253.00	0.00	0	55	3.6E-05	K.SIATCFGFFNSSSTEDVATGR.Y	
14	SPEN-like	C-GS	AT2G44950	HUB1	2/4	73	1.6E-03	13	24	21	/												
15	SPEN-like	C-GS	AT1G55250	HUB2	2/4	68	5.0E-03	18	23	12	/												
16	SPEN-like	C-GS	AT1G51580	KH domain-containing protein	3/4	161	2.6E-12	5	16	8	129	1	364	373	1154.66	1153.66	1153.66	0.00	0	24	3.8E-02	R.LLVHSPYIGR.L	
16												2	476	486	1325.64	1324.63	1324.63	0.00	0	6	5.7E+00	R.YHSPVGPFHER.H	
16												3	54	65	1368.70	1367.69	1367.69	0.00	0	21	1.7E-01	R.VIDDIPVPSEER.V	
16												4	420	431	1463.77	1462.76	1462.76	0.00	0	18	3.8E-01	K.TVQDALFQILCR.L	
16												5	8	22	1614.84	1613.83	1613.83	0.00	0	17	4.5E-01	K.RPATTATAAESVHFR.L	
16												6	404	419	1871.94	1870.94	1870.94	-0.01	0	42	1.1E-03	K.YESQHDEIVQVIGNLK.T	
17	SPEN-like	C-GS	AT1G27750	SPEN-like	4/4	130	3.3E-09	7	18	17	48	1	558	565	926.48	925.47	925.47	0.00	0	17	3.4E-01	K.GFALAEYR.S	
17												2	937	948	1331.71	1330.70	1330.70	0.00	0	31	2.2E-02	K.SGVHYSTIIAQR.L	

Table S2: List of proteins retrieved by TAP purification using HUB1 fusion with the original TAP tag. Number of independent purifications of the same TAP experiment in which the peptide has been identified. Protein scores evidenced in grey stand out on the other ones indicating that they are more likely part of the HUB1 interactome. In the lower table, list of proteins resulting from the experiment carried out using the modified HUB1 peptide, HUB1pm. Peptide count represents the number of hits of that particular peptide, the protein score represents the mascot score derived from peptide mass fingerprint (PMF) combined with MSMS (peptide sequence) data. Protein scores are dependent on the number of peaks/peptides that can be matched in a certain protein in the database, sequence coverage, presence of peptide sequence data and so on. The threshold score when searching the TAIR8 database in 58. Mascot provides additional guidance in the form of a significance level. By default, the significance level is set at 5%. That is, if the score for a particular match exceeds the significance level (threshold 58 for TAIR8), there is less than a 1 out of 20 chance that the observed match is a random event. The best ion score represents mascot scores coming from an individual peptide sequence data, the more fragments can be matched to the theoretical matrix of the different ions of a peptide, the higher the ion score for that particular peptide. There may be several ion scores for several different peptides belonging to the same protein: the one with the highest ion score is given in the best ion score column (the threshold for individual ion scores for TAIR8 is 26-28; for scores exceeding this threshold, there is less than a 1 out of 20 chance that the observed match is a random event).

Bait	Prey Name	AGI Code	N	Protein MW	Peptide Count	Protein Score	Best Ion Score
	TAO1, disease resistance induced TIR-NB-LRR protein	At5g44510	1	130497.4297	16	66	
	Expressed protein	At1g04900	1	51085.26172	11	67	
	Expressed protein	At1g55980	1	51310.55859	11	69	
	Expressed protein similar to geranylgeranylated protein ATGP4	At1g77870	1	13649.24023	9	72	
	HUB1	At2g44950	2	100740.2188	29	520	71
TAP-HUB1	HUB2	At1g55250	2	102008.6797	22	349	64
	Hypothetical protein	At5g36035	1	96451.78906	13	76	
	KH	At1g51580	2	67756.74219	18	390	88
	Pentatricopeptide (PPR) repeat-containing protein	At5g27460	1	56792.07813	13	69	
	Potassium channel tetramerisation domain-containing protein	At4g30940	1	49277.01953	1	40	40
	Putative non-LTR retroelement reverse transcriptase	At2g14430	1	147208.375	19	68	

Prey Name	AGI Code	N	Protein MW	Peptide Count	Protein Score	Best Ion Score
Ribosome recycling factor family protein / ribosome releasing factor	At3g01800	1	29267.41992	11	72	
SPT16, Component of the FACT complex	At4g10710	1	120967.1875	16	69	
SL	At1g27750	2	218243.1563	38	548	55
Ubiquitin-specific protease-related, similar to UBP5	At5g22035	1	29485.26953	9	71	
Ulp1 protease family protein	At1g34610	1	112269.8828	17	70	
Ulp1 protease family protein	At3g09170	1	116297.1875	17	72	
Expressed protein	At1g20310	1	35725.25	10	67	
Expressed protein similar to putative MYB family T.F.	At1g26580	1	56613.48828	11	66	
HUB1	At2g44950	2	100740.2188	33	577	49
HUB2	At1g55250	2	102008.6797	28	444	42
UDP-glucoronosyl/UDP-glucosyl transferase family protein	At3g11340	1	79288.36719	16	66	
Hypothetical protein	At5g40750	1	34448.33984	1	30	30
KH	At1g51580	2	67756.74219	10	164	38
MLP328, involved in copper ion binding	At2g01520	1	17615.57031	8	76	
ADNT1, mitochondrial substrate carrier family protein	At4g01100	1	38472.05078	10	66	
Expressed protein	At4g27595	1	138378.7344	10	71	
Tetratricopeptide repeat (TPR)-containing protein	At5g65160	1	65546.74219	13	68	
SL	At1g27750	2	218243.1563	36	430	28
U-box domain-containing protein, ubiquitin-protein ligase activity and binding	At5g65920	1	115142.6406	15	66	
Zinc finger (C3HC4-type RING finger) family protein	At1g18660	1	56197.14063	11	71	

Table S2 (continued)

Bait	Prey Name	AGI Code	Protein MW	Peptide Count	Protein Score	Best Ion Score
	aldo/keto reductase family protein	At3g53880	35185.24	11.00	80.40	
	cellulose synthase family protein	At4g38190	125712.82	17.00	69.20	
	DEAD/DEAH box helicase, putative	Aratho3g38860 (At3g46960)	141752.73	20.00	70.60	
	disease resistance protein (CC-NBS-LRR class), putative	At1g58410	104837.11	19.00	66.00	
	DNA-dependent ATPase, putative	At5g18620	124495.22	22.00	69.20	
	dyskerin, putative / nucleolar protein NAP57, putative	At3g57150	63329.12	9.00	76.20	31.04
	expressed protein	At5g25460	40214.58	3.00	62.00	51.96
	expressed protein	At5g22650	32385.63	4.00	55.80	37.72
	expressed protein	At2g30630	63855.78	15.00	71.50	
	fibrillarin 2	At4g25630	33803.49	10.00	112.00	41.96
TAP-HUB1pm	fructose-bisphosphate aldolase	Q9LPP8 (At1g18270)	29968.33	10.00	74.70	
	GCN5-related N-acetyltransferase (GNAT) family protein	At5g11340	18826.40	3.00	47.50	30.55
	glycosyl hydrolase family 9 protein	At1g71380	53639.34	8.00	202.00	53.17
	hypothetical protein	At1g04890	57206.01	15.00	66.50	
	La domain-containing protein	At4g35890	55804.33	7.00	69.20	
	myb family transcription factor	At1g58220	86456.37	14.00	66.40	
	nucleolar protein Nop56, putative	At1g56110	58864.53	7.00	113.00	34.09
	nucleolar RNA-binding Nop10p family protein	At2g20490	7443.89	5.00	104.00	36.61
	pentatricopeptide (PPR) repeat-containing protein	At1g60770	56097.85	15.00	72.00	
	preprotein translocase secA family protein	At1g21650	179241.06	21.00	67.20	
	putative retroelement gag/pol polyprotein	At2g11940	139581.31	18.00	66.70	

	Prey Name	AGI Code	Protein MW	Peptide Count	Protein Score	Best Ion Score
	tetratricopeptide repeat (TPR)-containing protein	At1g04190	40815.79	10.00	68.10	
	translational activator family protein	At1g64790	265798.19	22.00	68.30	
	zinc finger (C3HC4-type RING finger) family protein	At2g44950	100740.22	14.00	135.00	92.03
TAP-HUB1pm	adenylate kinase	At5g63400	27143.10	8.00	129.00	40.88
	expressed protein	At3g16270	75016.80	10.00	88.70	30.63
	formin homology 2 domain-containing protein	At5g58160	145366.48	3.00	44.70	32.75
	fructose-bisphosphate aldolase	Q9LPP8 (At1g18270)	29968.33	8.00	71.50	
	GCN5-related N-acetyltransferase (GNAT) family protein	At5g11340	18826.40	2.00	45.70	33.43
	isocitrate dehydrogenase, putative	At5g14590	54503.74	7.00	68.20	
	La domain-containing protein	O65626 (At4g35890)	49563.35	10.00	64.00	
	non-repetitive/WGA-negative nucleoporin family protein	At1g14850	161623.41	9.00	74.10	
	zinc finger (C3HC4-type RING finger) family protein	At2g44950	100740.22	5.00	120.00	93.66
	alpha-glucosidase I (GCS1) / KNOPF (KNF)	At1g67490	97800.84	14.00	68.80	
	BRCT domain-containing protein	Aratho4g02570 (At4g02110)	146806.44	18.00	66.80	
	DEAD box RNA helicase, putative	At3g22330	65547.17	22.00	126.00	
	DEAD box RNA helicase, putative (RH9)	At3g22310	63798.28	18.00	95.70	
	expressed protein	Q8GSG8 (At5g01010)	50458.31	11.00	67.90	
	ferredoxin--nitrite reductase, putative	At2g15620	65877.73	13.00	73.00	
	intracellular protein transport protein USO1-related	At2g46180	82873.06	16.00	68.00	
	kinesin motor protein-related	At1g59540	93774.93	17.00	64.80	
	L-ascorbate peroxidase, putative	At4g35970	28900.98	9.00	70.10	

Prey Name	AGI Code	Protein MW	Peptide Count	Protein Score	Best Ion Score
late embryogenesis abundant domain-containing protein	At2g03740	20004.22	10.00	66.60	
pentatricopeptide (PPR) repeat-containing protein	Arath01g53890 (At1g62260)	69154.04	13.00	65.90	
phytochrome D	At4g16250	130644.76	17.00	81.30	
RNA recognition motif (RRM)-containing protein	At5g32450	28955.01	9.00	68.10	
scarecrow-like transcription factor 11 (SCL11)	At5g59460	19118.83	8.00	77.60	
SEUSS transcriptional co-regulator	At1g43850	96513.86	15.00	69.20	
splicing factor, putative	At4g38780	272710.50	23.00	79.30	
SWIM zinc finger family protein	At2g07320	62560.25	15.00	69.10	
unknown	Arath02g44960	12889.51	5.00	64.30	
zinc finger (C3HC4-type RING finger) family protein	At2g44950	100740.22	10.00	187.00	111.00

Table S3. Number of significant differentially expressed (DE, up + downregulated) genes (*P*-value ≤5%) in *hub1-4, khd-1,* and *spen-1* as compared to Col-0 (wild type)

Name	Genes DE	% total DE* (0.5 threshold)	Genes DE	% total DE* (1 threshold)
hub1-4	2870	14.95	910	4.74
khd-1	2351	12.25	676	3.52
spen-1	994	5.18	308	1.60
hub1-4 + khd-1	1217	6.34	293	1.53
hub1-4 + spen-1	278	1.45	75	0.39
khd-1 + spen-1	212	1.10	55	0.29
hub1-4 + khd-1 + spen-1	117	0.61	27	0.14

* Total, 19196 genes.

Table S4. AGI codes of the 117 DEG common to the *hub1-4*, *khd-1*, and *spen-1* transcriptomes (-0,5 ≥log₂FC ≥ 0.5, *P*-value ≤0.05) manually curated with TAIR10.

Gene ID	REFGeneID	Function/process	HUB1 vs COL-0: log$_2$ FC	KHD vs COL-0: log$_2$ FC	SPEN vs COL-0: log$_2$ FC
AT3G30720	QQS	Starch biosynthetic process	-5.6626	-5.5745	-6.5275
AT4G08093	NA	Unknown	-3.7844	-5.5504	-4.0931
AT2G01422	NA	Unknown	-3.3395	-3.7738	-2.5119
AT4G04223	NA	Unknown	-3.1981	-2.3271	-3.6096
AT4G15320	ATCSLB06	Cellulose biosynthetic process	-1.9482	-2.2482	-2.0571
AT1G48740	F11I4_9	Oxidation reduction process	-1.7234	-1.2481	-1.8338
AT1G51055	NA	Unknown	-1.4514	-1.3610	-1.3864
AT1G55320	AAE18	Auxin metabolic process	-1.2355	-0.8119	-0.6587
AT4G08991	NA	Unknown	-1.2329	-1.9179	-1.3986
AT5G25970	T1N24.19	Transferase activity	-1.1978	-0.8172	-1.1685
AT5G07640	NA	Zinc ion binding	-1.1420	-0.9536	-0.9802
AT2G39460	ATRPL23A	RNA binding	-1.0806	-1.0022	-0.6850
AT3G05727	NA	Unknown	-0.9690	-0.6627	-1.0264
AT2G29570	PCNA2	DNA methylation	-0.9243	-0.7950	-0.5766
AT3G55660	ATROPGEF6	Unknown	-0.8981	-0.6359	-0.5877
AT5G22440	RPL10AC	RNA methylation	-0.8793	-0.8620	-0.7202
AT5G37010	NA	DNA replication	-0.8736	-0.7098	-0.4696
AT1G52770	F14G24.4	Response to light stimulus	-0.8589	-1.3647	-0.8099
AT3G16490	IQD26	Calmodulin binding	-0.8390	-0.8087	-0.8740
AT2G25880	AtAUR2	Histone kinase	-0.8332	-0.8656	-0.5894
AT2G28620	NA	DNA replication	-0.8305	-0.7375	-0.5404
AT2G01020	NA	Peptide biosynthetic process	-0.7982	-0.9755	-0.8181
AT2G33400	F4P9.17	Unknown	-0.7936	-0.5135	-0.6040
AT1G18370	HIK	Microtubule movement	-0.7906	-0.6073	-0.6042
AT5G01600	ATFER1	Iron ion binding	-0.7852	-1.0765	-0.6556
AT4G02800	T5J8.12	Microtubule cytoskeleton	-0.7802	-0.6539	-0.5214
AT4G03100	F4C21.2	Microtubule cytoskeleton	-0.7608	-0.8148	-0.5114
AT1G02780	emb2386	RNA methylation	-0.7545	-0.6800	-0.9208
AT3G23890	TOPII	DNA topoisomerase	-0.7470	-0.5620	-0.5724
AT4G35810	NA	Oxidation reduction process	-0.7201	-0.7203	-0.9608
AT3G01710	NA	Unknown	-0.7187	-0.5457	-0.5202
AT4G22505	NA	Lipid transport	-0.6991	-0.5741	-0.8263
AT5G38940	NA	Response to salt stress	-0.6947	-0.7681	-1.0002
AT2G38620	CDKB1	Regulation of cell cycle	-0.6756	-0.5173	-0.7126
AT5G15200	RPS9B	RNA methylation	-0.6751	-0.5741	-0.6052
AT3G58650	F14P22.240	DNA replication	-0.6746	-0.6901	-0.6336
AT5G60150	NA	Petal formation	-0.6702	-0.7296	-0.5222
AT1G05440	NA	DNA methylation	-0.6700	-0.7066	-0.5283

AT5G44560	VPS2.2	Protein binding	-0.6659	-0.5251	-0.5011
AT2G26760	CYCB1	Regulation of cell cycle	-0.6633	-0.7223	-0.6465
AT1G23790	F5O8.34	Cell proliferation	-0.6442	-0.7267	-0.5978
AT3G26050	NA	Unknown	-0.6299	-0.6320	-0.5259
AT5G67270	ATEB1C	Microtubule binding	-0.6257	-0.6774	-0.6385
AT3G19050	POK2	Microtubule movement	-0.6187	-0.5180	-0.5445
AT5G26742	emb1138	Embryo development	-0.5808	-0.9022	-0.6706
AT2G36885	NA	Unknown	-0.5808	-0.8775	-0.8374
AT4G24670	TAR2	Cotyledon development	-0.5388	-0.6692	-0.6080
AT2G45490	AtAUR3	Histone kinase	-0.5322	-0.5612	-0.7462
AT2G33560	BUBR1	Cell proliferation	-0.5258	-0.6428	-0.5698
AT4G37490	CYC1	Regulation of cell cycle	-0.5244	-0.7092	-0.6084
AT5G35935	NA	Transposon	3.8585	4.0484	3.9318
AT1G19510	ATRL5	Regulation of transcription	2.6802	1.7416	1.6497
AT3G10420	SPD1	Nucleoside-triphosphatase activity	2.4560	2.4592	2.6330
AT3G05660	AtRLP33	Kinase activity	2.4204	1.4367	1.4173
AT4G08040	ACS11	Biosynthetic process	1.8670	0.9910	1.2030
AT2G34010	T14G11.13	Negative regulation of transcription	1.7997	1.0896	0.8731
AT1G51820	NA	Proline transport	1.6036	1.9470	1.5766
AT2G26560	PLP2	Lipase activity	1.5401	1.4479	1.6085
AT1G43910	F9C16_7	Response to ABA stimulus	1.4203	1.3555	1.1442
AT3G16030	CES101	Immune response	1.3967	1.1568	1.0114
AT4G36280	CRH1	ATP binding	1.2300	0.7077	0.5734
AT5G15510	NA	Cell proliferation	1.1310	0.7409	1.2072
AT5G17860	CAX7	Transmembrane transport	1.1310	0.7409	1.2072
AT1G62510	NA	Lipid transport	1.1214	0.9785	0.8740
AT5G38970	BR6OX1	Oxidation reduction process	1.1193	1.2404	1.2257
AT1G52880	NAM	Regulation of transcription	1.1080	0.7682	0.9576
AT4G11900	NA	Protein phosphorylation	1.0676	0.7431	0.7588
AT3G53250	T4D2.180	Response to auxin stimulus	1.0341	0.9364	0.7971
AT3G62860	F26K9_290	Catalytic activity	1.0282	1.0083	0.7175
AT1G72430	T10D10.10	Response to auxin stimulus	0.9981	1.0623	0.8578
AT1G21270	WAK2	Oligosaccharide metabolic process	0.9727	0.7971	0.6735
AT5G64780	NA	Unknown	0.9604	0.6438	0.5608
AT2G39980	NA	Response to karrikin	0.9578	0.6103	0.5734
AT3G61430	PIP1A	Water channel activity	0.9367	0.7735	0.5416
AT4G18010	IP5PII	Inositol tri-phosphate metabolic process	0.8834	1.2286	0.6841
AT3G56000	ATCSLA14	Transferase activity	0.8726	0.9119	0.7815
AT3G48720	T8P19.230	Cutin biosynthetic process	0.8433	0.8613	0.6017
AT5G08150	SOB5	Cytokinin metabolism process	0.8382	1.1877	0.6384
AT1G23130	T26J12.10	Defense response	0.8248	0.9054	0.6017
AT3G12090	TET6	Transition metal ion transport	0.8139	0.6686	0.6863
AT5G24030	SLAH3	Nitrate transport	0.7619	0.9383	0.6074

AT2G31730	BHLH-BETA	Response to ethylene and GA stimulus	0.7106	0.8444	0.6729
AT5G07000	ATST2B	Sulfotransferase activity	0.6955	0.9848	0.6295
AT3G07340	BHLH62	Regulation of transcription	0.6624	0.6468	0.5896
AT4G23190	CRK11	Kinase activity	0.6350	0.7084	0.8002
AT5G23750	MRO11.3	Cell wall biogenesis	0.5664	0.6600	0.7512
AT4G32790	F4D11.10	Catalytic activity	0.5664	0.5992	0.5092
AT2G41330	NA	Cell redox homeostasis	0.5613	0.6276	0.7785
AT2G23690	NA	Protein myristoylation	0.5438	0.7003	0.8397
AT1G02820	F22D16.18	Embryo development	-1.7547	-1.2409	1.2362
AT1G62540	FMO GS-OX2	Oxidation reduction process	-1.4021	-0.9912	0.9452
AT4G26790	NA	Lipid metabolic process	-1.1570	-1.1056	0.8255
AT3G21670	NRT1.3	Oligopeptide transport	-1.1033	-1.0078	0.9084
AT1G16730	UP6	Fatty acid beta oxydation	-1.0651	-1.2906	1.0012
AT4G37310	CYP81H1	Oxidation reduction process	-1.0019	-0.7621	0.5620
AT2G46680	ATHB-7	Regulation of transcription	-0.9295	-0.6854	0.6970
AT1G73390	T9L24.40	Protein myristoylation	-0.9262	-0.6509	0.6113
AT2G17300	NA	Unknown	-0.7890	-0.5806	0.5410
AT5G03760	ATCSLA09	Calcium ion transport	-0.7349	-0.7330	0.7095
AT5G61290	NA	Oxidation reduction process	-0.6413	-0.7854	0.7625
AT1G64770	NDF2	Carbohydrate metabolic process	-0.5301	-0.5406	0.5175
AT4G37770	ACS8	Biosynthetic process	1.7545	2.0780	-1.8580
AT4G40065	NA	Unknown	1.4381	1.1595	-1.3468
AT2G23170	GH3.3	Response to auxin stimulus	1.4334	1.2295	-0.7410
AT2G18010	SAUR10	Response to auxin stimulus	1.3172	1.5038	-1.1684
AT3G42800	T21C14_20	Unknown	1.1613	1.4009	-0.8314
AT1G04610	YUC3	Oxidation reduction process	0.8388	1.2292	-1.9934
AT1G30420	ATMRP12	Transmembrane transport	0.5738	0.5111	-1.0747
AT1G51830	T14L22.4	Nitrate transport	-1.5491	1.2138	-1.0585
AT4G20320	F1C12.230	Pyrimidine nucleotide biosynthetic process	-1.4217	-0.8890	-0.5056
AT4G30170	PER45	Oxidation reduction process	-1.2226	1.4707	-1.1787
AT3G32925	NA	Transposon	2.4493	-2.0186	1.4498
AT5G59670	NA	Protein phosphorylation	1.2640	-1.1608	1.5756
AT1G73000	PYL3	Unknown	1.2088	-1.0563	1.6080
AT1G11070	NA	Unknown	0.9290	-0.6423	0.8314
AT1G78000	SULTR1	Nitrate transport	-1.5906	0.6725	0.8204
AT3G54160	F24B22.120	Unknown	0.9710	-1.2585	-1.0686

$^{\times}$p-values for all log$_2$FC are ≤0.05

Table S5. Primer sequences.

Gene	AGI code	Primer set	Forward Primer Sequence	Reverse Primer Sequence
Real-time qPCR				
SPEN1	At1g27750		CCCTGCATCAAGTCCCATGT	ACCGATCAAGCATTCCGAGG
KHD1	At1g51580		CCCCATTTGGACCGAGACAA	CCAGGACCATGACAATGCCT
CCA1	At2g46830		CCATGGAAGCCAAAGAAAGT	GGAAGCTTGAGTTTCCAACC
PP2A	At1g13320		TAACGTGGCCAAAATGATGC	GTTCTCCACAACCGCTTGGT
UBC	At5g25760		CTGCGACTCAGGGAATCTTCTAA	TTGTGCCATTGAATTGAACCC
FLC	At5g10140		CCTCTCCGTGACTAGAGCCAAG	AGGTGACATCTCCATCTCAGCTTC
FLC2			TTTGTCCAGCAGGTGACATC	AGCCAAGAAGACCGAACTCA
QQS	At3g30720		TCATTTTCTCCACAGCGACCA	TGGTTTGAAGCTTCTTTCAACG
PCNA2	At2g29570		CAACAGCAGGTGATATCGGGA	TCTTCAGGTTTGTCGACGGT
	At1g18990		CCGGTTTCAGATTTGCCTGT	TGCTTCCATTCTCTTTTTCTTCCT
	At5g56370		TTAACGAGACCCACGGCTAC	TGTTTCAAGAGAAAACTTGCG
	At1g66650		CGGAGGGTTTCATCACCCAA	GCTAGATGCCCATTATTACACTGA
COOLAIR			GCCGTAGGCTTCTTCACTGT	TGTATGTGTTCTTCACTTCTGTCAA
proxCOOLAIR			CACACCACCAAATAACAACCA	TTTTTTTTTTTTTTTACTGCTTCCA
distCOOLAIR			GGGGTAAACGAGAGTGATGC	TTTTTTTTTTTTTTTGCGGTACAC
CCA1α			GATCTGGTTATTAAGACTCGGAAGCCATATAC	GCCTCTTTCTCTACCTTGGAGA
CCA1β			GAATGTTCCTTGTGATAAGCCATAGAGG	AGGATCGTTCCACTTCCCGTCTT
ChIP-qPCR				
CCA1	At2g46830	P1	GAACAAGTTGATGTTAAGATGGAC	GGAGAAATCTCAGCCACTATAATTATC
		P2	GAAGTTGTGTAGAGGAGCTTAGTG	CTTCCTCAGTCCACCTTTCACGTTGC
		P3	ATCCTCGAAAGACGGGAAGT	GTCGATCTTCATTGGCCATC
		P4	AAGGCTCGATCTTCACTGGA	CCATCCTCTTGCCTTTCTGA
		P5	CTCAAGCTTCCACATGAGACTC	GTTACAGGAAGACTATGGACAAG
FLC	At5g10140	P1	GTTCGGGAGATTAACACAAATAATAAAGG	GAAAACAAGCTGATACAAGCATTTCAC
		P2	GCTGGACCTAACTAGGGGTGAAC	CCTCTTTGGTACGGATCTATAATGAATC
		P3	CCTCTCCGTGACTAGAGCCAAG	CTTCAACATGAGTTCGGTCTGC
		P4	CCTTGGATAGAAGACAAAAGAGAAAGTG	AGGTGACATCTCCATCTCAGCTTC
PCNA2	At2g29570	P1	TGGCCCAATTTAAACCCATGC	TGGCGCCATTTAGCGATTTT
		P2	TTCCCAGAAGATGTTGGAGCTT	GAACCCTGTGGTCGAACAGT
		P3	AGGGTTTTTGGTTTGGAATAAGGT	GGAAGGACTCATTCTCATCAAGC
		P4	TTGGTGTATCACTGCGAGGA	GCTGTCCCGATATCACCTGC
		P5	GGTCGTGGTGGAGTACAAGG	ACAAAGGACTCGAACGAAGACT
QQS		P1	CGGATTGATGTCGTGGCGAA	ATGGTGATTGGATCGTTTTGGC
		P2	ATGCTTCATTTTCTCCACAGGT	AACACCAACTGGTCGCTGAA
		P3	GGGTCGGGCTTCAGTTCTAC	TGGGCATTAGAACAAAATAACCAT
Cloning				
KHDN			ACAGGATCCAAACGTCCGGCGACGACA	ACAGTCGACTCAACTCGTCCCATGTTGGA
RRMSPEN			CACGGATCCACTCTACGGATCGTAGGAA	CACGTCGACTCAAATCCTTTCACTGGATCAAA
EMSA				
RNA			AAAACAAAAUAGCACCGUAAAGCAC	
DNA			AAAACAAAATACCAGCGTAAAGCAC	

Part II. ELONGATOR

Chapter 3 Plant   Elongator-mediated transcriptional control in a chromatin and epigenetic context

Magdalena Woloszynska [a,b], Sabine Le Gall [a,b], Mieke Van Lijsebettens [a,b],

[a] Department of Plant Systems Biology, VIB, 9052 Gent, Belgium
[b] Department of Plant Biotechnology and Bioinformatics, Ghent University, 9052 Gent, Belgium

Acknowledgments

Author contribution

This chapter was adapted from the published manuscript.

Woloszynska, M., Le Gall, S., Van Lijsebettens, M., 2016. Plant Elongator-mediated transcriptional control in a chromatin and epigenetic context. Biochimica et Biophysica Acta (BBA) - Gene Regulatory Mechanisms 1859, 1025–1033. doi:10.1016/j.bbagrm.2016.06.008

S.L.G made the Genevestigator meta-analysis and participated in the writing of the manuscript.

1 Abstract

Elongator (*Elp*) genes were identified in plants by the leaf growth-altering *elo* mutations in the yeast gene homologs. Protein purification of the Elongator complex from *Arabidopsis thaliana* cell cultures confirmed its conserved structure and composition. The Elongator function in plant growth, development and immune responses is well-documented in the *elp*/*elo* mutants and correlated with the histone acetyl transferase activity of the ELP3/ELO3 subunit at the coding part of key regulatory genes of developmental and immune response pathways. Here we will focus on additional roles in transcription, such as the cytosine demethylation activity of ELP3/ELO3 at gene promoter regions and primary microRNA transcription and processing through the ELP2 subunit interaction with components of the siRNA machinery. Furthermore, specific interactions and upstream regulators support a role for Elongator in transcription and might reveal mechanistic insights into the specificity of the histone acetyl transferase and cytosine demethylation activities for target genes.

2 Elongator activities in yeast, human, and plants

Elongator had been identified in yeast (*Saccharomyces cerevisiae*) as the major component of the elongating C-terminal repeat domain (CTD)-hyperphosphorylated RNA polymerase II (RNA pol II) holoenzyme under stringent conditions that allowed purification of the RNA pol II ternary complex-containing chromatin (Otero *et al.*, 1999). The first subunits identified by mass spectrometry and gene sequence were Elp1 and Elp3 (Otero *et al.*, 1999; Wittschieben *et al.*, 1999). The deletion mutants, *elp1Δ* and *elp3Δ*, grew more slowly when transferred to new growth conditions, with relevant inducible genes delayed in their activation, the mutants were sensitive to the nucleotide-depleting drug, 6-azauracil (6-AU) and to temperature, supporting an *in vivo* role for Elongator as a coactivator of post-initiation events in mRNA transcription. The yeast holo-Elongator consists of the core subcomplex containing Elp1, Elp2, and Elp3 and the accessory subcomplex of Elp4, Elp5, and Elp6. Single and double mutants had similar phenotypes, such as sensitivity to salt, caffeine, and temperature, with similar differentially expressed genes in their transcriptomes, indicating that holo-Elongator is a functional entity (Winkler *et al.*, 2001; Krogan and Greenblatt, 2001). The Elp1, Elp2, and Elp3 subunits

had also been identified through the *toxin target1* (*tot1*), *tot2*, and *tot3* mutants, respectively, that were resistant to the target toxin zymocin, secreted by *Kluyveromyces lactis* killer strains (Frohloff *et al.*, 2001). Structure and function of the Elongator subunits and subcomplexes are discussed by Glatt and Müller (2013).

Elp3 is highly conserved from Archaea to Eukaryotes, it contains a C-terminal histone acetyl transferase (HAT) domain that is phylogenetically related to the superfamily of Gcn5-related N-acetyltransferases (Pandey *et al.*, 2002). Elp3 is responsible for the *in vivo* HAT activity at the nucleosomal histone H3 lysine 14 and histone H4 lysine 8, when it is part of the holo-Elongator (Winkler *et al.*, 2002; Hawkes *et al.*, 2002). Elp3 contains a N-terminal Fe_4S_4 cluster domain that binds and cleaves *S*-adenosylmethionine (SAM) that catalyses transfer RNA (tRNA) U34 wobble uridine modification at C5 via a radical mechanism that, in archaea, also requires acetyl-CoA, the cofactor recruited by the Elp3 HAT domain activity (Selvadurai *et al.*, 2014). The high conservation of Elp3 between archaea and eukaryotes implies an ancient function for the HAT and SAM domain activities in the tRNA modification (Selvadurai *et al.*, 2014).

Elp2 contains two seven-bladed WD40 β propellers that are required for its binding to Elp1 and Elp3; intact Elp2 greatly affects HAT activity of the Elongator complex and is a hub in the formation of various complexes (Fellows *et al.*, 2000; Dong *et al.*, 2015).

Elp1 represents the largest subunit of the Elongator complex. Its conserved C-terminal basic region and phosphorylation promote tRNA binding and modification (Di Santo *et al.*, 2014; Abdel-Fattah *et al.*, 2015). Dimerization of Elp1 is essential for the Elongator complex assembly in human and yeast (Xu *et al.*, 2015). In human, the Elp1 gene corresponds to IKAP, a gene involved in familial dysautonomia that links the Elongator to a human developmental disorder of the sensory and autonomic nervous system (Anderson *et al.*, 2001; Slaugenhaupt *et al.*, 2001; Hawkes *et al.,* 2002).

The Elp4, Elp5, and Elp6 subunits have almost identical RecA folds forming a hexameric ring-like structure that resembles RecA-like ATPases to bind tRNAs in an ATP-dependent manner (Glatt *et al.*, 2012; Lin *et al.*, 2012). The Elongator structure and function are conserved in human. Indeed, the accessory subunit is required for hElp3 HAT activity and Elongator associates with the RNA pol II transcript elongation complex, like in yeast (Hawkes *et al.*, 2002).

Homologs of the genes coding for the Elongator subunits in yeast had been identified in the genome of the model plant *Arabidopsis thaliana* (Nelissen *et al.*, 2003) (Table 1). The evolutionary conservation of the Elongator subunit 3 that contains the two enzymatic activities, SAM and HAT, important for the Elongator functions, is presented in a phylogenetic analysis (Figure 1).
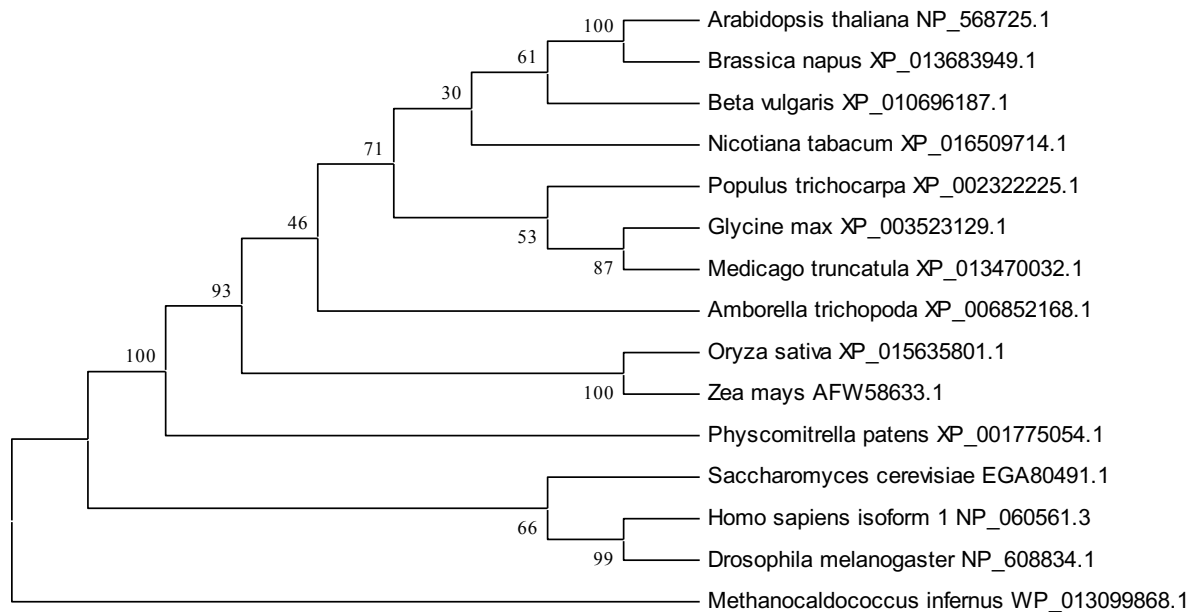
Figure 1. Phylogenetic analysis of ELP3. The evolutionary history was inferred with the Neighbor-Joining method (Saitou and Nei, 1987). The optimal tree with the sum of branch length = 1.21078652 is shown together with the percentage of replicate trees in which the associated taxa clustered together in the bootstrap test (500 replicates) (Felsenstein, 1985). The evolutionary distances were computed with the p-distance method (Nei and Kumar, 2000). The analysis involved 15 amino acid sequences. All positions containing gaps and missing data were eliminated and a total of 511 positions occurred in the final dataset. The analysis was conducted in MEGA5 (Tamura *et al.*, 2011).

Purification of Elongator subunits in *Arabidopsis* cell cultures revealed that the complex is conserved in higher plants (Nelissen *et al.,* 2010). Mutational analyses indicated that Elongator plays a role in growth, development, and stress-related processes. In plants, Elongator regulates transcription through several regulatory processes (Figure 2), i.e. histone acetylation during RNA pol II transcript elongation through the ELP3 HAT activity, DNA demethylation of cytosines through the ELP3 SAM activity (Nelissen *et al.*, 2010; DeFraia *et al.*, 2013; Wang *et al.*, 2013; Van Lijsebettens and Grasser, 2014; Ding and Mou, 2015; Jia *et al.*, 2015), and microRNA (miRNA) transcription and processing through

the ELP2 interaction with DICER-LIKE1 (DCL1) and SERRATE (SE), which are components of the microprocessor complex of the siRNA machinery (Fang *et al.*, 2015; Laubinger, 2015). In addition, the plant Elongator functions in translational control through tRNA wobble uridine modification by the ELP3 enzymatic activities (Fig. 2) (Mehlgarten *et al.*, 2010; Versées *et al.*, 2010; Leitner *et al.*, 2015). Here, we will review the state-of-the-art of Elongator research in plants with emphasis on its role in transcriptional regulation though various epigenetic mechanisms. We will focus on the HAT and the tRNA modification activities of the Elongator complex.
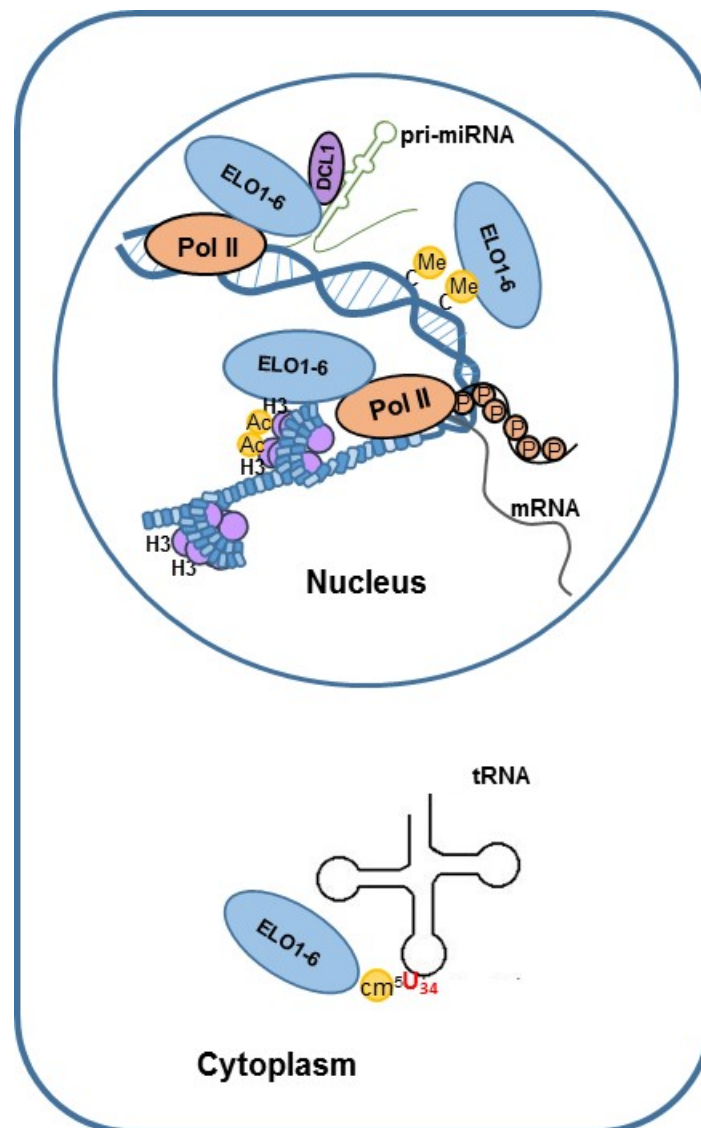

Figure 2. Activities of Elongator (represented as ELO1-6) located in nucleus and cytoplasm. Elongator interacts (directly or indirectly) with Pol II to regulate the mRNA transcription via the ELP3 HAT activity toward histone H3 (Ac) and the pri-miRNA transcription and processing via interaction with DCL1. The SAM activity of the ELP3

subunit of Elongator regulates cytosine demethylation and C5 modification of the tRNA wobble uridine in the nucleus and generation of carbonylmethyluridine (cm^5U) in the cytoplasm.

3   Elongator mutant phenotypes in plants

3.1   Mutant phenotypes in growth, immunity, and stress response

The occurrence and functionality of Elongator in plants had been suggested by the study of an *Arabidopsis* mutant with narrow leaves that identified the DEFORMED ROOTS AND LEAVES1 (DRL1)-encoding gene, a homolog of the Elongator-interacting TOT4/KTI12 protein in yeast (Nelissen *et al.*, 2003). The *drl1* leaf phenotype resembled that of the *elongata* (*elo*) mutants in an ethyl methanesulfonate-mutagenized collection of leaf mutants (Berná *et al.*, 1999). The rough map positions of the *elo* leaf mutants (Robles and Micol, 2001) colocalized with those of the *elp* homologs in the *Arabidopsis* genome; sequencing of *elp* Elongator subunit homologs in the *elo* mutants identified point mutations, hence proof for Elongator genes in *Arabidopsis* (Nelissen *et al.,* 2005). The *Arabidopsis* genes corresponding to the six Elongator subunits are listed in Table 1. Their function was studied in the model plant through mutants with developmental, biotic, or abiotic stress-related phenotypes, i.e. the *elp4/elo1*, *elp1/elo2*, and *elp3/elo3* mutants had elongated, narrow leaves, short primary roots, and a reduced number of lateral roots (Nelissen *et al.*, 2005, 2007, 2010). The *elp3/elo3* mutant was identified as enhancer of *as2*, with a role in leaf polarity (Kojima *et al.*, 2011), as suppressor of the *STIMPY* overexpression, and with a role in the cell cycle progression of the shoot meristem (Skylar *et al.*, 2013). The *elp2/drs1* mutant had a defective root development (Jia et al., 2015), whereas *elp1/abo1/elo2* was hypersensitive to abscisic acid (ABA) and was drought resistant (Chen *et al.*, 2006). The mutants *elp2* and *elp6* were hypersensitive to ABA, resistant to oxidative stress, and accumulated anthocyanins (Zhou et al., 2009). Additional phenotypic analyses demonstrated that Elongator regulates lateral growth in leaves (Falcone et al., 2007), transition to the differentiation state in the shoot apical meristem (Sanmartín et al., 2011), auxin-driven development, such as venation complexity, phyllotaxis, and apical dominance (Nelissen et al., 2010), mitotic cell cycle (Xu *et al.*, 2012), auxin responses (Leitner *et al.*, 2015), immune responses (DeFraia *et al.*, 2010, 2013; Wang *et al.*, 2013), and resistance to the necrotrophic fungal pathogens *Botrytis cinerea* and *Alternaria brassicicola* (Wang *et al.*, 2015). Indeed, in the *elp2* and

elp3 mutants, the expression of the Effect Trigger Immunity (ETI) genes (PR1, PR5, WRKY33, WRKY18, and ICS1) was delayed and that of the systemic acquired resistance genes (PR1, PR2, LURP1, GST11, EDR11, and SAG21) was reduced after exposure to *Pseudomonas syringae pv. maculicola* (Psm ES4326) or after treatment with the salicylic acid (SA) defense activator, or the strong, biologically active SA analog, benzo(1,2,3)thiadiazole-7-carbothioic acid *S*-methyl ester (BTH). Upon exposure to the necrotrophic fungal pathogen *B. cinerea*, the *PDF1.2*, *HEL*, and *CHIB* genes had a delayed and reduced expression in the *elp1*, *elp2*, *elp3*, *elp4,* and *elp5* mutants (Wang *et al.*, 2015). Mutations in the six genes coding for the Elongator complex subunits compromised exogenous NAD^+-induced PR gene expression and resistance to Psm ES4326 (An *et al.*, 2016). RNA interference of the *ELP2*-like gene of tomato (*Solanum lycopersicum*) resulted in tomato lines with reduced leaf growth, ABA hypersensitivity, accelerated leaf and sepal senescence, and dark-green fruits due to chlorophyll accumulation, suggesting that in an evolutionarily distant dicotyledonous species, Elongator has similar, but also divergent functions (Zhu *et al.*, 2015). At first sight, the Elongator mutant phenotypes are pleiotropic in plants, but a closer look shows that they are related to abiotic or biotic stress response pathways or growth processes which are inducible and part of a large network.

Phenotypes in leaf and primary and lateral root growth and development in the *elp/elo* mutants correlated well with the *ELP/ELO* gene expression in shoot and root apical meristems, lateral root meristems, and leaf primordia (Nelissen *et al.*, 2010; Kojima *et al.*, 2011; Skylar *et al.*, 2013; Jia *et al.*, 2015), whereas other gene expression studies in *elp/elo* mutants correlated with their stress-related phenotypes. Indeed, the *ELP1/ABO1/ELO2* promoter-β-glucuronidase (GUS) reporter gene was expressed in stomata which correlated with the stomatal closure hypersensitivity to ABA in the *elp1/abo1/elo2* mutant (Chen *et al.*, 2006), the reporter gene was expressed also in roots, hypocotyls, stems, leaves, flowers, and siliques.

Table 1. *Arabidopsis* **Elongator genes and function**

Gene Code	Locus Name	Protein domain[a]	Function	Reference
At5g13680	*ELP1/ELO2/ABO1*	WD40	Root and leaf growth	Nelissen et al. (2005)
			Abscisic acid sensitivity, drought tolerance, oxidative stress, anthocyanin synthesis	Chen et al. (2006)
			Immune response	Zhou et al. (2009)
			Auxin response	Leitner et al. (2015)
At1g49540	*ELP2*	WD40	Abscisic acid sensitivity, oxidative stress, anthocyanin synthesis	Zhou et al. (2009)
			Immune response	DeFraia et al. (2010, 2013), Wang et al. (2013)
			Biotic stress	Wang et al. (2015)
			Root development	Jia et al. (2015)
			Auxin response	Leitner et al. (2015) Fang et al. (2015)
At5g50320	*ELP3/ELO3*	Radical SAM, HAT	Root and leaf growth	Nelissen et al. (2005)
			Venation patterning, apical dominance, phylotaxis, auxin sensitivity	Nelissen et al. (2010)
			Auxin response	Leitner et al. (2015)
			Shoot meristem progression	Skylar et al. (2013)
At3g11220	*ELP4/ELO1*	RecA-like	Root and leaf growth	Nelissen et al. (2005)
			Oxidative stress, anthocyanin synthesis	Zhou et al. (2009)
			Auxin response	Leitner et al. (2015)
At2g18410	*ELP5*	RecA-like	Auxin response	Leitner et al. (2015) Fang et al. (2015)
At4g10090	*ELP6*	RecA-like	Oxidative stress, anthocyanin synthesis	Zhou et al. (2009)

[a] WD40 proteins acting as scaffolds that mediate structural integrity to protein complexes (Stirnimann *et al.*, 2010); radical SAM, *S*-adenosylmethionine-binding domain; HAT, histone acetyl transferase domain; RecA-like domain with tRNA-binding activity (Glatt *et al.*, 2012).

3.2 Meta-analysis of plant ELP gene expression upon biotic and abiotic stimuli

The literature on the Elongator gene expression upon environmental stress is limited. Therefore, the *Arabidopsis ELP* gene expression was assessed upon biotic and abiotic stimuli in mutant backgrounds by transcriptome meta-analyses with the Genevestigator gene expression database (Zimmermann *et al.*, 2004). Conditions of differential gene

expression correlated with described phenotypes in the *elp* mutants or were unexplored thus far, encouraging further research. Expression data of all Elongator subunits were retrieved from the Genevestigator database corresponding to the perturbation conditions. After conversion to fold change, the data were sorted to find similarities in induction or repression of the components of the core subunits and/or the accessory subunits, as well as in conditions that induce or repress differential expression of single *ELP* genes. The data were transformed into a heatmap format (Sturn *et al..*,2002) (Fig. 3). At all developmental stages (germinated seeds, seedlings, rosettes, flowers, siliques, and senescence), all six *ELP* genes were induced, among which the catalytic subunit gene *ELP3/ELO3* that had the highest expression at all stages, fitting the *in planta* expression analyses (Nelissen *et al*., 2010; Kojima *et al*., 2011; Skylar *et al*., 2013; Jia *et al*., 2015). By meta-analysis, stress conditions were investigated that could be linked to phenotypes of the *elp/elo* mutants or uncover conditions of the *ELP/ELO* induction or repression that were not yet explored. The shift from auxin inhibition on 1-*N*-naphthylphthalamic acid (NPA) to auxin induction on 1-naphthaleneacetic acid (NAA) and callus induction (involving auxin in the medium) triggered all six *ELP* genes (Fig. 3) and correlated very well with auxin-induced patterning defects in the *elp/elo* mutants, such as defects in leaf polarity and venation patterning, phyllotaxis and apical dominance, root stem cell and shoot apical meristem maintenance, supporting a role for Elongator in auxin signalling. Stratification, i.e., a cold treatment after seed imbibition prior to germination, induced *ELP1*, *ELP2*, *ELP4*, and *ELP6* (Fig. 3), whereas cold stress on leaves induced all three genes of the core complex, and a shift from high (28°C) to low (19°C) temperature triggered *ELP1* and *ELP4* (Fig. 3), suggesting that Elongator might be part of a temperature-sensing mechanism with epigenetic components (Kumar and Wigge, 2007, 2010). Germination itself repressed all Elongator genes with a larger effect on *ELP1*, *ELP2* and *ELP3* (Fig. 3). The plant hormone ABA induced *ELP1* (Fig. 3) and correlated well with the ABA hypersensitivity of the *elp1/elo2/abo1* mutant (Chen *et al*., 2006). Silencing of *ELP2* in tomato accelerated senescence and generated hypersensitivity to ABA (Zhu *et al*., 2015). ELP2 is strongly downregulated in the presence of ABA and the small ABA-downregulating molecule 5-(3,4-dichlorophenyl)furan-2-yl]-piperidine-1-ylmethanethione (DFPM). ABA and ethylene are senescence-promoting plant hormones. The effect of the tomato *ELP2* gene silencing correlated with the expression

of *ELP2* which was induced by the addition of ABA and ACC (ethylene precursor) and repressed by the ABA-antagonistic plant hormone gibberellic acid (GA) (Zhu *et al.*, 2015). The GA synthesis inhibitor paclobutrazole induced the Elongator core complex genes (Fig. 3) in analogy to ABA, antagonizer of GA, that triggered *ELP2* in tomato. *ELP3* is induced by high light (Fig. 3) and the core complex genes by norflurazon (Fig. 3), which mimics high light because this herbicide interferes with the carotenoid synthesis pathway that protects against light and oxygen radicals. All *ELP* genes were induced by drought and salt stresses and shifts to low pH (Fig.3). Lack of sulfur strongly triggers genes of the core subunits and *ELP4* (Fig.3). Pathogen infections have different effects on the *ELP* gene expression: *P. synringae pv.sSyringae* infection affects the *ELP3, ELP4,* and *ELP6* genes and represses the *ELP1, ELP2,* and *ELP5* genes (Fig. 3). The elicitor FLG22, which is the conserved N-terminal part of flagellin that is the main constituent of the bacterial flagellum, induced all Elongator genes, except *ELP6* (Fig. 3). Treatment with SA and ABA repressed all genes with an increased effect on the core subunits (Fig. 3). SA is a key signal and regulatory molecule in plant defense responses: it triggers responses at the infection site, but also at the systemic level. Therefore, SA is used to induce immune responses in plant studies. *ELP2* and *ELP3* have been shown to be required for hyperaccumulation of SA through regulation of *ICS1*, that is responsible for the SA biosynthesis upon pathogen infection and to function in the SA-mediated plant immunity pathways (DeFraia *et al.* 2010, 2013). Based on phenotype and expression analyses, the Elongator complex affects three major processes in plants, i.e. auxin signalling, immunity response, and abiotic stress response.
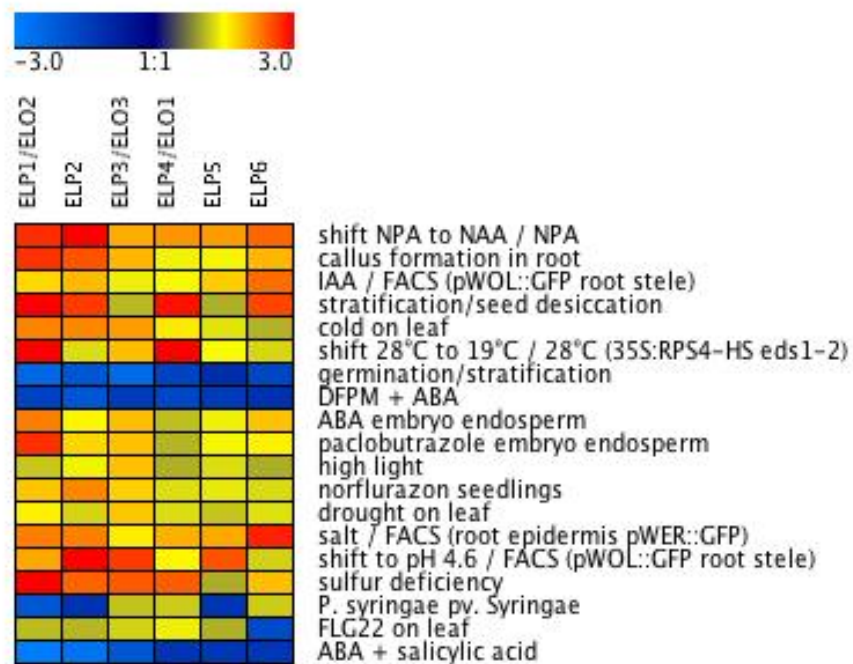
Figure 3. Heat map of *ELP* gene response to different perturbations by meta-analysis of the datasets in the Genevestigator database (Zimmermann *et al.*, 2004). Orange/yellow and blue colours represent up- and downregulation, respectively. Colour scale represents fold-change between -3.0 and +3.0, whereas the values beyond this range are shown in the same colour (Sturn *et al.*, 2002).

4   Plant Elongator composition, interactors, and nuclear functions

The Elongator complex in plants was purified by tandem affinity purifications (TAP) of extracts derived from *Arabidopsis* cell cultures overproducing GS-tagged ELO3/AtELP3, followed by NuPage gel separation and mass spectrometry. All six Elongator subunits ELO2/AtELP1, AtELP2, ELO3/AtELP3, ELO1/AtELP4, AtELP5, and AtELP6 were identified (Nelissen et al., 2010). TAP experiments with ELO2/AtELP1, ELO1/AtELP4, or AtELP5 as baits also purified the holo-Elongator. The tagged overexpression *ELO3/AtELP3* and *ELO1/AtELP4* constructs were tested for complementation and, indeed, restored the respective *elo3* and *elo1* mutant phenotypes to wild type which showed their functionality. Pairwise interactions between ELO1/AtELP4 and AtELP6, and between AtELP6 and AtELP5 were demonstrated by yeast two-hybrid that supports the assembly of the accessory subcomplex in plants (Nelissen *et al.*, 2010). Hence, the holo-Elongator complex structure consisting of six subunits is conserved from yeast and human to plant.

ELO3 was used as a proxy to investigate the subcellular localization of the complex in plants by an N-terminal fusion with the green fluorescent protein (GFP) that did not abolish its function in a complementation assay (Nelissen *et al.*, 2010). The GFP-ELO3 fusion protein was present in the nucleus and, to a lesser extent, in the cytoplasm. Deconvolution microscopy distinguished small and large "signal holes" in the nuclei, representing the heterochromatic centers and nucleolus. GFP-ELO3 immunolocalization had a signal overlap with the euchromatic marker, histone H3 lysine 4 dimethylation (H3K4me2); in contrast, the RNA pol II CTD phospho Ser5, GFP-ELO3 and the heterochromatic marker, H3K9me2, were mutually exclusive. Hence, the colocalization data supported a nuclear function for Elongator in plants.

Phenotypes of the double *elo swp1* mutant indicated epistasis of the SWP1 subunit of the MEDIATOR transcription initiation complex in genetic interactions with Elongator and revealed Elongator acts downstream of MEDIATOR (Nelissen *et al.*, 2003). Both the SUPPRESSOR of Ty4 (SPT4) transcript elongation factor and MINIYO (IYO, a RNA pol II-associated protein 1 homolog) interacted with the RBP subunits of RNA pol II, and pulled down ELP3/ELO3 and ELP1/ELO2 in *Arabidopsis* cell suspension cultures, confirming the nuclear localization of Elongator and supporting a role in transcription in plants (Sanmartín *et al.*, 2011; Dürr *et al.*, 2014; Van Lijsebettens *et al.*, 2014). Furthermore, the histone H3K14 acetylation levels were reduced in *Arabidopsis* Elongator mutants at the coding part of specific genes related to auxin response (Nelissen et al., 2010), immune response (Wang *et al.*, 2013), and root development (Jia et al., 2015), corresponding to reduced transcript levels of relevant genes and arguing for a conserved role of Elongator in histone H3K14 acetylation during RNA pol II transcript elongation in plants (Nelissen *et al.*, 2010; Van Lijsebettens and Grasser, 2014). Genetic interaction was demonstrated between mutants in *Arabidopsis* Elongator subunits and FACILITATES CHROMATIN TRANSCRIPTION (FACT) chaperone subunits (Lolas *et al.*, 2012) or HISTONE H2B MONOUBIQUITINATION1 (HUB1) (Himanen *et al.*, 2012), and added to a function for plant Elongator in transcript elongation. Histone chaperones, such as FACT, and histone-modifying complexes, such as Elongator (H3K14ac) and HUB1 (H2Bub), positively control the efficiency of the RNA pol II transcript elongation of subsets of genes in the chromatin context and contribute to the tuning of gene expression programs in higher organisms, including plants (Van

Lijsebettens and Grasser, 2014). Nuclear accumulation of the IYO protein is crucial for the switch to the differentiation state in *Arabidopsis*, because the *iyo* mutants have a delayed differentiation of all plant meristems and overexpression depletes plant meristems by consumption of stem cells, it interacts with RNA pol II to positively regulate the elongation phase of transcription (Sanmartín *et al.*, 2011). IYO interacted physically with ELP3/ELO3 and genetically with *ELP1, ELP3* and *DRL1*, i.e. their double mutants grew as undifferentiated callus, indicating a complete differentiation block. Sanmartín *et al.* (2012) hypothesize that factors like IYO and Elongator that promote transcript elongation might be crucial to turn on differentiation programs in plants by activating stalled RNA pol II, in analogy with the onset of developmental programs in *Drosophila melanogaster* (Muse *et al.*, 2007; Zeitlinger *et al.*, 2007).

The plant Elongator interacted with DCL1 and SE, resp. a major and an auxillary component of the microprocessor complex that is involved in the processing of primary (pri)-miRNAs and biogenesis of miRNAs (Fang *et al.*, 2015). Reduced accumulation of a number of specific miRNAs, increased transcript levels of their respective target genes, reduced DCL1 recruitment to chromatin and miRNA genes in the *elp/elo* mutants suggested that Elongator positively affects pri-miRNA processing by recruitment of the microprocessor complex (Fang *et al.*, 2015; Laubinger, 2015). Hence, a novel role for Elongator in epigenetic regulation has been discovered for the first time in plants that presumably does not depend on a new catalytic activity of one of the *ELP* genes, but rather involves the interaction with and activity of another complex, i.e. the microprocessor complex to steer functions in miRNA biogenesis.

An interaction network for ELP proteins has been investigated with *Arabidopsis thaliana* Protein Interaction Network (AtPIN) software (Brandão *et al.*, 2009), revealing 26 putative interactors of the plant Elongator. These putative interactors represent orthologs of yeast, human, *Drosophil*a, or bacterial proteins interacting with the ELP1, ELP2 or ELP3 subunits and were detected by copurification, affinity capture, yeast two-hybrid, pull down, or biochemical experiments. Of these interactors, 13 are particularly interesting with respect to known Elongator activities and functions in transcriptional regulation (Table 2). Three of the interactors represent the TATA-binding protein associated Factors TAF9, TAF14, and TAF14B, which are subunits of the general

transcription factor TFIID. The TAF14 and TAF14B subunits belong to the NuA4 complex that acetylates nucleosomal histones, whereas another interactor, ATSWC4, is a subunit of the SWR1-C complex that catalyzes the histone variant exchange reaction and interacts with NuA4. Moreover, the ELP3 subunit interacts with histone HTA9, one of the histone H2A.Z variants. All these interactors support a role for Elongator in histone acetylation related to histone variant exchange. In support of the role for plant Elongator as transcript elongation factor (Van Lijsebettens and Grasser, 2014), five RNA pol II subunits, NRPB1 to NRPB5 have been identified as interactors of the ELP2 subunit. Another interesting interactor is the U11/U12-65K protein, a U12-type spliceosomal protein that is an indispensable component of the minor spliceosome and plays a crucial role in U12 intron splicing and alternative splicing. Furthermore, the U11/U12-65K mutation affected splicing of many genes and resulted in developmental and growth defects in plants (Jung and Kang 2014). Taking into account the recently discovered function of the plant Elongator in miRNA processing, the protein encoded by the AT5G25800 gene that is similar to the small RNA-degrading nuclease 1 seems to be a relevant candidate for interaction with Elongator in plants, in addition to the interacting subunit of RNA polymerase V that plays a role in small interfering (si)RNA biogenesis and in the siRNA-directed DNA methylation pathway. Hence, the putative interactors retrieved from the AtPIN database support a role for Elongator in a number of nuclear processes related to chromatin and epigenetic regulation of gene expression and might be instrumental for further experimental research in plants.

Table 2. *Arabidopsis* **orthologs of Elongator interactors in yeast or** *Drosophila* **revealed by the AtPIN software**

AGI code	Gene	Description	Interactor of Elongator subunit			Experiment	Ortholog
			ELP1	ELP2	ELP3		
AT1G54140	*TAF9, TAFII21*	TATA BINDING PROTEIN ASSOCIATED FACTOR 21KDA SUBUNIT of general transcription factor IID (TFIID), TBP-ASSOCIATED FACTOR 9	x	x	x	Affinity capture-MS (Sanders et al., 2002)	Yeast

hold

Locus	Gene	Description			Method	Organism
AT5G45600	*TAF14B, YAF9A*	HOMOLOG OF YEAST YAF9 subunit of NuA4 complex acetylating nucleosomal histones; TAF14B, TBP-ASSOCIATED FACTOR 14B	x		Affinity capture-MS (Zhang et al., 2004)	Yeast
AT2G18000	*TAF14, YAF9B*	HOMOLOG OF YEAST YAF9 subunit of NuA4 complex acetylating nucleosomal histones; TAF14, TBP-ASSOCIATED FACTOR 14	x		Affinity capture-MS (Zhang et al., 2004)	Yeast
AT2G47210	*ATSWC4*	Subunit of SWR1-C complex catalyzing histone variant exchange reaction	x		Affinity capture-MS (Hazbun et al., 2003)	Yeast
AT1G52740	*HTA9*	Histone H2A protein 9		x	Biochemical (Keogh et al., 2006)	Yeast
AT4G35800	*NRPB1*	Encodes the unique largest subunit of nuclear DNA-dependent RNA polymerase II; the ortholog of budding yeast RPB1 and a homolog of the *E. coli* RNA polymerase β' subunit	x	x	Affinity capture-Western, copurification (Otero et al., 1999; Fichtner et al., 2003; Geisler-Lee et al., 2007; Fellows et al., 2000; Frohloff et al., 2003)	Yeast
AT4G21710	*NRPB2*	Encodes the unique second-largest subunit of DNA-dependent RNA polymerase II; the ortholog of budding yeast RPB2 and a homolog of the *E. coli* RNA polymerase β subunit		x	Affinity capture-Western, copurification, (Fellows et al., 2000)	Yeast
AT2G15430	*NRPB3*	Noncatalytic subunit of nuclear DNA-dependent RNA polymerases II, IV and V; homologous to budding yeast RPB3 and the *E. coli* RNA polymerase α subuni		x	Affinity capture-Western, copurification (Fellows et al., 2000)	Yeast
AT5G09920	*NRPB4*	Noncatalytic subunit specific to DNA-dependent RNA polymerase II; the ortholog of budding yeast RPB4		x	Affinity capture-Western, copurification (Fellows et al., 2000)	Yeast
AT3G22320	*NRPB5*	Noncatalytic subunit common to DNA-dependent RNA polymerases I, II, III and IV; homologous to budding yeast RPB5.		x	Affinity capture-Western, copurification (Fellows et al., 2000)	Yeast

AT1G09230	*U11/U12-65K*	U12-type spliceosomal protein that is an indispensible component of the minor spliceosome and plays a crucial role in U12 intron splicing	x		Y2H (Geisler-Lee et al., 2007; Giot et al., 2003)	*Drosophila*
AT5G25800		Polynucleotidyl transferase, ribonuclease H-like superfamily protein; BEST Arabidopsis thaliana protein match is: small RNA degrading nuclease 1 AT3G50100	x		Y2H (Geisler-Lee et al., 2007; Giot et al., 2003)	*Drosophila*
AT2G15400	*NRPE3B*	Non-catalytic subunit of nuclear DNA-dependent RNA polymerase V; homologous to budding yeast RPB3 and the *E. coli* RNA polymerase α subunit		x	Affinity capture-Western, copurification (Fellows et al., 2000)	Yeast

5   Molecular pathways and genes targeted by Elongator activities in plants

In yeast and animals, Elongator is involved in exocytosis, zymocin toxicity, sensitivity to DNA-damaging agents, zygotic paternal DNA demethylation, neuron development, and regulation of transcription and translation. Elongator might control molecular pathways and biological processes at the transcriptional or translational level via its enzymatic activities in protein acetylation, including histone acetylation (ELP3 HAT domain) and modifications of uridines at the wobble position in several tRNAs or DNA cytosine demethylation (ELP3 SAM domain). Transcriptome analyses in human and yeast were used for molecular phenotyping and supported a role in neuronal development (Cohen-Kupiec *et al*., 2011) and stress adaptation (Krogan and Greenblatt, 2001), respectively. However, elevated levels of Elongator-dependent tRNAs can rescue transcription defects in the yeast *elp* mutants or result in reduced production of transcription factors, thus affecting transcriptome indirectly as demonstrated in yeast (Esberg *et al*., 2006; Fernández-Vásquez *et al*., 2013). Hence, caution should be taken in assigning target genes, pathways, and processes to the Elongator activities.

In plants, morphological and molecular phenotypes of the *elo* mutants revealed cellular activities and pathways in which Elongator plays a role, i.e. growth and cell proliferation (Nelissen *et al*., 2005), leaf (Falcone *et al*., 2007) and root (Jia *et al*., 2015) development, immune response (Wang *et al*.,2013), cell cycle (Xu *et al*., 2011), tissue differentiation

(Sanmartin *et al.*, 2011), ABA responses (Chen *et al.*, 2006), oxidative stress resistance and anthocyanin biosynthesis (Zhou *et al.*, 2009). Plant growth (Nelissen *et al*, 2010), immune response (Wang *et al.*, 2013; Wang *et al.*, 2015) and root development (Jia *et al.*, 2015) pathways were found to be regulated by the histone acetylation and/or DNA demethylation enzymatic activities of Elongator during transcription.

5.1   Histone acetyl transferase activity of plant Elongator

The impact of the Elongator HAT on the activation of plant gene transcription is well established. Two auxin-related growth regulatory genes *SHORT HYPOCOTYL2* (*SHY2*, an auxin repressor) and *AUXIN TRANSPORTER-LIKE PROTEIN2* (*LAX2*, an auxin influx carrier) (Nelissen *et al.*, 2010), five genes of the SA defense pathway, i.e. *NONEXPRESSOR OF PATHOGENESIS-RELATED GENES1* (*NPR1*), *PHYTOALEXIN DEFICIENT4* (*PAD4*), *ENHANCED DISEASE SUSCEPTIBILITY1* (*EDS1*), *PATHOGENESIS-RELATED GENES2* (*PR2*) and *PR5* (Wang *et al.*, 2013), three genes of the jasmonic acid/ethylene (JA/ET) defense pathway, i.e. *WRKY33, OCTADECANOID-RESPONSIVE ARABIDOPSIS AP2/ERF59* (*ORA59*), *PLANT DEFENSIN1.2* (*PDF1.2*) (Wang *et al.*, 2015), and four transcription factor genes responsible for root development *PLETHORA1* (*PLT1*) and *PTL2 SHORT ROOT* (*SHR*), and *SCARECROW* (*SCR*) (Jia *et al.*, 2015) were identified as targets of the HAT activity of the Elongator (Fig. 4). Genes targeted by Elongator were identified based on lower histone H3 acetylation detected in their coding regions in the Arabidopsis *elp/elo* mutants as compared to wild type by means of the chromatin immunoprecipitation-quantitative polymerase chain reaction (ChIP-qPCR) method with antibodies against either H3K14Ac (Nelissen *et al.*, 2010) or H3K9/14Ac (Wang *et al.*, 2013, 2015; Jia *et al.*, 2015). Although the HAT domain is located in the ELP3 subunit, decreased histone H3 acetylation was found both in the *elp3* and *elp2* mutants, indicating that in plants, similarly as in yeast (Winkler *et al.*, 2002), Elongator as a complex is required for HAT activity. Elongator was found to modify histone acetylation selectively, because among eight assayed auxin-related genes, only two were targeted by the complex (Nelissen *et al.*, 2010) and among six analysed SA-induced genes (Wang *et al.*, 2013), five Elongator targets for HAT activity were detected. Genes with decreased basal levels of histone H3K14Ac in the *elp/elo* mutants had either a decreased basal expression or a reduced expression induction (in the case of genes triggered by pathogen infection). Decreased histone H3 acetylation was detected only in

the coding regions of the genes, but not in the promoters, implying that Elongator regulates transcription at the RNA pol II transcript elongation stage. Differences in the acetylation levels between the *elp/elo* mutants and the wild-type plants were moderate, maximally two folds. Thus, histone acetylation by Elongator is generally considered to activate basal or inductive expression of selected genes via facilitation of transcript elongation. Components of signalling cascades might activate or repress Elongator complex subunits through for example phosphorylation and could explain Elongator activity in certain environmental or developmental conditions or its putative "target gene specificity".
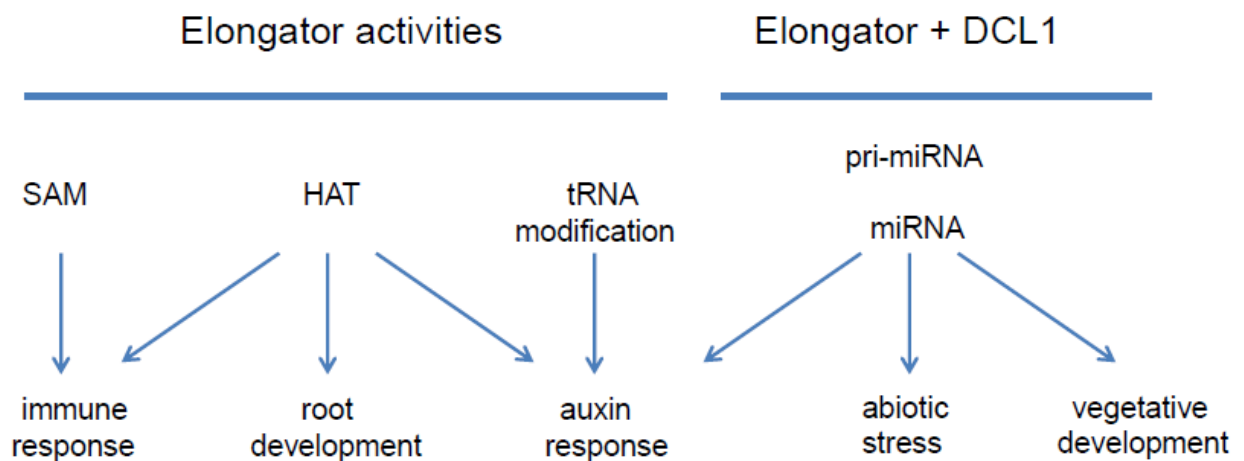
Figure 4. **Plant molecular pathways targeted by Elongator activities and by the DCL1 microprocessor interaction.** SAM, *S*-adenosyl methionine binding; HAT, histone acetyl transferase; pri-miRNA processing; miRNA transcription.

5.2   DNA demethylation activity of plant Elongator

The Elp3 subunit of Elongator contains also the radical SAM domain, originally assumed to be involved in histone demethylation (Chinenov, 2002). However, recent research in mice (*Mus musculus*) showed that Elongator, and more specifically, the radical SAM but not the HAT domain of Elp3, is required for paternal DNA demethylation in zygotes (Okada *et al.*, 2010). Hypothetically, a strong oxidizing agent, 5'-deoxyadenosyl, could be formed by the Elp3 SAM activity that might extract a hydroxyl group of 5 methyl cytosine to generate a powerful radical for further reactions (Okada *et al.*, 2010). The experimentally supported model for the tRNA modification by Elp3 SAM and HAT

activities is remarkably analogous in the first reaction steps in which the Elp3 SAM activity produces a SAM-derived 5'-deoxyadenosyl radical that extracts a hydrogen atom from the methyl group of acetyl-CoA bound by the Elp3 HAT domain to react with the C5 of the U34 tRNA (Selvadurai *et al.*, 2014). Hence, the seemingly distinct activities of the Elp3 SAM domain in DNA demethylation and tRNA modification might have biochemistry in common.

In plant *elp/elo* mutants, modified DNA methylation levels were identified by means of both gene-specific (Wang *et al.*, 2013; Jia *et al.*, 2015) and genome-wide approaches (Wang *et al.*, 2013). Two defense genes, *NPR1* and *PAD4*, with reduced expression in the *elp2* mutant and regulated by Elongator via histone acetylation, were assayed for DNA methylation levels (Wang *et al.*, 2013). The methylation of the *NPR1* promoter and *PAD4*-coding regions was higher in the *elp2* mutant than that of the wild type, but lower in the NPR1-coding part (Fig. 4). In the *B-type CYCLIN1* (*CYCB1*) gene that was upregulated in the *elp2* mutant, methylation levels were reduced both in the promoter and in the coding region (Jia *et al.*, 2015). The genome-wide bisulfite deep-sequencing analysis of the cytosine methylation patterns in the *elp2* mutant and wild type revealed that more cytosines were methylated in *elp2*, but that the average methylation level was lower than those of the wild type. When specific cytosines were analyzed, either increased or decreased methylation levels were detected in the *elp2* mutant, suggesting that Elongator is involved in both demethylation and methylation. Therefore, although cytosine methylation patterns indicate that Elongator modulates DNA methylation, it is unclear whether the complex is involved in cytosine methylation, demethylation, or both activities and how these modifications influence gene expression levels. Elongator may affect DNA methylation not only directly via the activity of its SAM domain, but also through regulation of transcript levels of DNA methyltransferases, as suggested by the enhanced expression of the *DRM7*, *DRM8*, and *MET1* genes in the silenced *ELP2* line of tomato (Zhu *et al.*, 2015).

5.3   Role of plant Elongator on pri-miRNA transcription and miRNA processing

Besides protein-coding genes transcriptionally regulated by Elongator via histone acetylation and DNA demethylation activities, genes encoding plant miRNAs also require Elongator to promote their transcription, although the exact mechanism of this

regulation is unknown. Indeed, the *elp2* and *elp5* mutants were obtained as suppressor mutations of the *ema1* mutant, overexpressing an artificial miRNA targeting three trichome regulators with a trichome-clustering phenotype (Fang *et al.*, 2015). Interestingly, through interaction with the DCL1 component of the microprocessor complex, Elongator is involved in further steps of miRNAs biogenesis such as the configuration of DCL1 in functional D-bodies and its association with chromatin. Therefore, Elongator positively regulates transcription of pri-miRNAs and facilitates cotranscriptional processing of pri-miRNAs into mature miRNAs by recruiting DCL1 to nascent pri-miRNAs. Endogenous miRNAs, such as *miR159*, *miR160*, *miR164*, *miR165*, *miR166*, *miR167*, and *miR398* were decreased in *elp2* and *elp5* mutants which resulted in increased transcript levels of their complementary target genes, such as *CUP-SHAPED COTYLEDON2* (*CUC2*) involved in leaf development and *AUXIN RESPONSE FACTOR17* (*ARF17*) and *ARF8* involved in auxin responses (Fig. 4). Hence, the Elongator function in miRNA transcription and biogenesis might contribute to the described phenotypes of the *elp*/*elo* mutants, such as narrow leaves and altered phyllotaxis, because miRNAs are known to reduce transcript levels of transcription factors, stress response proteins, and other proteins controlling growth, development, and plant physiology.

5.4 tRNA modification activity of plant Elongator might affect indirectly the transcriptome

An indirect effect on the transcriptome might be caused by the Elongator activity in tRNA wobble uridine modification that affects translation of certain proteins with a preference for those requiring Elongator-modified tRNAs for translation. Interestingly, in plants, regulation of tRNA maturation by Elongator is specifically important for auxin-controlled developmental processes and Elongator-mediated translational regulation of the PIN-FORMED (PIN) auxin transport protein seems to be a primary event in this pathway (Fig. 4) (Leitner *et al.*, 2015). Therefore, the plant Elongator regulates auxin responses via two different activities, histone acetylation and tRNA modification that operate at transcriptional and translational levels of gene expression, respectively. The crosstalk between the two Elongator activities that control the auxin pathway is unclear, but reduced abundance of the PIN1 protein and lack of decrease in *PIN1* transcript levels in the *elp*/*elo* mutants indicate that Elongator activities related to

transcription and translation might target different genes within the same molecular pathway.

5.5 Pathways shared by the plant Elongator and other transcript elongation factors

Elongator shares downstream target pathways and genes with a number of transcript elongation factors, such as SPT4/SPT5 and HUB1. Plants defective in SPT4/SPT5 activity had auxin-related phenotypes similar to those of the *elp/elo* mutants, i.e. reduced cell proliferation, reduced root growth, decreased lateral root density, and impaired leaf venation (Dürr *et al.*, 2014). Transcriptome analysis of plants depleted in SPT4 or ELO3 revealed common downregulated genes involved in auxin response and transport as well as in cell elongation and organ morphogenesis, indicating that Elongator and the SPT4/SPT5 elongation factors may work together during transcription of selected genes related to growth and development (Van Lijsebettens *et al.*, 2014). Genetic interaction between Elongator and the transcript elongation-facilitating HUB1 factor was apparent by the embryo lethality of the double *elo hub1* mutants with embryos arrested at the torpedo growth stage. Both Elongator and *HUB1* were expressed in all cells and tissues during the torpedo stage of embryogenesis, suggesting that they synergistically act on common processes during embryo development. Indeed, microarray analyses of the *elp3/elo3* and *hub1* mutants confirmed the high overlap between genes downregulated in both mutants, including genes highly expressed in embryos (Himanen *et al.*, 2012). Thus, Elongator can be viewed as an important player in the network of transcriptional regulators interacting with diverse partners and contributing to the regulation of different molecular pathways.

5.6 Interaction between pathways regulated by Elongator

In plants, Elongator positively regulates growth and immune responses (review Rojas *et al.*, 2014), two pathways known to interact negatively. Indeed, *Arabidopsis* mutants constitutively expressing defense genes are stunted, whereas plants defective in defense signalling are taller (Heil and Baldwin, 2002). At the metabolic level, plant-pathogen interactions result in a compensatory energy shift in which the expression of growth-related genes is downregulated in favour of upregulated immune response-related pathways. Elongator regulates growth via auxin-related pathways by its two activities linked to histone acetylation and tRNA maturation. In contrast, Elongator activates

immune responses by histone acetylation and DNA methylation/demethylation of genes of the SA and JA pathways. The interplay between SA, JA, and auxin signalling shapes the growth-defense balance (review Naseem *et al.*, 2015). High SA levels triggered by pathogen infection repress auxin signalling and defense is prioritized over growth, whereas in the absence of pathogens, auxin attenuates SA responses, with activation of growth programs as a consequence. Interactions between auxin and JA signalling occur at multiple levels and the crosstalk of these two pathways is highly complicated. The JA and auxin pathways positively and synergistically regulate plant defense, but the positive feedback loop from JA to auxin signalling results in overall growth inhibition. How Elongator contributes to the interplay between the SA, JA, and auxin pathways is unknown. However, in the absence of pathogen infection, Elongator might possibly act as a positive growth regulator in the auxin signalling pathway, whereas its role to maintain defense gene expression is only limited, as suggested by the comparable basal transcript levels of these genes in the noninfected wild type and *elo2* mutant plants (Wang *et al.*, 2013). Upon a pathogen attack, Elongator is necessary for fast induction of defense genes, but its positive growth regulation can be turned down either by dissociation or inactivation of the Elongator complex in the growth-related genes or by attenuation of growth pathways at another expression level, such as transcript initiation.

6 Conclusion and perspectives

The structure and enzymatic activities of the Elongator complex are conserved from yeast to human to plant. However, the complex localizes predominantly in the cytoplasm in mammals and yeast as opposed to the nucleus in plants, that might explain the evolution of different substrates as targets for the Elongator activities, i.e. proteins different from histones are acetylated in human and *Drosophila* (Creppe *et al.*, 2009; Miskiewicz *et al.*, 2011). Pathways regulated by Elongator also diverged over the kingdoms, reflecting diversification in inducibility of the *ELP* genes themselves. A number of environmental conditions that induce or repress Elongator genes were identified in the meta-analysis (Fig.3) and might be the starting point for further experimental research. In analogy, proteins steering Elongator activity might be only detected in sophisticated experimental set ups under specific growth conditions or upon a time course of inductive or repressive conditions. Indeed, the interaction between Elongator and the microprocessor complex revealed a role for Elongator in miRNA

transcription and biogenesis, described only in plants thus far (Fang *et al.*, 2015) and encourages mining for more interactors in future research. The various activities of the plant Elongator in transcription and translation contribute to specific *elp/elo* mutant phenotypes, such as the auxin biology-related ones (Nelissen *et al.*, 2010; Leitner *et al.*, 2015; Fang *et al.*, 2015), indicating a complex regulation at different levels that might allow a versatile and fast production of specific proteins and further research might reveal innovative insights in the cross-talk between transcriptional and translational regulation.

7 References

Abdel-Fattah, W., Jablonowski, D., Di Santo, R., Thüring, K.L., Scheidt, V., Hammermeister, A., ten Have, S., Helm, M., Schaffrath, R., and Stark, M.J.R. (2015). Phosphorylation of Elp1 by Hrr25 is required for Elongator-dependent tRNA modification in yeast. PLoS Genet. 11, e1004931.

An, C., Ding, Y., Zhang, X., Wang, C., and Mou, Z. (2016). Elongator plays a positive role in exogenous NAD-induced defense responses in *Arabidopsis*. Mol. Plant-Microbe Interact. 29, 5, 396-404

Anderson, S.L., Coli, R., Daly, I.W., Kichula, E.A., Rork, M.J., Volpi, S.A., Ekstein, J., and Rubin, B.Y. (2001). Familial dysautonomia is caused by mutations of the IKAP gene. Am. J. Hum. Genet. 68, 753-758.

Berná, G., Robles, P., and Micol, J.L. (1999). A mutational analysis of leaf morphogenesis in *Arabidopsis thaliana*. Genetics 152, 729-742.

Brandão, M.M., Dantas, L.L., and Silva-Filho, M.C. (2009). AtPIN: *Arabidopsis thaliana* Protein Interaction Network. BMC Bioinformatics 10, 454.

Chen, Z., Zhang, H., Jablonowski, D., Zhou, X., Ren, X., Hong, X., Schaffrath, R., Zhu, J.-K., and Gong, Z. (2006). Mutation in ABO1/ELO2, a subunit of Holo-Elongator, increase abscisic acid sensitivity and drought tolerance in *Arabidopsis thaliana*. Mol. Cell. Biol. 26, 6902-6912.
Chinenov, Y. (2002). A second catalytic domain in the Elp3 histone acetyltransferases: a candidate for histone demethylase activity? Trends Biochem. Sci. 27, 115-117.

Cohen-Kupiec, R., Pasmanik-Chor, M., Oron-Karni, V., and Weil, M. (2011). Effects of IKAP/hELP1 deficiency on gene expression in differentiating neuroblastoma cells: implications for familial dysautonomia. PLoS ONE 6, e19147.

Creppe, C., Malinouskaya, L., Volvert, M.-L., Gillard, M., Close, P., Malaise, O., Laguesse, S., Cornez, I., Rahmouni, S., Ormenese, S., Belachew, S., Malgrange, B., Chapelle, J.-P., Siebenlist, U., Moonen, G., Charlot, A., and Nguyen, L. (2009). Elongator controls the migration and differentiation of cortical neurons through acetylation of α-tubulin. Cell 136, 551-564.

DeFraia, C.T., Wang, Y., Yao, J., and Mou, Z. (2013). Elongator subunit 3 positively regulates plant immunity through its histone acetyltransferase and radical *S*-adenosylmethionine domains. BMC Plant Biol. 13, 102.

DeFraia, C.T., Zhong, X., and Mou, Z. (2010). Elongator subunit 2 is an accelerator of immune responses in *Arabidopsis thaliana*. Plant J. 64, 511-523.

Di Santo, R., Bandau, S., and Stark, M.J.R. (2014). A conserved and essential basic region mediates tRNA binding to the Elp1 subunit of the *Saccharomyces cerevisiae* Elongator complex. Mol. Microbiol. 92, 1227-1242.

Ding, Y., and Mou, Z. (2015). Elongator and its epigenetic role in plant development and responses to abiotic and biotic stresses. Front. Plant Sci. 6, 296.

Dong, C., Lin, Z., Diao, W., Li, D., Chu, X., Wang, Z., Zhou, H., Xie, Z., Shen, Y., and Long, J. (2015). The Elp2 subunit is essential for Elongator complex assembly and functional regulation. Structure 23, 1078-1086.

Dürr, J., Lolas, I.B., Sørensen, B.B., Schubert, V., Houben, A., Melzer, M., Deutzmann, R., Grasser, M., and Grasser, K.D. (2014). The transcript elongation factor SPT4/SPT5 is involved in auxin-related gene expression in *Arabidopsis*. Nucleic Acids Res. 42, 4332-4347.

Esberg, A., Huang, B., Johansson, M.J., and Byström, A.S. (2006). Elevated levels of two tRNA species bypass the requirement for Elongator complex in transcription and exocytosis. Mol. Cell 24, 139-148.

Falcone, A., Nelissen, H., Fleury, D., Van Lijsebettens, M., and Bitonti, M.B. (2007). Cytological investigations of the *Arabidopsis thaliana elo1* mutant give new insights into leaf lateral growth and Elongator function. Ann. Bot. 100, 261-270.

Fang, X., Cui, Y., Li, Y., and Qi, Y. (2015). Transcription and processing of primary microRNAs are coupled by Elongator complex in *Arabidopsis*. Nat. Plants 1, 15075.

Fellows, J., Erdjument-Bromage, H., Tempst, P., and Svejstrup, J.Q. (2000). The Elp2 subunit of Elongator and elongating RNA polymerase II holoenzyme is a WD40 repeat protein. J. Biol. Chem. 275, 12896-12899.

Felsenstein, J. (1985). Confidence limits on phylogenies: an approach using the bootstrap. Evolution 39, 783-791.

Fernández-Vázquez, J., Vargas-Pérez, I., Sansó, M., Buhne, K., Carmona, M., Paulo, E., Hermand, D., Rodríguez-Gabriel, M., Ayté, J., Leidel, S., and Hidalgo, E. (2013). Modification of tRNA$^{Lys}_{UUU}$ by Elongator is essential for efficient translation of stress mRNAs. PLoS Genet. 9, e1003647.

Frohloff, F., Fichtner, L., Jablonowski, D., Breunig, K.D., and Schaffrath, R. (2001). *Saccharomyces cerevisiae* Elongator mutations confer resistance to the *Kluyveromyces lactis* zymocin. EMBO J. 20, 1993-2003.

Frohloff, F., Jablonowski, D., Fichtner, L., and Schaffrath, R.. (2003). Subunit communications crucial for the functional integrity of the yeast RNA polymerase II Elongator (γ-toxin target (TOT)) complex. J. Biol. Chem. 278, 956-961.

Geisler-Lee, J., O'Toole, N., Ammar, R., Provart, N.J., Millar, A.H., and Geisler, M. (2007). A predicted interactome for Arabidopsis. Plant Physiol. 145, 317-329.

Giot, L., Bader, J.S., Brouwer, C., Chaudhuri, A., Kuang, B., Li, Y., Hao, Y.L., Ooi, C.E., Godwin, B., Vitols, E., Vijayadamodar, G., Pochart, P., Machineni, H., Welsh, M., Kong, Y., Zerhusen, B., Malcolm, R., Varrone, Z., Collis, A., Minto, M., Burgess, S., McDaniel, L., Stimpson, E., Spriggs, F., Williams, J., Neurath, K., Ioime, N., Agee, M., Voss, E., Furtak, K., Renzulli, R., Aanensen, N., Carrolla, S., Bickelhaupt, E., Lazovatsky, Y., DaSilva, A., Zhong, J., Stanyon, C.A., Finley, R.L. Jr., White, K.P., Braverman, M., Jarvie, T., Gold, S., Leach, M., Knight, J., Shimkets, R.A., McKenna, M.P., Chant, J., and Rothberg, J.M. (2003). A protein interaction map of *Drosophila melanogaster*. Science 302, 1727-1736.

Glatt, S., and Müller, C.W. (2013). Structural insights into Elongator function. Curr. Opin. Struct. Biol. 23, 235-242.

Glatt, S., Létoquart, J., Faux, C., Taylor, N.M.I., Séraphin, B., and Müller, C.W. (2012). The Elongator subcomplex Elp456 is a hexameric RecA-like ATPase. Nat. Struct. Mol. Biol. 19, 314-320.

Hawkes, N.A., Otero, G., Winkler, G.S., Marshall, N., Dahmus, M.E., Krappmann, D., Scheidereit, C., Thomas, C.L., Schiavo, G., Erdjument-Bromage, H., Tempst, P., and Svejstrup, J.Q. (2002). Purification and characterization of the human Elongator complex. J. Biol. Chem. 277, 3047-3052.

Hazbun, T.R., Malmström, L., Anderson, S., Graczyk, B.J., Fox, B., Riffle, M., Sundin, B.A., Aranda, J.D., McDonald, W.H., Chiu, C.-H., Snydsman, B.E., Bradley, P., Muller, E.G.D., Fields, S., Baker, D., Yates, J.E. III, and Davis, T.N. (2003). Assigning function to yeast proteins by integration of technologies. Mol. Cell 12, 1353-1365.

Heil, M., and Baldwin, I.T. (2002). Fitness costs of induced resistance: emerging experimental support for a slippery concept. Trends Plant Sci. 7, 61-67.

Himanen, K., Woloszynska, M., Boccardi, T.M., De Groeve, S., Nelissen, H., Bruno, L., Vuylsteke, M., and Van Lijsebettens, M. (2012). Histone H2B monoubiquitination is required to reach maximal transcript levels of circadian clock genes in Arabidopsis. Plant J. 72, 249-260.

Jia, Y., Tian, H., Li, H., Yu, Q., Wang, L., Friml, J., and Ding, Z. (2015). The *Arabidopsis thaliana* elongator complex subunit 2 epigenetically affects root development. J. Exp. Bot. 66, 4631-4642.

Jung, H.J., and Kang, H. (2014), The Arabidopsis U11/U12-65K is an indispensible component of minor spliceosome and plays a crucial role in U12 intron splicing and plant development. Plant J. 78, 799–810.

Keogh, M.-C., Mennella, T.A., Sawa, C., Berthelet, S., Krogan, N.J., Wolek, A., Podolny, V., Rocco Carpenter, L., Greenblatt, J.F., Baetz, K., and Buratowski, S. (2006). The *Saccharomyces cerevisiae* histone H2A variant Htz1 is acetylated by NuA4. Genes Dev. 20, 660-665.

Kojima, S., Iwasaki, M., Takahashi, H., Imai, T., Matsumura, Y., Fleury, D., Van Lijsebettens, M., Machida, Y., and Machida, C. (2011). ASYMMETRIC LEAVES2 and Elongator, a histone acetyltransferase complex, mediate the establishment of polarity in leaves of *Arabidopsis thaliana*. Plant Cell Physiol. 52, 1259-1273.

Krogan, N.J., and Greenblatt, J.F. (2001). Characterization of a six-subunit holo-Elongator complex required for the regulated expression of a group of genes in *Saccharomyces cerevisiae*. Mol. Cell. Biol. 21, 8203-8212.

Kumar, S.V., and Wigge, P.A. (2010). H2A.Z-containing nucleosomes mediate the thermosensory response in *Arabidopsis*. Cell 140, 136-147.

Kumar, V., and Wigge, P.A. (2007). Red sky in the morning, shepherd's warning. Nat. Genet. 39, 1309-1310.

Laubinger, S. (2015). Elongator caught in the act. Nat. Plants 1, 15076.

Leitner, J., Retzer, K., Malenica, N., Bartkeviciute, R., Lucyshyn, D., Jäger, G., Korbei, B., Byström, A., and Luschnig, C. (2015). Meta-regulation of *Arabidopsis* auxin responses depends on tRNA maturation. Cell Rep. 11, 516-526.

Lin, Z., Zhao, W., Diao, W., Xie, X., Wang, Z., Zhang, J., Shen, Y., and Long, J. (2012). Crystal structure of Elongator subcomplex Elp4-6. J. Biol. Chem. 287, 21501-21508.
Lolas, I.B., Himanen, K., Grønlund, J.T., Lyngaard, C., Houben, A., Melzer, M., Van Lijsebettens, M., and Grasser, K.D. (2010). The transcript elongation factor FACT affects *Arabidopsis* vegetative and reproductive development and functionally interacts with HUB1/2. Plant J. 61, 686-697.

Mehlgarten, C., Jablonowski, D., Wrackmeyer, U., Tschitschmann, S., Sondermann, D., Jäger, G., Gong, Z., Byström, A.S., Schaffrath, R., and Breunig, K.D. (2010). Elongator function in tRNA wobble uridine modification is conserved between yeast and plants. Mol. Microbiol. 76, 1082-1094.

Miśkiewicz, K., Jose, L.E., Bento-Abreu, A., Fislage, M., Taes, I., Kasprowicz, J., Swerts, J., Sigrist, S., Versées, W., Robberecht, W., and Verstreken, P. (2011). ELP3 controls active zone morphology by acetylating the ELKS family member Bruchpilot. Neuron 72, 776-788.

Muse, G.W., Gilchrist, D.A., Nechaev, S., Shah, R., Parker, J.S., Grissom, S.F., Zeitlinger, J., and Adelman, K. (2007). RNA polymerase is poised for activation across the genome. Nat. Genet. 39, 1507-1511.

Naseem, M., Kaltdorf, M., and Dandekar, T. (2015). The nexus between growth and defence signalling: auxin and cytokinin modulate plant immune response pathways. J. Exp. Bot. 66, 4885-4896.

Nei, M., and Kumar, S. (2000). *Molecular Evolution and Phylogenetics*. New York, Oxford University Press.

Nelissen, H., Boccardi, T.M., Himanen, K., and Van Lijsebettens, M. (2007). Impact of core histone modifications on transcriptional regulation and plant growth. Crit. Rev. Plant Sci. 26, 243-263.

Nelissen, H., Clarke, J.H., De Block, M., De Block, S., Vanderhaeghen, R., Zielinski, R.E., Dyer, T., Lust, S., Inzé, D., and Van Lijsebettens, M. (2003). DRL1, a homolog of the yeast TOT4/KTI12 protein, has a function in meristem activity and organ growth in plants. Plant Cell 15, 639-654.

Nelissen, H., De Groeve, S., Fleury, D., Neyt, P., Bruno, L., Bitonti, B., Vandenbussche, F., Van Der Straeten, D., Yamaguchi, T., Tsukaya, H., Witters, E., De Jaeger, G., Houben, A., and Van Lijsebettens, M. (2010). Plant Elongator regulates auxin-related genes during RNA polymerase II transcript elongation. Proc. Natl. Acad. Sci. USA 107, 1678-1683.

Nelissen, H., Fleury, D., Bruno, L., Robles, P., De Veylder, L., Traas, J., Micol, J.L., Van Montagu, M., Inzé, D., and Van Lijsebettens, M. (2005). The *elongata* mutants identify a functional Elongator complex in plants with a role in cell proliferation during organ growth. Proc. Natl. Acad. Sci. USA 102, 7754-7759.

Okada, Y., Yamagata, K., Hong, K., Wakayama, T., and Zhang, Y. (2010). A role for the elongator complex in zygotic paternal genome demethylation. Nature 463, 554-558.

Otero, G., Fellows, J., Li, Y., de Bizemont, T., Dirac, A.M.G., Gustafsson, C.M., Erdjument-Bromage, H., Tempst, P., and Svejstrup, J.Q. (1999). Elongator, a multisubunit component of a novel RNA polymerase II holoenzyme for transcriptional elongation. Mol. Cell 3, 109-118.

Pandey, R., Müller, A., Napoli, C.A., Selinger, D.A., Pikaard, C.S., Richards, E.J., Bender, J., Mount, D.W., and Jorgensen, R.A. (2002). Analysis of histone acetyltransferase and histone deacetylase families of *Arabidopsis thaliana* suggests functional diversification of chromatin modification among multicellular eukaryotes. Nucleic Acids Res. 30, 5036-5055.

Robles, P., and Micol, J.L. (2001). Genome-wide linkage analysis of *Arabidopsis* genes required for leaf development. Mol. Genet. Genomics 266, 12-19.

Rojas, C.M., Senthil-Kumar, M., Tzin, V., and Mysore, K.S. (2014). Regulation of primary plant metabolism during plant-pathogen interactions and its contribution to plant defense. Front. Plant Sci. 5, 17.

Saitou, N., and Nei, M. (1987). The neighbor-joining method: a new method for reconstructing phylogenetic trees. Mol. Biol. Evol. 4,:406-425.

Sanders, S.L., Jennings, J., Canutescu, A., Link, A.J., and Weil, P.A. (2002). Proteomics of the eukaryotic transcription machinery: identification of proteins associated with components of yeast TFIID by multidimensional mass spectrometry. Mol. Cell. Biol. 22, 4723-4738.

Sanmartín, M., Sauer, M., Muñoz, A., and Rojo, E. (2012). MINIYO and transcriptional elongation. Transcription 3, 25-28.

Sanmartín, M., Sauer, M., Muñoz, A., Zouhar, J., Ordóñez, A., van de Ven, W.T.G., Caro, E., de la Paz Sánchez, M., Raikhel, N.V., Gutiérrez, C., Sánchez-Serrano, J.J., and Rojo, E. (2011). A molecular switch for initiating cell differentiation in *Arabidopsis*. Curr. Biol. 21, 999-1008.

Selvadurai, K., Wang, P., Seimetz, J., and Huang, R.H. (2014). Archaeal Elp3 catalyzes tRNA wobble uridine modification at C5 via a radical mechanism. Nat. Chem. Biol. 10, 810-812.

Skylar, A., Matsuwaka, S., and Wu, X. (2013). *ELONGATA3* is required for shoot meristem cell cycle progression in *Arabidopsis thaliana* seedlings. Dev. Biol. 382, 436-445.

Slaugenhaupt, S.A., Blumenfeld, A., Gill, S.P., Leyne, M., Mull, J., Cuajungco, M.P., Liebert, C.B., Chadwick, B., Idelson, M., Reznik, L., Robbins, C.M., Makalowska, I., Brownstein, M.J., Krappmann, D., Scheidereit, C., Maayan, C., Axelrod, F.B., and Gusella, J.F. (2001). Tissue-specific expression of a splicing mutation in the *IKBKAP* gene causes familial dysautonomia. Am. J. Hum. Genet. 68, 598-605.

Stirnimann, C.U., Petsalaki, E., Russell, R.B., and Müller, C.W. (2010). WD40 proteins propel cellular networks. Trends Biochem. Sci. 35, 565-574.

Sturn, A., Quackenbush, J., and Trajanoski, Z. (2002). Genesis: cluster analysis of microarray data. Bioinformatics 18, 207-208.

Tamura, K., Peterson, D., Peterson, N., Stecher, G., Nei, M., and Kumar, S. (2011). MEGA5: Molecular Evolutionary Genetics Analysis using maximum likelihood, evolutionary distance, and maximum parsimony methods. Mol. Biol. Evol. 28, 2731-2739.

Van Lijsebettens, M., and Grasser, K.D. (2014). Transcript elongation factors: shaping transcriptomes after transcript initiation. Trends Plant Sci. 19, 717-726.

Van Lijsebettens,M., Dürr, J., Woloszynska, M., and Grasser, K.D. (2014). Elongator and SPT4/SPT5 complexes as proxy to study RNA polymerase II transcript elongation control of plant development. Proteomics 14, 2109-2114.

Versées, W., De Groeve, S., and Van Lijsebettens, M. (2010). Elongator, a conserved multitasking complex? Mol. Microbiol. 76, 1065-1069.

Wang, C., Ding, Y., Yao, J., Zhang, Y., Sun, Y., Colee, J., and Mou, Z. (2015). Arabidopsis Elongator subunit 2 positively contributes to resistance to the necrotrophic fungal pathogens *Botrytis cinerea* and *Alternaria brassicicola*. Plant J. 83, 1019-1033.

Wang, Y., An, C., Zhang, X., Yao, J., Zhang, Y., Sun, Y., Yu, F., Amador, D.M., and Mou, Z. (2013). The *Arabidopsis* Elongator complex subunit2 epigenetically regulates plant immune responses. Plant Cell 25, 762-776.

Winkler, G.S., Kristjuhan, A., Erdjument-Bromage, H., Tempst, P., and Svejstrup, J.Q. (2002). Elongator is a histone H3 and H4 acetyltransferase important for normal histone acetylation levels *in vivo*. Proc. Natl. Acad. Sci. USA 99, 3517-3522.

Winkler, G.S., Petrakis, T.G., Ethelberg, S., Tokunaga, M., Erdjument-Bromage, H., Tempst, P., and Svejstrup, J.Q. (2001). RNA polymerase II elongator holoenzyme is composed of two discrete subcomplexes. J. Biol. Chem. 276, 32743-32749.

Wittschieben, B.Ø., Otero, G., de Bizemont, T., Fellows, J., Erdjument-Bromage, H., Ohba, R., Li, Y., Allis, C.D., Tempst, P., and Svejstrup, J.Q. (1999). A novel histone acetyltransferase is an integral subunit of elongating RNA polymerase II holoenzyme. Mol. Cell 4, 123-128Xu et al., 2012

Xu, D., Huang, W., Li, Y., Wang, H., Huang, H., and Cui, X. (2012). Elongator complex is critical for cell cycle progression and leaf patterning in *Arabidopsis*. Plant J. 69, 792-808.

Xu, H., Lin, Z., Li, F., Diao, W., Dong, C., Zhou, H., Xie, X., Wang, Z., Shen, Y., and Long, J. (2015). Dimerization of elongator protein 1 is essential for Elongator complex assembly. Proc. Natl. Acad. Sci. USA 112, 10697-10702.

Zeitlinger, J., Stark, A., Kellis, M., Hong, J.-W., Nechaev, S., Adelman, K., Levine, M., and Young, R.A. (2007). RNA polymerase stalling at developmental control genes in the *Drosophila melanogaster* embryo. Nat. Genet. 39, 1512-1516.

Zhang, H., Richardson, D.O., Roberts, D.N., Utley, R., Erdjument-Bromage, H., Tempst, P., Côté, J., and Cairns, B.R. (2004). The Yaf9 component of the SWR1 and NuA4 complexes is required for proper gene expression, histone H4 acetylation, and Htz1 replacement near telomeres. Mol. Cell. Biol. 24, 9424-9436.

Zhou, X., Hua, D., Chen, Z., Zhou, Z., and Gong, Z. (2009). Elongator mediates ABA responses, oxidative stress resistance and anthocyanin biosynthesis in Arabidopsis. Plant J. 60, 79-90.

Zhu, M., Li, Y., Chen, G., Ren, L., Xie, Q., Zhao, Z., and Hu, Z. (2015). Silencing *SlELP2L*, a tomato Elongator complex protein 2-like gene, inhibits leaf growth, accelerates leaf, sepal senescence, and produces dark-green fruit. Sci. Rep. 5, 7693.

Zimmermann, P., Hirsch-Hoffmann, M., Hennig, L., and Gruissem, W. (2004). GENEVESTIGATOR. Arabidopsis microarray database and analysis toolbox. Plant Physiol. 136, 2621-2632.

Chapter 4 The Elongator complex regulates hypocotyl growth in darkness and during photomorphogenesis

Magdalena Woloszynska[1,2], Olimpia Gagliardi[1,2], Filip Vandenbussche[3], Steven De Groeve[1,2], Luis Alonso Baez[1,2], Pia Neyt[1,2], Sabine Le Gall[1,2], Jorge Fung[4], Paloma Mas[4], Dominique Van Der Straeten[3] and Mieke Van Lijsebettens[1,2*]

[1] Ghent University, Department of Plant Biotechnology and Bioinformatics, 9052 Ghent, Belgium
[2] VIB Center for Plant Systems Biology, 9052 Ghent, Belgium
[3] Ghent University, Department of Physiology, Laboratory of Functional Plant Biology, 9000 Ghent, Belgium
[4] Center for Research in AgriGenomics (CRAG), Consortium CSIC-IRTA-UAB-UB, 08193 Barcelona, Spain

Author contributions

This chapter was adapted from the published manuscript.

Woloszynska, M., Gagliardi, O., Vandenbussche, F., De Groeve, S., Baez, L.A., Neyt, P., Le Gall, S., Fung, J., Mas, P., Van Der Straeten, D., Van Lijsebettens, M., 2017. Elongator regulates hypocotyl growth in darkness and during photomorphogenesis. Journal of Cell Science jcs.203927. https://doi.org/10.1242/jcs.203927

S.L.G. made the RNA-seq in blue light and analysis, made the crosses and did partially the genotyping for the Luciferase reporter lines, helped with RNA extraction and subsequent RT-qPCR and ChIP-qPCR, performed the hypocotyl growth experiment of Ws background mutants.

1 Abstract

The Elongator complex promotes RNA polymerase II-mediated transcript elongation through epigenetic activities such as histone acetylation. Elongator regulates growth, development, immune response and sensitivity to drought and abscisic acid. We demonstrate that *elo* mutants exhibit defective hypocotyl elongation but have a normal apical hook in darkness and are hyposensitive to light during photomorphogenesis. These *elo* phenotypes are supported by transcriptome changes, including downregulation of circadian clock components, positive regulators of skoto- or photomorphogenesis, hormonal pathways and cell wall biogenesis-related factors. We show that that genes related to skoto- and photomorphogenesis are activated by the light signal but still significantly downregulated in the mutant. The downregulated genes *LHY*, *HFR1* and *HYH* are selectively targeted by Elongator for histone H3K14 acetylation in darkness. The role of Elongator in early seedling development in darkness and light is supported by hypocotyl phenotypes of mutants defective in components of the gene network regulated by Elongator, and by double mutants between *elo* and mutants in light or darkness signalling components. A model is proposed in which Elongator represses the plant immune response and promotes hypocotyl elongation and photomorphogenesis via transcriptional control of positive photomorphogenesis regulators and a growth-regulatory network that converges on genes involved in cell wall biogenesis and hormone signalling.

2 Introduction

The conserved Elongator complex (hereafter Elongator) is a transcript elongation factor that binds in yeast to CTD-phosphorylated RNA polymerase II (RNAPII) at the coding part of genes and facilitates transcript elongation via histone acetyl transferase (HAT) activity, preferentially targeting lysine 14 of histone H3 (Otero *et al.*, 1999; Woloszynska *et al.*, 2016; Van Lijsebettens and Grasser, 2014). The Elongator complex consists of six subunits, ELP1 to ELP6, and two subcomplexes ELP1-ELP3 and ELP4-ELP6, with ELP3 conferring HAT and DNA demethylation activities (Nelissen *et al.*, 2005, 2010; Glatt and Müller, 2013; DeFraia *et al.*, 2013). The ELP4-ELP6 subcomplex plays a role in the modification of uridines at the wobble position in transfer RNAs (Glatt and Müller, 2013). In plants, an epigenetic role for Elongator in transcription and processing of primary

microRNAs has been shown (Fang *et al.*, 2015). Analysis of *Arabidopsis* mutants impaired in the expression of Elongator subunits revealed that Elongator regulates growth, development, and responses to environmental stimuli (Ding and Mou, 2015). Elongator is expressed in meristematic tissues, which correlates with delayed growth, shortened primary roots, reduced lateral root density, abnormal leaves, defective inflorescence phylotaxis and reduced apical dominance in *elongata (elo)* mutants (Nelissen *et al.*, 2010; Skylar *et al.*, 2013; Jia *et al.*, 2015). In addition, *elo* mutants have altered sensitivities to drought and abscisic acid (Chen *et al.*, 2006; Zhou *et al.*, 2009), whereas genes of the plant immune response are down- or upregulated (DeFraia *et al.*, 2010; Wang *et al.*, 2013; Wang *et al.*, 2015). Reduced histone H3K14 acetylation of auxin response-related genes (Nelissen *et al.*, 2010), transcription factors essential for root development (Jia *et al.*, 2015), and genes coding for salicylic acid, jasmonic acid, and ethylene signalling (An *et al.*, 2017; Wang *et al.*, 2013, Wang *et al.*, 2015) correlated with their reduced gene expression and the specific phenotypes in *elo* mutants.

Following germination, seedlings develop according to the skotomorphogenic program, in which hypocotyls elongate (so-called etiolation), apical hooks are closed and cotyledons are folded. When seedlings reach the soil surface, the developmental program switches to photomorphogenesis, resulting in de-etiolation, in which hypocotyl elongation is inhibited, while the apical hook opens and cotyledons expand. Morphological changes are driven by light-stimulated transcriptional or posttranscriptional shifts in the accumulation of positive skoto- and photomorphogenesis regulators, controlled by photoreceptors and the circadian clock. Interestingly, chromatin modifications modulate the expression of genes encoding regulators of skoto- and photomorphogenesis, such as the phytochrome A (PHYA) photoreceptor, the positive photomorphogenesis regulators ELONGATED HYPOCOTYL 5 (HY5) and HY5-HOMOLOG (HYH) (Cloix and Jenkins, 2008), the positive skotomorphogenesis regulator SUPPRESSOR OF PHYA-105 1 (SPA1) (Bourbousse et al., 2012), the EARLY LIGHT-INDUCIBLE PROTEIN 1 (ELIP1) (Cloix and Jenkins, 2008) and the circadian clock genes CIRCADIAN CLOCK ASSOCIATED 1 (CCA1), LATE ELONGATED HYPOCOTYL (LHY), TOC1(TIMING OF CAB EXPRESSION 1), LUX (LUX ARRHYTHMO), ELF4 (EARLY FLOWERING 4), PRR7 (PSEUDO RESPONSE REGULATOR 7), and PRR9 (Hemmes et al., 2012; Himanen et al., 2012;

Malapeira et al., 2012) . Blue light is involved through cryptochromes in the regulation of photomorphogenic responses such as cell elongation and photoperiodic flowering and through phototropin in phototropism (Lin, 2002).

Here we show that Elongator regulates seedling development in darkness and light via a growth-regulatory network of genes that converge on cell wall biogenesis and positive photomorphogenesis factors, some of which are targeted by the Elongator HAT activity specifically in darkness, suggesting target gene selection.

3   Results

3.1   Phenotypes of the elo seedlings in darkness and light

Narrow, elongated, and hyponastic leaves and petioles of *elo* mutants that resemble those of photoreceptor mutants (Fig. S1A), suggested that Elongator plays a role in light response. Therefore, we investigated the role of Elongator in early *Arabidopsis* development in darkness or light (during etiolation or de-etiolation, respectively) by scoring hypocotyl elongation and apical hook formation, two characteristics of seedling growth that differ between the skoto- and photomorphogenetic developmental programs. Seeds of *elo3-6* and Col-0 were sown, stratified for 48h, illuminated for 6h in white light to induce germination, and transferred to either darkness or to red, far-red or blue light. Representative seedling phenotypes are shown at 4 days after germination (DAG) (Fig. 1A). The hypocotyl length and seedling morphology was compared between the *elo3-6* mutant and Col-0 wild type every day between 3 and 7 DAG (Fig. 1A,B; Fig.S1B). Darkness-grown *elo3-6* seedlings had shorter hypocotyls as compared to Col-0 (Fig. 1B), but cotyledons and apical hooks were similar (Fig. 1A; Fig.S1B), indicating that the mutation affected only hypocotyl growth. The hypocotyl length difference between Col-0 and *elo3-6* seedlings was maximal at 3 DAG (0.55 cm and 0.33 cm, respectively) (Fig. 1B). At 5 DAG, hypocotyl elongation nearly stopped for Col-0, whereas *elo3-6* hypocotyls still elongated, ultimately reaching lengths similar to those of the wild type at 7 DAG (Fig. 1B). This is probably due to a delay in growth rather than a compensation mechanism, because Arabidopsis hypocotyls have a fixed number of 20 cells and grow only by elongation (Gendreau *et al.,* 1997) and we see that they grow longer than wild

type in light conditions. Measurement of the cell length and cell number in the hypocotyl in darkness and at the different light qualities, at different time points could distinguish between the two hypotheses. The *elo3-6* seedlings grown in red, far-red or blue light had reduced de-etiolation, visible as longer hypocotyls between 3 and 7 DAG (Fig. 1B), reduced cotyledon expansion and hyponastic growth of the cotyledons (Fig. 1A; Fig. S1B), showing that the mutant is hyposensitive to all light qualities. Light inhibited hypocotyl elongation in the Col-0 seedlings already at 3 or 4 DAG, whereas in the *elo3-6* mutant, hypocotyls elongated until 5 to 7 DAG, depending on the light quality (Fig. 1B).

The seedling phenotypes of the *elo3-1* Landsberg *erecta* (Ler) mutant grown in darkness, red, far-red or blue light were assessed at 4 and 6 DAG relative to the Ler control and the alterations were comparable to those of the *elo3-6* Col-0 allele (Fig. 1C), confirming that ELP3 regulates hypocotyl growth in darkness and in light. Hypocotyl lengths of the *elo1-1* (mutation in the accessory subunit *ELP4* gene), *elo2* (the core subunit *ELP1* gene), *elo4/drl1-4* and *drl1-2* (the Elongator interactor *DRL1/ELO4* gene) mutants, and the wild-type Ler were assayed at 4 and 6 DAG and results were similar to those obtained for the *elo3-1* and *elo3-6* mutants were obtained (Fig. 1C). Similar phenotypes are observed in the different Elongator subunits (Fig. 1C) suggesting that the Elongator as an integral complex regulates hypocotyl elongation in darkness and different light conditions in *Arabidopsis*.
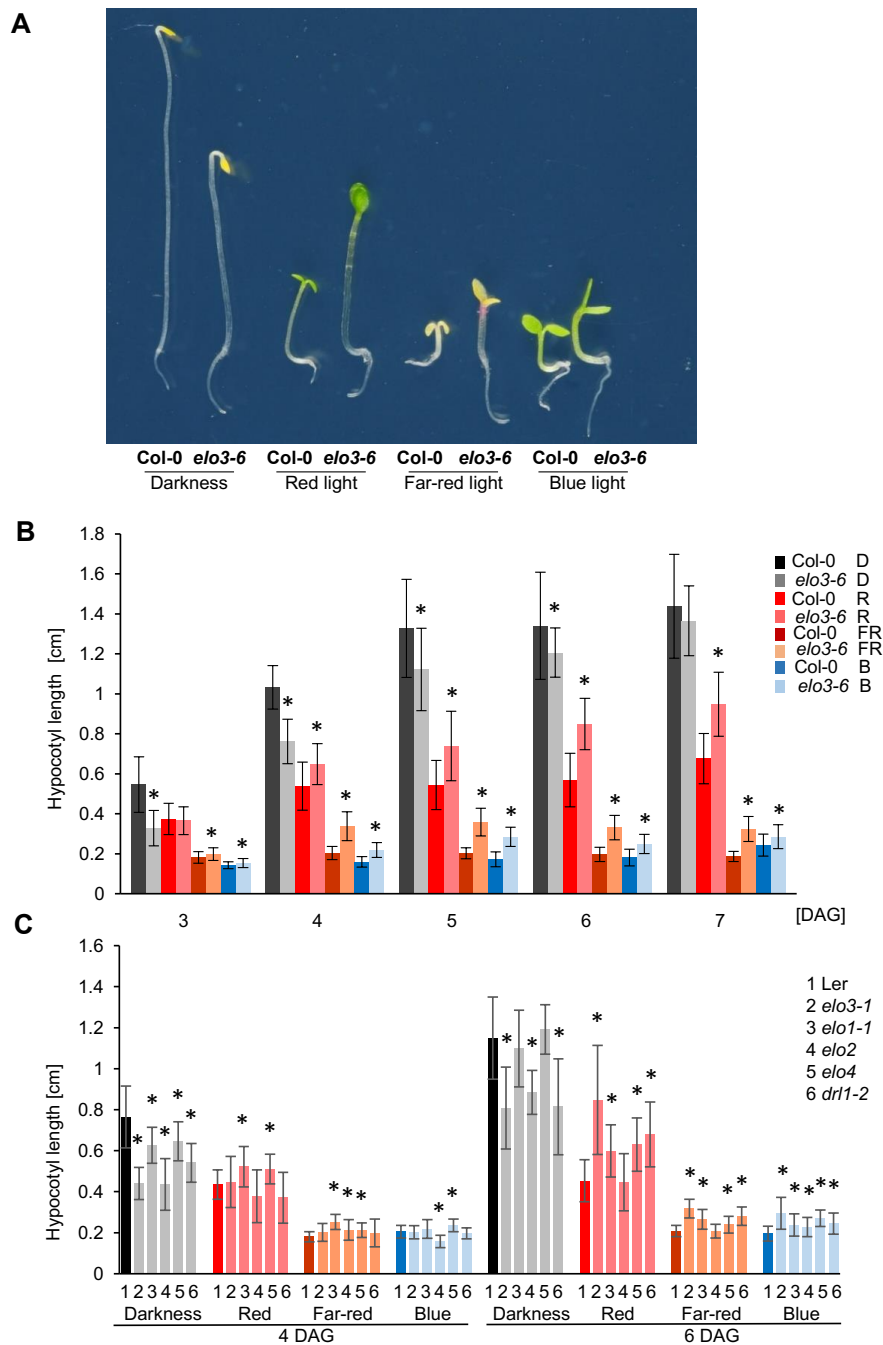
Figure 1. Phenotypes of *elo3-6* seedlings grown in darkness or under different light conditions. (A) Representative seedlings germinated and grown on half-strength MS medium for 4 days in darkness or under continuous monochromatic light of different wavelengths. (B) Hypocotyl lengths of Col-0 and *elo3-6* seedlings grown in darkness, or under continuous red, far-red, and blue light. (C) Hypocotyl lengths of mutants of different Elongator subunits in Ler background grown on half-strength MS medium in darkness or under continuous monochromatic light of different wavelengths. Bars represent mean hypocotyl length of 25 seedlings (mean ± s.d.). Differences between mutant and wild type were statistically analyzed with an unpaired two-tailed Student's *t*-test and significant differences are indicated with asterisks ($P<0.05$).

3.2 Genetic interactions for hypocotyl growth between Elongator and light-dependent receptors and regulators

To examine the role of Elongator in the regulation of hypocotyl growth, the *elo3-1* (Ler) or *elo3-6* (Col-0) mutants were used as proxy for the Elongator complex and combined with the *phyB-1, phyA-201, hfr1-101* and *pif3-3 pif4-1* mutants in light-dependent receptors and regulators. Hypocotyl length was compared between the control, the parental lines and their double or triple mutant combinations grown in darkness or in red or far-red light at 4 and 6 DAG (Fig. 2).

The *phyB-1* (Fig. 2A) and, *phyA-201* (Fig. 2B) mutants had significantly longer hypocotyls than the Ler control in darkness and light, because a decrease in active phytochrome molecules results in increased levels of PHYTOCHROME INTERACTING FACTORS (PIFs), which stimulate cell elongation (Leivar *et al.*, 2008a and b). Hypocotyl lengths of double mutants combining *phyB-1* or *phyA-201* with *elo3-1* were significantly longer than those of *elo3-1*, but shorter than those of *phy* single mutants (Fig 2A,B). This intermediate phenotype likely results from the additive effect of the *phyB-1* or *phyA-201* mutations, leading to increased hypocotyl elongation (comparable to the effect of darkness on the wild type) and the *elo3-1* mutation that disables hypocotyl elongation under such conditions. Therefore, the deficit of Elongator results in two defects leading to opposite changes in hypocotyl growth. Firstly, the *elo3-1* mutant has decreased light sensitivity, resulting in longer hypocotyls in light-grown seedlings and secondly, it grows more slowly in conditions of strongly enhanced cell elongation, such as darkness or the *phy* background. These results confirm that Elongator is indispensable for the light response and for the fast growth stimulation that occurs in darkness or upon *phy* mutation.

The hypocotyl length of the *elo3-6* mutant grown in darkness was reduced more than that of the *pif3-3 pif4-2* mutant compared to the Col-0 control (Fig. 2C), indicating that Elongator regulates hypocotyl growth via factors different or additional to PIF3 and PIF4. The combination of *elo3-6* and *pif3-3 pif4-2* mutations in the triple mutant resulted in only slightly shorter hypocotyls than *elo3-6*, suggesting that the PIFs pathway positively regulating hypocotyl elongation could have been already downregulated in *elo3-6* in darkness. Therefore, in darkness, Elongator may control hypocotyl elongation via PIFs and other pathways. In red light, the hypocotyl length of *pif3-3 pif4-2* was significantly

shorter than that of the Col-0 control, whereas it was intermediate in the *elo3-6 pif3-3 pif4-2* triple mutant compared to its parental lines. This effect was a result of the additive effect of mutations inversely regulating hypocotyl length in red light. The findings suggest that the PIF pathway is not affected by Elongator during growth in red light.

The *hfr1-101* mutant had significantly longer hypocotyls than the Col-0 control in darkness, indicating that HFR1 (LONG HYPOCOTYL IN FAR-RED 1), a positive photomorphogenesis regulator and suppressor of PIF action, is active in the absence of light and counteracts exaggerated hypocotyl elongation (Fig.2D). The *hfr1-101* mutation did not increase the hypocotyl elongation of *elo3-6* in the *elo3-6 hfr1-101* double mutant in darkness, indicating that Elongator and HFR1are involved in the same pathway regulating hypocotyl elongation in darkness and Elongator is located upstream of HFR1. In far-red light, hypocotyls of the *elo3-6* and *hfr1-101* mutants were longer than those of Col-0, and the *elo3-6 hfr1-101* double mutant had hypocotyls longer than those of both parents, indicating a synergistic interaction between Elongator and HFR1 in hypocotyl elongation. This result suggests that in the far-red light, in contrast to darkness, the *ELO3* and *HFR1* activities converge on the same process of hypocotyl elongation leading to a dramatic elongation of the double-mutant hypocotyl.

In conclusion, double-mutant analyses show that Elongator is required for fast hypocotyl elongation in darkness and that this Elongator function is involved in growth-stimulating mechanisms other than the PIF pathway. Under light conditions, Elongator promotes inhibition of hypocotyl growth, by acting in far-red light via an HFR1-interacting pathway.
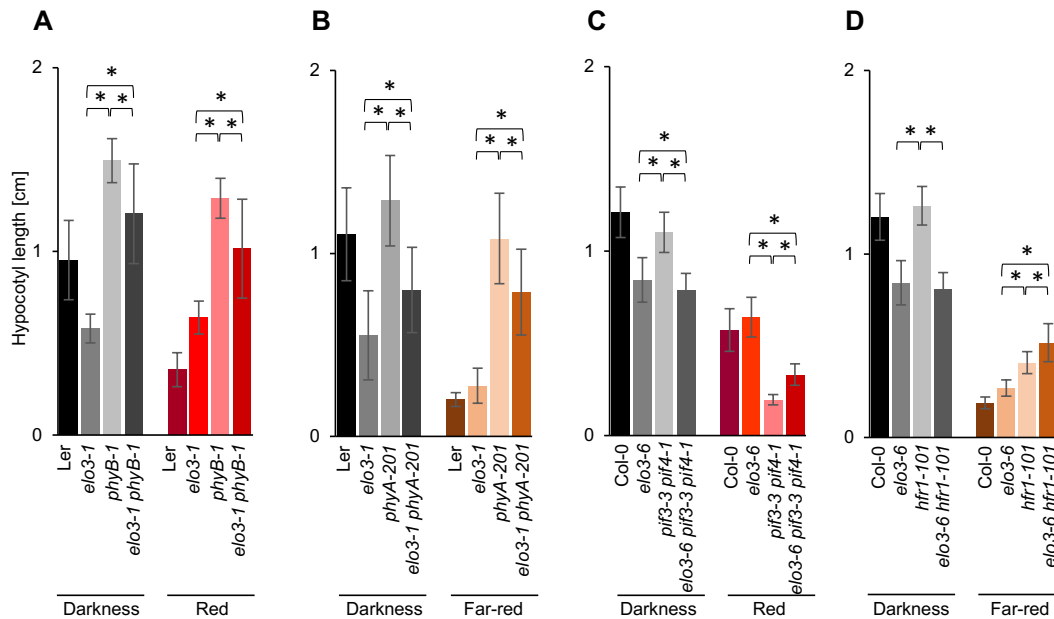
Figure 2. Genetic interactions for hypocotyl growth between Elongator and phyA, phyB, PIF, or HFR1. (A) Seedlings of *Arabidopsis* Ler (A,B) or Col-0 (C,D) wild types, and *elo3-1* (A,B), *elo3-6* (C, D), *phyB1* and *elo3-1 phyB-1* (A), *phyA-201* and *elo3-1 phyA-201* (B), *pif3-3 pif4-1* and *elo3-6 pif3-3 pif4-1* (C), and *hfr1-101* and *elo3-6 hfr1-101* (D) mutants were grown for 4 days on half-strength MS medium without sucrose in darkness, continuous red or far-red light. Hypocotyl lengths were quantified. Error bars represent mean values of hypocotyl length of 25 seedlings with standard deviation (mean±s.d.). Differences between genotypes were statistically analyzed with an unpaired two-tailed Student's *t*-test and significant differences are indicated with asterisks (*P*<0.05). Differences in hypocotyl length between single, double or triple mutants and their respective wild types were always statistically significant and are therefore not indicated in the graphs. The experiment was repeated twice.

3.3   elo3-6 mutant transcriptome in darkness

The gene regulatory network underlying the hypocotyl elongation phenotype of *elo3-6* was compared with that of Col-0 in the microarray dataset of 4-day-old darkness-grown seedlings: 2,489 genes were downregulated and 2,533 genes were upregulated in the mutant, at -0.5 ≥ log2FC ≥ 0.5, *P*<0.05 (data are available at NCBI, Gene Expression Omnibus, accession number GSE42053).

Upregulated genes in *elo3-6* clustered in two large Gene Ontology (GO) categories (Table S1), i.e. "Response to stimuli" (defense response genes and genes induced by light, cold, osmotic stress, oxidative stress, water, desiccation, salt, carbohydrates, metal ions,

hormones and other organisms) and "Metabolic process" (genes related to catabolism of carbohydrate coding for enzymes driving glycolysis, pentose phosphate pathway, TCA cycle, starch breakdown, photorespiration and Calvin cycle, and genes involved in biosynthesis of amino acids, lipids, nucleotides, gibberellins and flavones). The GO category "Defense response" contains 140 genes including those encoding important defense regulators and showing moderate, maximally 2- to 3-fold upregulation. Phytoalexin Deficient 4 PAD4 is a component of basal immunity against virulent pathogens and also contributes to effector-triggered immunity and systemic acquired resistance (Louis *et al*., 2012). PAD3/CYP71B15 catalyzes biosynthesis of camalexin determining elicitor induced resistance against fungal pathogens (Ferrari *et al*., 2007), its upregulated transcripts are markers for camalexin biosynthesis (Prince *et al*., 2014). Cytochrome P450s (CYP79B2 and CYP79B3) are involved in tryptophan metabolism and biosynthesis of pathogen defense components. PENETRATION 3 (PEN3) plays a role in focal immune response and response to fungal and bacterial pathogens and is a marker of plant – pathogen interactions (Xin *et al*., 2013). ELICITOR PEPTIDE 2 and 3 PRECURSORS (PROPEP2 and 3) are massively upregulated following pathogen challenges and recognized by PERP1/PERP2 receptors of defense signalling. Upregulation of GLYCERALDEHYDE-3-PHOSPHATE DEHYDROGENASE C SUBUNIT 1 (GAPC1) enhances glycolysis providing ATP and pyruvate (reactive oxygen species scavenger) for plants undergoing immune response (Henry *et al*., 2015). Other genes with a confirmed positive effect on plant immunity were also upregulated in *elo3-6*: AZELAIC ACID INDUCED 1 (AZI1), LONG-CHAIN ACYL-COA SYNTHETASE 2 (LACS2), ENHANCED DISEASE SUSCEPTIBILITY 5 (EDS5), GRETCHEN HAGEN 3.12 (GH3.12), ARABIDOPSIS THALIANA SULFOTRANSFERASE 1 (ATSOT1), ACTIVATED DISEASE RESISTANCE 1 (ADR1) and ADR1-LIKE 1. Some of the genes involved in carbohydrates catabolism together with genes coding for subunits of the mitochondrial electron transport chain and ATP synthase were grouped in the overrepresented GO category "Energy derivation by oxidation of organic compounds". Two smaller GO categories of upregulated genes were identified: "Cell wall organization or biogenesis" containing genes related to defense and/or cell wall firmness (chitinases, pectin methylesterases), and "Localization" including the genes coding for transporters of sugars, amino acids, proteins, lipids and metal ions. In summary, the set of genes

upregulated in the *elo3-6* mutant in darkness matches transcriptome profiles typical for plant response to pathogen (Rojas *et al.*, 2014), in which the upregulation of defense-related pathways is followed by the upregulation of primary metabolism genes involved in energy production (carbohydrates catabolism, mitochondrial electron transport, nucleotides and amino acid biosynthesis) or synthesis of signalling molecules (carbohydrates and lipids). The upregulation of defense-related genes results in energy deprivation, which activates compensatory downregulation of other pathways ultimately leading to growth deceleration as observed in the *elo3-6* mutant in darkness.

GO categories with significantly downregulated genes were: "Response to light stimulus", "Response to hormone stimulus", "Cell wall biogenesis", "Regulation of transcription", "Regulation of developmental processes" and "Regulation of cell cycle" with the large proportion of transcription factors within each GO category. From the downregulated GO categories, a growth-controlling network was deduced that consisted of four main hubs: circadian clock, regulators of skoto- and photomorphogenesis, different hormone response pathways, and primary and secondary cell wall biogenesis (Table S2). Downregulated genes encoded both positive upstream regulators and direct downstream effectors of growth, in line with the delayed hypocotyl elongation observed for *elo3-6* seedlings grown in darkness. Some of these pathways were functionally analyzed by means of reporter gene constructs or hypocotyl growth experiments upon treatment.

3.4   elo3-6 mutant transcriptome in red, far-red and blue light

The hypocotyl assays and microarray data indicated that Elongator could be involved in skotomorphogenesis of seedlings in darkness, photomorphogenesis in red light, shade avoidance syndrome induced by low red to far-red light ratio and in response to blue light. It is also known that SHY2, an identified target of Elongator (Nelissen *et al.,* 2010), has an expression dependent on light (Tian *et al.,* 2002). To explore the link between Elongator and the early response to light transcriptome analyses were performed on seedlings exposed to 1hr of different light qualities and compared to seedlings grown in darkness. The gene regulatory network underlying the hypocotyl elongation phenotype of *elo3-6* was compared to Col-0 in the microarray dataset of 4-day-old seedlings exposed

to 1 hr red or far-red light as well as in the RNA-sequencing dataset of 4-day-old seedlings exposed to 1 hr blue light. Differentially Expressed Genes (DEG) in the microarray and RNA-Seq results were scored at a threshold of -0.5≥ log2FC≥ 0.5 for down or up regulation, respectively, together with a corrected p-value of 5% to compare *elo3-6* to WT in the same condition (Figure 3).

In a first analysis, we compared the results obtained in darkness in the microarray and RNA-seq datasets (Figure 3A&E). In the RNA-Seq data 1,502 genes were downregulated and 2,442 genes were upregulated in the mutant while in the microarray data, 2,490 genes were downregulated and 981 were upregulated in the mutant. The 807 common downregulated DEG correspond to 32% of the downregulated DEG in the microarray and 53% of the downregulated DEG in the RNA-Seq. While for the upregulated DEG 443 are in common, which corresponds to 45% of the upregulated DEG in the microarray data and 18% of the RNA-Seq DEG. In the GO category "response to light", amongst a selection of 17 genes significantly downregulated in the microarray, 6 are not significantly downregulated in the RNA-Seq (Table 1).
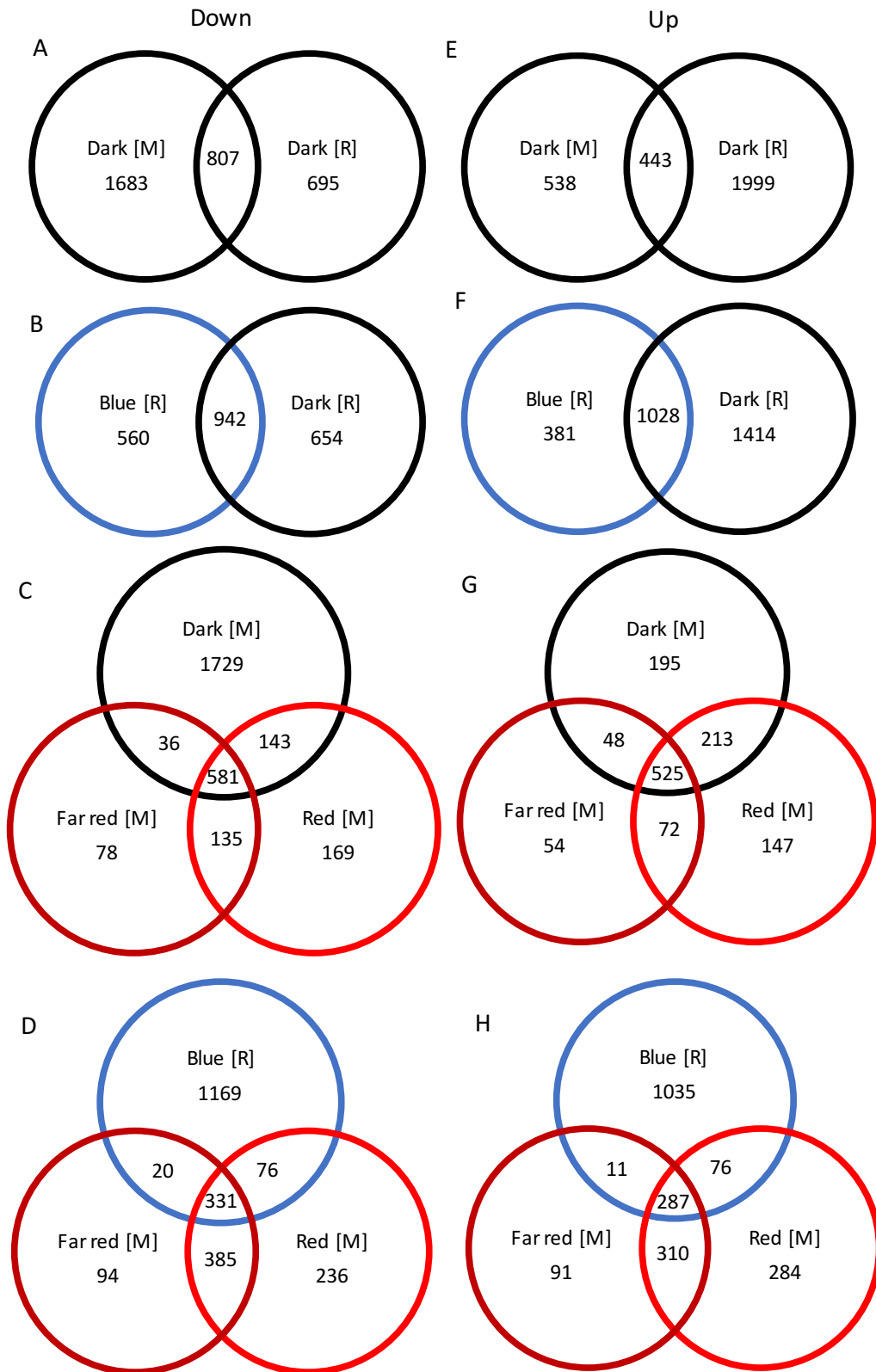
Down

Up

Figure 3. Comparison of differentially expressed genes (DEG) in *elo3-6* to wild type using a microarray [M] dataset obtained in darkness, and by red and far-red light induction, and using an RNA-Seq [R] dataset obtained in darkness and by blue light induction. A-D, downregulated DEG at -0.5 ≥ log2FC, *P*<0.05. E-H, upregulated DEG at log2FC ≥ 0.5, *P*<0.05.

Table 1: Selection of genes related to response to light categories in microarray (dark, red and far-red 1h induction) **and RNA-Seq** (dark and blue light 1h induction) **datasets**. Differential gene expression between *elo3-6* and wild type. Shaded are DEGs at threshold -0.5 ≥log2FC≥ + 0.5 and P value ≤ 0.05.

	AGI code	gene	Darkness (microarray)		Red (microarray)		Far-red (microarray)		Blue (RNA-Seq)		Darkness (RNA-Seq)	
			log2FC	p-value	log2FC	p-value	log2FC	p-value	log2FC	p-value	log2FC	p-value
Regulators of skoto- and photomorphogenesis	AT5G11260	HY5	-0.65	3.76E-14	-0.18	1.11E-04	-0.07	9.09E-02	-0.16	4.08E-01	-0.77	9.59E-06
	AT3G17609	HYH	-2.32	9.53E-16	-1.39	3.15E-11	-1.44	2.73E-11	-0.62	7.59E-02	-1.16	4.05E-04
	AT1G02340	HFR1	-0.33	1.55E-05	-0.20	6.40E-03	-0.26	6.13E-04	-0.18	2.12E-01	-0.67	1.19E-08
	AT2G26670	HY1	-0.65	1.16E-09	-0.66	3.60E-09	-0.55	1.22E-07	-0.40	2.03E-03	-0.26	7.10E-02
	AT2G46340	SPA1	-0.76	2.80E-12	-0.34	6.70E-06	-0.35	6.45E-06	0.01	9.84E-01	-0.24	2.05E-01
	AT4G02440	EID1	-0.57	2.97E-12	-0.57	1.16E-11	-0.62	5.46E-12	-0.56	1.09E-03	-0.70	3.48E-05
	AT2G43010	PIF4	-0.71	2.02E-12	-0.60	1.43E-10	-0.46	2.11E-08	-0.53	4.74E-02	-0.77	2.09E-03
	AT2G31380	STH/ BBX25	-1.07	1.11E-09	-1.14	1.57E-09	-1.34	1.64E-10	-0.68	4.22E-03	-0.47	1.11E-01
	AT1G06040	BBX24	-0.54	4.20E-08	-0.30	5.28E-04	-0.25	3.32E-03	-0.10	5.89E-01	-0.28	8.80E-02

Circadian clock	AT1G01060	*LHY*	-0.94	*3.74E-06*	-0.80	*8.59E-05*	-1.07	*2.28E-06*	-0.13	*6.02E-01*	-0.15	*5.41E-01*
	AT2G46830	*CCA1*	-0.54	*2.53E-05*	-0.47	*3.38E-04*	-0.70	*3.20E-06*	-0.36	*1.21E-01*	-0.33	*1.59E-01*
	AT3G09600	*RVE8*	-0.57	*8.19E-08*	-0.78	*1.75E-09*	-0.64	*6.73E-08*	-0.54	*2.01E-03*	-0.54	*2.99E-03*
	AT5G02840	*LCL1/ RVE4*	-0.74	*1.37E-13*	-0.71	*1.53E-12*	-0.56	*1.56E-10*	-0.54	*1.12E-05*	-0.65	*6.24E-08*
	AT5G37260	*RVE2*	-0.68	*1.58E-10*	-0.69	*4.32E-10*	-0.48	*2.77E-07*	-0.35	*1.58E-01*	-0.60	*8.24E-03*
	AT4G00760	*PRR8*	-0.50	*3.69E-07*	-0.64	*2.61E-08*	-0.49	*2.76E-06*	-0.64	*3.63E-03*	-0.71	*9.16E-04*
	AT5G61380	*TOC1*	-0.40	*1.92E-08*	-0.31	*3.26E-06*	-0.19	*1.28E-03*	-0.42	*1.75E-02*	-0.61	*3.65E-04*
Early light-induced protein	AT4G14690	*ELIP2*	-1.42	*1.58E-09*	-1.35	*1.59E-08*	-1.62	*1.03E-09*	-0.80	*3.55E-02*	-1.24	*5.40E-04*

In the RNA-seq dataset, blue light-exposed seedlings had 1,596 downregulated and 1,409 upregulated genes in the mutant. The RNA-Seq showed 942 downregulated DEG common between darkness and blue light induction, which represents 63% of the blue light induced downregulated DEG and 59% of the in darkness downregulated ones (Figure 3B). Moreover, 1028 upregulated DEG are in common between the two conditions which corresponds to 73% of the blue induced upregulated DEG and 42% of the in darkness DEG (Figure 3F).

In order to investigate the role of Elongator in the early light response, genes with a reduced expression between *elo3-6* and Col-0 were selected as a first step to identify putative target genes for Elongator ELP3 histone acetylation activity. In blue light, GO analysis revealed categories linked to cell growth and division (cell cycle, secondary cell wall, membrane), to hormone signalling (auxin, ethylene, salicylic acid, gibberellin), to responses to pathogens (regulation of immune response, chitin response, defense response), to light response (photoperiod, circadian cycle). Similar categories were observed in darkness.

However, the GO category stomatal development was enriched in blue light only, which is in line with previous reports on the role of blue light in stomatal opening through phototropin signalling, triggering the action of H+ATPases (Zeiger, 2000), and in stomatal development through a crosstalk between the cryptochrome-phytochrome-COP1 and the mitogen-activated protein kinase signalling pathways (Kang *et al.*, 2009). Most genes related to blue light receptors and signal transduction from the RNA-Seq dataset (Table 2) were not significantly differentially expressed except for the circadian clock regulatory gene *ZTL*, and the chalcone synthase (*CHS*) gene, which plays a role in oxidative stress reaction by light and is regulated by the light signalling.

Table 2: **Differential expression of genes related to blue light perception and response in the RNA-Seq dataset**. Genes were selected from Lin, 2002. Differential gene expression between elo3-6 and wild type. Shaded are DEGs at threshold -0.5 ≥log2FC≥ + 0.5 and P value ≤ 0.05.

	AGI ID	Gene ID	Description	Blue		Darkness	
				Log-ratio	p-value	Log-ratio	p-value
Blue photoreceptor	AT4G08920	CRY1	cryptochrome 1	-0.194	0.198	-0.278	0.049
	AT1G04400	CRY2	cryptochrome 2	-0.026	0.905	-0.016	0.941
	AT3G45780	PHOT1	phototropin 1	0.095	0.702	0.038	0.892
	AT5G58140	PHOT2	phototropin 2	-0.436	0.058	-0.019	0.955
Light signalling	AT5G64330	NPH3	Phototropic-responsive NPH3 family protein	0.173	0.336	0.098	0.622
	AT5G20730	NPH4	Transcriptional factor B3 family protein / auxin-responsive factor AUX/IAA-related	-0.149	0.357	-0.281	0.054
	AT2G30520	RPT2	Phototropic-responsive NPH3 family protein	-0.112	0.699	-0.812	0.000
	AT2G32950	COP1	Transducin/WD40 repeat-like superfamily protein	-0.071	0.685	-0.092	0.614
Circadian clock	AT5G57360	ZTL	Galactose oxidase/kelch repeat superfamily protein	-0.278	0.047	-0.403	0.004
Light dependent gene expression	AT5G13930	CHS	Chalcone and stilbene synthase family protein	-0.486	0.023	-0.230	0.349
Ion homeostasis	AT4G08810	SUB1	calcium ion binding	-0.090	0.624	0.006	0.979

In blue light, regulatory genes related to light perception and signalling, i.e. *HY5 (long hypocotyl 5), HYH (HY5 homolog), HFR1 (long hypocotyl in far red1), SPA1, BBX24, LHY, CCA1* and *RVE2* were not significantly differentially expressed while in darkness, *HY1, SPA1, LHY* and *CCA1* were significantly differentially expressed. Strikingly, the transcription factors *HYH* and *HY5* were significantly downregulated after 1h of blue light induction when tested by RT-qPCR (Figure 7 A), which may be explained by the higher sensitivity of the RT-qPCR method. After blue light induction, *EID1, PIF4, LCL1/RVE4, PRR8, TOC1* and *ELIP2* were still downregulated but to a lesser degree as compared to darkness. *RVE8* expression was not changed by blue light induction. Thus, the blue light induction activated these genes but the mutation in *ELO3* resulted in a downregulation.

Red and far-red treatment were then compared to their darkness control in the microarray dataset. In red light, 1,028 genes were downregulated and 957 genes were upregulated in the mutant. In far red light, 830 genes were downregulated and 699 genes were upregulated in the mutant. Comparison of the three conditions, darkness, red and far-red induction, showed that only a few DEG are specifically up- or downregulated in light treated samples compared to darkness (Figure 3C&G). In red light, 70% of the downregulated DEG are in common with DEG identified in darkness and 74% in far-red light. The percentage is higher for the upregulated DEG, 77% in red light and 82% in far red light, respectively.

In red and far-red light, regulatory genes related to light perception and signalling such as *HY5, HYH, HFR1, SPA1, PIF4, BBX24* and circadian clock genes *LCL1* and *TOC1* were less downregulated as compared to darkness condition (Table 1). *LHY* and *ELIP2* were activated only by the red light while *HY1, RVE2* and *PRR8* were activated by the far-red light. Thus, the light induction activated these genes but the mutation in *ELO3* resulted in a downregulation.

The different light qualities share pathways and integrators such as *HY5* or *COP1* (Chen *et al.*, 2004). A large overlap of DEG was observed between the different light conditions (Figure 3D&H). Red and far-red condition shared respectively 70% and 86% of downregulated DEG and respectively 62% and 85% of up regulated DEG. But comparing

red and far-red conditions to blue, only 27% of downregulated DEG and 26% of upregulated DEG were in common. This may be explained by different receptors and pathways for red/far-red and blue light response but also because of the different transcriptome profiling techniques used. We see that we obtain a greater number of DEG in the blue condition with the RNA-Seq that in red and far-red with the microarray.

In conclusion, the effect of the mutated *ELO3* (downregulation of the genes) are cumulated with the effect of the light (upregulation) resulting in genes less downregulated in the light treated condition compared to darkness (Table 1). This is the case for *HY5, HYH, HFR1, SPA1, PIF4, BBX24, LCL1/RVE4* and *TOC1* for all lights; *HY1, RVE2, PRR8* and *ELIP2* for blue and far-red light; and *LHY* for blue and red light, whereas *BBX24* is more downregulated in all light qualities. Elongator and light have an effect on several categories of genes related to cell growth and division, hormone signalling, circadian clock and cell wall biogenesis. Red and far-red are triggering more similar responses than blue light.

3.5   Circadian clock

The circadian clock is one of the four main hubs of the growth-regulatory network downregulated in *elo3-6* in darkness. Seven genes from this hub (*LHY, CCA1, RVE8, CIR1, LCL1/RVE4, RVE2* and *PRR8*) showed decreased expression levels in *elo3-6* in darkness (Table S2, Fig. 4A). To check whether downregulation of two key circadian clock components, CCA1 and LHY, may contribute to the *elo* phenotype, we assayed the hypocotyl length of the *lhy-21 cca1-11, cca1-1lhy RNAi* and *lhy-21* mutants together with their wild type Wassilewskija (Ws). In darkness, similarly to the *elo* mutants, the hypocotyls of the circadian clock-regulatory mutants were significantly shorter than those of the wild type at 2 and 4 DAG, but the apical hooks remained closed and cotyledons did not expand (Fig. 4B). The effects in the *lhy-21 cca1-11* double and the *lhy-21* single mutants were comparable, indicating that mutation of *LHY* is sufficient to cause decreased hypocotyl length and therefore lowered expression of the *LHY* gene in the *elo* mutant may contribute to the observed short hypocotyl phenotype in darkness.

Next, the diurnal expression profiles of the *CCA1* and *LHY* genes were examined in wild-type and *elo3-6* mutant plants synchronized under short-day conditions. Samples were taken every 4 hours during 48 hours under short-day or under continuous light conditions following the synchronization. The diurnal fluctuations of the *CCA1* and *LHY* transcripts in the *elo3-6* mutant followed a similar oscillatory trend to that observed in wild-type plants but the mRNA accumulation was clearly reduced in the *elo3-6* mutant under both conditions (Fig. 4C). These results indicate that functionality of ELO3 is important for proper amplitude of the *CCA1* and *LHY* genes expression.

The downregulation of circadian clock components was further examined by monitoring bioluminescence of reporter lines expressing the *LUCIFERASE* (*LUC*) gene fused to the *CCA1* and *TOC1* promoters (*pCCA1::LUC* and *pTOC1::LUC*) in *elo3-6*. Our results show that the amplitude of the circadian activity for both promoters was decreased in the *elo3-6* mutant compared to the wild type and that the circadian period was not affected by the *elo3-6* mutation (Fig. 4D). These results are consistent with the decreased *CCA1* and *LHY* expression observed by quantitative polymerase chain reaction (qPCR) analysis (Fig. 4C) and suggest that altered clock function by mis-expression of oscillator components might contribute to the *elo3* hypocotyl phenotype.
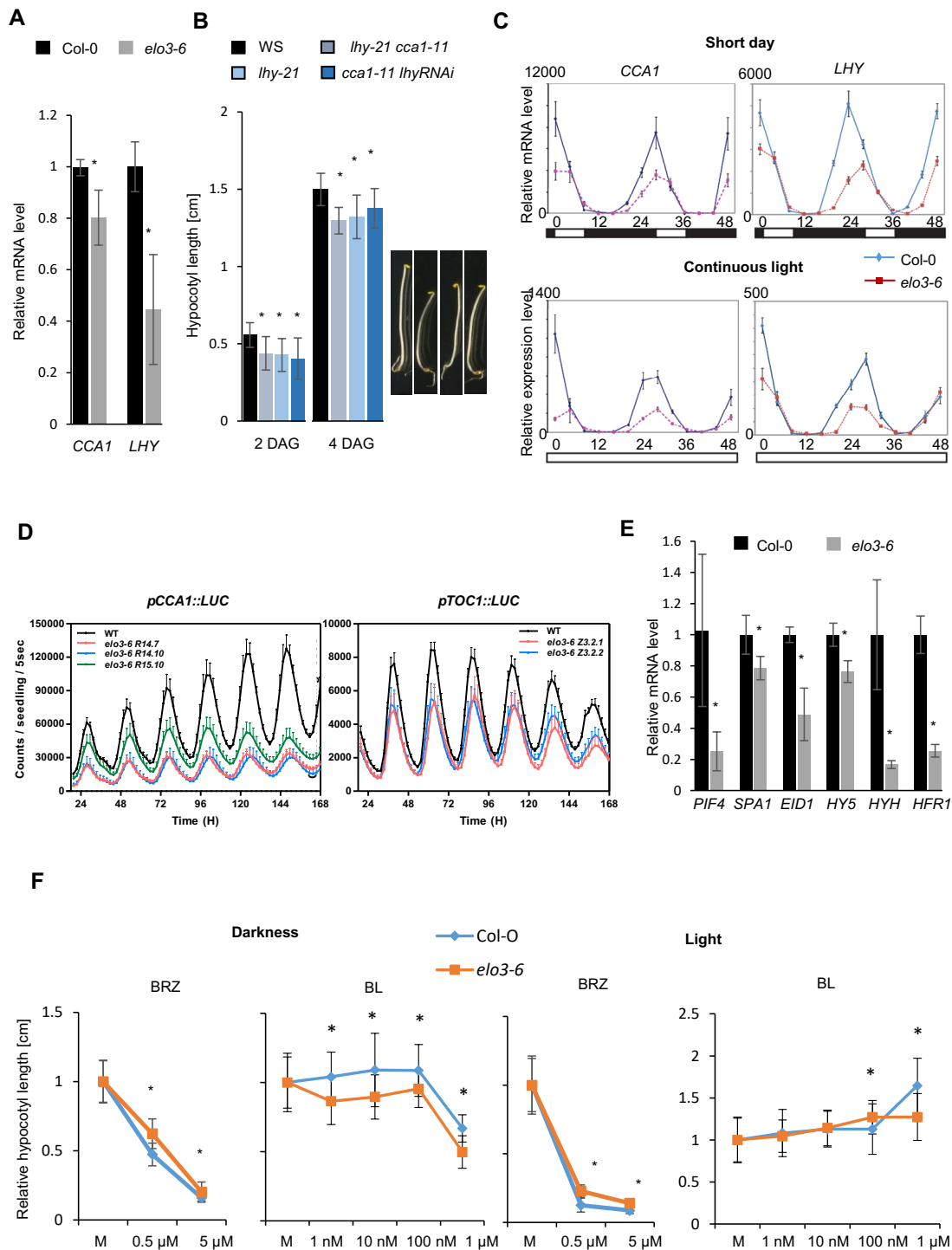
Figure 4. Expression of circadian clock and skoto- and photomorphogenesis regulatory genes, circadian clock assays and response to BL and BRZ of the *elo3-6* mutant. (A) Relative expression levels of *CCA1* and *LHY* genes in seedlings of *elo3-6* and Col-0 wild type. (B) Hypocotyl length of single and double mutants of *CCA1* and *LHY* genes (*lhy-21*, *lhy-21 cca1-11*, and *cca1-11 lhyRNAi*) compared to Ws wild type in darkness. Thirty seedlings were photographed and hypocotyls were measured with the ImageJ software. (C) qPCR assessing relative expression levels of *CCA1* and *LHY* genes in the Col-0 and *elo3-6* seedlings grown for 12 days in a short-day photoperiod and analyzed for 48 hours in short-day conditions or continuous white light with samples

taken every 4 hours. White and black boxes below the graphs indicate alternation of light and dark, respectively. (D) Bioluminescence of *pCCA1::LUC* and *pTOC1::LUC* reporter lines measured in the Col-0 wild type and *elo3-6* mutant (R14.7, R14.10 and R15.10 lines for *pCCA1* and the Z3.2.1 and Z3.2.2 lines for *pTOC1*) in a time-course analysis under constant white light conditions. (E) Relative expression levels by qPCR of positive regulators of skotomorphogenesis (*PIF4*, *SPA1*, and *EID1*) and positive regulators of photomorphogenesis (*HY5*, *HYH*, and *HFR1*) in darkness. (F) Relative hypocotyl lengths of the Col-0 wild type and *elo3-6* seedlings grown in constant darkness or white light in the absence (mock control M) or presence of indicated concentrations of BL or BRZ. In A, E and F 4-day-old seedlings grown on half-strength MS medium were analyzed. In A and E, the relative expression levels were detected by qPCR with six biological replicates and *PP2A* and *SAND* genes as references (Czechowski *et al.*, 2005). The experiments were repeated two times. Bars represent mean values ± s.d. In B and F mean values of hypocotyl length of at least 25 seedlings are presented. Differences between mutant and wild type were statistically analyzed with an unpaired two-tailed Student's *t*-test and significant differences are indicated with asterisks ($P<0.05$).

3.6 Regulators of skoto- and photomorphogenesis

The *PHYTOCHROME INTERACTING FACTOR 4* gene (*PIF4*) and genes encoding other positive skotomorphogenesis regulators, such as *SPA1* and *EMPFINDLICHER IM DUNKELROTEN LICHT 1* (*EID1*) (Fig. 4E), and B-box zinc finger proteins *BBX24* and *BBX25* (Table S2) showed significantly lower expression in the *elo3-6* mutant. Downregulation of such factors reduced hypocotyl elongation, as shown in *pif4* and multiple *pif* mutants (Leivar *et al.*, 2012), *spa1 det1-1* (Nixdorf and Hoecker, 2010), *bbx24 cop1-4*, and *bbx25 cop1-4* (Gangappa *et al.*, 2013). Such downregulation might contribute to the reduced hypocotyl elongation in *elo3-6* in darkness. PIF4 is the key player among factors positively regulating hypocotyl growth, and reduced relative mRNA level of *PIF4* in *elo3-6* in darkness is in line with genetic interactions between PIF4 and Elongator observed in the triple *elo3-6 pif3-3 pif4-2* mutant. Indeed, the genes downregulated in the *elo3-6* transcriptome in darkness largely overlapped with PIF4 targets identified by chromatin immunoprecipitation-sequencing (ChIP-seq) in 5-day-old etiolated seedlings (Oh *et al.*, 2014). There was 41% overlap in the GO category "Response to hormones", 38% in "Response to light", 36% in "Secondary cell wall biogenesis", and 23% in "Regulation of transcription".

In addition to genes that are positive skotomorphogenesis regulators, including *PIF4*, the positive photomorphogenesis regulator genes *HY5*, *HYH*, *HFR1* (Fig. 4E), and *HY1*

(Table S2) were also downregulated in the *elo3-6* mutant in darkness. Decreased expression of these regulators leads to hypocotyl elongation and prevents opening of the apical hook and cotyledon expansion. Considering that positive regulators of skoto- and photomorphogenesis are known to interact and suppress each other's phenotypes (Ang and Deng, 1994; Xu *et al.*, 2014; Srivastava *et al.*, 2015), coincidental downregulation of positive regulators of both skoto- and photomorphogenesis in the *elo3-6* mutant may blend into the combinatorial phenotype of a moderately shorter hypocotyl and a closed apical hook. This mechanism is supported by the hypocotyl length of the *elo3-6 hfr1-101* double mutant, which is the same as in *elo3-6*, indicating that introduction of the *hfr1* mutation into *elo3-6* does not result in additional hypocotyl elongation because the *hfr1* expression is decreased by the *elo3-6* mutation.

The basic leucine zipper (bZIP) transcription factors LONG HYPOCOTYL 5 (HY5) and HY5 HOMOLOG (HYH) are highly similar and play important roles in light-induced gene expression (Holm *et al.,* 2002). They exist in vivo in an equilibrium of homo- and heterodimers allowing for a dynamic control of transcription in response to the light stimuli. In darkness, HYH has a low expression while HY5 expression is 10 times higher (Sibout *et al.*, 2006). After an hour in light, HYH expression has increased by 50 to 100-fold, and HY5 by 10 to 12-fold. At 6 hours of light exposition, HY5 and HYH reach an equilibrium where HY5 decreases to reach 2-fold of the darkness level while HYH steadily increases to reach the level of HY5. Loss-of-function *hy5* mutants display dark-grown characteristics in the light (Oyama e*t al.,* 1997), i.e. a loss of the inhibition of hypocotyl elongation. While *hy5* mutants display this phenotype in all light conditions, mutants in *hyh* show a similar but very weak phenotype only in blue light. Since we have shown that *HYH* expression is affected in darkness and after 1h light induction in the mutant (Table 1 and Figure 4E), we are comparing the hypocotyl phenotypes of loss-of-function of *HYH* to loss-of-function *ELO3*. The hypocotyl length was compared between the *elo3-2* mutant (*ELO3* T-DNA insertion mutant in Ws background), the *hyh* mutant and the Ws wild type at 4 and 6 DAG in darkness and in white light condition (Figure 5). Upon light exposure, the hypocotyls of *elo3-2*, *hyh* and Ws present no differences in length. Darkness-grown *elo3-2* seedlings had shorter hypocotyls as compared to Ws at 4 and 6 DAG. The hypocotyl length of *hyh* was bigger than Ws at 4

DAG but becomes significant at 6 DAG. *hyh* and *elo3-2* have opposite effects on the hypocotyl growth and taking into account reduced *hyh* expression in *elo3-6*, this suggests that the observed reduction in hypocotyl growth in *elo3-6 / elo3-2* is not linked to the reduction of *HYH* expression.
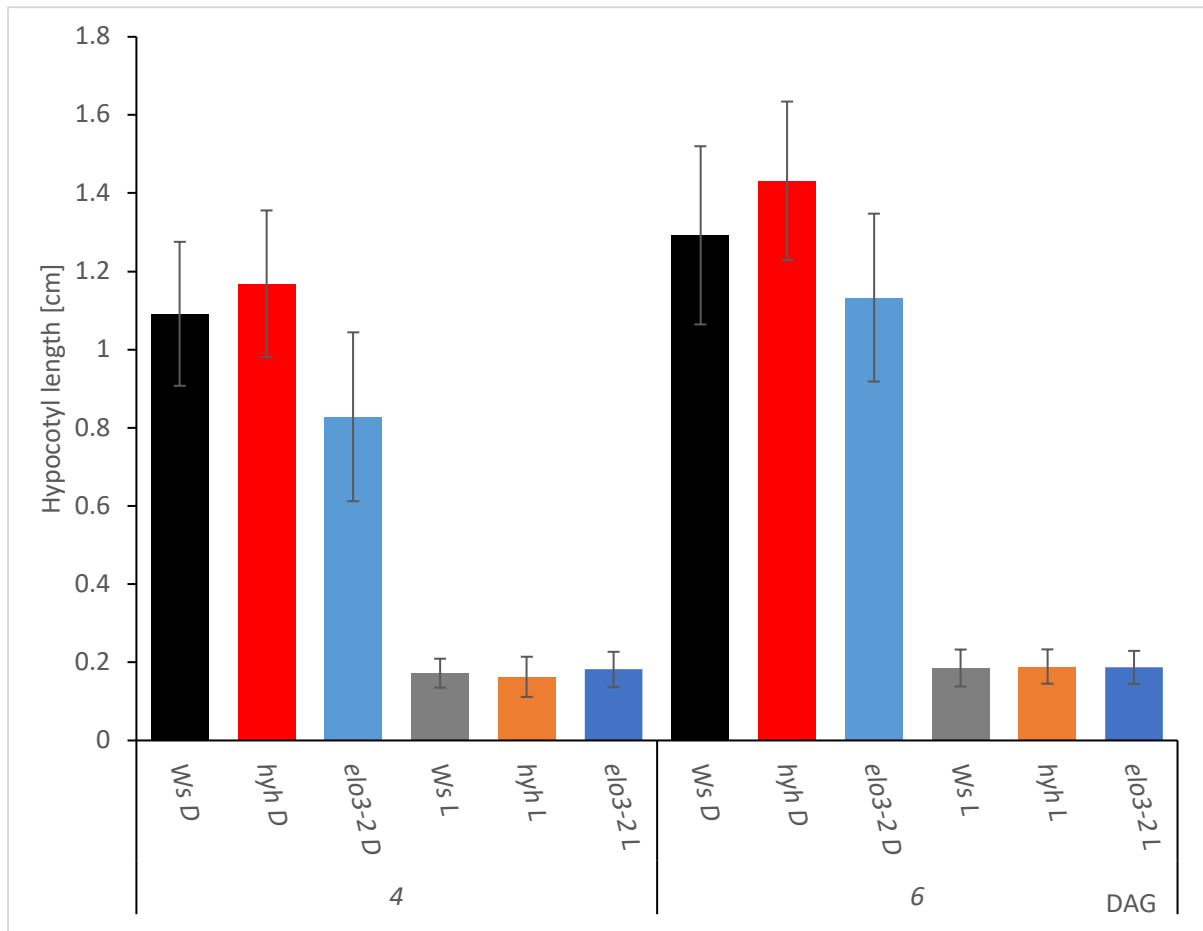
Figure 5. Phenotypes of *elo3-6* seedlings grown in darkness or under light conditions in comparison to *hyh*. Hypocotyl length of wild type (Ws), *hyh* mutant and *elo3-2* mutant were measured at 4 and 6 DAG after being grown in darkness (D) or in light condition (L). At least thirty seedlings were photographed and hypocotyls were measured with the ImageJ software. Mean values of hypocotyl length of at least 25 seedlings are presented. Error bars represent standard errors. Asterisks indicate statistically significant differences to Col-0 (* $p<0.05$, ** $p<0.01$, *** $p<0.001$).

3.7 Hormone response

Downregulated genes of the growth-regulatory network are related to hormonal pathways (Table S2), in particular those encoding the brassinosteroid (BR) pathway components. These genes were well represented and included three enzymes crucial for BR synthesis (*CPD, DWF4* and *CYP90D1*), the signalling component *BSU1*, and five

genes (*VH1, MERI5, THE1, TCH4,* and *IBH1*) encoding response proteins related to control of cell elongation via cell wall modification. To check whether a defective BR pathway contributes to the reduced hypocotyl elongation in *elo3-6*, we tested the mutant sensitivity to the BR biosynthesis inhibitor brassinazole (BRZ) and exogenous brassinolide (BL) by means of the hypocotyl elongation assay in darkness. Both Col-0 and *elo3-6* responded with reduced hypocotyl elongation to 0.5 and 5 μM BRZ, but the decrease in hypocotyl length was smaller in the mutant (Fig. 4F). The result hints at BRZ hyposensitivity and reduced activity of BR biosynthesis enzymes, in line with their decreased expression in *elo3*-6 as compared to Col-0. BL treatment did not reverse the short hypocotyl phenotype of *elo3-6,* indicating that BR deficiency caused by reduced biosynthesis gene expression is not the primary reason for the short hypocotyl mutant phenotype. The *elo3-6* mutant showed a moderate hypersensitivity to BL with a decreased hypocotyl length even at the lowest (1nM) BL concentration, whereas only the highest concentration of 1 μM BL decreased hypocotyl length in the wild type (Fig. 4F). BRZ hypo- and BL hypersensitivity of *elo3-6* resembled those of the *bzr1-1D* mutant, which contains increased amounts of the BRASSINAZOLE-RESISTANT 1 (BZR1) transcription factor activated by BRs that dimerize with PIF4 to promote cell elongation in etiolated hypocotyls (Wang *et al.*, 2002). Like *bzr1-1D,* also *elo3-6* might have increased levels of free BZR1 caused by downregulation of PIF4 and hence reduced amount of PIF4-BZR1 dimers and a retarded cell elongation. High BZR1 levels in *elo3-6* were suggested by fewer transcripts of BR biosynthesis enzymes, implying feedback inhibition as also detected in *bzr1-1D* (Wang *et al.*, 2002). BRZ and BL sensitivities were modestly affected in *elo3-6,* suggesting that malfunction of the BR pathway contributes only partially to the short *elo3-6* hypocotyls. As indicated by the transcriptome, other growth-related hormonal pathways that might contribute to defective hypocotyl elongation are downregulated in *elo3-6*. For example, downregulation of *PIF4* may affect the auxin responses, because PIF4 stimulates the expression of the auxin biosynthetic gene *YUCCA8* (Sun *et al.*, 2012), whose expression is reduced in *elo3-6* (Table S2).

3.8   Cell wall biogenesis

Hormone pathways regulate growth by convergence to the cell wall biogenesis pathways. In the *elo3-6* mutant, more than 40 genes related to cell wall formation were downregulated in darkness; these included three genes (*IRX9, IRX10, IRX14-L*) encoding enzymes of the xylan biosynthesis, which is involved in the generation of both primary and secondary cell walls. The irx9, irx10, and irx14-L mutants are similar to elo3-6, in that they have moderately shorter hypocotyls than the wild type in darkness and no opened cotyledons (Faik et al., 2014). In the elo3-6 mutant, genes regulating secondary cell wall synthesis are downregulated. These genes include xylem differentiation factors (ATHB15, REV, PHV), and NAC and MYB transcription factors (VND2-6, MYB46, MYB83, MYB103, XND1, SND2, MYB52, MYB54, C3H14, and MYB85) representing all three tiers of the transcription factor cascade (Hussey et al., 2013); and enzymes of cellulose (CESA4, CESA7, CESA8, and IRX6/COBL4), hemicellulose (IRX8, IRX9, IRX10, IRX14L, FRA8, and GUX1) and lignin (LAC4, LAC10, and LAC17) synthesis (Table S2).

3.9   H3K14 acetylation activity of Elongator at LHY, HYH and HFR1 in darkness

The expression of the *CCA1* and *LHY* genes was correlated with the level of the histone H3 modifications, H3K4Me2 and H3K9Ac (Ni *et al.*, 2009). Similarly, some of the light- and/or darkness-related regulatory genes are controlled by histone modifications, suggesting that they might also be direct targets of Elongator HAT activity. Hence, ChIP-qPCR was carried out on chromatin of *elo3-6* and Col-0 4-day-old seedlings germinated in darkness. The analysis used antibodies against acetylated histone H3K14 and primers for promoter and coding regions of the circadian clock *CCA1* and *LHY* genes (Fig. 6A,B) and of the regulatory genes *PIF4* (Fig. 6C)*, HYH, HFR1,* (Fig. 6D,E) *SPA1, EID1* and *HY5*. Results were normalized versus both input and the *ACTIN2* gene. To check whether Elongator targets downstream transcription factors related to hormone and cell wall pathways, ChIP-qPCR was done on the *CPD, DWF4, CYP90D1*, and *BSU1* genes from the BR pathway, the *CGA* and *GNC* cytokinin response genes; the secondary cell wall regulator-encoding genes *PHAV, REV, VND4, MYB46, MYB83*, and *MYB103*, and the structural genes *CESA4, CESA7*, and *CESA8* (Table S2).

Of the 20 analyzed genes, the H3K14 acetylation was only significantly decreased in the coding regions of the *LHY, HYH* and *HFR1* genes in *elo3-6* seedlings. The results show that *LHY, HYH* and *HFR1* are direct targets of Elongator HAT activity in darkness (Fig. 6B,D,E) and suggesting that Elongator provides selective epigenetic control to a few of the highest order transcription factors. Identification of *LHY* as a target for histone H3K14 acetylating activity of Elongator together with decreased expression of *LHY* in *elo3-6* and similar hypocotyl phenotypes of *lhy* and *elo3-6* mutants in darkness, indicate that epigenetic control of *LHY* expression via Elongator HAT activity might contribute to hypocotyl growth regulation. Targeting of *HYH* and *HFR1* by Elongator in darkness suggests a fine-tuning mechanism of hypocotyl growth regulation whereby positive regulators of photomorphogenesis prevent exaggerated elongation. None of the positive skotomorphogenesis regulators showing decreased expression in *elo3-6* was targeted by Elongator HAT activity, as illustrated for *PIF4* (Fig. 6C). These factors might be regulated via other activities of Elongator or via HAT regulation of the higher-order regulators. For example, because *PIF4* is controlled by the circadian clock (Yamashino *et al.* 2003; Kidokoro *et al.* 2009), it is possible that the downregulation of *PIF4* in the *elo3-6* mutant is a consequence of the downregulation of *CCA1* and Elongator target *LHY*.
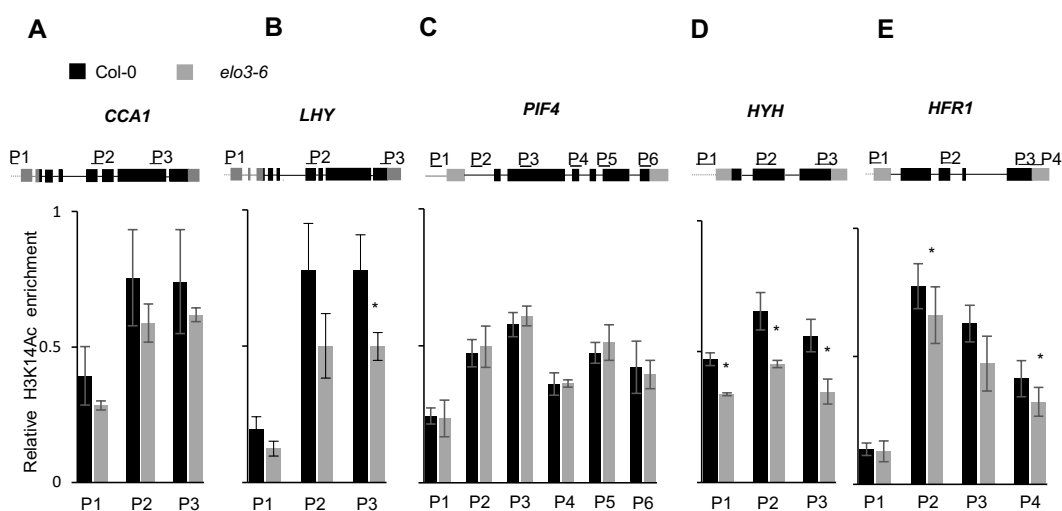
Figure 6. Histone acetylation of circadian clock and skoto- and photomorphogenesis regulatory genes in the *elo3-6* mutant in darkness. Histone H3K14 acetylation level in the *CCA1, LHY, PIF4, HYH* and *HFR1* promoter and coding regions. The relative H3K14Ac enrichment was established with antibodies against H3K14Ac for ChIP and primers (P1–P6, Table S5), amplifying fragments of promoter and coding sequences, for qPCR. Results were normalized versus input and actin reference

gene. The experiment was repeated four (*LHY* and *HYH*) or two (*CCA1*, *PIF4*, and *HY5*) times with four biological replicates each time. Four-day-old seedlings grown in darkness on half-strength MS medium were analyzed. Bars represent mean values ± s.d. Differences between mutant and wild type were statistically analyzed with an unpaired two-tailed Student's *t*-test and significant differences are indicated with asterisks ($P<0.05$).

3.10 Gene expression in the elo3-6 mutant in light

The transcriptome analysis showed that the expression of some transcription factor i.e. *HYH* or *HY5* were downregulated in *elo3-6* under the different light qualities therefore some of these genes were tested for their expression and acetylation.

Expression levels of genes encoding the main regulators of skoto- and photomorphogenesis, light response, and cell wall-related and brassinosteroid biosynthesis were assayed by qPCR in 4-day-old *elo3-6* and Col-0 seedlings grown in continuous red, far-red, or blue light. The genes of positive regulators of photomorphogenesis (*HY5*, *HYH*, and *HFR1)*, and of skotomorphogenesis (*EID1*), were downregulated under at least one light condition, whereas *PIF4*, downregulated in darkness, was upregulated in far-red and blue light (Fig. 7A). The *HY5* gene, encoding the main positive photomorphogenesis regulator, was downregulated in all light qualities, but *HYH* and *HFR1*, encoding two HY5 interactors, were downregulated in red light, *HYH*, which plays an important role in blue light photomorphogenesis, also showed lower transcript levels in blue light. Reduced expression of these regulators, which cooperate in inhibition of hypocotyl elongation and promotion of apical hook opening and cotyledon growth, was consistent with the increased hypocotyl length and unexpanded and hyponastic cotyledons of the light-grown *elo3-6* seedlings. *HY5* downregulation in *elo3-6* coincided with extreme upregulation of *WALL-ASSOCIATED KINASE 1* (*WAK1*), moderate upregulation of *INCREASED SIZE EXCLUSION LIMIT 2* (*ISE1*) (Fig. 5A), and no difference in expression of *ARF2*, *UBP15*, *ATHB-2*, *ATASE2*, *APG3*, and *MSL3*, which are all HY5 target genes (Zhang *et al.*, 2011). Indeed, *WAK1* is negatively regulated by HY5 (Zhang *et al.*, 2011), plays a positive role in cell elongation (Lally *et al.*, 2001), and is the receptor of oligogalacturonides, which are cell wall-integrity signalling components that induce defense responses. High *WAK1* expression might contribute to enhanced hypocotyl elongation and/or immune response activation, in line with downregulation of secondary cell wall genes under red-light (Fig. 7A) (Miedes *et al.*,

2014). Decreased expression of the BR biosynthesis genes *CPD*, *CYP90C11*, and *DWFA2* in the *elo3-6* mutant under red light (Fig. 7A) might result from negative feedback regulation by free BZR1 proteins. Free BZR1 might overaccumulate in *elo3-6* due to lower *HY5* levels and, consequently lower the formation of BZR1/HY5 dimers, which suppresses hypocotyl elongation (Li and He, 2016). Accordingly, *elo3-6* was hyposensitive to BL and BZR in light (Fig. 3F), confirming that BR signalling was affected in *elo3-6*.

ChIP-qPCR was applied to check whether Elongator promotes photomorphogenesis via histone H3K14 acetylation of the regulatory genes *HY5*, *HYH*, and *HFR1* in light. Chromatin isolated from *elo3-6* and Col-0 seedlings grown for 4 days in red, far-red, or blue light did not differ in histone acetylation, indicating that Elongator-mediated HAT activity did not target *HY5*, *HYH* (Fig. 7B), or *HFR1* in light. Thus, Elongator is necessary for the expression of *HY5*, *HYH*, and *HFR1*, which encode the main photomorphogenesis regulators, and for the downstream pathways controlled by HY5 during photomorphogenesis, but not via Elongator HAT activity.
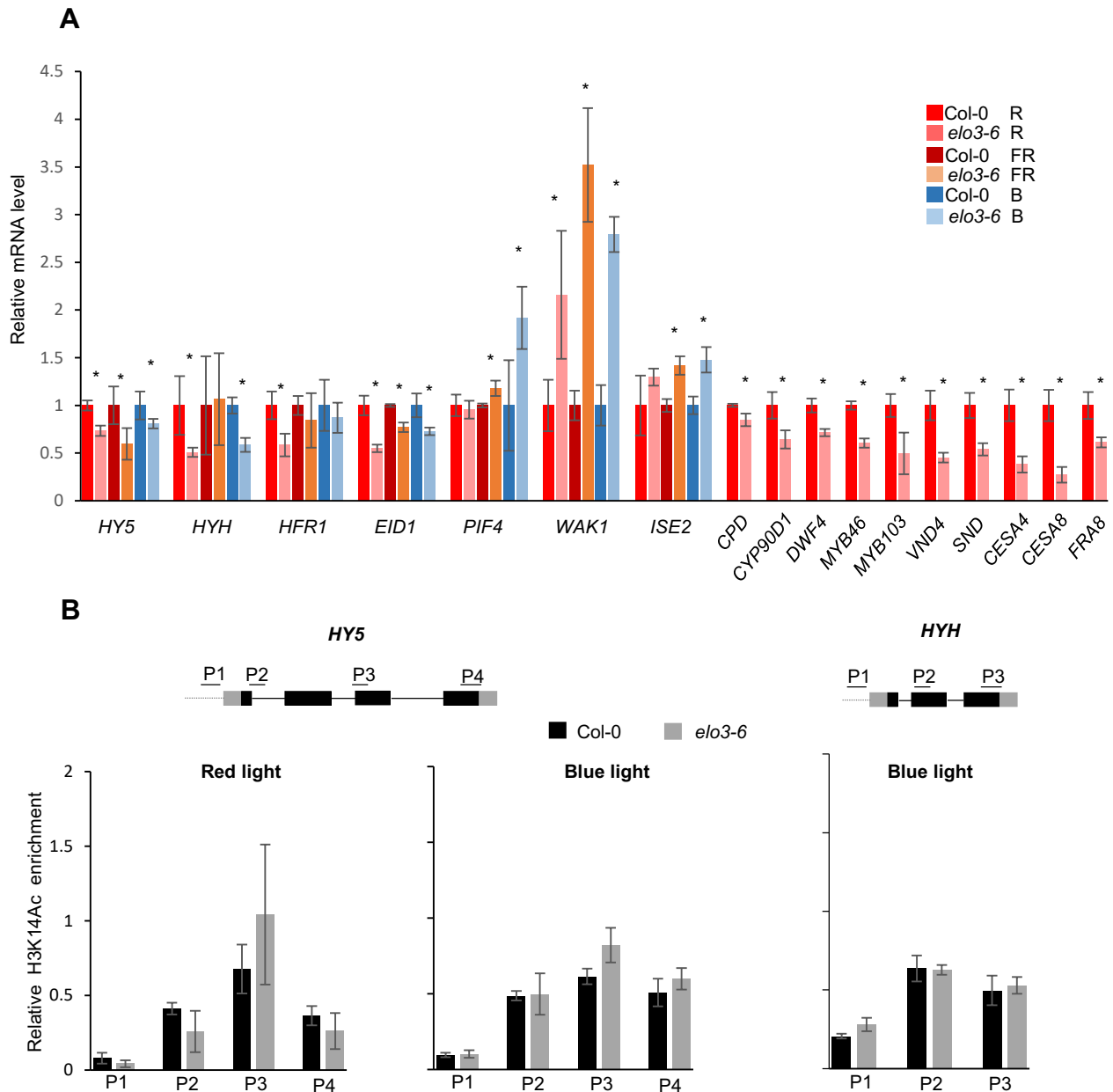
Figure 7. Expression of genes encoding photomorphogenesis regulators and cell wall biogenesis genes, and histone acetylation of *HY5* and *HYH* in monochromatic light. (A) Relative expression levels of indicated genes determined by qPCR in 4-day-old *elo3-6* and Col-0 seedlings grown under continuous monochromatic light. Expression was normalized using *PP2A* and *SAND* as reference genes. (B) Histone H3K14 acetylation in the *HY5* and *HYH* promoter and coding regions. The relative H3K14Ac enrichment was established with antibodies against H3K14Ac for ChIP and primers (P1–P4, Table S5), amplifying fragments of promoter and coding sequences, for qPCR. Results were normalized versus input and actin reference genes. Average values of six (qPCR) or four (ChIP-qPCR) biological replicates are presented with standard deviation (mean±s.d.). Differences between mutant and wild type were statistically analyzed with an unpaired two-tailed Student's *t*-test and significant differences are indicated with asterisks ($P<0.05$).

4   Discussion

We show that the Elongator complex modulates hypocotyl growth and photomorphogenesis via the regulation of a growth-controlling network consisting of circadian clock regulator, skoto- and photomorphogenesis regulators, hormone pathways and cell wall biogenesis. The regulatory role of Elongator is supported by the hypocotyl phenotypes of the *elo3-6* and *elo3-1* and the growth-related mutants, identification of the *LHY*, *HYH*, and *HFR1* regulators as direct targets of Elongator HAT activity, hormone sensitivity assays, *LUC* reporter gene activity in the *elo3-6* mutant background, and genetic interactions studies with skotomorphogenesis and light response regulators.

4.1   Elongator affects early growth in darkness and light through a growth-controlling network

Unlike de-etiolation mutants such as *cop1* and *pif*, which combine short hypocotyls with expanded cotyledons in darkness, *elo3-6* has a short hypocotyl, although apical hook and cotyledon folding remain normal. Cotyledons expand in darkness in *cop1* due to high levels of HY5, HYH, and/or HFR1; they also expand in multiple *pif* mutants, especially those including mutations in *PIF1*, which is the main cotyledon folding suppressor in darkness (Leivar *et al.*, 2012). Cotyledons of *elo3-6* do not expand in darkness, because the expression of *HY5*, *HYH*, and *HFR1* is lowered and of all *PIF*s only *PIF4* is downregulated. Hypocotyl phenotypes similar to those of *elo3-6* were observed in *lhy-21*, *lhy-21 cca1-11*, *cca1-11 lhyRNAi* (Fig. 4B), *pif4* (Leivar *et al.*, 2012), and *irx9, irx10*, and *irx14-L* (Faik et al., 2014) that represent main hubs of the growth-controlling network downregulated in *elo3-6,* indicating that the *elo3-6* hypocotyl phenotype is the result of multiple reduced gene activities. This observation is in line with the network topology that consists of upstream regulatory transcription factor pathways converging on cell wall biogenesis and resulting in a cumulative repressing effect on hypocotyl growth. The importance of cell wall biosynthesis for growth and cell elongation has been demonstrated in mutants affected in their cell wall composition (Desnos *et al.*, 1996; McCarthy *et al.*, 2010; Faik *et al.*, 2014). However, growth seems to be reduced in response to cell wall-integrity signalling that activates plant immune responses (Hématy *et al.*, 2007), rather than inhibited directly by a physically weakened cell wall.

Mutants defective in the MYB46 regulator of cell wall formation (Ramírez *et al.*, 2011) or in CESA4, CESA7, and CESA8 cellulose synthase subunits required for secondary cell wall synthesis (Hernández-Blanco *et al.*, 2007) activate the plant immune response, leading to growth attenuation (Rojas *et al.*, 2014). Downregulation of over 40 cell wall-related genes (including *MYB46*, *CESA4*, *CESA7*, and *CESA8*) and upregulation of defense response genes (including important key regulators) and of metabolic genes involved in the plant immune response coincide in *elo3-6*; hence, the hypocotyl growth defects in this mutant might be a result of reduced cell wall biosynthesis and, eventually, activation of the plant immune response (Figure 8). Decreased pathogen resistance has been shown for the *elo2* mutant, confirming positive regulation of the plant immune response by Elongator via the targeting of genes encoding important components of the salicylic acid pathway (*NPR1*, *PR2*, *PR5*, *EDS1*, and *PAD4*) (Wang *et al.*, 2013) and the jasmonate/ethylene pathway (*WRKY33*, *ORA59*, and *PDF1.2*) (Wang *et al.*, 2015) for histone acetylation and/or DNA methylation. Elongator controls also the reactive oxygen species–salicylic acid amplification loop and targets important defense genes for histone acetylation, including the homolog *AtrbohD*, that encodes the *Arabidopsis* respiratory burst oxidase, and the salicylic acid biosynthesis gene *ISOCHORISMATE SYNTHASE1* (An *et al.*, 2017). The incongruity between our data and results of others (Wang *et al.*, 2013) related to the Elongator role in immune response may correspond to different mutants (*elo3* vs *elo2*) and/or diverse developmental stages or different growth conditions applied in the studies. For example, delayed induction and lower expression of some defense genes (including *PAD4*) in the *elo2* mutant were observed only after pathogen infection, whereas basal expression was similar in the mutant and the wild type (Wang *et al.*, 2013). Moderately increased expression of selected immunity pathways in *elo3-6* may result in growth inhibition but does not necessarily trigger constitutive activation of plant defense pathways, which requires high levels of upregulation (usually in response to pathogen infection) to exceed the defense activation threshold (Kwon *et al.*, 2009). Therefore, in addition to well-established direct positive regulation of plant immune response, Elongator may under some conditions play an opposite and possibly indirect role acting as a positive regulator of cell wall-related genes. Elongator may contribute independently and inversely to

different immune response pathways, and may modulate the growth–defence balance (Hématy *et al.*, 2007).

Alternatively, the increased levels of jasmonic acid (JA), increased JA biogenesis and responsive gene expression levels (Nelissen *et al.*, 2010), and the induction of the jasmonate-controlled MYC2 transcriptional cascade (Wang *et al.*, 2015) were reported earlier for the *elo* mutants. The plant response to wounding, similar to immune response, has a negative JA-mediated effect on growth. However, we did not find JA-related genes among those differentially regulated in *elo3-6* in our microarray dataset. Moreover, JA acts during skotomorphogenesis to reduce hypocotyl length but at the same time JA also promotes cotyledon opening in etiolated seedlings (Zheng *et al.*, 2017), resulting in the constitutively photomorphogenic phenotype. This is not the case for the darkness-grown *elo3* seedlings, which are shorter but have normal apical hooks arguing against the role of JA and wounding in the *elo3* phenotype.
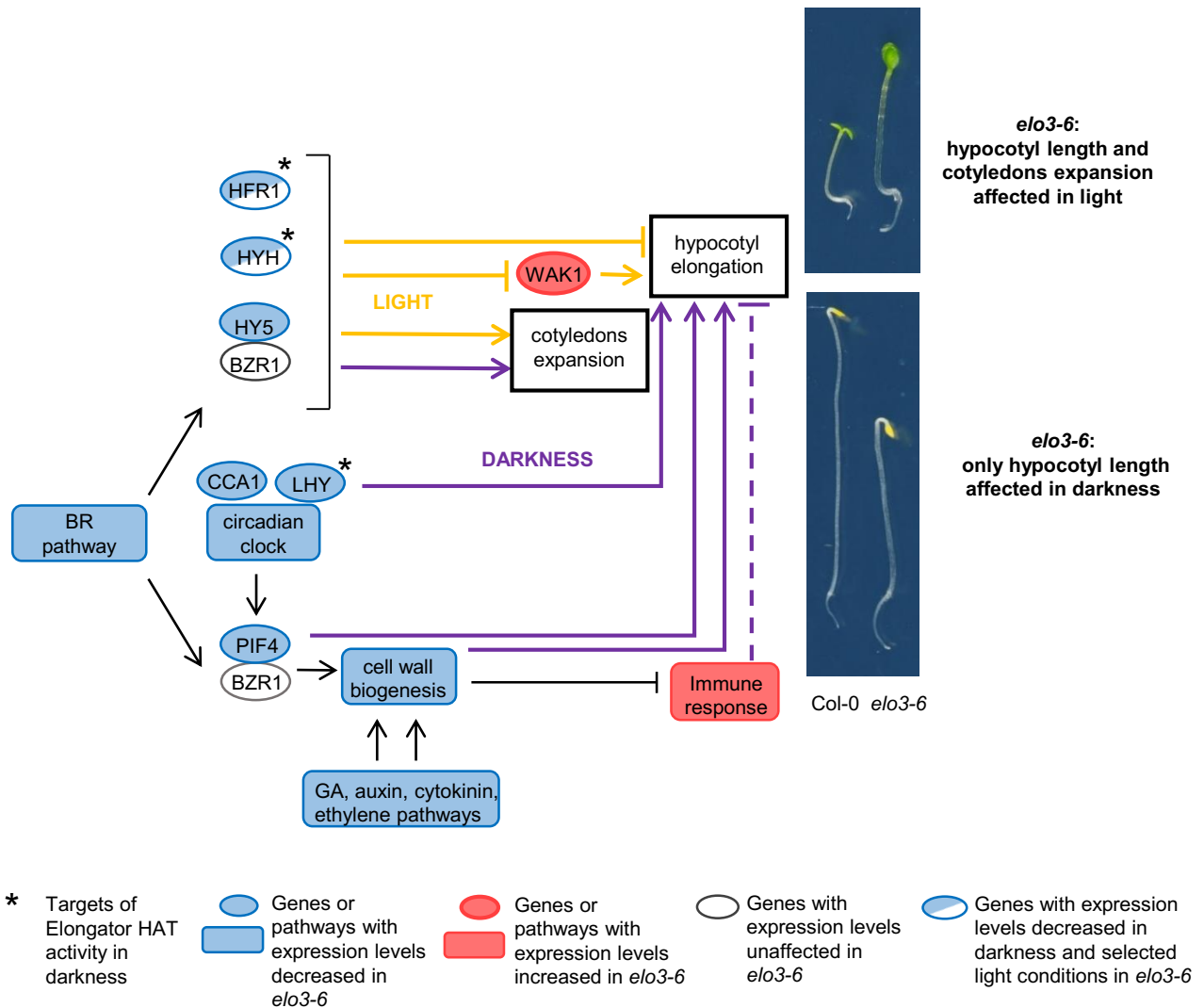
Figure 8. Model for Elongator transcriptional control of hypocotyl growth in darkness and photomorphogenesis. Elongator controls hypocotyl elongation via several pathways: elongation-suppressing pathways involving positive regulators of photomorphogenesis (HY5, HYH, and HFR1) or immune response genes, and elongation-stimulating pathways including circadian clock, PIF4, hormone biosynthesis or signalling, and cell wall biogenesis. In darkness (purple arrows), downregulation of genes in pathways stimulating hypocotyl elongation and upregulation of immune response genes suppressing elongation prevail, resulting in a shorter hypocotyl of the *elo3-6* mutant. In light (yellow arrows), hypocotyl elongation is inhibited very early in the wild type, whereas in the *elo3-6* mutant, elongation inhibition fails due to downregulation of positive photomorphogenesis regulators and strong upregulation of WAK1 which stimulates cell elongation and results in a longer hypocotyl. Elongator also regulates cotyledon expansion via positive regulators of photomorphogenesis. The *HY5* gene was downregulated under red, far-red and blue light (blue filling), *HYH* under red and blue light and *HFR1* under red light only (blue-white filling). Expression of BR pathway and cell wall biogenesis genes was assayed in darkness and red light. Pictures present 4-day-old seedlings grown in darkness (lower panel) or in red light (upper panel). The asterisks indicate targets of Elongator HAT activity in darkness. Blue or red

colours indicate respectively lower or higher expression level of given gene or pathway. Genes half-shaded with blue colour have expression levels downregulated in darkness and selected light conditions. The expression level of *BZR1* gene is unaffected as indicated by transparent circles. Downregulation of hypocotyl elongation by immune response is represented with the dashed line since it is not clear whether downregulation of the cell wall biogenesis-related genes affects hypocotyl elongation directly or via immune response as suggested by higher transcription of genes involved in immune response in *elo3-6*.

4.2 Elongator affects major regulators of light signalling

Transcriptomes of *elo3-6* and wild type were compared in darkness and upon 1 hour induction in red, far-red and blue light using microarrays and RNA-seq platforms. A number of genes related to light perception and response were downregulated in the *elo3-6* mutant but still inducible by light (slight upregulation) suggesting an effect of Elongator on these genes (Table 1). It has been shown that after 1h of exposure to blue light 18% of transcription factors are regulated and that the number rises to 26% after 24h of exposure (Jiao *et al.*, 2003), which can explain why little difference between DEG in darkness vs light induced samples is seen.

Upon 1hr of exposure to blue light, specific genes of blue light response had DEG in *elo3-6*. DEG were also compared for light response specific genes under red and far-red light 1hr exposure. Cryptochromes are the major blue light receptors and CRY1 is known to regulate through light induction the expression of flavonoid biosynthesis genes like *CHS* (Wade *et al.*, 2001). Chalcone synthase is the first step in the flavonoid biosynthesis. Elongator mutants accumulate anthocyanin and have increased *CHS* expression under white light that is regulated by MYBL2, a negative transcription factor of the anthocyanin pathway (Zhou *et al.*, 2009). The reduction of *CRY1*, *CRY2* and *MYBL2* may explain the reduction in *CHS* by cascade. Less photoreceptors lead to reduced responses. Cryptochrome also interacts with ZTL, altering the circadian clock function (Jarillo *et al.*, 2001). But ZTL is also directly affected by blue light via its LOV domain (Kim *et al.*, 2007). ZTL is responsible for the degradation of TOC1 and insuring the normal running of the clock. Like other clock genes, *ZTL* is constitutively expressed and its levels fluctuate throughout the day. We show that the amplitude of the clock is reduced in *elo* mutants and that *LHY* is a target of acetylation by Elongator which may

explain the reduced expression of ZTL in *elo3-6*. It could also be that ZLT is a direct target of acetylation by Elongator.

Blue light controls stomatal opening and stomatal development (Kang *et al.*, 2009). Upon blue light induction, *elo3-6* mutation leads to an enrichment in GO categories in downregulated genes related to stomatal development, indicating that Elongator is necessary for normal development of stomata through blue light signalling. Interestingly, the *BBX25* that promotes the expression of *COP1*, coding for a key repressor in the light-promoted stomatal development (Gangappa *et al.*, 2013) is downregulated in *elo3-6*, suggesting *BBX25* as a putative target of ELO3.

Phytochromes are responsible for detection of red and far-red light. These wavelengths function together in the detection of shade by the plant (Casal, 2013). Light qualities that are detected by the different photoreceptors have similar effects on the transcriptome due to integration points such as *HY5, CCA1* and *LHY* (Jiao *et al.*, 2007). During the early light response, we showed that transcription of *HYH, HY5* and *HFR1* was downregulated and *PIF4* upregulated in the different light qualities and that genes downstream in the light response pathway are also affected such as *WAK1*.

4.3 Transcription-based model of the role of Elongator in early plant development

We propose a model for the role of Elongator in early plant development that elucidates why hypocotyl growth of the *elo* mutants is slower in darkness but photomorphogenesis is defective in light, resulting in a longer hypocotyl and unexpanded cotyledons (Fig. 8). Elongator regulates hypocotyl elongation and cotyledon expansion by controlling cell wall biogenesis genes and positive photomorphogenesis regulators. Depending on the light conditions, one of the pathways becomes restrictive and Elongator promotes opposite growth behaviours.

In darkness, expression of the circadian clock regulator *LHY* and of the positive photomorphogenesis regulators *HFR1* and *HYH* is activated by Elongator-mediated transcript elongation-facilitating histone acetylation. As shown by the hypocotyl growth analysis of the *lhy-21, lhy-21 cca1-11 and cca1-11 lhyRNAi* mutants, the circadian clock components LHY and CCA1 positively regulate hypocotyl elongation. One of the possible mechanisms of this regulation involves PIF4 which is controlled by circadian

clock (Nozue *et al.*, 2007) at the transcription level and stimulates expression of genes involved in hypocotyl elongation. Indeed, because the *LHY*, *CCA1*, and *PIF4* genes are downregulated in darkness in *elo3-6* mutants, which affects the expression of many transcription factors, such as components of hormonal and cell wall biosynthesis pathways that slow down hypocotyl elongation partially via activation of the plant immune response (Hématy *et al.*, 2007). Lower level of PIF4 reduces formation of complexes with the BZR1 transcription factor of the BR pathway and compromises induction of cell wall biogenesis genes (Lozano-Durán *et al.*, 2013). In conclusion, in darkness, the *elo3-6* hypocotyl phenotype is determined by the combined effect of decreased levels of cell wall biogenesis genes, reduced expression of clock regulators and decreased expression of *HY5*, *HYH*, and *HFR1*, consequently inhibiting hypocotyl elongation. The final phenotype of short hypocotyls indicates that the defect in cell wall biogenesis prevails. Low expression of *HY5*, *HYH*, and *HFR1* also prevents cotyledon expansion in *elo3-6*.

Elongator is also required for light responses, because the genes of the major positive photomorphogenesis regulators *HY5*, *HYH*, and *HFR1* are downregulated in *elo3-6* although, strikingly, their H3K14Ac levels are unaffected in light. The HAT activity of Elongator might be very dynamic and difficult to capture in a ChIP-qPCR assay using acetylated histone antibodies, which could explain the limited number of genes targeted for Elongator-mediated histone acetylation. In plants, the interaction between Elongator subunits and the SPT4/SPT5 transcript elongation complex (Van Lijsebettens *et al.*, 2014) suggests that Elongator might affect RNAPII transcript elongation indirectly, next to its histone acetylation activity (Antosz *et al.*, 2017). An alternative explanation is that, in light, another epigenetic activity of Elongator such as DNA demethylation (DeFraia *et al.*, 2013; Wang *et al.*, 2013) or processing of primary microRNAs (Fang *et al.*, 2015) might be responsible for decreased expression of *HY5*, *HYH* and *HFR1*. In light, hypocotyl elongation is inhibited very early in wild-type seedlings by diverse factors including HY5, HYH, and HFR1, possibly involving suppression of the cell elongation activity of WAK1 (Fig. 8). In the *elo3-6* mutant, decreased expression of *HY5* leads to a higher accumulation of *WAK1* mRNA and induced hypocotyl elongation. On the other hand, upregulation of *WAK1* may trigger

immune responses as suggested by decreased levels of cell wall biogenesis genes, and may suppress hypocotyl elongation. The two pathways contribute to a final hypocotyl length that is longer in *elo3-6* than in the wild type, indicating that the pathway promoting cell elongation prevails. Lower expression of *HY5*, *HYH*, and *HFR1* in the mutant results also in less expanded cotyledons yielding the phenotype typical of photomorphogenesis defect.

In conclusion, Elongator is known as an enzymatic complex with diverse activities that directly or indirectly, positively or negatively influence expression of genes located in various pathways. Here, we showed that Elongator acts as an interface between growth, immune responses and photomorphogenesis and plays a fine-tuning role in mutual regulatory interactions of those processes at the transcriptional level.

5   Material and methods

5.1   Plant mutants and reporter lines

The *drl1-2* (Nelissen *et al.*, 2003), *elo1-1*, *elo2-1*, *elo3-1*, *elo4* (Nelissen *et al.*, 2005) mutants corresponding to alleles of *ELP4*, *ELP1*, *ELP3*, and *DRL1* genes in Ler and the *elo3-6* mutant in Col-0 (GABI-KAT collection code GABI555_H06, Nelissen *et al.*, 2010) are described previously. *pCCA1::LUC* (Salome and McClung, 2005) and *pTOC1::LUC* (Portoles and Mas, 2007) are reporter lines in Col-0. The mutants *phyB-9*, *hfr1-101* and *pif3-3 pif4-2* in Col-0 and *phyA-201*, *phyB-1* and *phyA-201 phyB-5* in Ler were purchased at the Nottingham *Arabidopsis* Stock Centre (NASC). The *lhy-21 cca1-11* (N9380) and *lhy-21* (N9379) mutants in Ws background were also obtained from NASC. The *cca1-11 lhyRNAi* mutant in Ws background was a kind gift of Steve Kay (The Scripps Research Institute, La Jolla, CA, USA). The double or triple mutants *elo3-6 hfr1*, *elo3-6 pif3-3 pif4-2*, *elo3-1 phyB-1* and *elo3-1 phyA-201* were generated by crossing. Homozygous individuals were identified by PCR genotyping with primers listed in Table S3. *elo3-2* (FLAG_219E08, in WS) (Nelissen *et al.*, 2005), *hyh* (in Ws) seeds were a gift from X.W. Deng (Yale University, New Haven, CT, USA).

5.2   Growth conditions and assays

For hypocotyl assays, seeds were sterilized in 5% (v/v) bleach with 0.05% (v/v) Tween 20 for 10 min, washed in water, sown on half-strength Murashige and Skoog (MS) medium (Murashige and Skoog, 1962) without sucrose and stratified at 4°C for 48 h. Seeds were exposed for 6 h to white light (100 μmol m^{-2} s^{-1}) to induce germination and plants were grown in either darkness, white (Cool white fluorescent light, Philips), red (Cool white fluorescent light, filtered through red plastic (Rohm and Haas) and red cellophane, (UCB-Sidac, Gent, Belgium)), far-red (Incandescent light combined with a 700-nm long pass filter), or blue light (dragon tape LEDs, 470 nm, Osram), all at the high fluence rate of 10 μmol m^{-2} s^{-1} for the indicated time at 21°C. Seedlings analyzed for hypocotyl length were put on 1% (w/v) agar, photographed, and hypocotyl length of at least 25 seedlings for each genotype/condition was measured with the ImageJ 1.45 software. Significant differences were recovered with the two-tailed Student's *t*-test in Microsoft Excel.

For the hormone assays, BL (24-epibrassinolide, Duchefa-Direct, Cat. E0940.0010) or BRZ (TCI Europe, Cat. B2829) were used at concentrations of 10^{-3}, 10^{-2}, 10^{-1}, 1 μM or 0.5 and 5 μM, respectively.

The clock reporter lines expressing *pCCA1::LUC* and *pTOC1::LUC* were crossed into the *elo3-6* mutant. F1 was tested for the presence of the LUC reporter and F2 was tested for the presence of the LUC reporter and selection of homozygote *elo3-6* individuals using primers presented in Fig S2. The F3 progeny of positive individuals were tested for homozygosity of LUC with primers and of *elo3-6* based on phenotype and P. Lines homozygous for the *elo3-6* mutation and the *pCCA1::LUC* reporter (R14.7, R14.10, R15.10) and a line homozygous for the *elo3-6* mutation and the *pTOC1::LUC* reporter (Z3.2.1 and Z3.2.2) were analyzed by in vivo luminescence assays. Plants were stratified for 3 days at 4ºC on MS agar medium and grown for 7 days under LD cycles (12-h light/12-h dark) with 60 μmol m^{-2} s^{-1} white light at 22ºC. Seedlings were subsequently transferred to 96-well plates containing MS agar and 3mM luciferine (Promega). Luminescence rhythms were monitored using a luminometer LB-960 (Berthold Technologies) and the software MikroWin 2000, version 4.34 (Mikrotek Laborsysteme) for the analysis.

5.3   RNA isolation, cDNA synthesis, and qPCR

For gene expression analyses, six biological replicates were used. RNA was isolated with the RNeasy Plant Kit (Qiagen) with on-column DNase digestion. The manufacturer's protocol was modified by two additional washes of RNeasy spin columns with the RPE buffer. cDNA was synthesized with SuperScript III First-strand synthesis kit (Life-Invitrogen, CAT. 18080051).

The PCR reactions were performed in technical triplicates with the LightCycler 480 SYBR Green I Master reagent and the Janus robot (PerkinElmer) for pipetting. The LightCycler 480 Real-Time PCR System was used for amplification (95°C for 10 min, 45 cycles of 95°C/10 s, 60°C/15 s, 72°C/30 s, followed by melting curve analysis). The qPCR results were analyzed with the qBase Plus software (Biogazelle). The *PP2A* (At1g13320) and *SAND* (At2g28390) genes were used as references for gene expression normalization. For the primer sequences, see Table S4.

5.4   Microarray analysis

Whole 4-day-old seedlings grown in continuous darkness were harvested, RNA was isolated and analyzed using *Arabidopsis* (V4) Gene Expression Microarray 4x44K (Agilent Technologies). The data are available at NCBI, Gene Expression Omnibus, accession number GSE42053.

5.5   RNA-seq analysis

For transcriptome sequencing, RNA was extracted from 4-day-old seedlings grown in continuous darkness and grown in darkness then exposed to 1h of blue light. TruSeq RNA sequencing libraries (Illumina) were generated and sequenced on Illumina HiSeq.

5.6   ChIP-qPCR

ChIP was done as described (Bowler et al., 2004) with 4-day-old seedlings. The isolated chromatin was sonicated in SONICS Vibra-cell sonicator with four 15-s pulses at 20% amplitude and immunoprecipitated with 5 µl of anti-acetyl-histone H3 (Lys14) antibodies (Millipore, Cat. no. 7-353). Protein A agarose (Millipore, Cat. No. 16-157) was used to collect immunoprecipitated chromatin. After reverse cross-linking and

proteinase K digestion, DNA was purified with the MinElute PCR Purification Kit (Qiagen) and eluted with elution buffer supplemented with RNase A (10 µg/ml). Samples were analyzed by real-time qPCR with primers in the promoter and coding regions of the analyzed genes (Table S5) and the amount of immunoprecipitated DNA was calculated relatively to the actin reference gene (At3g18780) and input.

There are several controls used for the ChIP. The efficiency of the sonication is verified on agarose gel. The input corresponds to crosslinked DNA that did not go over the process of the immunoprecipitation, is used to control the qPCR efficiency and the difference with the immunoprecipitated sample shows the enrichment. Finally, a mock sample where no antibodies are added is also used to control the immunoprecipitation efficiency, there should be no enrichment to the input in these mock samples. Another action can be taken to control the immunoprecipitation of histone modification by also performing an immunoprecipitation of the histone that is modified, it was not performed in this study.

6   References

An, C., Wang, C., Mou, Z., 2017. The Arabidopsis Elongator complex is required for nonhost resistance against the bacterial pathogens *Xanthomonas citri* subsp. *citri* and *Pseudomonas syringae* pv. *phaseolicola* NPS3121. New Phytologist 214, 1245–1259. https://doi.org/10.1111/nph.14442

Ang, L.-H., Deng, X.-W., 1994. Regulatory hierarchy of photomorphogenic loci: allele-specific and light-dependent interaction between the HY5 and COP1 loci. The Plant Cell 6, 613–628. https://doi.org/10.1105/tpc.6.5.613

Antosz, W., Pfab, A., Ehrnsberger, H.F., Holzinger, P., Köllen, K., Mortensen, S.A., Bruckmann, A., Schubert, T., Längst, G., Griesenbeck, J., Schubert, V., Grasser, M., Grasser, K.D., 2017. The Composition of the Arabidopsis RNA Polymerase II Transcript Elongation Complex Reveals the Interplay between Elongation and mRNA Processing Factors. The Plant Cell 29, 854–870. https://doi.org/10.1105/tpc.16.00735

Bourbousse, C., Ahmed, I., Roudier, F., Zabulon, G., Blondet, E., Balzergue, S., Colot, V., Bowler, C., Barneche, F., 2012. Histone H2B Monoubiquitination Facilitates the Rapid Modulation of Gene Expression during Arabidopsis Photomorphogenesis. PLoS Genetics 8, e1002825. https://doi.org/10.1371/journal.pgen.1002825

Bowler, C., Benvenuto, G., Laflamme, P., Molino, D., Probst, A.V., Tariq, M., Paszkowski, J., 2004. Chromatin techniques for plant cells. The Plant Journal 39, 776–789. https://doi.org/10.1111/j.1365-313X.2004.02169.x

Casal, J.J., 2013. Photoreceptor Signaling Networks in Plant Responses to Shade. Annual Review of Plant Biology 64, 403–427. https://doi.org/10.1146/annurev-arplant-050312-120221

Chen, M., Chory, J., Fankhauser, C., 2004. Light Signal Transduction in Higher Plants. Annual Review of Genetics 38, 87–117. https://doi.org/10.1146/annurev.genet.38.072902.092259

Chen, Z., Zhang, H., Jablonowski, D., Zhou, X., Ren, X., Hong, X., Schaffrath, R., Zhu, J.-K., Gong, Z., 2006. Mutations in ABO1/ELO2, a Subunit of Holo-Elongator, Increase Abscisic Acid Sensitivity and Drought Tolerance in Arabidopsis thaliana. Molecular and Cellular Biology 26, 6902–6912. https://doi.org/10.1128/MCB.00433-06

Cloix, C., Jenkins, G.I., 2008. Interaction of the Arabidopsis UV-B-Specific Signaling Component UVR8 with Chromatin. Molecular Plant 1, 118–128. https://doi.org/10.1093/mp/ssm012

Czechowski, T., Stitt, M., Altmann, T., Udvardi, M.K., Scheible, W.-R., 2005. Genome-Wide Identification and Testing of Superior Reference Genes for Transcript Normalization in Arabidopsis. PLANT PHYSIOLOGY 139, 5–17. https://doi.org/10.1104/pp.105.063743

DeFraia, C.T., Wang, Y., Yao, J., Mou, Z., 2013. Elongator subunit 3 positively regulates plant immunity through its histone acetyltransferase and radical S-adenosylmethionine domains. BMC plant biology 13, 102. https://doi.org/10.1186/1471-2229-13-102

DeFraia, C.T., Zhang, X., Mou, Z., 2010. Elongator subunit 2 is an accelerator of immune responses in Arabidopsis thaliana: Function of AtELP2 in plant immunity. The Plant Journal 64, 511–523. https://doi.org/10.1111/j.1365-313X.2010.04345.x

Desnos, T., Orboic, V., Bellini, C., Kronenberger, J., Caboche, M., Traas, J., Höfte, H., 1996. Procuste1 mutants identify two distinct genetic pathways controlling hypocotyl cell elongation, respectively in dark- and light-grown Arabidopsis seedlings. Development 122, 683–693. https://doi.org/PubMed 8625819

Ding, Y., Mou, Z., 2015. Elongator and its epigenetic role in plant development and responses to abiotic and biotic stresses. Frontiers in plant science 6. https://doi.org/10.3389/fpls.2015.00296

Faik, A., Jiang, N., Held, M.A., 2014. Xylan Biosynthesis in Plants, Simply Complex, in: McCann, M.C., Buckeridge, M.S., Carpita, N.C. (Eds.), Plants and BioEnergy. Springer New York, New York, NY, pp. 153–181. https://doi.org/10.1007/978-1-4614-9329-7_10

Fang, X., Cui, Y., Li, Y., Qi, Y., 2015. Transcription and processing of primary microRNAs are coupled by Elongator complex in Arabidopsis. Nature Plants 1, 15075. https://doi.org/10.1038/nplants.2015.75

Ferrari, S., Galletti, R., Denoux, C., De Lorenzo, G., Ausubel, F.M., Dewdney, J., 2007. Resistance to Botrytis cinerea Induced in Arabidopsis by Elicitors Is Independent of Salicylic Acid, Ethylene, or Jasmonate Signaling But Requires PHYTOALEXIN DEFICIENT3. PLANT PHYSIOLOGY 144, 367–379. https://doi.org/10.1104/pp.107.095596

Gangappa, S.N., Holm, M., Botto, J.F., 2013. Molecular interactions of BBX24 and BBX25 with HYH, HY5 HOMOLOG, to modulate *Arabidopsis* seedling development. Plant Signaling & Behavior 8, e25208. https://doi.org/10.4161/psb.25208

Gendreau, E., Traas, J., Desnos, T., Grandjean, O., Caboche, M., Hofte, H., 1997. Cellular basis of hypocotyl growth in Arabidopsis thaliana. Plant physiology 114, 295–305. https://doi.org/10.1104/pp.114.1.295

Glatt, S., Müller, C.W., 2013. Structural insights into Elongator function. Current Opinion in Structural Biology 23, 235–242. https://doi.org/10.1016/j.sbi.2013.02.009

Hématy, K., Sado, P.-E., Van Tuinen, A., Rochange, S., Desnos, T., Balzergue, S., Pelletier, S., Renou, J.-P., Höfte, H., 2007. A Receptor-like Kinase Mediates the Response of Arabidopsis Cells to the Inhibition of Cellulose Synthesis. Current Biology 17, 922–931. https://doi.org/10.1016/j.cub.2007.05.018

Hemmes, H., Henriques, R., Jang, I.-C., Kim, S., Chua, N.-H., 2012. Circadian Clock Regulates Dynamic Chromatin Modifications Associated with Arabidopsis CCA1/LHY and TOC1 Transcriptional Rhythms. Plant and Cell Physiology 53, 2016–2029. https://doi.org/10.1093/pcp/pcs148

Henry, E., Fung, N., Liu, J., Drakakaki, G., Coaker, G., 2015. Beyond glycolysis: GAPDHs are multi-functional enzymes involved in regulation of ROS, autophagy, and plant immune responses. PLoS genetics 11, e1005199.

Hernandez-Blanco, C., Feng, D.X., Hu, J., Sanchez-Vallet, A., Deslandes, L., Llorente, F., Berrocal-Lobo, M., Keller, H., Barlet, X., Sanchez-Rodriguez, C., Anderson, L.K., Somerville, S., Marco, Y., Molina, A., 2007. Impairment of Cellulose Synthases Required for Arabidopsis Secondary Cell Wall Formation Enhances Disease Resistance. THE PLANT CELL ONLINE 19, 890–903. https://doi.org/10.1105/tpc.106.048058

Himanen, K., Woloszynska, M., Boccardi, T.M., De Groeve, S., Nelissen, H., Bruno, L., Vuylsteke, M., Van Lijsebettens, M., 2012. Histone H2B monoubiquitination is required to reach maximal transcript levels of circadian clock genes in Arabidopsis: *HUB1 regulates transcript levels*. The Plant Journal 72, 249–260. https://doi.org/10.1111/j.1365-313X.2012.05071.x

Holm, M., Ma, L.-G., Qu, L.-J., Deng, X.-W., 2002. Two interacting bZIP proteins are direct targets of COP1-mediated control of light-dependent gene expression in Arabidopsis. Genes & Development 16, 1247–1259.

Hussey, S.G., Mizrachi, E., Creux, N.M., Myburg, A.A., 2013. Navigating the transcriptional roadmap regulating plant secondary cell wall deposition. Frontiers in Plant Science 4. https://doi.org/10.3389/fpls.2013.00325

Jarillo, J.A., Capel, J., Tang, R.-H., Hong-Quan, Y., others, 2001. An Arabidopsis circadian clock component interacts with both CRY1 and phyB. Nature 410, 487. https://doi.org/10.1038/35068589

Jia, Y., Tian, H., Li, H., Yu, Q., Wang, L., Friml, J., Ding, Z., 2015. The *Arabidopsis thaliana* elongator complex subunit 2 epigenetically affects root development. Journal of Experimental Botany 66, 4631–4642. https://doi.org/10.1093/jxb/erv230

Jiao, Y., 2003. A Genome-Wide Analysis of Blue-Light Regulation of Arabidopsis Transcription Factor Gene Expression during Seedling Development. PLANT PHYSIOLOGY 133, 1480–1493. https://doi.org/10.1104/pp.103.029439

Jiao, Y., Lau, O.S., Deng, X.W., 2007. Light-regulated transcriptional networks in higher plants. Nature Reviews Genetics 8, 217–230. https://doi.org/10.1038/nrg2049

Kang, C.-Y., Lian, H.-L., Wang, F.-F., Huang, J.-R., Yang, H.-Q., 2009. Cryptochromes, Phytochromes, and COP1 Regulate Light-Controlled Stomatal Development in Arabidopsis. THE PLANT CELL ONLINE 21, 2624–2641. https://doi.org/10.1105/tpc.109.069765

Kidokoro, S., Maruyama, K., Nakashima, K., Imura, Y., Narusaka, Y., Shinwari, Z.K., Osakabe, Y., Fujita, Y., Mizoi, J., Shinozaki, K., Yamaguchi-Shinozaki, K., 2009. The Phytochrome-Interacting Factor PIF7 Negatively Regulates DREB1 Expression under Circadian Control in Arabidopsis. PLANT PHYSIOLOGY 151, 2046–2057. https://doi.org/10.1104/pp.109.147033

Kim, W.-Y., Fujiwara, S., Suh, S.-S., Kim, J., Kim, Y., Han, L., David, K., Putterill, J., Nam, H.G., Somers, D.E., 2007. ZEITLUPE is a circadian photoreceptor stabilized by GIGANTEA in blue light. Nature 449, 356–360. https://doi.org/10.1038/nature06132

Kwon, S.I., Kim, S.H., Bhattacharjee, S., Noh, J.-J., Gassmann, W., 2009. *SRFR1* , a suppressor of effector-triggered immunity, encodes a conserved tetratricopeptide repeat protein with similarity to transcriptional repressors. The Plant Journal 57, 109–119. https://doi.org/10.1111/j.1365-313X.2008.03669.x

Lally, D., Ingmire, P., Tong, H.-Y., He, Z.-H., 2001. Antisense expression of a cell wall–associated protein kinase, WAK4, inhibits cell elongation and alters morphology. The Plant Cell 13, 1317–1332.

Leivar, P., Monte, E., Al-Sady, B., Carle, C., Storer, A., Alonso, J.M., Ecker, J.R., Quail, P.H., 2008. The Arabidopsis Phytochrome-Interacting Factor PIF7, Together with PIF3 and PIF4, Regulates Responses to Prolonged Red Light by Modulating phyB Levels. THE PLANT CELL ONLINE 20, 337–352. https://doi.org/10.1105/tpc.107.052142

Leivar, P., Monte, E., Oka, Y., Liu, T., Carle, C., Castillon, A., Huq, E., Quail, P.H., 2008. Multiple Phytochrome-Interacting bHLH Transcription Factors Repress Premature Seedling Photomorphogenesis in Darkness. Current Biology 18, 1815–1823. https://doi.org/10.1016/j.cub.2008.10.058

Leivar, P., Tepperman, J.M., Cohn, M.M., Monte, E., Al-Sady, B., Erickson, E., Quail, P.H., 2012. Dynamic Antagonism between Phytochromes and PIF Family Basic Helix-Loop-Helix Factors Induces Selective Reciprocal Responses to Light and Shade in a Rapidly Responsive Transcriptional Network in *Arabidopsis*. The Plant Cell 24, 1398–1419. https://doi.org/10.1105/tpc.112.095711

Li, Q.-F., He, J.-X., 2016. BZR1 Interacts with HY5 to Mediate Brassinosteroid- and Light-Regulated Cotyledon Opening in Arabidopsis in Darkness. Molecular Plant 9, 113–125. https://doi.org/10.1016/j.molp.2015.08.014

Lin, C., 2002. Blue light receptors and signal transduction. The Plant Cell 14, S207–S225. https://doi.org/10.1105/tpc.000646

Louis, J., Gobbato, E., Mondal, H.A., Feys, B.J., Parker, J.E., Shah, J., 2012. Discrimination of Arabidopsis PAD4 Activities in Defense against Green Peach Aphid and Pathogens. PLANT PHYSIOLOGY 158, 1860–1872. https://doi.org/10.1104/pp.112.193417

Lozano-Durán, R., Macho, A.P., Boutrot, F., Segonzac, C., Somssich, I.E., Zipfel, C., 2013. The transcriptional regulator BZR1 mediates trade-off between plant innate immunity and growth. Elife 2, e00983. https://doi.org/10.7554/eLife.00983.001

Malapeira, J., Khaitova, L.C., Mas, P., 2012. Ordered changes in histone modifications at the core of the Arabidopsis circadian clock. Proceedings of the National Academy of Sciences 109, 21540–21545. https://doi.org/10.1073/pnas.1217022110

McCarthy, R.L., Zhong, R., Fowler, S., Lyskowski, D., Piyasena, H., Carleton, K., Spicer, C., Ye, Z.-H., 2010. The Poplar MYB Transcription Factors, PtrMYB3 and PtrMYB20, are Involved in the Regulation of Secondary Wall Biosynthesis. Plant and Cell Physiology 51, 1084–1090. https://doi.org/10.1093/pcp/pcq064

Miedes, E., Vanholme, R., Boerjan, W., Molina, A., 2014. The role of the secondary cell wall in plant resistance to pathogens. Frontiers in Plant Science 5. https://doi.org/10.3389/fpls.2014.00358

Nelissen, H., De Groeve, S., Fleury, D., Neyt, P., Bruno, L., Bitonti, M.B., Vandenbussche, F., Van Der Straeten, D., Yamaguchi, T., Tsukaya, H., Witters, E., De Jaeger, G., Houben, A., Van Lijsebettens, M., 2010. Plant Elongator regulates auxin-related genes during RNA polymerase II transcription elongation. Proceedings of the National Academy of Sciences 107, 1678–1683. https://doi.org/10.1073/pnas.0913559107

Nelissen, H., Fleury, D., Bruno, L., Robles, P., De Veylder, L., Traas, J., Micol, J.L., Van Montagu, M., Inzé, D., Van Lijsebettens, M., 2005. The elongata mutants identify a functional Elongator complex in plants with a role in cell proliferation during organ growth. Proceedings of the National Academy of Sciences of the United States of America 102, 7754–7759. https://doi.org/10.1073/pnas.0502600102

Ni, Z., Kim, E.-D., Ha, M., Lackey, E., Liu, J., Zhang, Y., Sun, Q., Chen, Z.J., 2009. Altered circadian rhythms regulate growth vigour in hybrids and allopolyploids. Nature 457, 327–331. https://doi.org/10.1038/nature07523

Nixdorf, M., Hoecker, U., 2010. SPA1 and DET1 act together to control photomorphogenesis throughout plant development. Planta 231, 825–833. https://doi.org/10.1007/s00425-009-1088-y

Nozue, K., Covington, M.F., Duek, P.D., Lorrain, S., Fankhauser, C., Harmer, S.L., Maloof, J.N., 2007. Rhythmic growth explained by coincidence between internal and external cues. Nature 448, 358–361. https://doi.org/10.1038/nature05946

Oh, E., Zhu, J.-Y., Bai, M.-Y., Arenhart, R.A., Sun, Y., Wang, Z.-Y., 2014. Cell elongation is regulated through a central circuit of interacting transcription factors in the Arabidopsis hypocotyl. Elife 3, e03031. https://doi.org/10.7554/eLife.03031.001

Otero, G., Fellows, J., Li, Y., de Bizemont, T., Dirac, A.M., Gustafsson, C.M., Erdjument-Bromage, H., Tempst, P., Svejstrup, J.Q., 1999. Elongator, a multisubunit component of a novel RNA polymerase II holoenzyme for transcriptional elongation. Molecular cell 3, 109–118. https://doi.org/10.1016/S1097-2765(00)80179-3 show

Oyama, T., Shimura, Y., Okada, K., 1997. The Arabidopsis HY5 gene encodes a bZIP protein that regulates stimulus-induced development of root and hypocotyl. Genes & Development 11, 2983–2995. https://doi.org/PMC316701

Portolés, S., Más, P., 2007. Altered oscillator function affects clock resonance and is responsible for the reduced day-length sensitivity of CKB4 overexpressing plants: CKB4 and clock resonance with the environment. The Plant Journal 51, 966–977. https://doi.org/10.1111/j.1365-313X.2007.03186.x

Prince, D.C., Drurey, C., Zipfel, C., Hogenhout, S.A., 2014. The Leucine-Rich Repeat Receptor-Like Kinase BRASSINOSTEROID INSENSITIVE1-ASSOCIATED KINASE1 and the Cytochrome P450 PHYTOALEXIN DEFICIENT3 Contribute to Innate Immunity to Aphids in Arabidopsis. PLANT PHYSIOLOGY 164, 2207–2219. https://doi.org/10.1104/pp.114.235598

Ramirez, V., Agorio, A., Coego, A., Garcia-Andrade, J., Hernandez, M.J., Balaguer, B., Ouwerkerk, P.B.F., Zarra, I., Vera, P., 2011. MYB46 Modulates Disease Susceptibility to Botrytis cinerea in Arabidopsis. PLANT PHYSIOLOGY 155, 1920–1935. https://doi.org/10.1104/pp.110.171843

Rojas, C.M., Senthil-Kumar, M., Tzin, V., Mysore, K.S., 2014. Regulation of primary plant metabolism during plant-pathogen interactions and its contribution to plant defense. Frontiers in Plant Science 5. https://doi.org/10.3389/fpls.2014.00017

Salome, P.A., McClung, C.R., 2005. PSEUDO-RESPONSE REGULATOR 7 and 9 Are Partially Redundant Genes Essential for the Temperature Responsiveness of the Arabidopsis Circadian Clock. THE PLANT CELL ONLINE 17, 791–803. https://doi.org/10.1105/tpc.104.029504

Sibout, R., Sukumar, P., Hettiarachchi, C., Holm, M., Muday, G.K., Hardtke, C.S., 2006. Opposite Root Growth Phenotypes of hy5 versus hy5 hyh Mutants Correlate with Increased Constitutive Auxin Signaling. PLoS Genetics 2, e202. https://doi.org/10.1371/journal.pgen.0020202

Skylar, A., Matsuwaka, S., Wu, X., 2013. ELONGATA3 is required for shoot meristem cell cycle progression in Arabidopsis thaliana seedlings. Developmental Biology 382, 436–445. https://doi.org/10.1016/j.ydbio.2013.08.008

Srivastava, A.K., Senapati, D., Srivastava, A.K., Chakraborty, M., Gangappa, S.N., Chattopadhyay, S., 2015. SHW1 Interacts with HY5 and COP1, and Promotes COP1-mediated Degradation of HY5 During Arabidopsis Seedling Development. Plant Physiology pp.01184.2015. https://doi.org/10.1104/pp.15.01184

Sun, J., Qi, L., Li, Y., Chu, J., Li, C., 2012. PIF4–Mediated Activation of YUCCA8 Expression Integrates Temperature into the Auxin Pathway in Regulating Arabidopsis Hypocotyl Growth. PLoS Genetics 8, e1002594. https://doi.org/10.1371/journal.pgen.1002594

Tian, Q., 2002. Arabidopsis SHY2/IAA3 Inhibits Auxin-Regulated Gene Expression. THE PLANT CELL ONLINE 14, 301–319. https://doi.org/10.1105/tpc.010283

Van Lijsebettens, M., Grasser, K.D., 2014. Transcript elongation factors: shaping transcriptomes after transcript initiation. Trends in Plant Science 19, 717–726. https://doi.org/10.1016/j.tplants.2014.07.002

Wade, H.K., Bibikova, T.N., Valentine, W.J., Jenkins, G.I., 2001. Interactions within a network of phytochrome, cryptochrome and UV-B phototransduction pathways regulate chalcone synthase gene expression in Arabidopsis leaf tissue. The Plant Journal 25, 675–685. https://doi.org/10.1046/j.1365-313x.2001.01001.x

Wang, C., Ding, Y., Yao, J., Zhang, Y., Sun, Y., Colee, J., Mou, Z., 2015. Arabidopsis Elongator subunit 2 positively contributes to resistance to the necrotrophic fungal pathogens *Botrytis cinerea* and *Alternaria brassicicola*. The Plant Journal 83, 1019–1033. https://doi.org/10.1111/tpj.12946

Wang, Y., An, C., Zhang, X., Yao, J., Zhang, Y., Sun, Y., Yu, F., Amador, D.M., Mou, Z., 2013. The Arabidopsis Elongator Complex Subunit2 Epigenetically Regulates Plant Immune Responses. The Plant Cell 25, 762–776. https://doi.org/10.1105/tpc.113.109116

Wang, Z.-Y., Nakano, T., Gendron, J., He, J., Chen, M., Vafeados, D., Yang, Y., Fujioka, S., Yoshida, S., Asami, T., others, 2002. Nuclear-localized BZR1 mediates brassinosteroid-induced growth and feedback suppression of brassinosteroid biosynthesis. Developmental cell 2, 505–513. https://doi.org/10.1016/S1534-5807(02)00153-3 show

Woloszynska, M., Le Gall, S., Van Lijsebettens, M., 2016. Plant Elongator-mediated transcriptional control in a chromatin and epigenetic context. Biochimica et Biophysica Acta (BBA) - Gene Regulatory Mechanisms 1859, 1025–1033. https://doi.org/10.1016/j.bbagrm.2016.06.008

Xin, X.-F., Nomura, K., Underwood, W., He, S.Y., 2013. Induction and Suppression of PEN3 Focal Accumulation During *Pseudomonas syringae* pv. *tomato* DC3000 Infection of *Arabidopsis*. Molecular Plant-Microbe Interactions 26, 861–867. https://doi.org/10.1094/MPMI-11-12-0262-R

Xu, X., Paik, I., Zhu, L., Bu, Q., Huang, X., Deng, X.W., Huq, E., 2014. PHYTOCHROME INTERACTING FACTOR1 Enhances the E3 Ligase Activity of CONSTITUTIVE PHOTOMORPHOGENIC1 to Synergistically Repress Photomorphogenesis in Arabidopsis. The Plant Cell 26, 1992–2006. https://doi.org/10.1105/tpc.114.125591

Yamashino, T., Matsushika, A., Fujimori, T., Sato, S., Kato, T., Tabata, S., Mizuno, T., 2003. A link between circadian-controlled bHLH factors and the APRR1/TOC1 quintet in Arabidopsis thaliana. Plant and Cell Physiology 44, 619–629. https://doi.org/10.1093/pcp/pcg078

Zeiger, E., 2000. Sensory transduction of blue light in guard cells. Trends in Plant Science 5, 183–185. https://doi.org/10.1016/S1360-1385(00)01602-2

Zhang, H., He, H., Wang, X., Wang, X., Yang, X., Li, L., Deng, X.W., 2011. Genome-wide mapping of the HY5-mediated genenetworks in Arabidopsis that involve both transcriptional and post-transcriptional regulation: Regulation of HY5-mediated gene networks. The Plant Journal 65, 346–358. https://doi.org/10.1111/j.1365-313X.2010.04426.x

Zheng, Y., Cui, X., Su, L., Fang, S., Chu, J., Gong, Q., Yang, J., Zhu, Z., 2017. Jasmonate inhibits COP1 activity to suppress hypocotyl elongation and promote cotyledon opening in etiolated Arabidopsis seedlings. The Plant Journal 90, 1144–1155. https://doi.org/10.1111/tpj.13539

Zhou, X., Hua, D., Chen, Z., Zhou, Z., Gong, Z., 2009. Elongator mediates ABA responses, oxidative stress resistance and anthocyanin biosynthesis in Arabidopsis. The Plant Journal 60, 79–90. https://doi.org/10.1111/j.1365-313X.2009.03931.x

7 Supplemental figures and tables
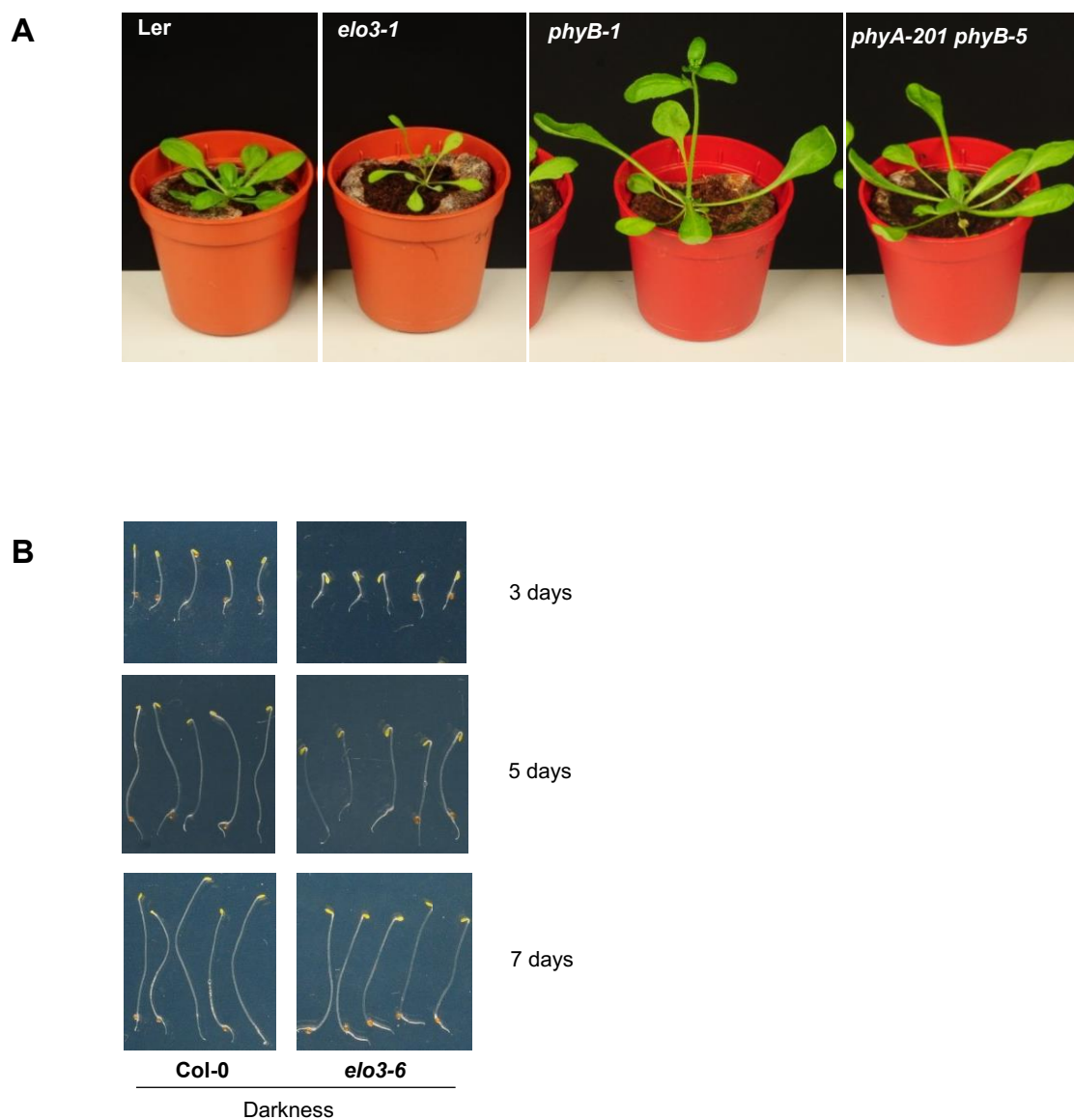
Figure S1 Phenotype of *elo3-6* seedlings grown in long day photoperiod or in darkness. (A) Morphology of *elo3-1*, *phyB-1* and *phyA-201phyB-5* mutant seedlings grown for three weeks in long-day photoperiod (16-h light/8-h darkness). (B) Col-0 and *elo3-6* seedlings grown for 3, 5 or 7 days on half-strength MS medium in darkness.
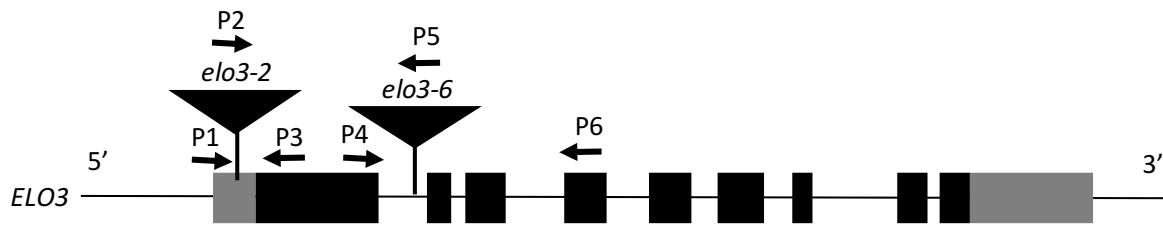
Primer name	Primer sequence
P1	TACTCCTTCTCCACAATAGTTGGAGAGGACT
P2	GACTGAATGCCCACAGGCCGTCGAG
P3	AATAGCTCGCATGCTGGTAGGCT
P4	ACCGTAAATCAGCATTTGTCG
P5	ATATTGACCATCATACTCATTGC
P6	TGGGGTTTAGGTAGTTTTGGG
LUC-forward	GCGTCGACCATGGAAGACGCCAAAAAC
LUC-reverse	ACGGATCCTTACACGGCGATCTTTCCG

Figure S2 Genotyping of *elo3-6*, *elo3-2* and Luciferase reporter lines. Scheme of the *ELO3* gene with primer position and list of the primer used. P1+P3 for wild type *elo3-2*, P2+P3 for *elo3-2*, P4+P5 for *elo3-6*, P4+P6 for wild type *elo3-6*. LUC-forward and LUC-reverse are complementary to the *LUC* gene in *pCCA1::LUC* and *pTOC1::LUC*.

Table S1: PLAZA enrichment of Biological Process Gene Ontology (GO) categories identified within genes upregulated in the *elo3-6* mutant in darkness as compared to the wild-type

GO category description	Log2-enrichment	*P* value
Response to stimulus	0.77	2.03E-52
Defense response	0.77	2.46E-7
Response to chemical stimulus	0.89	7.72E-41
Response to stress	0.88	1.47E-38
Response to abiotic stimulus	0.98	2.31E-32
Response to organic substance	0.73	4.08E-15
Response to endogenous stimulus	0.68	3.12E-8
Response to inorganic substance	1.37	4.68E-27
Response to osmotic stress	1.38	5.79E-29
Response to salt stress	1.41	7.71E-29
Response to biotic stimulus	0.74	1.47E-7
Response to hormone stimulus	0.58	1.44E-4
Response to metal ion	1.45	6.42E-27
Response to other organism	0.73	4.73E-7
Response to cadmium ion	1.48	8.34E-22
Response to cold	1.26	6.25E-14
Response to light stimulus	0.86	2.87E-7
Response to radiation	0.84	5.85E-7
Response to temperature stimulus	1.07	6.15E-12
Response to carbohydrate stimulus	0.96	1.44E-4
Response to external stimulus	0.72	0.01
Response to oxidative stress	1.23	2.37E-9
Response to water	0.83	0.01
Response to water deprivation	0.82	0.02
Response to chitin	0.90	0.05
Response to UV	1.28	8.19E-5
Response to UV-B	1.35	1.40E-4
Response to zinc ion	1.95	5.52E-12
Response to desiccation	2.11	0.01

Response to herbivore	1.96	0.02
Metabolic process	0.38	8.06E-33
Primary metabolic process	0.29	2.47E-13
Cellular metabolic process	0.27	1.78E-10
Biosynthetic process	0.41	5.63E-13
Cellular biosynthetic process	0.40	9.71E-12
Nitrogen compound metabolic process	0.36	4.02E-6
Anatomical structure development	0.59	6.56E-10
Small molecule metabolic process	0.99	3.77E-28
Carbohydrate metabolic process	1.08	1.17E-22
Oxidation reduction	0.97	1.29E-15
Carboxylic acid metabolic process	1.06	1.73E-15
Catabolic process	0.61	1.37E-4
Organic acid metabolic process	1.06	2.12E-15
Oxoacid metabolic process	1.06	1.73E-15
Small molecule biosynthetic process	1.21	3.61E-20
Cellular ketone metabolic process	1.04	6.37E-15
Lipid metabolic process	0.93	4.00E-10
Cellular carbohydrate metabolic process	1.17	1.62E-14
Cellular catabolic process	0.61	3.23E-4
Amine metabolic process	1.01	2.22E-10
Secondary metabolic process	1.33	1.04E-17
Cellular amino acid and derivative metabolic process	0.97	4.53E-9
Cellular nitrogen compound metabolic process	0.84	2.19E-6
Carboxylic acid biosynthetic process	1.17	2.70E-9
Heterocycle metabolic process	0.99	1.39E-6
Monocarboxylic acid metabolic process	1.19	5.49E-10
Organic acid biosynthetic process	1.17	2.70E-9
Polysaccharide metabolic process	1.35	4.66E-12
Cellular aromatic compound metabolic process	1.18	1.01E-9
Cellular lipid metabolic process	0.85	1.60E-4
Alcohol metabolic process	1.29	1.02E-8

Carbohydrate catabolic process	1.76	1.32E-17
Lipid biosynthetic process	0.80	0.02
Small molecule catabolic process	1.40	1.96E-8
Cellular amine metabolic process	0.81	0.01
Cellular amino acid derivative metabolic process	1.14	1.24E-6
Cellular carbohydrate catabolic process	1.79	1.48E-15
Cellular nitrogen compound biosynthetic process	1.00	1.63E-5
Amine biosynthetic process	1.16	0.0020
Aminoglycan metabolic process	1.43	1.75E-7
Aromatic compound biosynthetic process	1.21	8.49E-6
Carbohydrate biosynthetic process	0.86	0.03
Fatty acid metabolic process	1.05	0.01
Glucose metabolic process	1.78	2.83E-7
Glycoside metabolic process	1.25	0.0015
Hexose metabolic process	1.70	4.36E-9
Monosaccharide metabolic process	1.56	1.42E-8
Nucleoside phosphate metabolic process	1.03	0.01
Nucleotide metabolic process	1.03	0.01
Phenylpropanoid biosynthetic process	1.41	4.24E-5
Phenylpropanoid metabolic process	1.28	8.19E-5
Sulfur metabolic process	1.01	0.01
Chitin metabolic process	1.45	1.08E-7
Cellular amino acid derivative biosynthetic process	1.29	1.60E-6
Cellular nucleobase, nucleoside and nucleotide metabolic process	1.08	6.33E-4
Cellular polysaccharide metabolic process	1.32	2.13E-4
Alcohol catabolic process	1.70	2.38E-6
Diterpenoid metabolic process	2.24	0.0050
Gibberellin metabolic process	2.28	0.0034
Glucan catabolic process	2.87	5.65E-5
Glucan metabolic process	1.38	8.95E-4
Glucose catabolic process	1.82	9.08E-7
Glucosinolate catabolic process	1.93	0.0031

Glucosinolate metabolic process	1.34	0.02
Glutamine family amino acid biosynthetic process	2.48	5.77E-4
Glutamine family amino acid metabolic process	1.89	0.0011
Glycolysis	1.97	4.69E-6
Glycoside catabolic process	1.79	9.51E-4
Glycosinolate catabolic process	1.93	0.0031
Glycosinolate metabolic process	1.34	0.02
Hexose catabolic process	1.82	9.08E-7
Isoprenoid metabolic process	1.16	0.02
Monosaccharide catabolic process	1.77	2.36E-6
Nitrile biosynthetic process	2.03	0.01
Nitrile metabolic process	2.07	0.0038
Polysaccharide catabolic process	2.14	9.97E-6
Ribonucleotide biosynthetic process	1.28	0.02
Ribonucleotide metabolic process	1.21	0.04
S-glycoside catabolic process	1.93	0.0031
S-glycoside metabolic process	1.34	0.02
Starch metabolic process	2.07	0.0038
Sulfur compound catabolic process	1.80	0.01
Cellular glucan metabolic process	1.38	0.0013
Cellular polysaccharide catabolic process	2.79	1.16E-4
Oxidative phosphorylation	1.57	0.01
Cell wall organization or biogenesis	1.04	4.65E-4
Cell wall macromolecule metabolic process	1.28	6.54E-6
Cell wall chitin metabolic process	1.36	2.27E-5
Cell wall organization	1.36	2.27E-5
Cell wall polysaccharide metabolic process	1.26	1.21E-4
Cell wall modification	1.29	0.0047
Energy derivation by oxidation of organic compounds	1.25	0.02
Generation of precursor metabolites and energy	1.38	8.38E-13

Localization	0.41	0.0032
Establishment of localization	0.40	0.01
Lipid localization	1.40	5.76E-5
Transport	0.41	0.01
Ion transport	0.78	0.01
Lipid transport	1.52	8.54E-6
Transition metal ion transport	1.54	0.02

Table S2. Gene classes identified as overrepresented by PLAZA 2.5 software within genes downregulated in the *elo3-6* mutant in continuous darkness as compared to the wild type.

Gene class	AGI code	Gene	Log2FC		ChIP-qPCR[a]
Response to light stimulus					
Regulators of skoto- and photomorphogenesis	AT5G11260	*HY5*	-0.65	C	NT
	AT3G17609	*HYH*	-2.32	C	T
	AT1G02340	*HFR1*	-0.33	C	T
	AT2G26670	*HY1*	-0.65		
	AT2G46340	*SPA1*	-0.76	C	NT
	AT4G02440	*EID1*	-0.57	C	NT
	AT2G43010	*PIF4*	-0.71	C	NT
	AT2G31380	*STH/BBX25*	-1.07		
	AT1G06040	*BBX24*	-0.55		
Circadian clock	AT1G01060	*LHY*	-0.94	C	T
	AT2G46830	*CCA1*	-0.54	C	NT
	AT3G09600	*RVE8*	-0.57		
	AT5G37260	*CIR1*	-0.68		
	AT5G02840	*LCL1/RVE4*	-0.75		
	AT5G37260	*RVE2*	-0.68		
	AT4G00760	*PRR8*	-0.50		
Early light-induced protein	AT4G14690	*ELIP2*	-1.42	C	NT
Hormone response					
ABA receptor	AT5G53160	*RCAR3*	-0.74		
ABA response	AT1G03880	*CRU2*	-0.62		
	AT1G05470	*CVP2*	-0.99		
	AT1G18100	*MFT*	-0.52		
	AT1G66600	*ABO3/WRKY63*	-0.81		
	AT1G76180	*ERD14*	-0.71		
	AT2G26980	*CIPK3/SNRK3.17*	-0.55		
	AT2G40170	*ATEM6*	-1.43		
	AT3G02140	*AFP4/TMAC2*	-0.51		
	AT5G37770	*CML24/TCH2*	-0.63		

	AT5G50720	*HVA22E*	-0.52
	AT1G48000	*MYB112*	-0.56
	AT2G01430	*ATHB17*	-0.53
	AT5G25160	*ZPF3*	-0.50
	AT5G49620	*MYB78*	-0.69
	AT2G47770	*ATTSPO*	-0.51
Auxin biosynthesis	AT4G28720	*YUC8*	-0.68
Response to auxins	AT1G15580	*IAA5*	-0.54
	AT1G04100	*IAA10*	-0.66
	AT1G04550	*IAA12*	-0.67
	AT2G33310	*IAA13*	-0.77
	AT4G14550	*IAA14*	-0.65
	AT5G25890	*IAA28*	-0.69
	AT5G57420	*IAA33*	-0.72
	AT1G19220	*ARF19*	-0.70
	AT1G35240	*ARF20*	-1.32
	AT1G34390	*ARF22*	-0.74
	AT2G14960	*GH3.1*	-0.57
	AT3G50060	*MYB77*	-0.51
	AT4G03400	*DFL2*	-0.76
	AT5G12330	*LRP1*	-0.69
	AT4G34790	*SAUR3*	-0.72
	AT5G66260	*SAUR11*	-0.61
	AT2G21220	*SAUR12*	-1.02
	AT5G53590	*SAUR30*	-0.96
	AT2G45210	*SAUR36*	-1.04
	AT2G37030	*SAUR46*	-0.98
	AT4G34750	*SAUR49*	-0.66
	AT1G76190	*SAUR56*	-0.67
	AT3G60690	*SAUR59*	-0.71
	AT1G29430	*SAUR62*	-0.51

	AT1G29440	*SAUR63*	-0.62		
	AT1G29450	*SAUR64*	-0.68		
	AT1G29500	*SAUR66*	-0.78		
	AT1G29510	*SAUR67*	-0.63		
	AT1G17345	*SAUR77*	-0.58		
	AT1G72430	*SAUR78*	-0.85		
Brassinosteroid biosynthesis	AT5G05690	*CPD*	-0.69	C	NT
	AT3G50660	*DWF4*	-0.78	C	NT
	AT3G13730	*CYP90D1*	-0.80	C	NT
Brassinosteroid signalling and response	AT1G03445	*BSU1*	-1.05	C	NT
	AT2G01950	*VH1/BRL2*	-0.73	C	
	AT4G30270	*MERI5*	-0.88	C	
	AT5G54380	*THE1*	-0.54		
	AT5G57560	*TCH4/XTH22*	-0.68		
	AT2G43060	*IBH1*	-0.61		
Cytokinin receptors	AT5G35750	*AHK2*	-0.58		
	AT1G27320	*AHK3*	-0.58		
Cytokinin response	AT1G05850	*CTL1*	-1.04		
	AT1G13430	*ST4C*	-0.67		
	AT4G26150	*CGA1*	-3.24	C	NT
Ethylene biosynthesis	AT2G22810	*ACS4*	-0.75		
Ethylene signalling and response	AT1G13260	*EDF4*	-0.55		
	AT3G23230	*ERF98*	-0.85		
	AT5G07580	*ERF106*	-0.81		
	AT5G61600	*ERF104*	-0.65		
	AT5G51190	*ERF105*	-1.15		
	AT5G07310	*ERF115*	-1.35		

	AT5G61890	*EBE*	-0.86	
	AT5G61590	*DEWAX*	-0.55	
	AT5G18560	*PUCHI*	-1.41	
	AT5G47230	*ERF5*	-0.53	
Gibberellin response	AT1G74670	*GASA6*	-1.49	
	AT3G02885	*GASA5*	-1.49	
	AT5G17490	*RGL3*	-0.52	
	AT5G41030	*TCP6*	-0.79	C
	AT1G58100	*TCP8*	-0.59	C
	AT3G47620	*TCP14*	-0.51	C
	AT1G69690	*TCP15*	-0.62	C
	AT3G02150	*TCP13*	-0.57	
	AT2G31070	*TCP10*	-0.86	
	AT5G08070	*TCP17*	-0.8	
Cell wall biogenesis				
Primary cell wall biogenesis	AT5G64570	*XYL4*	-0.55	
	AT4G17030	*EXLB1*	-1.32	C
	AT5G56320	*EXPA14*	-1.08	C
Primary and secondary cell wall biogenesis	AT2G37090	*IRX9*	-1.57	C
	AT1G27440	*IRX10*	-1.11	C
	AT5G67230	*IRX14-L*	-0.54	
Secondary cell wall biogenesis structural genes	AT2G38080	*LAC4*	-1.19	C
	AT5G01190	*LAC10*	-1.70	C
	AT5G60020	*LAC17*	-1.04	C
	AT5G15630	*IRX6/COBL4*	-1.46	C
	AT5G15630	*IRX8*	-1.07	C
	AT3G55990	*ESK1/TBL29*	-0.96	
	AT2G28110	*FRA8*	-0.73	C
	AT3G18660	*GUX1*	-1.40	
	AT1G75500	*WAT1*	-0.91	

209

	AT4G14940	*AO1*	-1.11	C	
	AT5G01360	*TBL3*	-1.40	C	
	AT3G16920	*CTL2*	-1.43		
	AT5G57550	*XTH25*	-1.00	C	
	AT5G44030	*CESA4*	-1.29	C	NT
	AT5G17420	*CESA7*	-1.33	C	NT
	AT4G18780	*CESA8*	-1.35	C	NT
Xylem differentiation factors	AT1G52150	*ATHB15*	-0.87		
	AT5G60690	*REV*	-0.43	C	NT
	AT1G30490	*PHV*	-1.00	C	NT
Transcription factors regulating secondary cell wall biogenesis	AT1G68200	*ATC3H15/CDM1*	-1.68		
	AT1G66810	*ATC3H14*	-0.84		
	AT4G34610	*BLH6*	-1.15		
	AT4G12350	*MYB42*	-0.62		
	AT5G16600	*MYB43*	-1.16		
	AT5G12870	*MYB46*	-1.47	C	NT
	AT3G08500	*MYB83*	-1.04	C	NT
	AT4G22680	*MYB85*	-0.64		
	AT1G63910	*MYB103*	-1.95	C	NT
	AT1G17950	*MYB52*	-1.13	C	
	AT1G73410	*MYB54*	-1.42	C	
	AT4G29230	*NAC075*	-0.77		
	AT4G28500	*SND2*	-1.50	C	
	AT4G36160	*VND2*	-1.08	C	
	AT5G66300	*VND3*	-1.15	C	
	AT1G12260	*VND4*	-1.00	C	NT
	AT1G62700	*VND5*	-0.75		
	AT5G62380	*VND6*	-1.17	C	
	AT5G64530	*XND1*	-1.28		

[a] C, downregulation of the gene in elo3-6 in darkness was confirmed by the qPCR assay; T, target of Elongator HAT activity detected by the ChIP-qPCR assay as decreased

H3K14Ac level; NT, nontarget of Elongator HAT activity detected by the ChIP-qPCR assay as unchanged H3K14Ac level.

Table S3. Primer sets and sequences used for the ChIP-qPCR analysis.

Gene	Primer set	Forward primer sequence	Reverse primer sequence
ACT2	Reference	ACGAGCAGGAGATGGAAACC	TCCATTCCCACAAACGAGGG
BSU1	P1	GATTTTTCGGAAAGAAATCTAGTCA	TTTATCGACCGGACCGGAAT
	P2	CAACATGGAGCTGTATGTGGAA	TTGAGTTCTCACCAAGCCA
	P3	CTGTACGTTACCAGGGCGAG	TAGAAGTGCAGCAAGCGGAA
	P4	GAACATCGAGATGCCGCCT	TTCCGGTACACTTGTGCAGCTT
CCA1	P1	GAACAAGTTGATGTTAAGATGGAC	GGAGAAATCTCAGCCACTATAATTATC
	P2	ATCCTCGAAAGACGGGAAGT	GTCGATCTTCATTGGCCATC
	P3	AAGGCTCGATCTTCACTGGA	CCATCCTCTTGCCTTTCTGA
CESA4	P1	CTGAGCTGTCTCCTTCTTCCA	AGGTTGTACCAAACTGTGAGTG
	P2	AAGTCTGTGGCGATGAGGTC	CAAACCGGGTAAACGCACAC
	P3	ACACCAGCCAAAGACGCATA	CCAAGAGAGAGCGAACCAGA
	P4	TCCCGGGATGATTCAGGTCA	TGCTCCTTCTTTGCCGAGAT
	P5	ATCATCGACGGAGGCGATTT	ACGTCGACGCAATAAACACAG
	P6	TTATCTGATCGGTTGCACCAAG	TCCCCAAGCATACCACAAAGG
	P7	CTCCGGTGGAGTGGTGTAAG	GAGATGAGCTGAGACACCGC
	P8	GGATTGATCCGTTCTTGCCG	TGGCTCAAAATAGCGGTCCA
CESA7	P1	TGGCGCAGAGGAATTGTCAT	GCAAGCCAAGTTACGTTCCC
	P2	CAGGTTTAACCATTTTAATCGCTGT	TCTTCAGAGGCTTTGGCTGTT
	P3	TGTGGTAGGGAGTGAGGGAG	TGGCCCAAGATTTCCATGCT
	P4	TCTGACGACGGTGCTTCAAT	GAAGTACATCTCCGGTGCCC
	P5	TTCTGTCAGGTTCGAGTGGC	ACACATTGCTTCCCTCACGG
	P6	ATCAAGTCCTGCAGTGCTCC	CCTCAGTTCCCCACTCAGTC
	P7	ACCCATTCCTCAAAGGTCTGAT	AGGTCCTTTGGTCTTGAGCAC
	P8	GGATCTGGGTTTATTGTGAGCG	TTGTGGGTTTTCACTGCAACT

CESA8	P1	GCTAGTATCTGCCGCTGGTTA	TTGCGGGAAAGTGAAGGAAAGT
	P2	CGTTGCGGCAATCCTTACG	AGATGTCTTTGTCTCAACATCATCA
	P3	CGTTGATTTGGTCTCTGCCG	AGCCAAGATGATCAACCGCA
	P4	ACAACACTCGTGACCATCCC	GCGAGCACCGCTATATCCAA
	P5	TACGGGTCGATCACCGAAGA	CGTAGAACCTGGTGAAGCCT
	P6	CTTGATCCCTCCGACGTCAC	CCAAACAAAGGTCCCCAAGC
	P7	TCGATTGCTAAGAGAAGATACGTT	CCCGCCAAGACTTGTTGCTA
CGA1	P1	ACATTTGTTTCTGCTCGTGGTC	GCACAAAAGAGAGGGAAGACG
	P2	CCCTCTTCTTTGATGTCACCGT	ACCTCGAGAGGTTGGGAGATA
	P3	TGCGTGATTAGGATTTGCTCC	AATACCTTGGGACCTCTCGGA
	P4	AATGGCTCTATCGCACGGAA	ACTAGCTATGAGGGCTTATGGT
CPD	P1	CCTATGATTCATCAGTTCCTCCA	ATCGATCGGTTTGTTGATGACA
	P2	ATGCTCGCACTTTCAACCCT	TACCGAGTTGCTCTGTTCCAC
	P3	TACCCGATCTTCGTGAAGCG	CACTAGACCCACAAGGAGGC
CYP90D1	P1	TGGGCATGCATGTATCCTGTA	GGTATTTTGGGTGCGCCTTC
	P2	TGCAAAGGATGTTGTGGATGTG	AGGAATTTGACGGCAAGGGT
	P3	GTGGTCAGAGATTGTGCCCT	AAGCGAGTGACAAGATGGTGA
	P4	CACAATCATAAACTTCCCAACGGT	ACACTCGTGTGACTTCTTTAACCTT
DWF4	P1	AGCCTATACGCGCTCAAAGT	TCCCAATTCTGAATCGCACCA
	P2	TGCCGGACATGAGACTTCTTC	TCTTCAACGGCTTTAGGGCA
	P3	CGATGGTACCACGGCTTTGA	AACCAGTCAACGTGGCAGAA
	P4	CCTATTAGGGTTTCTCGTATTCTG	CCCTTTTCTCAAACCCGAACTA
EID1	P1	AGTTCAGTCCGTACGATGTCA	ACTGTTATGGGTCCGGTACG
	P2	TACTATTCCCGCTCCTCCTC	CTTCCTTCGTTTCCTTACCG
	P3	GAGCTTATGTTTGTGAGAATGGTC	TGAGACTTGAGACCGTGGAA
ELIP2	P1	GGGCCTATCATTTTCCTTCACC	AGATGGAGTTGGTTTGAGGTGT
	P2	GATCCTTCTGTGCCCTCGAC	CTGGTGGAGGAGGAGACTGT
	P3	CAATGGTTGGATTCGTGGCG	CCTAGAAACCACCCGACACC
	P4	TCATGACTTCAGACGCCGAG	CCAGTGACGTACTCGGTGAA
HFR1	P1	CGGTGTACGCAACAAACGAA	TCAGCTACATTGGTGACCCAC
	P2	CCTTCAGTTACTCGAAAAGGTTCC	GGTACGAGTTGCTGTAGCTT
	P3	GATGTCAACAGTGGGGGTGA	ATTTAGGCCGTGAGCCGAAG
	P4	TCCCATGCGATGAGAAGACTA	TGGTTCACACAAACTGTCCTA

HY5	P1	TGGGCCATGTGACAGAATGA	CGTGGGTGGATTTTAGCCGT
	P2	CAAGCAGCGAGAGGTCATCA	GAGATCACTCGTTGGGAGAAGA
	P3	ATAACGGTTGCGTGATGGGG	TCCAACTCGCTCAAGTAAGCC
	P4	GTAGATTCTGAAGAACACAACAGGA	CAAGAAGAAGAAGGAGATCAAAGGC
HYH	P1	AGGGGTCCCTTGAGTGATACA	GTGGCATATCGACCGACCAA
	P2	GTTGATGGTTCCTGACATGG	AAGCTCCGGATTGTTGACTC
	P3	CAATGACCAGCTCGAAGAGA	CACTGAACAATGGATTAAAGGG
LHY	P1	GCGTAAAAGTGAGGCCCATA	TGGTGGTCCACAATTGCTTA
	P2	CCGAAAAATTCGGGTCAGTA	GGCGGAATTTCTATGTCCAA
	P3	GCCATTGGCTCCTAATTTCA	TCGAAGCCTTTTGCAGACTT
MYB46	P1	ACACAACATTTGCTTACCTTGAA	TCTAATTCGTTAACCTTACGTGTG
	P2	TGTTGCGAAAAACGCAGGAC	CCTGTTGCCGAGGATGGAAT
	P3	TGTTTGTTTTAAGGACGAGTTTTCA	CGACCAAACTTTATCCTTCCACG
	P4	AAGGCTTCGTCAACCCTTCC	TGGCTGATCATGTTTCCCGT
	P5	AGCCTTGAGGTGCCATGTAA	TCAATCTTCTCCATTGCTACTTGA
MYB83	P1	CCGTGCTCCATCATTACTTGC	GCGCATGCAAAAATCAGCTT
	P2	GGATGTTGGAGTGACATCGC	GTAATTGATCCAGCGAAGGCG
	P3	GCGGCTTAAGAACAACAGCA	TGAAGTTGAGTTGCCTCCCAT
	P4	CCCCTCGGAGAATACCAACG	GCAAGGATCAAGGGCCTGTA
	P5	TGGAGGAACCAATCACCATGC	CACTGCTGTGTGGGCCATTA
MYB103	P1	GGGCTTCGGAAATTATTAGAAAGA	AGTACTTGATGGCCGCAAAC
	P2	TGAAGAGAGGGCTTTGGTCAC	ATCACCTGCTTTTTCAGGGACT
	P3	AGATACGAAAACCGCACCATC	CGATGTAGTGTCCGCATTCA
	P4	TACCGGCGCTAATAGAGGGA	TGTGGACGCCATTTCTCCAT
	P5	CATGTTGCAAGGCAATACGGT	TTTGCCATGGCCTGTACGTG
PIF4	P1	GACGTATAGCAAAAGACTTGAAGA	GTCAAATCACAATCATCTATAGCGT
	P2	GCAAGCTTTCCTAGATTGCCA	AAGCAAGTCCATGAGTCCGT
	P3	AGCCCTAAGATCCAGCACCT	GTCGGGTTCGAATGGGTCTT
	P4	TTTGCAGGCAATCGGTAACA	AACTTCAGCTGCTCGACTCC
	P5	GTGATGTGGATGGGGAGTGG	GGTTGAACTCCGGGGAACAT
	P6	ATTTAGTTCACCGGCGGGAC	AGTGGTCCAAACGAGAACCG
SPA1	P1	TCTTCGACTATACACAGAATACAA	TCCCAGATATCGAGAGAGATCACA
	P2	GTCCTAGGGCTGGCAAGTTT	CAAGATCCCCATCTCCTGCC

	P3	GCTATGCCATTGCGAGTCAG	TTGGTGGGAGAATCCGATGG
	P4	TGTTTTTCGAGGGGTTGTGC	ATCCCAGCTGCTGCTATGTG
	P5	AGTTTGTGTCGAGCGTCTGT	AAAGTCCAATGCCCGCAGTA
	P6	ATTGATTGCTTGGTGGCGTG	GTCTCTCGCGAAAGCAGAGG
VND4	P1	AATAATACAGTGACATGCCAACCT	AACGATATTGCTGGTTTGATGGTA
	P2	TCATTTTCCCACGTCCCTCC	TGGGATTGGGCAAACCTTGA
	P3	GGATGGGTTGTGTGTAGGGT	GAGAATCCGTCGTTGACCGT
	P4	ATACATGAACAGCGGCAACG	GCATTGCTTGTGTCCTTGGC

Table S3. Primer sequences and detection assays used for genotyping double or triple *Arabidopsis* mutants.

Mutant	Mutation	Detection	Forward primer sequence	Reverse primer sequence	Restriction enzyme	Product size (bp)	
						Wild type	Mutant
elo3-1	Point mutation	dCAPS	AGCTTTCCCTCCTATGTTTCTGTT	AGGGTGGGATATTTTTAACAGAT	*Bgl*II		238
elo3-6	T-DNA insertion	PCR	TGGGGTTTAGGTAGTTTTGGG	ACCGTAAATCAGCATTTGTCG		1182	
			TGGGGTTTAGGTAGTTTTGGG	ATATTGACCATCATACTCATTGC			589
phyA-201	Point mutation	dCAPS	GAAGTGTTGACTGCTTCCACGAGT	TAGCAAGATGCACAGAACGCC	*Hinf*I	212, 29	241
phyB1	Point mutation	PCR-RFLP	TATTGCGTCTTTAGCAATGGC	AAGCAACCACTCCACAACATC	*Alw*NI	247, 174	421
phyB5	Point mutation	PCR-RFLP	CGTGACGCGCCTGCTGGAATTGTT	TCCATTGATGCAGCCTCCGGCA	*Bsa*BI	666	375, 291
hfr1-101	Deletion	PCR	AATTTAGGATGAATCGGAGGAG	AGTTGCTGTAGCTTACGCATC		117	104
pif3-3	Deletion	PCR	TTTTCTTAAATCTACTTTTGACCCG	TTAGGCCAAGAAAAACTTGCC		2850	343
pif4-2	T-DNA insertion	PCR	ACCTCCTCAAGTCATGGTTAAGCCTAAGCC	TCCAAACGAGAACCGTCGGT		1400	
			TAGCATCTGAATTTCATAACCAATCTCGATACAC	TCCAAACGAGAACCGTCGGT			300

Table S4. Primer sequences used for qPCR.

Gene	Forward primer sequence	Reverse primer sequence
AO1	CCATCAGAGTTGGGGTGGAT	TTCTTCGCCACCAGTGTACC
BSU1	CAAAGCATGGATGCAGGAGC	ACACCTCTTCAACCGCACAA
CCA1	CCATGGAAGCCAAAGAAAGT	GGAAGCTTGAGTTTCCAACC
CESA4	CGACGTTGATGGAGAACGGA	TCCATCCAATCTCTTTGCCCC
CESA7	ATCAAGTCCTGCAGTGCTCC	ATCCAACCCAGCTCAGTTCC
CESA8	GGTCTCCCATCTGCAACACT	ACGCAAGCAAATTCTTCGACC
CGA1	CCAGAGCAACTCCACGATGT	TTCCGTGCGATAGAGCCATT
CPD	TTCAACCCTTGGAGATGGCAGAG	CTCGTAACCGGGACATAGCC
CYP90D1	GGAGATGGCAAGAAAGGGACA	ACGAGCCAAATCGAGACCAG
DWF4	GGCAACAGCAAAACAACGGA	GCTAGCTCTGAACCAGCACA
EID1	GTTTGTGCGATGAGACTTGG	TAAAGCAGTCCAAGCACCAG
ELIP1	GTTGGCGTTCACTGAGTTCG	TCCTCCCCATAACGTGCTCT
ELIP2	TCATGACTTCAGACGCCGAG	CCAGTGACGTACTCGGTGAA
EXLB1	AAGTCTGGCAGGAGGATTGC	GATTCCTGCGCTTCCGTAGA
EXPA14	AATACCGGAGAGTGGCTTGC	TGCCAACGTGTATTGGTTCCT
FRA8	ATAGCAAGCGTGTAAGGACGA	TTCTGACTGGTAACCGGCAA
HFR1	TCATCTCCGATATCTCTTTAACTAACA	TAGACGATCTTCATCACTTCTTGC
HY5	TCAGAACGAGAACCAGATGC	GAAGGAGATCAAAGGCTTGC
HYH	CAATGACCAGCTCGAAGAGA	CACTGAACAATGGATTAAAGGG
IRX10	TTGCCTCTCCGCCATTCTTC	ACATCACCAGCACTTCCTGA
IRX6	CACCATAACTCCTTGCCCGT	AGAATCAGCCTTGACGCAGC
IRX8	ATCATTGGCTTGACGAGAACTT	AATCAGCCCAGGAGGCAAAG
IRX9	GAAGGCACCAAACAGGATTCG	GCCGGAAGTCCCTTCAACTT
ISE2	ATCGACAAGTTTCAGAGATTGGCT	TCGGAGCAGAAACCACAACA
LAC10	CATACTCGGTGAGTGGTGGA	CGAAACCGGGATGACCGTTA
LAC17	TGGGAATTTCGACCCGAACA	TGCATGAACCACACTCCTGG
LAC4	TAATCCCGGGGTTTGGTTCA	ATTGGGTCCTTTGCCGTTCT
LHY	GAGACAGACAGGATTTAAGCCA	GAAGCTTCTCCTTCCAATCG
MERI5	GAATCATATTGACCGTCGATGACA	CTTGTTGCCCAATCGTCTGC
MYB103	GTCCCTGAAAAAGCAGGGCT	TCCCACAACTCCATGAAGGC

MYB46	GGCAACAGGTGGTCTCAGAT	TGTGTTGGGTGATGAGGATGA
MYB52	TTGGCAACCACAACCGCTAT	GTTTGGTCTATTGCTCCTTCTTGT
MYB54	TCGCTTTAAATCACAAAGCAAATCA	TGTCCGAGTCACTGCGTTTG
MYB83	TCCATTCTTGGTAACAGGTGGT	TGCTGTTGTTCTTAAGCCGC
PIF4	AGGGAAACAGAAATGGAACAG	AGCCACCTGATGAGGAACTT
PP2A	GTTCTCCACAACCGCTTGGT	AAGACAGTGAAGGTGCAACCTTACT
SAND	AACTCTATGCAGCATTTGATCCACT	TGATTGCATATCTTTATCGCCATC
SND2	TTTCACGAACAGGCTGGGAT	CCTTGCCTTCAAGATGCTCC
SPA1	TGGAGGTAGGGATTCGAAGA	CTGGATTACGTGCATCAACC
TBL3	AGCCAATGGGAATCGTTCGT	AGTCGCATTGTATTCCTTTGCT
TCP14	TCCTTCTCATTTCCGCTCCG	TAGGTGCACGTCCCTGTAGA
TCP15	ACAGCCTTTGGCTTCTGGTT	ATCTCCGTCACGGTTTTGCT
TCP6	AAGGCTGTCTCAAGTTGGGG	CTGCACTCTGCTGCTGATCT
TCP8	AATCTCGGGATGTTAGCCGC	ACCGCATTGTTCGCTTGTTC
VH1/BRL2	CAGAGGAAGGGAAACGTGCT	ATACAAACCGAAGCAGCGGA
VND2	ACAGATGAAGAGCTCGTTGGTT	CGATTCGGCAGCTCTCTTGT
VND3	ACCCATCCTTCTTCCTGTGG	CTCCACAGGAAGAAGGATGGG
VND4	CGTCCCTCCGGGTTTTAGATT	CACAACTCTTGAAGGTCCCAT
VND6	GCCATGGGACATCCAAGAGTT	GGTTCGTGTCCCAGTTGGAT
WAK1	TTCTTCTTGTAACCACCATCGG	AGCTTGGTGTCCTTCAGGTG
XTH25	CGATCCAACCGCTGATTTCC	TCATCAACCATGAAAACGATGTGA

Table S5. Primer sets and sequences used for the ChIP-qPCR analysis.

Gene	Primer set	Forward primer sequence	Reverse primer sequence
ACT2	Reference	ACGAGCAGGAGATGGAAACC	TCCATTCCCACAAACGAGGG
BSU1	P1	GATTTTTCGGAAAGAAATCTAGTCA	TTTATCGACCGGACCGGAAT
	P2	CAACATGGAGCTGTATGTGGAA	TTGAGTTCTCACCAAGCCA
	P3	CTGTACGTTACCAGGGCGAG	TAGAAGTGCAGCAAGCGGAA
	P4	GAACATCGAGATGCCGCCT	TTCCGGTACACTTGTGCAGCTT
CCA1	P1	GAACAAGTTGATGTTAAGATGGAC	GGAGAAATCTCAGCCACTATAATTATC
	P2	ATCCTCGAAAGACGGGAAGT	GTCGATCTTCATTGGCCATC
	P3	AAGGCTCGATCTTCACTGGA	CCATCCTCTTGCCTTTCTGA

CESA4	P1	CTGAGCTGTCTCCTTCTTCCA	AGGTTGTACCAAACTGTGAGTG
	P2	AAGTCTGTGGCGATGAGGTC	CAAACCGGGTAAACGCACAC
	P3	ACACCAGCCAAAGACGCATA	CCAAGAGAGAGCGAACCAGA
	P4	TCCCGGGATGATTCAGGTCA	TGCTCCTTCTTTGCCGAGAT
	P5	ATCATCGACGGAGGCGATTT	ACGTCGACGCAATAAACACAG
	P6	TTATCTGATCGGTTGCACCAAG	TCCCCAAGCATACCACAAAGG
	P7	CTCCGGTGGAGTGGTGTAAG	GAGATGAGCTGAGACACCGC
	P8	GGATTGATCCGTTCTTGCCG	TGGCTCAAAATAGCGGTCCA
CESA7	P1	TGGCGCAGAGGAATTGTCAT	GCAAGCCAAGTTACGTTCCC
	P2	CAGGTTTAACCATTTTAATCGCTGT	TCTTCAGAGGCTTTGGCTGTT
	P3	TGTGGTAGGGAGTGAGGGAG	TGGCCCAAGATTTCCATGCT
	P4	TCTGACGACGGTGCTTCAAT	GAAGTACATCTCCGGTGCCC
	P5	TTCTGTCAGGTTCGAGTGGC	ACACATTGCTTCCCTCACGG
	P6	ATCAAGTCCTGCAGTGCTCC	CCTCAGTTCCCCACTCAGTC
	P7	ACCCATTCCTCAAAGGTCTGAT	AGGTCCTTTGGTCTTGAGCAC
	P8	GGATCTGGGTTTATTGTGAGCG	TTGTGGGTTTTCACTGCAACT
CESA8	P1	GCTAGTATCTGCCGCTGGTTA	TTGCGGGAAAGTGAAGGAAAGT
	P2	CGTTGCGGCAATCCTTACG	AGATGTCTTTGTCTCAACATCATCA
	P3	CGTTGATTTGGTCTCTGCCG	AGCCAAGATGATCAACCGCA
	P4	ACAACACTCGTGACCATCCC	GCGAGCACCGCTATATCCAA
	P5	TACGGGTCGATCACCGAAGA	CGTAGAACCTGGTGAAGCCT
	P6	CTTGATCCCTCCGACGTCAC	CCAAACAAAGGTCCCCAAGC
	P7	TCGATTGCTAAGAGAAGATACGTT	CCCGCCAAGACTTGTTGCTA
CGA1	P1	ACATTTGTTTCTGCTCGTGGTC	GCACAAAAGAGAGGGAAGACG
	P2	CCCTCTTCTTTGATGTCACCGT	ACCTCGAGAGGTTGGGAGATA
	P3	TGCGTGATTAGGATTTGCTCC	AATACCTTGGGACCTCTCGGA
	P4	AATGGCTCTATCGCACGGAA	ACTAGCTATGAGGGCTTATGGT
CPD	P1	CCTATGATTCATCAGTTCCTCCA	ATCGATCGGTTTGTTGATGACA
	P2	ATGCTCGCACTTTCAACCCT	TACCGAGTTGCTCTGTTCCAC
	P3	TACCCGATCTTCGTGAAGCG	CACTAGACCCACAAGGAGGC
CYP90D1	P1	TGGGCATGCATGTATCCTGTA	GGTATTTTGGGTGCGCCTTC
	P2	TGCAAAGGATGTTGTGGATGTG	AGGAATTTGACGGCAAGGGT
	P3	GTGGTCAGAGATTGTGCCCT	AAGCGAGTGACAAGATGGTGA

		Forward	Reverse
	P4	CACAATCATAAACTTCCCAACGGT	ACACTCGTGTGACTTCTTTAACCTT
DWF4	P1	AGCCTATACGCGCTCAAAGT	TCCCAATTCTGAATCGCACCA
	P2	TGCCGGACATGAGACTTCTTC	TCTTCAACGGCTTTAGGGCA
	P3	CGATGGTACCACGGCTTTGA	AACCAGTCAACGTGGCAGAA
	P4	CCTATTAGGGTTTCTCGTATTCTG	CCCTTTTCTCAAACCCGAACTA
EID1	P1	AGTTCAGTCCGTACGATGTCA	ACTGTTATGGGTCCGGTACG
	P2	TACTATTCCCGCTCCTCCTC	CTTCCTTCGTTTCCTTACCG
	P3	GAGCTTATGTTTGTGAGAATGGTC	TGAGACTTGAGACCGTGGAA
ELIP2	P1	GGGCCTATCATTTTCCTTCACC	AGATGGAGTTGGTTTGAGGTGT
	P2	GATCCTTCTGTGCCCTCGAC	CTGGTGGAGGAGGAGACTGT
	P3	CAATGGTTGGATTCGTGGCG	CCTAGAAACCACCCGACACC
	P4	TCATGACTTCAGACGCCGAG	CCAGTGACGTACTCGGTGAA
HFR1	P1	CGGTGTACGCAACAAACGAA	TCAGCTACATTGGTGACCCAC
	P2	CCTTCAGTTACTCGAAAAGGTTCC	GGTACGAGTTGCTGTAGCTT
	P3	GATGTCAACAGTGGGGGTGA	ATTTAGGCCGTGAGCCGAAG
	P4	TCCCATGCGATGAGAAGACTA	TGGTTCACACAAACTGTCCTA
HY5	P1	TGGGCCATGTGACAGAATGA	CGTGGGTGGATTTTAGCCGT
	P2	CAAGCAGCGAGAGGTCATCA	GAGATCACTCGTTGGGAGAAGA
	P3	ATAACGGTTGCGTGATGGGG	TCCAACTCGCTCAAGTAAGCC
	P4	GTAGATTCTGAAGAACACAACAGGA	CAAGAAGAAGAAGGAGATCAAAGGC
HYH	P1	AGGGGTCCCTTGAGTGATACA	GTGGCATATCGACCGACCAA
	P2	GTTGATGGTTCCTGACATGG	AAGCTCCGGATTGTTGACTC
	P3	CAATGACCAGCTCGAAGAGA	CACTGAACAATGGATTAAAGGG
LHY	P1	GCGTAAAAGTGAGGCCCATA	TGGTGGTCCACAATTGCTTA
	P2	CCGAAAAATTCGGGTCAGTA	GGCGGAATTTCTATGTCCAA
	P3	GCCATTGGCTCCTAATTTCA	TCGAAGCCTTTTGCAGACTT
MYB46	P1	ACACAACATTTGCTTACCTTGAA	TCTAATTCGTTAACCTTACGTGTG
	P2	TGTTGCGAAAAACGCAGGAC	CCTGTTGCCGAGGATGGAAT
	P3	TGTTTGTTTTAAGGACGAGTTTTCA	CGACCAAACTTTATCCTTCCACG
	P4	AAGGCTTCGTCAACCCTTCC	TGGCTGATCATGTTTCCCGT
	P5	AGCCTTGAGGTGCCATGTAA	TCAATCTTCTCCATTGCTACTTGA
MYB83	P1	CCGTGCTCCATCATTACTTGC	GCGCATGCAAAAATCAGCTT
	P2	GGATGTTGGAGTGACATCGC	GTAATTGATCCAGCGAAGGCG

	P3	GCGGCTTAAGAACAACAGCA	TGAAGTTGAGTTGCCTCCCAT
	P4	CCCCTCGGAGAATACCAACG	GCAAGGATCAAGGGCCTGTA
	P5	TGGAGGAACCAATCACCATGC	CACTGCTGTGTGGGCCATTA
MYB103	P1	GGGCTTCGGAAATTATTAGAAAGA	AGTACTTGATGGCCGCAAAC
	P2	TGAAGAGAGGGCTTTGGTCAC	ATCACCTGCTTTTTCAGGGACT
	P3	AGATACGAAAACCGCACCATC	CGATGTAGTGTCCGCATTCA
	P4	TACCGGCGCTAATAGAGGGA	TGTGGACGCCATTTCTCCAT
	P5	CATGTTGCAAGGCAATACGGT	TTTGCCATGGCCTGTACGTG
PIF4	P1	GACGTATAGCAAAAGACTTGAAGA	GTCAAATCACAATCATCTATAGCGT
	P2	GCAAGCTTTCCTAGATTGCCA	AAGCAAGTCCATGAGTCCGT
	P3	AGCCCTAAGATCCAGCACCT	GTCGGGTTCGAATGGGTCTT
	P4	TTTGCAGGCAATCGGTAACA	AACTTCAGCTGCTCGACTCC
	P5	GTGATGTGGATGGGGAGTGG	GGTTGAACTCCGGGGAACAT
	P6	ATTTAGTTCACCGGCGGGAC	AGTGGTCCAAACGAGAACCG
SPA1	P1	TCTTCGACTATACACAGAATACAA	TCCCAGATATCGAGAGAGATCACA
	P2	GTCCTAGGGCTGGCAAGTTT	CAAGATCCCCATCTCCTGCC
	P3	GCTATGCCATTGCGAGTCAG	TTGGTGGGAGAATCCGATGG
	P4	TGTTTTTCGAGGGGTTGTGC	ATCCCAGCTGCTGCTATGTG
	P5	AGTTTGTGTCGAGCGTCTGT	AAAGTCCAATGCCCGCAGTA
	P6	ATTGATTGCTTGGTGGCGTG	GTCTCTCGCGAAAGCAGAGG
VND4	P1	AATAATACAGTGACATGCCAACCT	AACGATATTGCTGGTTTGATGGTA
	P2	TCATTTTCCCACGTCCCTCC	TGGGATTGGGCAAACCTTGA
	P3	GGATGGGTTGTGTGTAGGGT	GAGAATCCGTCGTTGACCGT
	P4	ATACATGAACAGCGGCAACG	GCATTGCTTGTGTCCTTGGC

Chapter 5   Glutaredoxin   GRXS17 associates with the cytosolic iron-sulfur cluster assembly pathway

Sabrina Iñigo[2], Astrid Nagels Durand[2], Andrés Ritter, Sabine Le Gall, Martin Termathe, Roland Klassen, Takayuki Tohge, Barbara De Coninck, Jelle Van Leene, Rebecca De Clercq, Bruno P.A. Cammue, Alisdair R. Fernie, Kris Gevaert, Geert De Jaeger, Sebastian A. Leidel, Raffael Schaffrath, Mieke Van Lijsebettens, Laurens Pauwels[3], and Alain Goossens[3,*]

[2,3] These authors contributed equally to the article.

Department of Plant Systems Biology, VIB, B-9052 Ghent, Belgium (S.I., A.N.D., A.R., S.L.G., B.D.C., J.V.L., R.D.C., B.P.A.C., G.D.J., M.V.L., L.P., A.G.); Department of Plant Biotechnology and Bioinformatics, Ghent University, B-9052 Ghent, Belgium (S.I., A.N.D., A.R., S.L.G., J.V.L., R.D.C., G.D.J., M.V.L., L.P., A.G.); Max Planck Research Group for RNA Biology, Max Planck Institute for Molecular Biomedicine, 48149 Muenster, Germany (M.T., S.A.L.); Cells-in-Motion Cluster of Excellence, University of Muenster, 48149 Muenster, Germany (M.T., S.A.L.); Faculty of Medicine, University of Muenster, 48149 Muenster, Germany (S.A.L.); Institut für Biologie, Fachgebiet Mikrobiologie, Universität Kassel, D-34132 Kassel, Germany (R.K., R.S.); Max-Planck-Institute of Molecular Plant Physiology, D-14476 Potsdam-Golm, Germany (T.T., A.R.F.); Centre of Microbial and Plant Genetics, KU Leuven, B-3001 Leuven, Belgium (B.D.C., B.P.A.C.); Department of Medical Protein Research, VIB, B-9000 Ghent, Belgium (K.G.); Department of Biochemistry, Ghent University, B-9000 Ghent, Belgium (K.G.)

Author contribution

This chapter contains work from the published manuscript.

S.L.G. made the root, hypocotyl and leaf phenotyping. S.L.G. wrote this chapter.

1 Abstract

Cytosolic monothiol glutaredoxins (GRXs) are required in iron-sulfur (Fe-S) cluster delivery and iron sensing in yeast and mammals. In plants, GRXs associate with the CIA (Cytosolic Fe-S assembly) complex, as in other eukaryotes, and contribute to, but are not essential for, the correct functioning of client Fe-S proteins in unchallenged conditions. *Arabidopsis thaliana* (*Arabidopsis*) has a sole cytosolic monothiol GRX encoded by *GRXS17*. The conserved 6 subunit Elongator complex has pleiotropic phenotypes associated with its double activity in transcript elongation via histone acetylation and in translation via tRNA modification of the wobble uridine 34.

Here, we used comparison between *grxs17* and *elo3* loss-of-function mutants to unravel common phenotypes associated with their tRNA modification processes. We found that several root and leaf growth phenotypes are phenocopied as well as upregulation of a number of genes. Similar to mutant plants with defective CIA components, the loss-of-function mutants of GRXs and Elongator showed hypersensitivity to DNA damage and elevated expression of DNA-damage marker genes. We also found that some phenotypes like hypocotyl growth differ between the grxs17 and the elo3 mutant, suggesting they are not related to the tRNA modification activity of the respective genes, but rather to the HAT or another activity of Elongator. The results support a shared, but not necessarily identical role in the functioning of particular processes such as tRNA modification in GRXS17 and Elongator.

2 Introduction

2.1 tRNAs modifications in yeast and plants

During translation, ribosomes provide the structural units to catalyse the reaction that links amino acids to make a new protein while transfer RNAs (tRNAs) carry the amino acids to the ribosome, matching a codon in an mRNA with its amino acid. Each tRNA contains a set of three nucleotides, called anticodon, binding a specific mRNA codon and carries the corresponding amino acid.

Cytosolic tRNAs in eukaryotes carry several chemical modifications, often at the anticodon loop. Uridines at the first position of the anticodon (U_{34}) of tRNAs tK(UUU), tE(UUC), and tQ(UUG) are modified to 5-methoxycarbonylmethyl-2-thiouridine (mcm5s2U) in eukaryotes. Furthermore, this evolutionarily conserved modification (Mehlgarten *et al.*, 2010) is essential for unperturbed translation and cellular signalling (Zinshteyn and Gilbert, 2013; Scheidt *et al.*, 2014; Nedialkova and Leidel, 2015). The 2-thiolation (s2) step of mcm5s2U is catalysed by the UBIQUITIN-RELATED MODIFIER (URM1) pathway and requires the CIA complex in yeast (Nakai *et al.*, 2007; Leidel *et al.*, 2009). The mcm5 modification is catalysed by the elongator (ELP) pathway and requires the Elp3/ELO3 catalytic subunit, i.e. a [4Fe-4S] protein (Huang et al., 2005; Paraskevopoulou et al., 2006; Selvadurai et al., 2014), together with the Trm9/Trm112 complex, which is a tRNA methyltransferase necessary for the last step of mcm5 formation (Kalhor and Clarke, 2003; Chen et al., 2011; Leihne et al., 2011). The presence of the mcm5 chain is needed for an effective thiolation of tRNAs (Leidel et al., 2009; Chen et al., 2011). Although in vivo data are scarce, tRNA modifications might have a regulatory function, because certain open reading frames (ORFs) are enriched in codons recognized by modified tRNAs. In yeast, genes involved in the DNA-damage response are enriched in GAA, AAA, and CAA codons and elongator mutants defective in mcm5s2 modification are hypersensitive to DNA stress (Chen et al., 2011).

2.2 The glutaredoxin GRXS17

Glutaredoxins (GRXs) together with thioredoxins (TRXs) are thiol oxidoreductases that are able to control the redox state of proteins and are present in most organisms (Herrero and de la Torre-Ruiz, 2007). The yeast GRX proteins Grx3/4 and the mammalian ortholog GRX3/PKC-interacting cousin of TRX (PICOT) have been associated with the CIA pathway and contain themselves [2Fe-2S] clusters (Picciocchi et al., 2007; Haunhorst et al., 2010). Deletion of Grx3/4 in yeast leads to defects in cytosolic and mitochondrial Fe-S assembly, deregulation of iron homeostasis, and defects in proteins containing di-iron centers (Mühlenhoff et al., 2010). Yeast Grx3/4 and human GRX3 belong to the PICOT protein family and contain one N-terminal TRX and one (Grx3/4) or two (GRX3) C-terminal GRX domains, also known as PICOT

homology domains (Haunhorst *et al.*, 2010). Because they contain only a single Cys residue in their GRX active sites, they are classified as monothiol GRXs. They are conserved and present in a broad range of organisms, including bacteria, yeasts, plants, and mammals (Isakov *et al.*, 2000). Whereas there are other monothiol GRXs present in mitochondria, Grx3/4 and GRX3 are the only nucleocytosolic-localized monothiol GRXs (Herrero and de la Torre-Ruiz, 2007).

The sole class II *Arabidopsis* (*Arabidopsis thaliana*) nucleocytosolic monothiol GRX is GRXS17, which contains one N-terminal TRX and three C-terminal GRX domains. GRXS17 dimers are capable of associating with three [2Fe-2S] clusters *in vitro* (Knuesting *et al.*, 2015). Its physiological and molecular role in plants is not well understood (Couturier *et al.*, 2013). GRXS17 function has been associated with protection against oxidative stress in *Arabidopsis* and thermotolerance in *Arabidopsis* and tomato (Cheng *et al.*, 2011; Wu *et al.*, 2012; Knuesting *et al.*, 2015). *Arabidopsis* GRXS17 loss-of-function plants (*grxs17*) are hypersensitive to heat stress and show alterations in auxin sensitivity and polar transport (Cheng *et al.*, 2011). The molecular function of an association of cytosolic monothiol GRX with Fe-S clusters and the CIA pathway has been a subject of debate, and a role in Fe, Fe-S, or oxidative signalling has been proposed, in addition to a role in delivery or repair of Fe-S clusters (Couturier *et al.*, 2015). Recently, delivery of an Fe-S cluster by human GRX3 to the CIA pathway component DRE2/Anamorsin has been demonstrated (Banci *et al.*, 2015).

Using tandem affinity purification (TAP) with GRXS17 as bait, several proteins of the Fe-S cluster assembly and tRNA metabolism were purified (Iñigo *et al.*, 2016). Among the GRXS17-associated proteins that we identified by TAP were CTU1 (CYTOSOLIC THIOURIDYLASE SUBUNIT1) and CTU2, two proteins essential for the thiolation of uridine at the wobble position of cytosolic tRNA in eukaryotes (Björk *et al.*, 2007; Schlieker *et al.*, 2008; Leidel *et al.*, 2009). CTU1 presents homology with *Escherichia coli* TtcA, the protein responsible for the thioltransferase activity necessary for s^2C_{32} tRNA thiolation, a tRNA modification not present in eukaryotes (Jäger *et al.*, 2004). *E. coli* TtcA was shown to bind, through three conserved Cys residues, Fe-S clusters that are

essential for its activity (Bouvier *et al.*, 2014). The conserved motifs Cys-X_1-X_2 - Cys present in *E. coli* TtcA and *Arabidopsis* CTU1 suggest that *Arabidopsis* CTU1(L) proteins could be Fe-S client proteins. GRXS17 could be involved in the transfer of putative Fe-S clusters to a CTU1(L)/CTU2 complex. Y2H and BiFC assay showed an interaction between GRXS17 and CTU1 and CTU2 as well as a cytosolic-interaction between GRXS17 and CTU2 (Iñigo *et al.,* 2016). Visualization of the thiolated total tRNA in *grxs17-1* showed levels similar to wild type as compared to mutants *ctu1* and *ctu2*, known for their loss of thiolated tRNA, whereas *elo3-6* showed significant reduction of thiolated tRNA (Iñigo *et al.,* 2016).

Several proteins already known to bind Fe-S clusters were also found in the GRXS17 TAP interactome, including BolA2 and XDH1 (XANTHINE DEHYDROGENASE1). Interactions between GRX and BolA proteins are conserved in yeast, humans, and plants. In all of these eukaryotes, it has been demonstrated that the GRX and BolA domains are bridged by the binding of a [2Fe-2S] cluster (Li *et al.*, 2009a, 2012; Couturier *et al.*, 2014). However, GRXS17 can also bind Fe-S clusters independently of BolA2 interaction, through the formation of Fe-S bridged homodimers, and it can contribute to the activity of cytosolic Fe-S enzymes (Knuesting *et al.*, 2015). XDH1 belongs to the family of XORs and is a central player in purine catabolism. In Arabidopsis, two XOR-encoding genes are present with a strict XDH activity, i.e. XDH1 and XDH2. According to the function of XDH1 in purine catabolism, precursors of uric acid (hypoxanthine and xanthine) are significantly more abundant in XDH1-deficient plants, whereas downstream products (allantoic acid and urea) are less abundant (Nakagawa *et al.,* 2007; Brychkova *et al*., 2008). Quantification of these metabolites in grxs17-1 plants indicated that these purine catabolism intermediates also accumulate differentially in the absence of GRXS17, reflecting a perturbed flux through the purine salvage pathway (Iñigo *et al*., 2016).

The function of many CIA components in yeast, mammals, and *Arabidopsis* has been associated with genomic stability, DNA repair, and metabolism, because many proteins necessary for DNA replication and repair are known to contain Fe-S clusters. The CIA

pathway is responsible for providing Fe-S clusters to respective apoproteins in the cytosol and the nucleus (Bernard *et al*., 2013). In yeast and humans, Met-18/MMS19 (METHIONINE REQUIRING18/ METHYL METHANESULFONATE19) has been shown to associate not only with several other CIA components, but also with Fe-S target proteins involved in DNA metabolism and to mediate the maturation of certain Fe-S proteins involved in DNA repair and replication (DNA helicases, polymerases, nucleases or glycosylases; Gari et al., 2012; Stehling et al., 2012; van Wietmarschen et al., 2012). The human MMS19 has been shown to be necessary for the maturation of only certain Fe-S proteins, mostly involved in DNA metabolism, but not for the activity of cytosolic aconitase iron regulated protein1 (IRP1) or Gln phosphoribosylpyrophosphate amidotransferase (Stehling et al., 2012). Human GRX3 is able to bind, in addition to [2Fe-2S] clusters, [4Fe-4S] clusters in vitro, which is necessary for the maturation of apo-IRP1 into aconitase (Xia et al., 2015), thus suggesting that GRX3/GRXS17, and not MMS19/MET18, is involved in the transfer of [4Fe-4S] clusters necessary for IRP1 maturation. This hypothesis is in accordance with the decrease in cytosolic aconitase activity observed in the Arabidopsis grxs17-1 mutant (Knuesting et al., 2015). Several members of the CIA pathway were found in the TAP interactome of GRXS17 i.e. MET18 and DRE2 (Iñigo et al., 2016). An elevated DNA-damage response was found in Arabidopsis mutants deficient in CIA complex components, such as ae-7 and met18 (Luo et al., 2012; Han et al., 2015), or in Fe-S cluster containing proteins, such as elo3 (Xu et al., 2012). A network (or regulon) was uncovered that comprises genes involved in the genotoxic (DNA- damage) stress response to be up-regulated in the *grxs17-1* mutant (Iñigo *et al.,* 2016). Accordingly, *grxs17* plants present some degree of hypersensitivity to the DNA-alkylating agent MMS.

2.3   Cytoplasmic role of the Elongator complex

In yeast, Elongator mutants defective in any of the Elongator subunit genes (ELP1 to ELP6) are lacking tRNA modifications at wobble uridines or thiouridines in position 34 of the anticodon (Huang et al., 2005; Karlsborn et al., 2014). Evidence for ELP acting particularly in tRNA modification came from studies in yeast, demonstrating that selective overexpression of two individual tRNAs can bypass major elp mutant phenotypes, presumably via compensating for the loss of translational fidelity that

results from defects in Elongator (Esberg et al., 2006). In addition to its HAT domain, Elp3 contains a N-terminal Fe4S4 cluster domain that binds and cleaves S-adenosylmethionine (SAM). This domain catalyzes transfer RNA (tRNA) U34 wobble uridine modification at C5 via a radical mechanism that, in archaea, also requires acetyl-CoA, the cofactor recruited by the Elp3 HAT domain activity (Selvadurai *et al.,* 2014). The ELP3 gene of Saccharomyces cerevisiae is essential for formation of mcm5 and ncm5 side chains in mcm5s2U, mcm5U, 5-carbamoylmethyluridine (ncm5U) and 5-carbamoylmethyl-2'-O-methyluridine (ncm5Um) at U34 in tRNA (Huang *et al.*, 2005). *Arabidopsis* Elongator has a role in tRNA maturation at wobble position 34, to improve wobbling accuracy and translational fidelity (Johansson *et al.,* 2008; Mehlgarten *et al.*, 2010).

The pleiotropic phenotypes of yeast Elongator mutants in diverse processes such as translation, exocytosis, filamentous growth and transcriptional silencing (Rahl *et al.*, 2005; Johansson *et al.*, 2008; Abdullah and Cullen, 2009; Li *et al.*, 2009b) might be explained by effects of improper tRNA modification or by multiple acetylation substrates for Elongator.

One of these tRNA modifications, 5-methoxycarbonyl-methyl-2-thiouridine (mcm^{5}s^{2}U), renders *Saccharomyces cerevisiae* sensitive to a toxin (zymocin) secreted by *Kluyveromyces lactis* (Schaffrath and Breunig, 2000) and ELP genes render zymocin-resistance to yeast cells (Frohloff *et al*., 2001).

An indirect effect on the transcriptome might be caused by the Elongator activity in tRNA wobble uridine modification that affects translation of certain proteins with a preference for those requiring Elongator-modified tRNAs for translation. In plants, regulation of tRNA maturation by Elongator is specifically important for auxin-controlled developmental processes. Elongator-mediated translational regulation of the PIN-FORMED (PIN) auxin transport protein seems to be a primary event in this pathway (Leitner et al., 2015). The plant Elongator regulates auxin responses via two different activities, histone acetylation and tRNA modification that operate at transcriptional and translational levels, respectively (Nelissen et al., 2010; Leitner et al.,

2015; Woloszynska et al., 2016; Chapter 3). The crosstalk between the two Elongator activities that control the auxin pathway is unclear, but reduced abundance of the PIN1 protein and lack of decrease in PIN1 transcript levels in the elp/elo mutants indicate that Elongator activities related to transcription and translation might target different genes within the same molecular pathway.

The high conservation of Elp3 between archaea and eukaryotes implies an ancient function for the HAT and SAM domain activities in the tRNA modification (Selvadurai *et al.,* 2014; Karlsborn *et al.,* 2014).

3   Results

3.1   A comparative leaf growth analysis between *elo* and *grsx17* mutants

Whereas CTU1 and CTU2 are essential for 2-thiolation of mcm^5-modified tRNA anticodons, the ncm^5U_{34} modification itself is dependent on Elongator (Huang *et al.,* 2005; Selvadurai *et al.,* 2014), a complex that is structurally and functionally conserved between *Saccharomyces cerevisiae* and *Arabidopsis* (Mehlgarten *et al.,* 2010). ELO3, the *Arabidopsis* ortholog of yeast elongator subunit Elp3 (Nelissen *et al.,* 2005), contains histone acetyltransferase and radical sterile alpha motif domains, which were recently shown to be catalytically critical for the tRNA modification function of archaeal Elp3 (Selvadurai *et al.,* 2014).

grxs17-1 and *grxs17-2* mutant plants exhibit an elongated leaf phenotype with larger leaf length/width ratio as compared to wild type (Fig. 1 A and E), which is typical of *elo* mutants (Nelissen *et al.,* 2005). Therefore, we investigated the possibility of a link between GRXS17 and Elongator through the study of leaf, hypocotyl and root phenotypes. The overall vegetative phenotype of 19 days-old *grxs17-1*, *grxs17-2* and *elo3-6* seedlings showed longer petioles and similar size and shape of the rosette leaves, and altered phylotaxis in all three mutants (Fig 1A). Leaf series were made and total leaf areas measured in *elo3-6* and the two *grxs17* mutant alleles relative to wild-type plants. Notably, all three mutants had a similar growth profile: (1) larger juvenile leaves 1, 2, and 3, which are fully expanded at 24 d after germination (DAG); (2) a larger leaf 4, which is

the transition to adult stage; and (3) smaller adult leaves 6, 7, and 8 because of a delay in growth in the mutants (Fig. 1B). This is also reflected in the absence of leaf 8 and cauline leaves at the 24 DAG time point in some of the mutant genotypes. We examined the cellular basis of the changes in the fully developed leaf 3, of which the total cell number and final cell area are representative of cell proliferation and growth activities during its development. We observed that the cell area in all mutant lines was similar to that of the Col-0 control. However, the calculated number of cells per leaf was significantly higher in the two grxs17 mutant genotypes and in the elo3-6 line as compared to wild type (Fig. 1 C and D), indicating that the larger leaf 3 area is the result of more cell proliferation in grxs17 and elo3-6 mutant lines. Leaf lamina length/width ratios were calculated and showed similar profiles amongst the three mutants, all displaying increased length relative to width which is a measure for their elongated shape (Fig. 1E).

Next, we compared our RNA-Seq dataset with previously published microarray datasets of the elongator mutants elo2-1 and elo3-1 (Nelissen *et al.,* 2005, Iñigo *et al.,* 2016). Although the latter dataset was performed on mutants in the Landsberg erecta ecotype and with a different experimental setup, we observed a large overlap between the top 100 genes induced in grxs17-1, elo2-1, and elo3-1 (Fig. 2A). The overlap comprised the DNA-damage network (Iñigo *et al.*, 2016). Indeed, loss of ELO3 has been reported to lead to a DNA-damage response (Xu *et al.*, 2012). We assessed this observation further by analysing gene expression in the grxs17 and elo3-6 mutants and in the T-DNA insertion lines of CTU1 and CTU2, called ctu1 and ctu2, all in the Col-0 background (Fig. 2B). Indeed, all genes tested that were up-regulated in grxs17 mutants were also up-regulated in elo3-6. Similarly, also in ctu1 and ctu2 we observed an upregulation of many grxs17-up-regulated genes, although more modest. In agreement with these results, ctu1 and ctu2 also showed some degree of sensitivity to the DNA-damage agent MMS (Fig. 2C).
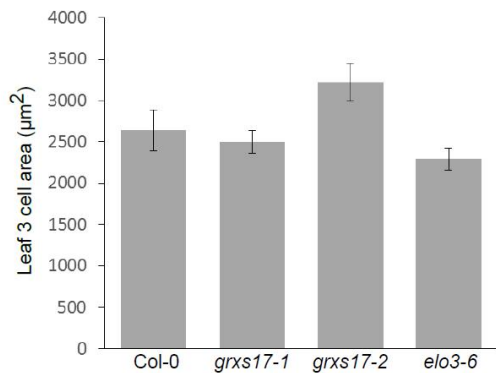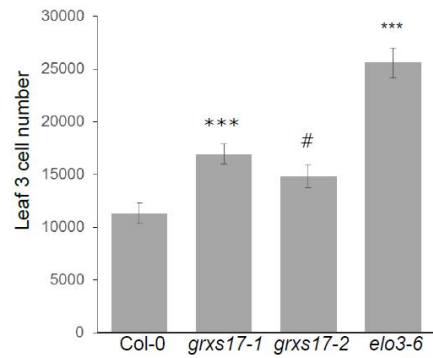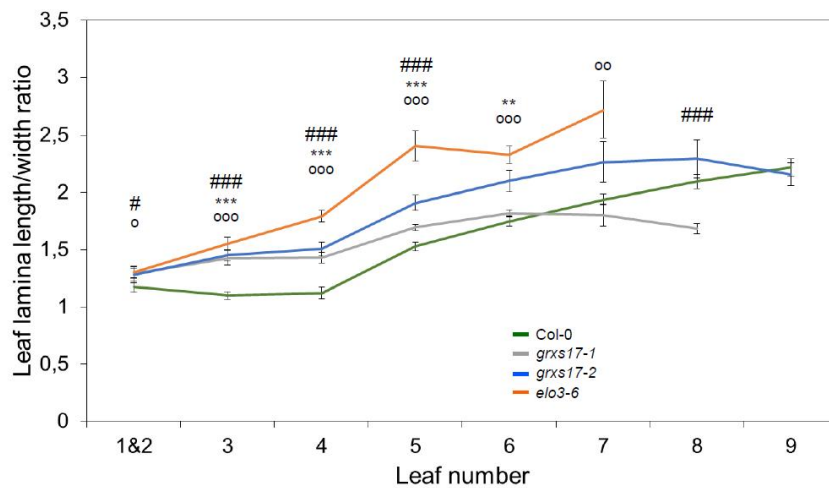
A

Col-0   grxs17-1   grxs17-2   elo3-6
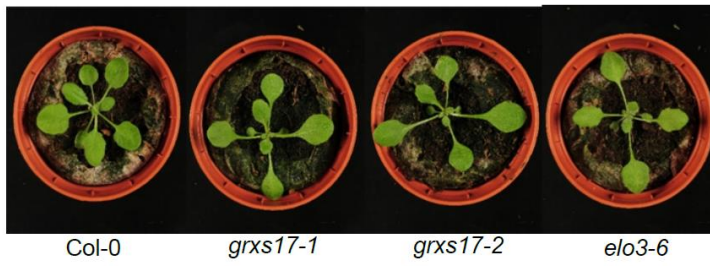
B
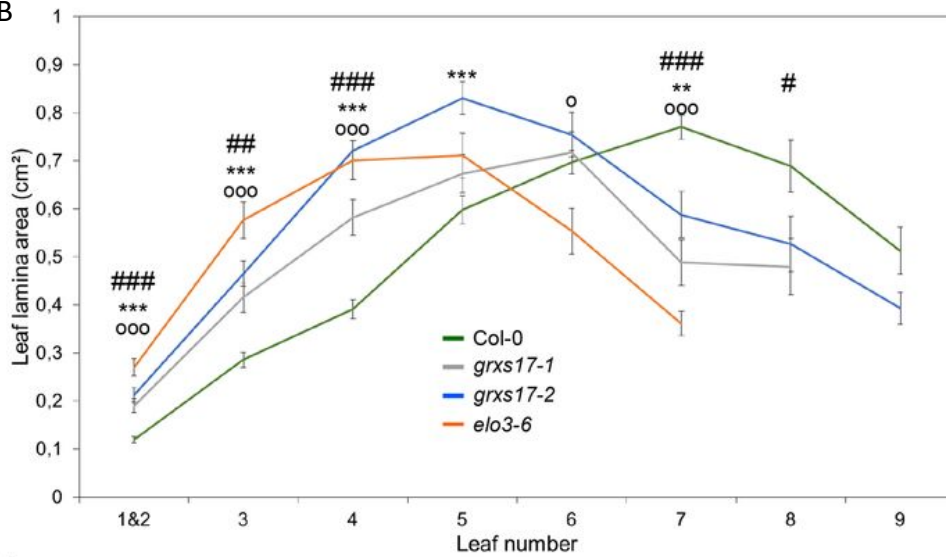
C

D

E

Figure 1. *grxs17* **and** *elo3-6* **mutants have similar developmental defects.** A. Representative plant phenotypes, 19 days after germination (DAG) of left to right: Col-0, *grxs17-1, grxs17-2* and *elo3-6*. B. Lamina area of leaf series of 24-d-old plants germinated in soil (n=10) Bars represent means ± SE (*P, 0.05; **P, 0.01; ***P, 0.001, Student's t test, # comparison between Col-0 and *grxs17-1*, * between Col-0 and *grxs17-2*, and °between Col-0 and *elo3-6*). C. C and D, Cellular analysis of leaf 3 (n=5): mean of cell area (C) and calculated number of cells (D) (***, P<0.001; #, P=0.06, Student's t-test). E. Ratio between leaf lamina length and width of leaf series of plants, 24 DAG, grown in soil (n≥10) (*, P<0.05; **, P<0.01; ***, P<0.001, Student's t-test, # comparison between Col-0 and grxs17-1; * between Col-0 and *grxs17-2* and º between Col-0 and *elo3-6*. Bars represent SE.

Finally, previous reports indicated that the elongator subunits ELP2 and ELP3/ELO3 are involved in the salicylic acid signalling pathway (DeFraia *et al.,* 2010, 2013) and that the elongator complex is required for *Arabidopsis* resistance to necrotrophic fungal pathogens such as *Botrytis cinerea* and *Alternaria brassicicola* (Wang *et al.*, 2015). Therefore, we tested the susceptibility of the *grxs17-1* mutant to *B. cinerea*. Compared with wild-type plants, *grxs17-1* plants were more susceptible to *B. cinerea* infection (Fig. 2D), suggesting that GRXS17 plays a role in the defence response against *B. cinerea*.

Taken together, our data indicate that *grxs17* and *elo3* mutants have similar phenotypes at the molecular, cellular, and physiological level, both in growth and in defence, and thus support a joined, but not necessarily identical, role in the functioning of particular processes such as tRNA modification.
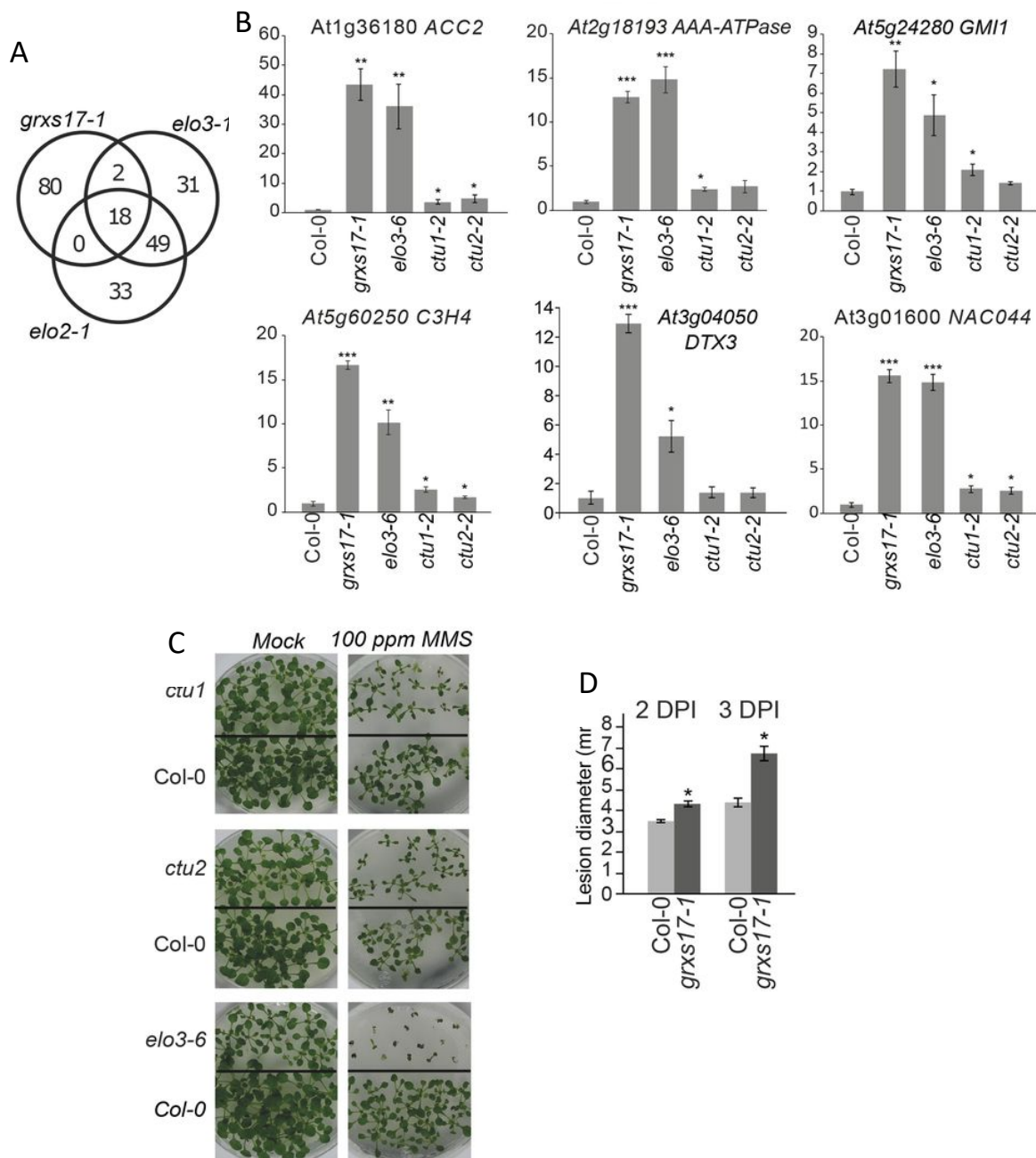
Figure 2. *grxs17* and *elo3-6* mutants show similar physiological and molecular defects. A. Overlap between the top 100 genes up-regulated in *grxs17-1* for which a probes et is present on the ATH1 microarray and the top 100 probe sets significantly up-regulated in *elo2-1* and *elo3-1*. B. qPCR validation of gene expression in *grxs17-1, elo3-6, ctu1-2*, and *ctu2-2* mutants. The expression ratio relative to that in wild-type Col-0 seedlings is plotted (set at 1). Bars represent means ± SE of n = 3 (*P, 0.05; **P, 0.01; ***P, 0.001, Student's t test). C. Hypersensitivity of *ctu1, ctu2*, and *elo3-6* to MMS. Seedlings were grown for 17 d on 0.01% v/v MMS or under control conditions (mock). D. Hypersensitivity of *grxs17-1* mutants to the necrotrophic pathogen *B. cinerea*. Lesion diameter in *grxs17-1* and Col-0 plants infected with *B. cinerea*, 2 and 3 d post-inoculation. Bars represents means ±SE with n=32 (* P<0.05, Student's t-test).

3.2   Root phenotypes

In *A. thaliana* several auxin-related genes were found to be differentially expressed in wild type and *elo* mutants and two of these genes SHY2 and LAX2 were also affected in histone H3K14 acetylation (Nelissen *et al.*, 2010). These were taken as evidence for the role of Elongator in transcript elongation of specific genes explaining the influences on cell proliferation and development in *elo* mutants. Thus, in plants, Elongator has a function in auxin signalling whereas, in the animal kingdom, Elongator has a role in neuron development. Studies on the role of Elongator in these processes might reveal how a conserved protein complex with conserved enzymatic activities can fulfill specific functions in different organisms. Elongator regulates growth via auxin-related pathways by its two activities linked to histone acetylation and tRNA maturation (Nelissen *et al.*, 2010; Leitner *et al.*, 2015; Woloszynska *et al.,* 2016; Chapter 3).

Observations of the *elo* mutants showed that they are characterized by narrow leaves and reduced root growth resulting from a decreased cell division rate (Nelissen *et al.*, 2005) and that Elongator genes are strongly expressed in meristems (Nelissen *et al.*, 2010). It indicates a role of Elongator in root and leaf development. *shy2* has a short primary root and reduced lateral root formation as a result of auxin-resistance, resembling the phenotype of *elo* mutants. Hence, we examined primary root length, auxin sensitivity of root growth, lateral root initiation and adventitious root formation. The *elo3-6* and the two *grxs17* mutant alleles had a reduced primary root growth (Fig. 3A), which was correlated with a reduced number of cortex cells in the root apical meristem (Fig. 3B), suggesting a faster transition to differentiation. Growth media were complemented with increasing amounts of the auxin IAA (Indole-3-acetic acid) (Fig. 3D). In the presence of low concentration of auxin, *elo3-6* primary root growth is increased while that in wild type is reduced. *grxs17-1* primary root growth is reduced with increasing auxin concentration in the same way as wild type. It was shown previously that low concentrations of IAA applied to *elo1-10* and *elo3-10* reduced root growth (Nelissen *et al*. 2010).
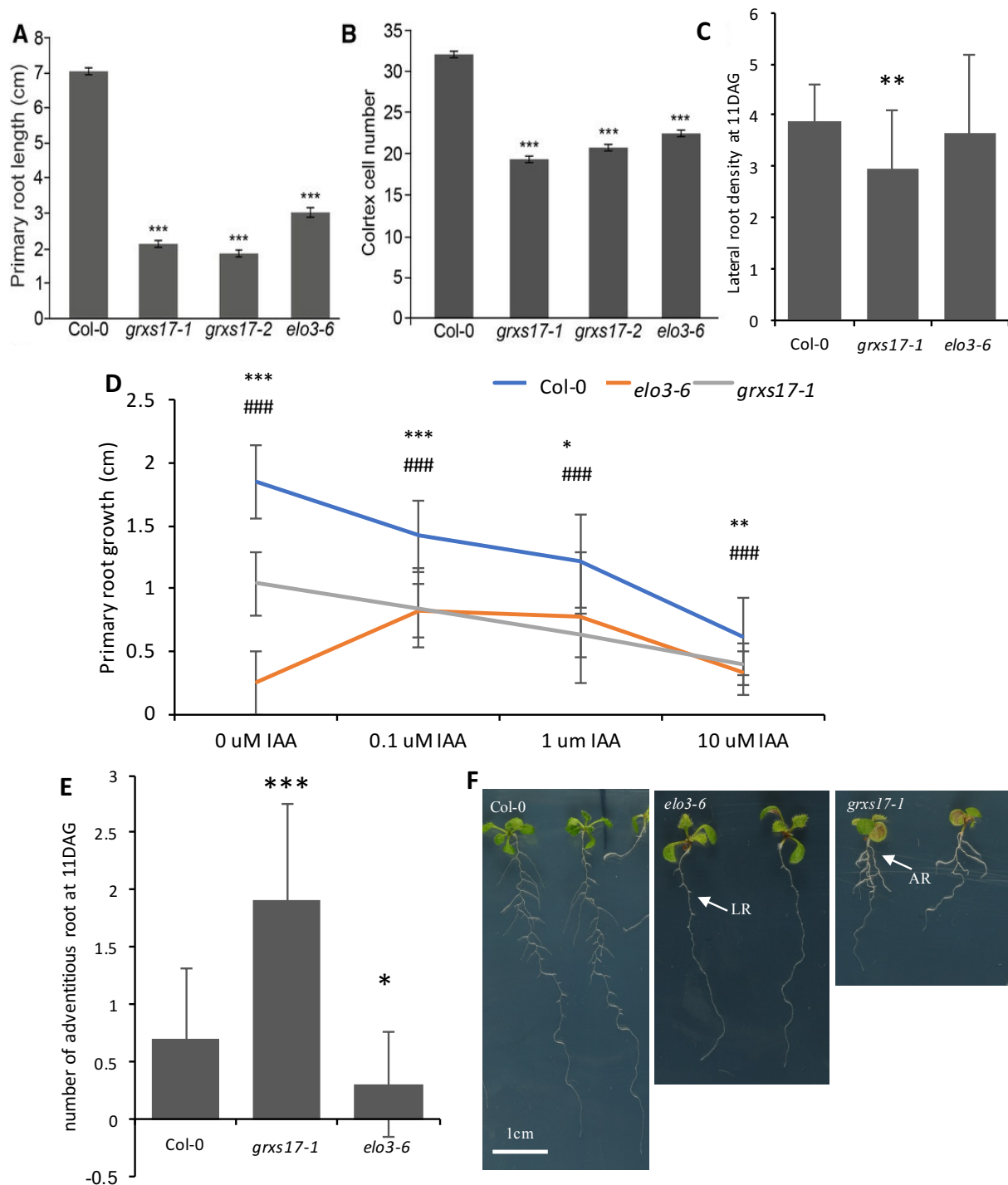
Figure 3: Root comparison of elo3-6 and grxs17-1 at 11 days after germination. A. Primary root length of 11-d-old Col-0, grxs17-1, grxs17-2, and elo3-6 seedlings grown on Murashige and Skoog (n=21). B. Number of cortex cells in the root apical meristem of seedlings 5 DAG (n=34). A-B. Bars represents means ±SE. C. Lateral root density (number of lateral root (LR)/length of primary root (PR)) at 11DAG. D. Primary root length at 11DAG on MS media complemented with 0.1M, 1M or 10M of IAA (* comparison between Col-0 and elo3-6, # comparison between Col-0 and grxs17-1). E. Adventitious root number at 11DAG. F. Representative plants at 11DAG grown vertically grown in vitro. All plants were grown in vitro on vertical MS plates with continuous light for 11

days. LR indicates lateral roots and AR adventitious roots. * and # indicate significant difference (*, P<0.05; **, P<0.01; ***, P<0.001, Student's t-test). C-E. Bars represents means ±SD.

Lateral root formation is a process that depends on the coordinated distribution of auxin (Benkova *et al.*, 2003). The lateral roots are post-embryonic, being formed by the primary root pericycle cells. The quiescent center is established in the lateral root tip at stage VII of primordium development (Malamy and Benfey, 1997). Lateral root density, calculated as the number of lateral roots/primary root length, is reduced in *grxs17-1* as compared to wild type, while in *elo3-6* the lateral root density is not significantly reduced (Fig. 3C). In *elo3-6* the outgrowth of lateral roots is reduced (Fig. 3F). The slower speed of primary root growth may also be related to the delay of emergence of the lateral roots and is consistent with a role of Elongator in transmission of instructive auxin signals during root morphogenesis tRNA maturation has been linked to root organogenesis, potentially via mechanisms orchestrating PIN activities and associated adjustments in auxin distribution (Leitner *et al.*, 2015).

Adventitious roots emerge from organs other than the primary root, such as hypocotyls, stems and leaves. In *Arabidopsis*, they originate from the hypocotyl pericycle, at the hypocotyl - primary root transition zone (Falasca and Altamura, 2003). Usually they are present in a low number, but mutants overproducing adventitious roots, e.g. *superroot2-1* (*sur2-1*) a modulator of auxin homeostasis, are known (Delarue *et al.*, 1998). Auxin and cytokinin control the formation of the quiescent centre of the adventitious root of *Arabidopsis* (Della Rovere *et al.*, 2013). Surprisingly, the number of adventitious roots is significantly bigger in *grxs17-1* than in wild type while significantly smaller in *elo3-6* (Fig. 3E).

Taken together these parameters showed that the general root architecture is very different between *grxs17-1, elo3-6* and Col-0 (Fig. 3F). Compared to Col-0, *elo3-6* is shorter and has a lower number of adventitious roots while *grxs17-1* is shorter and has a lower number of lateral roots and a larger number of adventitious roots.

Both *elo3-6* and *grxs17-1* had a reduced primary root growth and meristem size but they showed different phenotypes in lateral and adventitious root initiation and growth. The generation of secondary meristems in the primary root is due to the auxin gradients (Della Rovere *et al.*, 2013; Benkova *et al.*, 2003) also observed as a different response to the application of ectopic auxin in *elo3-6* and *grxs17-1*. Taken together, phenotypes related to the auxin pathway may be regulated by the HAT activity of Elongator on SHY2 and LAX2 rather than tRNA maturation (Nelissen *et al.*, 2010), while the phenotypes of the primary meristem and primary root are likely due to the tRNA modification defect of the mutant. This coincides with previously described Elongator root phenotypes that have been shown to be influenced by the two activities of Elongator (Nelissen *et al.*, 2005, 2010; Leitner *et al.*, 2015).

3.3   GRXS17 and elo in early development

Elongator controls hypocotyl growth in darkness via its HAT activity (Woloszynska *et al.*, 2017; Chapter 4). In darkness, Elongator mutants are characterized by shorter hypocotyls than Col-0 but similar apical hooks and cotyledons. The maximum difference of the hypocotyl length between elo3-6 and WT is measured at 3DAG. Seeds were sown, stratified for 48h, illuminated for 6h in white light to induce germination, and transferred to darkness. Hypocotyl length was measured at 4DAG in grxs17-1 and elo3-6. Only elo3-6 had a significantly reduced hypocotyl length (Fig. 4). The apical hook and cotyledons in grxs17-1 are similar to wild-type. In darkness, the elo3-6 hypocotyl phenotype is determined by the combined effect of decreased levels of cell wall biogenesis genes, reduced expression of clock regulators and decreased expression of HY5, HYH, and HFR1, consequently inhibiting hypocotyl elongation (Woloszynska *et al.*, 2017; Chapter 4). Low expression of *HY5*, *HYH*, and *HFR1* also prevents cotyledon expansion in *elo3-6*. Thus, hypocotyl elongation is reduced in darkness in *elo3-6* and this phenotype is not present in *grxs17-1*, indicating it is related to the role of Elongator in transcription.
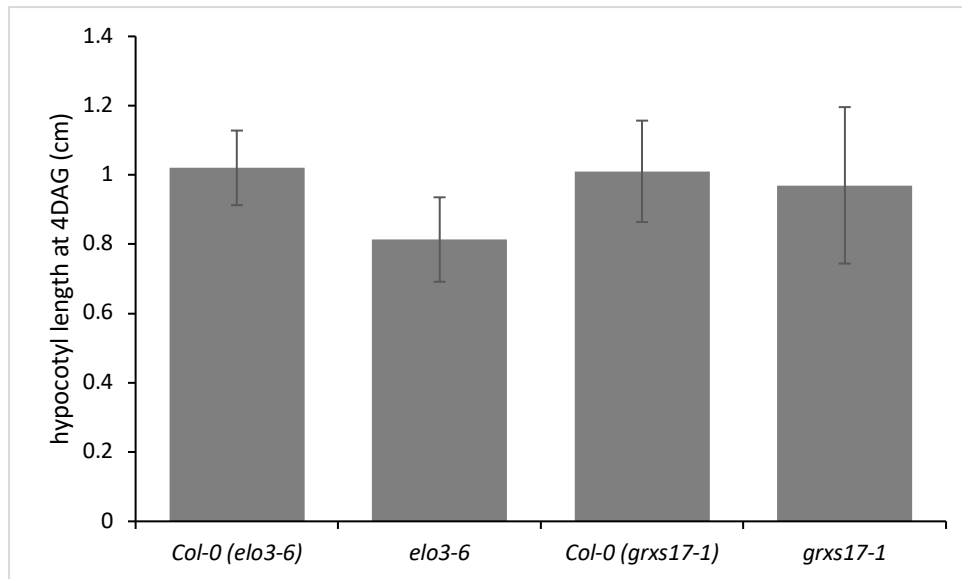
Figure 4: Phenotypes of *elo3-6* and *grxs17-1* seedlings grown in darkness conditions in comparison to Col-0. Hypocotyl length of wild type (Col-0), *grxs17-1* mutant and *elo3-6* mutant was measured at 4 DAG after being grown in darkness condition. At least thirty seedlings were photographed and hypocotyls were measured with the ImageJ software. Mean values of hypocotyl length of at least 25 seedlings are presented. Error bars represent standard errors. Asterisks indicate statistically significant differences to Col-0 (* $p<0.05$, ** $p<0.01$, *** $p<0.001$). Bars represents means ±SD.

4   Discussion

Cytosolic monothiol GRXs are required in Fe-S cluster delivery, associate with CIA components and contribute to their functioning. GRXS17 is associated with CTU proteins essential for thiolation of uridine at the wobble position of cytosolic tRNA in eukaryotes (Björk *et al.,* 2007; Schlieker *et al.,* 2008; Leidel *et al.,* 2009). CTU1 and CTU2 are essential for 2-thiolation of mcm^5-modified tRNA anticodons, the ncm^5U_{34} modification itself is dependent on the Elongator complex (Huang *et al.,* 2005; Selvadurai *et al.,* 2014). Therefore, we investigated phenotypes in common between GRXS17 and Elongator to reveal processes affected by Elongator function in tRNA modification.

In *elo3-6* mutants, in contrast to *grxs17-1,* almost no thiolated tRNA were observed (Iñigo *et al.,* 2016). These results suggest that *grxs17-1* presents no strong defect in mcm^5 modification in plants based on the absence of a strong thiolation defect. However, in yeast and plants, the GRXs Grx3/4 and GRXS17 may have a potential influence on elongator tRNA modification function, which has been previously shown to be

conserved and functionally exchangeable between *S. cerevisiae* and *Arabidopsis* (Mehlgarten *et al.*, 2010). In the light of these findings, it is interesting to note that the GRX3 gene was identified previously as a high-copy suppressor in yeast of growth inhibition by zymocin, a fungal tRNase ribotoxin complex (Jablonowski *et al.*, 2001; Jablonowski and Schaffrath, 2007). Zymocin activity targets elongator-dependent mcm^{5}s^{2}U$_{34}$ modifications in tRNA anticodons (Lu *et al.*, 2005; Jablonowski *et al.*, 2006) and eventually kills *S. cerevisiae* cells. *elp3/elo3* and *elp6* have a reduction in the occurrence of 5-methoxycarbonyl-methyl-2-thiouridine (mcm^{5}s^{2}U) and of 5-carbamoyl-methyluridine (ncm^{5}U) in both mutant alleles (Leitner *et al.*, 2015). Therefore, loss of tRNA modification in elongator (*elp*) or tRNA methyltransferase (*trm9*) mutants protects against zymocin, making the tRNase a useful tool for diagnosing elongator function and, hence, tRNA modification in yeast (Nandakumar *et al.*, 2008) and potentially in *Arabidopsis* (Mehlgarten *et al.*, 2010; Leitner *et al.*, 2015). In a yeast, ELP3 depletion strain resistance to zymocin is observed due to loss of mcm^{5}s^{2}U$_{34}$ modification (Iñigo *et al.,* 2016). However, when GRX3/4 were deleted, yeast cells could not grow in the presence of the toxin, although previous data show that high-copy GRX3 confers zymocin resistance (Jablonowski *et al.*, 2001), which might indicate that the absence of GRX3/4 function differentially affects mcm^5 or mcm^{5}s^2 modifications at U$_{34}$.

We showed that *grxs17* and *elo3* mutants have similar molecular, physiological and cellular phenotypes i.e. primary root size reduction, reduction of root cortex cell number, leaf size and shape, upregulation of *ACC2, AAA-ATPase, GMI1, C3H4, DTX3* and *NAC044*, overlap of gene upregulation, hypersensitivity to *B. cinerea* and hypersensitivity to the DNA damage agent MMS. This supports a shared role in in tRNA modification. But both mutants also differ in specific phenotypes such as hypocotyl growth in darkness, lateral root density, adventitious root number and root growth in response to ectopic application of IAA. The differences observed in the mutants can be explained by different function of GRX17 and Elongator i.e. GRX17 association with the purine pathway (Iñigo *et al.,* 2016) or Elongator histone acetylation activity.

The use of zymocin that targets degradation of tRNA modified by Elongator is expected to give growth defect related to tRNA maturation. It resulted in auxin-related defects, resembling those of *elp* mutants (Leitner *et al., *2015) i.e. defects in root growth,

cotyledon formation and aberrations in lateral organ positioning at inflorescence axes. PIN1::GFP reporter signals were reduced in seedlings producing zymocin in meristem, while *PIN1* transcript levels were unaffected, indicating that zymocin interferes with post-transcriptional control of *PIN1*. However, phenotypes of *elp6* and zymocin treated plants are synergistic suggesting an incomplete overlap of activities.

In conclusion, Elongator and GRXs have a shared function in tRNA modification, but the exact function needs to be further examined.

5   Material and Methods

5.1   Plant Material and Growth Conditions

All mutant lines used in this study were in the Col-0 ecotype background. *grxs17-1* (SALK_021301), *grxs17-2* (antisense line), *rol5-2/ctu1-2* (GK-709D04), *ctu2-2* (GK-686B10) and *elo3-6* (GK-555H06) mutants were described previously (Leiber *et al.*, 2010; Nelissen *et al.*, 2010; Chen *et al.*, 2011; Luo *et al.*, 2012; Philipp *et al.*, 2014). *Arabidopsi*s (*Arabidopsis thaliana*) seeds were sterilized by the chlorine gas method and sown on sterile plates containing Murashige and Skoog medium supplemented with 1% (w/v) Suc, 0.8% (w/v) agarose, pH 5.7. Plates were kept 2 d in the dark for stratification at 4°C before being transferred to a growth room at 21°C with a 16-h light/8-h dark regime, with a light intensity of 80 mmol $m^{22} s^{21}$, unless mentioned otherwise.

For hypocotyl assays, seeds were sterilized in 5% (v/v) bleach with 0.05% (v/v) Tween 20 for 10 min, washed in water, sown on half-strength Murashige and Skoog (MS) medium (Murashige and Skoog, 1962) without sucrose and stratified at 4°C for 48 h. Seeds were exposed for 6 h to white light (100 µmol $m^{-2} s^{-1}$) to induce germination and plants were grown in darkness for the indicated time at 21°C. Seedlings analyzed for hypocotyl length were put on 1% (w/v) agar, photographed, and hypocotyl length of at least 25 seedlings for each genotype/condition was measured with the ImageJ 1.45 software. Significant differences were recovered with the two-tailed Student's *t*-test in Microsoft Excel.

5.2   RNA-Seq

Seedlings were grown in vertical plates in three biological repeats for 14 d in Murashige and Skoog medium supplemented with 1% (w/v) Suc. Seedlings were frozen in liquid nitrogen, and total RNA was extracted using the RNeasy plant mini kit (Qiagen) and DNase I (Promega) treatment. A TruSeq RNA-Seq library (Illumina) was generated and sequenced as 50-bp single read using the Illumina HiSEquation 2000 technology at GATC Biotech. Read quality control, filtering, mapping to The Arabidopsis Information Resource 10 version of the Arabidopsis genome, and read counting were carried out using the Galaxy portal running on an internal server (http://galaxyproject.org/). Sequences were filtered and trimmed with the Filter FASTQ v1 and FASTQ Quality Trimmer v1 tools, respectively, with default settings (http://www.bioinformatics.babraham.ac.uk/projects/fastqc/). Reads were subsequently mapped to The Arabidopsis Information Resource 10 version of the Arabidopsis genome using GSNAPv2 (Wu and Nacu, 2010), allowing a maximum of five mismatches. The concordantly paired reads that uniquely map to the genome were used for quantification on the gene level with HTSeq-count from the HTSeq python package (Anders *et al.,* 2015). Data were normalized using TMM, implemented in edgeR (Robinson *et al.,* 2010), and common dispersion was then estimated using the conditional maximum likelihood method (Robinson and Smyth, 2008). Differentially expressed genes were defined by a 2-fold difference between mutant lines and the wild-type control with P-value of $\leq$ 0.05. The false discovery rate was limited to 5% according to Benjamini and Hochberg (1995).

5.3   Gene Expression Analysis

Seedlings were grown in the same conditions described for RNA-Seq, and total RNA was isolated as mentioned above. One microgram of RNA was used for cDNA synthesis using the iScript kit (Bio-Rad). Quantitative reverse transcriptase-PCR was performed on a LightCycler 480 system (Roche) using the Fast Start SYBR Green I PCR mix (Roche). At least three biological repeats and two technical repeats were used for each analysis. Data were analyzed using the second derivative maximum method, and relative expression levels were determined using the comparative cycle threshold method. Primer sequences are provided in Supplemental Table S1.

5.4 DNA-Damage Agent

Sterilized seeds were geminated in Murashige and Skoog medium, transferred after 4 d to Murashige and Skoog plates supplemented or not with 0.01% v/v MMS (Sigma) and scored after 17 d. The experiment was performed in triplicate.

5.5 Root Phenotype Analysis

Seeds were germinated and seedlings grown vertically at 21°C under 24-h light conditions (75 mmol m22 s21)for 11 days were used for root length analysis. The root meristem size was determined 5 DAG as the number of cells in the cortex cell file from the Quiescent center (QC) to the first elongated cell (Casamitjana-Martínez et al., 2003). The samples were mounted with clearing solution (80 g chloral hydrate, 30 mL glycerol, and 10 mL dH_2O) and observed immediately. The main root length was determined 11 DAG using ImageJ software (http://imagej.nih.gov/ij/), adventitious root and emerged lateral root were counted. At least 23 seedlings of each line were analyzed.

5.6 Leaf Phenotype Analysis

Plants, 24 DAG in soil at 21°C under a 16-h light/8-h dark regime with a light intensity of 75 mmol m22 s21were used for leaf series on 1% agar plates, picture taking, and image analysis of leaf lamina area, length, and width as described (Cnops et al., 2004). Leaf 3 was chosen for epidermal cell imaging because of its full expansion at 24 DAG (Fig. 1B; Pyke et al., 1991; Medford et al., 1992). Leaves were fixed overnight in 100% ethanol and mounted with 90% lactic acid. The leaf area was measured with the ImageJ software. The epidermal cells on the abaxial side were drawn with a Leica DMLB microscope equipped with a drawing tube and differential interference contrast objectives. The total number of cells per leaf was calculated as described previously (De Veylder *et al.,* 2001). We estimated the total number of cells per leaf by dividing the leaf area by the mean cell area (averaged between the tip and basal positions). Means between samples were compared by a two-tailed Student's t-test.

5.7   Pathogen Infection

Cultivation and spore harvesting of Botrytis cinerea strain B05.10 (provided by Rudi Aerts, Katholieke Hogeschool Kempen, Belgium) was performed as described previously (Broekaert et al., 1990). Arabidopsis wild-type (Col-0) and mutant plants were grown for 4 weeks in soil ("DCM potgrond voor Zaaien en Stekken"; DCM, Sint-Katelijne-Waver, Belgium) in a growth chamber at 21°C, 75% humidity, and a 12-h day/light cycle with a light intensity of approximately 120 mmol m22 s21. A 5-mL drop of a B. cinerea spore suspension (5 3 105/mL in half-strength potato dextrose broth) was inoculated on three leaves per plant. Plants were kept in transparent, sealed boxes to retain almost 100% humidity after inoculation. Disease symptoms were scored by measuring the diameter of the necrotic lesions at 2 and 3 d post-inoculation. Thirty-two plants per line were analyzed. Two independent assays with similar results were performed.

6   References

Abdullah, U., Cullen, P.J., 2009. The tRNA Modification Complex Elongator Regulates the Cdc42-Dependent Mitogen-Activated Protein Kinase Pathway That Controls Filamentous Growth in Yeast. Eukaryotic Cell 8, 1362–1372. doi:10.1128/EC.00015-09

Anders, S., Pyl, P.T., Huber, W., 2015. HTSeq--a Python framework to work with high-throughput sequencing data. Bioinformatics 31, 166–169. doi:10.1093/bioinformatics/btu638

Banci, L., Ciofi-Baffoni, S., Gajda, K., Muzzioli, R., Peruzzini, R., Winkelmann, J., 2015. N-terminal domains mediate [2Fe-2S] cluster transfer from glutaredoxin-3 to anamorsin. Nature Chemical Biology 11, 772–778. doi:10.1038/nchembio.1892

Benjamini, Y., Hochberg, Y., 1995. Controlling the false discovery rate: a practical and powerful approach to multiple testing. Journal of the royal statistical society. Series B (Methodological) 289–300. https://www.jstor.org/stable/2346101

Benková, E., Michniewicz, M., Sauer, M., Teichmann, T., Seifertová, D., Jürgens, G., Friml, J., 2003. Local, efflux-dependent auxin gradients as a common module for plant organ formation. Cell 115, 591–602. https://doi.org/10.1016/S0092-8674(03)00924-3 show

Bernard, D.G., Netz, D.J.A., Lagny, T.J., Pierik, A.J., Balk, J., 2013. Requirements of the cytosolic iron-sulfur cluster assembly pathway in Arabidopsis. Philosophical Transactions of the Royal Society B: Biological Sciences 368, 20120259–20120259. doi:10.1098/rstb.2012.0259

Bjork, G.R., Huang, B., Persson, O.P., Bystrom, A.S., 2007. A conserved modified wobble nucleoside (mcm5s2U) in lysyl-tRNA is required for viability in yeast. RNA 13, 1245–1255. doi:10.1261/rna.558707

Bouvier, D., Labessan, N., Clémancey, M., Latour, J.-M., Ravanat, J.-L., Fontecave, M., Atta, M., 2014. TtcA a new tRNA-thioltransferase with an Fe-S cluster. Nucleic Acids Research 42, 7960–7970. doi:10.1093/nar/gku508

Broekaert, W.F., Terras, F.R.G., Cammue, B.P.A., Vanderleyden, J., 1990. An automated quantitative assay for fungal growth inhibition. FEMS Microbiology Letters 69, 55–59. doi:10.1111/j.1574-6968.1990.tb04174.x

Brychkova, G., Alikulov, Z., Fluhr, R., Sagi, M., 2008. A critical role for ureides in dark and senescence-induced purine remobilization is unmasked in the Atxdh1 Arabidopsis mutant. The Plant Journal 54, 496–509. doi:10.1111/j.1365-313X.2008.03440.x

Casamitjana-Martınez, E., Hofhuis, H.F., Xu, J., Liu, C.-M., Heidstra, R., Scheres, B., 2003. Root-specific CLE19 overexpression and the sol1/2 suppressors implicate a CLV-like pathway in the control of Arabidopsis root meristem maintenance. Current Biology 13, 1435–1441. https://doi.org/10.1016/S0960-9822(03)00533-5 show

Chen, C., Huang, B., Eliasson, M., Rydén, P., Byström, A.S., 2011. Elongator Complex Influences Telomeric Gene Silencing and DNA Damage Response by Its Role in Wobble Uridine tRNA Modification. PLoS Genetics 7, e1002258. doi:10.1371/journal.pgen.1002258

Cheng, N.-H., Liu, J.-Z., Liu, X., Wu, Q., Thompson, S.M., Lin, J., Chang, J., Whitham, S.A., Park, S., Cohen, J.D., Hirschi, K.D., 2011. Arabidopsis Monothiol Glutaredoxin, AtGRXS17, Is Critical for Temperature-dependent Postembryonic Growth and Development via Modulating Auxin Response. Journal of Biological Chemistry 286, 20398–20406. doi:10.1074/jbc.M110.201707

Cnops, G., Jover-Gil, S., Peters, J.L., Neyt, P., De Block, S., Robles, P., Ponce, M.R., Gerats, T., Micol, J.L., Van Lijsebettens, M., 2004. The rotunda2 mutants identify a role for the LEUNIG gene in vegetative leaf morphogenesis. Journal of Experimental Botany 55, 1529–1539. doi:10.1093/jxb/erh165

Couturier, J., Przybyla-Toscano, J., Roret, T., Didierjean, C., Rouhier, N., 2015. The roles of glutaredoxins ligating Fe–S clusters: Sensing, transfer or repair functions? Biochimica et Biophysica Acta (BBA) - Molecular Cell Research 1853, 1513–1527. doi:10.1016/j.bbamcr.2014.09.018

Couturier, J., Touraine, B., Briat, J.-F., Gaymard, F., Rouhier, N., 2013. The iron-sulfur cluster assembly machineries in plants: current knowledge and open questions. Frontiers in Plant Science 4. doi:10.3389/fpls.2013.00259

Couturier, J., Wu, H.-C., Dhalleine, T., Pégeot, H., Sudre, D., Gualberto, J.M., Jacquot, J.-P., Gaymard, F., Vignols, F., Rouhier, N., 2014. Monothiol Glutaredoxin–BolA Interactions: Redox Control of Arabidopsis thaliana BolA2 and SufE1. Molecular Plant 7, 187–205. doi:10.1093/mp/sst156

De Veylder, L., Beeckman, T., Beemster, G.T., Krols, L., Terras, F., Landrieu, I., Van Der Schueren, E., Maes, S., Naudts, M., Inzé, D., 2001. Functional analysis of cyclin-dependent kinase inhibitors of Arabidopsis. The Plant Cell 13, 1653–1668. https://doi.org/10.1105/TPC.010087

DeFraia, C.T., Wang, Y., Yao, J., Mou, Z., 2013. Elongator subunit 3 positively regulates plant immunity through its histone acetyltransferase and radical S-adenosylmethionine domains. BMC plant biology 13, 102. https://doi.org/10.1186/1471-2229-13-102

DeFraia, C.T., Zhang, X., Mou, Z., 2010. Elongator subunit 2 is an accelerator of immune responses in Arabidopsis thaliana: Function of AtELP2 in plant immunity. The Plant Journal 64, 511–523. doi:10.1111/j.1365-313X.2010.04345.x

Delarue, M., Prinsen, E., Van Onckelen, H., Caboche, M., Bellini, C., 1998. Sur2 mutations of Arabidopsis thaliana define a new locus involved in the control of auxin homeostasis. The Plant Journal 14, 603–611. https://doi.org/10.1046/j.1365-313X.1998.00163.x

Della Rovere, F., Fattorini, L., D'Angeli, S., Veloccia, A., Falasca, G., Altamura, M.M., 2013. Auxin and cytokinin control formation of the quiescent centre in the adventitious root apex of arabidopsis. Annals of Botany 112, 1395–1407. doi:10.1093/aob/mct215

Esberg, A., Huang, B., Johansson, M.J.O., Byström, A.S., 2006. Elevated Levels of Two tRNA Species Bypass the Requirement for Elongator Complex in Transcription and Exocytosis. Molecular Cell 24, 139–148. doi:10.1016/j.molcel.2006.07.031

Falasca, G., Altamura, M.M., 2003. Histological analysis of adventitious rooting in Arabidopsis thaliana (L.) Heynh seedlings. Plant biosystems 137, 265–273. https://doi.org/10.1080/11263500312331351511

Frohloff, F., Fichtner, L., Jablonowski, D., Breunig, K.D., Schaffrath, R., 2001. Saccharomyces cerevisiae Elongator mutations confer resistance to the Kluyveromyces lactis zymocin. The EMBO journal 20, 1993–2003. https://doi.org/10.1093/emboj/20.8.1993

Gari, K., León Ortiz, A.M., Borel, V., Flynn, H., Skehel, J.M., Boulton, S.J., 2012. MMS19 Links Cytoplasmic Iron-Sulfur Cluster Assembly to DNA Metabolism. Science 337, 243–245. doi:10.1126/science.1219664

Han, Y.-F., Huang, H.-W., Li, L., Cai, T., Chen, S., He, X.-J., 2015. The Cytosolic Iron-Sulfur Cluster Assembly Protein MMS19 Regulates Transcriptional Gene Silencing, DNA Repair, and Flowering Time in Arabidopsis. PLOS ONE 10, e0129137. doi:10.1371/journal.pone.0129137

Haunhorst, P., Berndt, C., Eitner, S., Godoy, J.R., Lillig, C.H., 2010. Characterization of the human monothiol glutaredoxin 3 (PICOT) as iron–sulfur protein. Biochemical and Biophysical Research Communications 394, 372–376. doi:10.1016/j.bbrc.2010.03.016

Herrero, E., de la Torre-Ruiz, M.A., 2007. Monothiol glutaredoxins: a common domain for multiple functions. Cellular and Molecular Life Sciences 64, 1518–1530. doi:10.1007/s00018-007-6554-8

Huang, B., Johansson, M.J.O., Byström, A.S., 2005. An early step in wobble uridine tRNA modification requires the Elongator complex. RNA 11, 424–436. doi:10.1261/rna.7247705

Iñigo, S., Nagels Durand, A., Ritter, A., Le Gall, S., Termathe, M., Klassen, R., Tohge, T., De Coninck, B., Van Leene, J., De Clercq, R., Cammue, B.P.A., Fernie, A.R., Gevaert, K., De Jaeger, G., Leidel, S.A., Schaffrath, R., Van Lijsebettens, M., Pauwels, L., Goossens, A., 2016.

Glutaredoxin GRXS17 Associates with the Cytosolic Iron-Sulfur Cluster Assembly Pathway. Plant Physiology 172, 858–873. doi:10.1104/pp.16.00261

Isakov, N., Witte, S., Altman, A., 2000. PICOT-HD: a highly conserved protein domain that is often associated with thioredoxin and glutaredoxin modules. TRENDS in Biochemical Sciences 25, 537–539. https://doi.org/10.1016/s0968-0004(00)01685-6

Jablonowski, D., Frohloff, F., Fichtner, L., Stark, M.J., Schaffrath, R., 2001. Kluyveromyces lactis zymocin mode of action is linked to RNA polymerase II function via Elongator. Molecular microbiology 42, 1095–1105. https://doi.org/10.1046/j.1365-2958.2001.02705.x

Jablonowski, D., Schaffrath, R., 2007. Zymocin, a composite chitinase and tRNase killer toxin from yeast. Portland Press Limited.

Jablonowski, D., Zink, S., Mehlgarten, C., Daum, G., Schaffrath, R., 2006. tRNA ^{Glu} wobble uridine methylation by Trm9 identifies Elongator's key role for zymocin-induced cell death in yeast: tRNA ^{Glu}, a potential toxin target in yeast. Molecular Microbiology 59, 677–688. doi:10.1111/j.1365-2958.2005.04972.x

Jager, G., Leipuviene, R., Pollard, M.G., Qian, Q., Bjork, G.R., 2004. The Conserved Cys-X1-X2-Cys Motif Present in the TtcA Protein Is Required for the Thiolation of Cytidine in Position 32 of tRNA from Salmonella enterica serovar Typhimurium. Journal of Bacteriology 186, 750–757. doi:10.1128/JB.186.3.750-757.2004

Johansson, M.J.O., Esberg, A., Huang, B., Bjork, G.R., Bystrom, A.S., 2008. Eukaryotic Wobble Uridine Modifications Promote a Functionally Redundant Decoding System. Molecular and Cellular Biology 28, 3301–3312. doi:10.1128/MCB.01542-07

Kalhor, H.R., Clarke, S., 2003. Novel Methyltransferase for Modified Uridine Residues at the Wobble Position of tRNA. Molecular and Cellular Biology 23, 9283–9292. doi:10.1128/MCB.23.24.9283-9292.2003

Karlsborn, T., Tükenmez, H., Mahmud, A.K.M.F., Xu, F., Xu, H., Byström, A.S., 2014. Elongator, a conserved complex required for wobble uridine modifications in Eukaryotes. RNA Biology 11, 1519–1528. doi:10.4161/15476286.2014.992276

Knuesting, J., Riondet, C., Maria, C., Kruse, I., Bécuwe, N., König, N., Berndt, C., Tourrette, S., Guilleminot-Montoya, J., Herrero, E., Gaymard, F., Balk, J., Belli, G., Scheibe, R., Reichheld, J.-P., Rouhier, N., Rey, P., 2015. Arabidopsis Glutaredoxin S17 and Its Partner, the Nuclear Factor Y Subunit C11/Negative Cofactor 2α, Contribute to Maintenance of the Shoot Apical Meristem under Long-Day Photoperiod. Plant Physiology 167, 1643–1658. doi:10.1104/pp.15.00049

Leiber, R.-M., John, F., Verhertbruggen, Y., Diet, A., Knox, J.P., Ringli, C., 2010. The TOR Pathway Modulates the Structure of Cell Walls in Arabidopsis. The Plant Cell 22, 1898–1908. doi:10.1105/tpc.109.073007

Leidel, S., Pedrioli, P.G.A., Bucher, T., Brost, R., Costanzo, M., Schmidt, A., Aebersold, R., Boone, C., Hofmann, K., Peter, M., 2009. Ubiquitin-related modifier Urm1 acts as a sulphur carrier in thiolation of eukaryotic transfer RNA. Nature 458, 228–232. doi:10.1038/nature07643

Leihne, V., Kirpekar, F., Vågbø, C.B., van den Born, E., Krokan, H.E., Grini, P.E., Meza, T.J., Falnes, P.Ø., 2011. Roles of Trm9- and ALKBH8-like proteins in the formation of modified wobble uridines in Arabidopsis tRNA. Nucleic Acids Research 39, 7688–7701. doi:10.1093/nar/gkr406

Leitner, J., Retzer, K., Malenica, N., Bartkeviciute, R., Lucyshyn, D., Jäger, G., Korbei, B., Byström, A., Luschnig, C., 2015. Meta-regulation of Arabidopsis Auxin Responses Depends on tRNA Maturation. Cell Reports 11, 516–526. doi:10.1016/j.celrep.2015.03.054

Li, H., Mapolelo, D.T., Dingra, N.N., Naik, S.G., Lees, N.S., Hoffman, B.M., Riggs-Gelasco, P.J., Huynh, B.H., Johnson, M.K., Outten, C.E., 2009a. The Yeast Iron Regulatory Proteins Grx3/4 and Fra2 Form Heterodimeric Complexes Containing a [2Fe-2S] Cluster with Cysteinyl and Histidyl Ligation. Biochemistry 48, 9569–9581. doi:10.1021/bi901182w

Li, Q., Fazly, A.M., Zhou, H., Huang, S., Zhang, Z., Stillman, B., 2009b. The Elongator Complex Interacts with PCNA and Modulates Transcriptional Silencing and Sensitivity to DNA Damage Agents. PLoS Genetics 5, e1000684. doi:10.1371/journal.pgen.1000684

Lu, J., Huang, B., Esberg, A., Johansson, M.J.O., Byström, A.S., 2005. The Kluyveromyces lactis g -toxin targets tRNA anticodons. RNA 11, 1648–1654. https://doi.org/10.1261/ rna.2172105.

Luo, D., Bernard, D.G., Balk, J., Hai, H., Cui, X., 2012. The DUF59 Family Gene *AE7* Acts in the Cytosolic Iron-Sulfur Cluster Assembly Pathway to Maintain Nuclear Genome Integrity in *Arabidopsis*. The Plant Cell 24, 4135–4148. doi:10.1105/tpc.112.102608

Malamy, J.E., Benfey, P.N., 1997. Organization and cell differentiation in lateral roots of Arabidopsis thaliana. Development 124, 33–44. https://doi.org/PubMed 9006065

Medford, J.I., Behringer, F.J., Callos, J.D., Feldmann, K.A., 1992. Normal and abnormal development in the Arabidopsis vegetative shoot apex. The Plant Cell 4, 631–643. https://doi.org/10.1105/tpc.4.6.631

Mehlgarten, C., Jablonowski, D., Wrackmeyer, U., Tschitschmann, S., Sondermann, D., Jäger, G., Gong, Z., Byström, A.S., Schaffrath, R., Breunig, K.D., 2010. Elongator function in tRNA wobble uridine modification is conserved between yeast and plants: Plant Elongator function in tRNA modification. Molecular Microbiology 76, 1082–1094. doi:10.1111/j.1365-2958.2010.07163.x

Mühlenhoff, U., Molik, S., Godoy, J.R., Uzarska, M.A., Richter, N., Seubert, A., Zhang, Y., Stubbe, J., Pierrel, F., Herrero, E., Lillig, C.H., Lill, R., 2010. Cytosolic Monothiol Glutaredoxins Function in Intracellular Iron Sensing and Trafficking via Their Bound Iron-Sulfur Cluster. Cell Metabolism 12, 373–385. doi:10.1016/j.cmet.2010.08.001

Nakagawa, A., Sakamoto, S., Takahashi, M., Morikawa, H., Sakamoto, A., 2007. The RNAi-Mediated Silencing of Xanthine Dehydrogenase Impairs Growth and Fertility and Accelerates Leaf Senescence in Transgenic Arabidopsis Plants. Plant and Cell Physiology 48, 1484–1495. doi:10.1093/pcp/pcm119

Nakai, Y., Nakai, M., Lill, R., Suzuki, T., Hayashi, H., 2007. Thio Modification of Yeast Cytosolic tRNA Is an Iron-Sulfur Protein-Dependent Pathway. Molecular and Cellular Biology 27, 2841–2847. doi:10.1128/MCB.01321-06

Nandakumar, J., Schwer, B., Schaffrath, R., Shuman, S., 2008. RNA Repair: An Antidote to Cytotoxic Eukaryal RNA Damage. Molecular Cell 31, 278–286. doi:10.1016/j.molcel.2008.05.019

Nedialkova, D.D., Leidel, S.A., 2015. Optimization of Codon Translation Rates via tRNA Modifications Maintains Proteome Integrity. Cell 161, 1606–1618. doi:10.1016/j.cell.2015.05.022

Nelissen, H., De Groeve, S., Fleury, D., Neyt, P., Bruno, L., Bitonti, M.B., Vandenbussche, F., Van Der Straeten, D., Yamaguchi, T., Tsukaya, H., Witters, E., De Jaeger, G., Houben, A., Van Lijsebettens, M., 2010. Plant Elongator regulates auxin-related genes during RNA polymerase II transcript elongation. Proceedings of the National Academy of Sciences 107, 1678–1683. doi:10.1073/pnas.0913559107

Nelissen, H., Fleury, D., Bruno, L., Robles, P., De Veylder, L., Traas, J., Micol, J.L., Van Montagu, M., Inzé, D., Van Lijsebettens, M., 2005. The elongata mutants identify a functional Elongator complex in plants with a role in cell proliferation during organ growth. Proceedings of the National Academy of Sciences of the United States of America 102, 7754–7759. https://doi.org/10.1073/pnas.0502600102

Paraskevopoulou, C., Fairhurst, S.A., Lowe, D.J., Brick, P., Onesti, S., 2006. The Elongator subunit Elp3 contains a Fe4S4 cluster and binds S-adenosylmethionine. Molecular Microbiology 59, 795–806. doi:10.1111/j.1365-2958.2005.04989.x

Picciocchi, A., Saguez, C., Boussac, A., Cassier-Chauvat, C., Chauvat, F., 2007. CGFS-Type Monothiol Glutaredoxins from the Cyanobacterium *Synechocystis* PCC6803 and Other Evolutionary Distant Model Organisms Possess a Glutathione-Ligated [2Fe-2S] Cluster [†]. Biochemistry 46, 15018–15026. doi:10.1021/bi7013272

Pyke, K.A., Marrison, J.L., Leech, A.M., 1991. Temporal and Spatial Development of the Cells of the Expanding First Leaf of Arabidopsis thaliana (L.) Heynh. Journal of Experimental Botany 42, 1407–1416. doi:10.1093/jxb/42.11.1407

Rahl, P.B., Chen, C.Z., Collins, R.N., 2005. Elp1p, the Yeast Homolog of the FD Disease Syndrome Protein, Negatively Regulates Exocytosis Independently of Transcriptional Elongation. Molecular Cell 17, 841–853. doi:10.1016/j.molcel.2005.02.018

Robinson, M.D., McCarthy, D.J., Smyth, G.K., 2010. edgeR: a Bioconductor package for differential expression analysis of digital gene expression data. Bioinformatics 26, 139–140. doi:10.1093/bioinformatics/btp616

Robinson, M.D., Smyth, G.K., 2007. Small-sample estimation of negative binomial dispersion, with applications to SAGE data. Biostatistics 9, 321–332. doi:10.1093/biostatistics/kxm030

Schaffrath, R., Breunig, K.D., 2000. Genetics and Molecular Physiology of the Yeast Kluyveromyces lactis. Fungal Genetics and Biology 30, 173–190. doi:10.1006/fgbi.2000.1221

Scheidt, V., Baer, C., Klassen, R., Schaffrath, R., Molecular Oncology Program, Spanish National Cancer Centre (CNIO), Melchor Fernandez Almagro 3, Madrid, Spain., 2014. Loss of wobble uridine modification in tRNA anticodons interferes with TOR pathway signaling. Microbial Cell 1, 416–424. doi:10.15698/mic2014.12.179

Schlieker, C.D., Van der Veen, A.G., Damon, J.R., Spooner, E., Ploegh, H.L., 2008. A functional proteomics approach links the ubiquitin-related modifier Urm1 to a tRNA modification pathway. Proceedings of the National Academy of Sciences 105, 18255–18260. https://doi.org/10.1073/pnas.0808756105

Selvadurai, K., Wang, P., Seimetz, J., Huang, R.H., 2014. Archaeal Elp3 catalyzes tRNA wobble uridine modification at C5 via a radical mechanism. Nature Chemical Biology 10, 810–812. doi:10.1038/nchembio.1610

Stehling, O., Vashisht, A.A., Mascarenhas, J., Jonsson, Z.O., Sharma, T., Netz, D.J., Pierik, A.J., Wohlschlegel, J.A., Lill, R., 2012. MMS19 assembles iron-sulfur proteins required for DNA metabolism and genomic integrity. Science 337, 195–199. https://doi.org/10.1126/science.1219723

van Wietmarschen, N., Moradian, A., Morin, G.B., Lansdorp, P.M., Uringa, E.-J., 2012. The Mammalian Proteins MMS19, MIP18, and ANT2 Are Involved in Cytoplasmic Iron-Sulfur Cluster Protein Assembly. Journal of Biological Chemistry 287, 43351–43358. doi:10.1074/jbc.M112.431270

Wang, C., Ding, Y., Yao, J., Zhang, Y., Sun, Y., Colee, J., Mou, Z., 2015. Arabidopsis Elongator subunit 2 positively contributes to resistance to the necrotrophic fungal pathogens *Botrytis cinerea* and *Alternaria brassicicola*. The Plant Journal 83, 1019–1033. doi:10.1111/tpj.12946

Woloszynska, M., Gagliardi, O., Vandenbussche, F., De Groeve, S., Baez, L.A., Neyt, P., Le Gall, S., Fung, J., Mas, P., Van Der Straeten, D., Van Lijsebettens, M., 2017. Elongator regulates hypocotyl growth in darkness and during photomorphogenesis. Journal of Cell Science jcs.203927. doi:10.1242/jcs.203927

Woloszynska, M., Le Gall, S., Van Lijsebettens, M., 2016. Plant Elongator-mediated transcriptional control in a chromatin and epigenetic context. Biochimica et Biophysica Acta (BBA) - Gene Regulatory Mechanisms 1859, 1025–1033. doi:10.1016/j.bbagrm.2016.06.008

Wu, Q., Lin, J., Liu, J.-Z., Wang, X., Lim, W., Oh, M., Park, J., Rajashekar, C.B., Whitham, S.A., Cheng, N.-H., Hirschi, K.D., Park, S., 2012. Ectopic expression of Arabidopsis glutaredoxin AtGRXS17 enhances thermotolerance in tomato: Ectopic expression of AtGRXS17 in tomato. Plant Biotechnology Journal 10, 945–955. doi:10.1111/j.1467-7652.2012.00723.x

Wu, T.D., Nacu, S., 2010. Fast and SNP-tolerant detection of complex variants and splicing in short reads. Bioinformatics 26, 873–881. doi:10.1093/bioinformatics/btq057

Xia, H., Li, B., Zhang, Z., Wang, Q., Qiao, T., Li, K., 2015. Human glutaredoxin 3 can bind and effectively transfer [4Fe–4S] cluster to apo-iron regulatory protein 1. Biochemical and Biophysical Research Communications 465, 620–624. doi:10.1016/j.bbrc.2015.08.073

Xu, D., Huang, W., Li, Y., Wang, H., Huang, H., Cui, X., 2012. Elongator complex is critical for cell cycle progression and leaf patterning in Arabidopsis: Elongator promotes cell cycle progression. The Plant Journal 69, 792–808. doi:10.1111/j.1365-313X.2011.04831.x

Zinshteyn, B., Gilbert, W.V., 2013. Loss of a conserved tRNA anticodon modification perturbs cellular signaling. PLoS genetics 9, e1003675. https://doi.org/10.1371/journal.pgen.1003675

7   Supplemental figures and tables

Table S1: primer used in the study

For qRT-PCR	
AT1G36180 ACC2-F	5'-CATGGAGTGGTTCCCATGTT-3'
AT1G36180 ACC2-R	5'-CCTCGGGGACAGTTACCA-3'
AT2G18193-F	5'-TCACCCTCAAAACCTTCCTG-3'
AT2G18193-R	5'-TTCCATATGCCTGCACTGTC-3'
AT5G24280 GMI1-F	5'-ATACGTCTTGATGACGGTTCTG-3'
AT5G24280 GMI1-R	5'-CGGTGTCAAATCCCACAAGT-3'
AT5G60250 C3H4-F	5'-TCTTATCCGATTTTCCAATACGTC-3'
AT5G60250 C3H4-R	5'-TGTTGCATGATGCTTTGAAGA-3'
AT5G53240 DUF295-F	5'-ATGGCGCTCAAACGTACCTA-3'
AT5G53240 DUF295-R	5'-CTCGGGAGGCACCTTTTT-3'
AT3G01600 NAC044-F	5'-TCACCCTCAAAACCTTCCTG-3'
AT3G01600 NAC044-R	5'-TTCCATATGCCTGCACTGTC-3'

Part III. CONCLUSION

Chapter 6 General discussion and perspectives

1 The RNA pol II elongation complex is a hub for RNA processing

The central dogma of molecular biology states that DNA makes RNA through transcription that makes proteins through translation. In order to react to external stimuli or proceed with developmental processes, living organism have developed control mechanisms of expression at the different levels. Plants being fixed to their substrate and having no way to flee or hide from biotic or abiotic stresses, a fast and finely tuned gene expression is crucial to their survival.

Histone modifying multi-subunit complexes alter the chromatin structure by changing the conformational state or the mobilization of the nucleosome (Chapter 1). Transcript elongation is a crucial step of transcription and is associated with RNA processing. Indeed, purification of the elongating RNA pol II showed that the elongation complex associates with additional chromatin factors, such as Nucleosome Assembly Protein 1 (NAP1), Chromatin Remodelling complexes (CRCs); enzymes involved in histone modification such as histone (de)acetylation (i.e., Elongator and HDACs); histone H2B monoubiquitination (HUB1), histone methyltransferases (SDG4, WDR5A) and mRNA processing factors (splicing factors and polyadenylation proteins) (Antosz e*t al*., 2017).

HUB1 and Elongator have been first identified in *Arabidopsis* as leaf mutants respectively *ang4-1* and *elo* (Berná *et al*., 1999; Nelissen *et al*., 2005; Fleury *et al*., 2007). Their mutants have numerous but distinct growth and developmental defects that show an important role in plant transcription regulation in several biological processes. Both HUB1 and Elongator have been purified in the RNA pol II transcript elongation complex (Antosz e*t al*., 2017).

2 Questions related to the HUB1 and Elongator research

This thesis had the goal of extending current knowledge of histone modifiers and their specificity of action. HUB1 and Elongator have been identified and their action on chromatin has been characterized, however, the mechanisms behind their specificity and the choice of their targets are still unknown.

They are both part of the RNA pol II transcript elongation complex but their specific role in the complex is still uncharacterized. It is unclear how they interact with the RNA

pol II transcript elongation complex. Proteins that are part of their interaction network are unknown. The effect of upstream regulation on their activity and target gene selection is unexplored.

In, addition, downstream target pathways and thus related phenotypes regulated by HUB1 and Elongator should be further studied.

The study was divided into two parts, focussing on the one hand on HUB1 and on the other hand on Elongator.

HUB1 has a broad role in general histone H2B monoubiquitination but also a specific one in the targeting of particular genes. To better understand how the specificity of the HUB complex is directed we have taken an approach via the search of interactors that may serve as a link between the complex and the targeted gene. After identification and phylogenetic characterization of interactors, their mutant phenotypes were compared to those of HUB1 to find commonly affected pathways both at physiological and molecular level. Being RNA binding proteins, the HUB1 interactors were further studied on two known targets of HUB1 that linked to phenotypes observed in the interactor mutants. A mechanistic insight into H2Bub and mRNA processing through the action of the RNA binding HUB1 interactors was obtained. Our data are in line with the published RNA pol II transcript elongation complex and advance the functional and mechanistic insight of the different molecular processes that are at work at this platform.

Elongator is characterized by a number of roles in addition to histone modification. The aim was to identify the target genes/pathways of the different functions of Elongator and to investigate whether these targets can explain the specificity of the Elongator complex for different pathways. One approach was using a peculiar hypocotyl phenotype of the Elongator mutant to unravel how Elongator affects the transcriptional regulation of different pathways that result in this phenotype. Physiological phenotypic comparison of *elo* to other mutants presenting similar phenotypes was used as a basis for molecular phenotyping. A second approach used comparison between an Elongator mutant and a mutant for tRNA modification, in order to identify common phenotypes that may be due to tRNA modification activity of Elongator.

3   SPEN links H2Bub to RNA processing

In yeast and metazoa, splicing and polyadenylation are linked to transcript elongation and there is a close relationship between ongoing transcription and mRNA processing (Perales and Bentley, 2009). The RNA pol II elongation rate under the control of transcript elongation factors is known to influence splicing and polyadenylation efficiency (Elkon *et al.,* 2013; Saldi *et al.,* 2016). TFIIS and PAF1-C have been connected to splicing (Dolata *et al.*, 2015; Li *et al.*, 2016). In yeast, PAF1-C is involved in recruiting certain polyadenylation factors to transcribed regions and can modulate 3'end processing (Nagaike *et al.,* 2011; Nordick *et al.,* 2008). In *Arabidopsis*, a range of splicing factors were copurified with CstF77, a polyadenylation factor (Antosz e*t al.*, 2017). Recent studies show a close cooperation of mRNA splicing and polyadenylation, particularly at the last exons (Kaida, 2016; Misra and Green, 2016). These studies support a close cooperation between splicing and polyadenylation during transcript elongation via the RNA pol II. HUB1 is also copurified with the RNA pol II elongation complex (Antosz e*t al.*, 2017).

In our study (Chapter 2), we showed that SPEN, an RNA binding protein that copurified with the HUB complex, is involved in the alternative splicing control of the *CCA1* gene. Like *hub1,* the *spen* mutant has reduced expression of CCA1 and a decreased level of H2Bub along the CCA1 gene (Figure 3 Chapter 2) and a disrupted period of the circadian clock. Quantitative observation of the alternatively spliced form of CCA1 in the *spen* mutant showed an altered intron 4 retention compared to wild type. Transcript elongation rate is known to influence splicing efficiency, slow elongation rate is associated with intron retention (Luco *et al.*, 2011). In *hub1,* reduction of H2Bub might slow down the speed of transcript elongation and therefore increase the splicing efficiency. *spen* has reduced H2Bub in the first part of the *CCA1* gene where the alternative splice site is located, suggesting a role in the recruitment of HUB1/2 at the splice site for maximum H2Bub which might function as a signal for splice site selection. It suggests that SPEN might connect with the nascent RNA via its RRM domain, and with a large group of interacting proteins involved in elongation and splicing via HUB1 and the SPOC domain of SPEN. Histone modifications are emerging as major regulators of alternative splicing via chromatin structure and interaction of histone modifiers with

the spliceosome (Luco *et al.*, 2011). The histone acetyltransferase Gcn5 in yeast and SAGA in humans physically interact with U2 snRNPs, and the histone arginine methyltransferase CARM1 interacts with U1 snRNP proteins suggesting a role of chromatin complexes in facilitating the correct assembly of the pre-spliceosome on pre-mRNA. In humans, a model has emerged involving direct physical crosstalk between chromatin and the splicing machinery via an adaptor complex (Sims *et al.*, 2007; Luco *et al.*, 2010). SPEN might be such an adaptor for H2Bub modification, SPEN would make the link between the nascent RNA via its RRM domain and the H2Bub via interaction with HUB1/2 by its SPOC domain, thus bridging the H2Bub to the pre-mRNA.

We showed that SPEN is a positive regulator of the splicing of the FLC antisense lncRNA COOLAIR (Chapter 2). However, this regulation is not directly linked to the activity of HUB1 in H2B monoubiquitination. The *spen* mutation is correlated with an increase of FLC expression and no change in H2Bub enrichment along the FLC gene (Figure 4 Chapter 2). The distal form of COOLAIR is increased in *spen* which can be explained by a defect in splicing or polyadenylation of COOLAIR. The data support a role for SPEN in splicing or polyadenylation regulation and specificity of COOLAIR. A number of genes tested by ChIP-qPCR are not affected in the *spen* mutant while their transcript level is. The dual function of SPEN on specific genes at coding RNA and non-coding RNA links the RNA pol II elongation complex to mRNA processing but also to long non-coding RNA processing and represents an additional level of transcriptional regulation. This reminds of the double activity of the SR like protein Npl3 in yeast that interacts with Bre1 (homolog of HUB1) and which is necessary for correct splicing together with Bre1 (Moehle *et al.*, 2012). In humans, the splicing factor SART3 binds histones H2A, H2B, H3 and H4 and enhances deubiquitination of H2B (Long *et al.*, 2014). In yeast, the ubiquitin-like protein Hub1 (not an homolog of the AtHUB1) binds to the DEAD-box helicase Prp5, a key regulator of early spliceosome assembly, and stimulates its ATPase activity thereby enhancing splicing and relaxing fidelity (Karaduman *et al.,* 2017). These observations confirm our hypothesis that, in plants, modification of the histone H2B by monoubiquitination plays a role in splicing regulation via adaptors, such as SPEN, that might help in the recruitment or stabilization of the nascent transcript to facilitate the splicing.

We showed that KHD binds ssRNA and interacts with HUB1 and HUB2. However, no link was demonstrated between H2Bub and KHD (Chapter 2). KHD was also found in the mRNA binding proteome of *Arabidopsis* etiolated seedling (Reichel *et al.,* 2016) while SPEN was not found in plant mRNA binding protein interactomes (reviewed in Köster *et al.*, 2017). KHD is also localized in the nucleus and cytoplasm contrary to SPEN. Altogether, it suggests a wider role for KHD in mRNA stability, export or translation.

In conclusion, the RNA pol II elongation complex is an interaction site for different proteins such as transcript elongation factors and histone modifiers as well as mRNA processing factors and proteins like SPEN that link indirectly, through its association with HUB1, different processes such as histone modification and splicing. HUB1 was shown to have a broad effect on gene regulation by H2Bub (Chapter 2, Fleury *et al.*, 2007) and in addition to have specific target genes like *CCA1* and *FLC* (Himanen *et al.*, 2012; Xu *et al.*, 2009). Interaction of SPEN with HUB1 was shown here to be part of this specific targeting. Supposedly, other HUB1 interactors could exist that would facilitate targeting to specific genes similar to the SPEN-mediated targeting, and could be identified via tandem affinity purification of HUB1.

4   Perspectives on the HUB interactors study

4.1   RNA binding of SPEN and KHD

Studies on the functional roles of RBPs (RNA binding proteins) in plant growth, development and stress response are emerging in recent years because not much is known about their roles (Lee and Kang, 2016). In particular investigation of the chaperone activity of RBPs will provide clues about their roles and mechanisms of action in the RNA metabolism. A major task for the future is to identify RNA targets and to understand how RBPs recognize substrate RNAs and how RBPs interact with other protein factors to regulate posttranscriptional RNA metabolism during plant growth and development under normal as well as stressful conditions.

We have shown that SPEN and KHD are RNA binding with EMSA on recombinant protein. However, we were not able to produce the full length proteins this could still

be tried with other types of cells (yeast, insects cells) and other tags (maltose binding protein, calmodulin binding protein) (Kimple *et al.*, 2013). Proteins with mutation in or missing the RNA binding domain could also be produced for functional analysis. EMSA could be repeated with specific RNA sequences and using the affinity MST (MicroScale Thermophoresis) RNA binding assay that would allow higher resolution and to test affinity at lower concentrations. Most RNA binding domains recognition sites are comprised of only 3 to 8 nucleotides, but they can tolerate a high degree of sequence variation in these sites (Jankowsky and Harris, 2015). This explains why proteins can bind with similar affinity to a range of divergent sequences. The protein concentration also influences the affinity. At limiting concentrations of protein, low affinity non-consensus sites in highly expressed RNAs can efficiently compete for protein binding with high affinity consensus sites in an RNA expressed at a lower level. Thus, explaining differences that can be seen *in vitro* vs *in vivo*.

New technologies such as RIP-seq (RNA immunoprecipitation sequencing) or CLIP-seq (cross-linking immunoprecipitation sequencing) or iCLIP (individual nucleotide resolution CLIP) might reveal more on the type of RNA bound by KHD and SPEN. The information obtained using these techniques might contribute to our knowledge on RNA-binding proteins in plants and on the function of putative non-coding RNAs. However, interaction of RNA-binding proteins might be transient and dynamic during transcript elongation which would complicate its analysis.

4.2   Protein interaction with HUB1

Improvements in different aspects of the TAP technology will increase sensitivity and no doubt, will reveal additional interactors of HUB, that could be other factors guiding HUB-mediated gene targeting.

The results of the TAP experiments used in this thesis were performed already in 2009, while due to technological advancements of the TAP method and mass spectrometry instruments increased sensitivities in protein interaction detection may be achieved today. New tags allow the elution at low temperatures which could help with the identification of unstable proteins. In addition, the protocol could be further improved, e. g. with trypsin digestion during beads purification or single step pull down (magnetic

IgG beads), increasing the identification of transient, weak or low abundant interactions. These interactions could be stabilized by crosslinking, further improving the sensitivity.

Beside the sensitivity, improvements were also made to the specificity (identification of false-positives). With every TAP, false positives are detected. They may be divided into two main groups. Firstly, some background proteins are found with most baits as they are very abundant and very interactive ("sticky"). Secondly, general non-specific interactors also co-purify because they help in bait translation, folding or transfer. Finally, some false positives are due to false positive interactions because during protein extraction all cell compartments are mixed, putting in contact sub-cellular proteomes, that are separated in intact cells.

The cell culture system can also give rise to false negative interactions because of the missing developmental context. A protein can take part in different complexes that are, for instance, developmental stage and tissue-specific. Since all our recombinant gene constructs are under the control of the 35S promoter the respective tagged proteins are much more abundant than under their endogenous promoters. As a consequence, their putative interactors, that are expressed under their endogenous promoters, are present in lower quantities and represent the limiting factors, resulting in lower number of purified complexes.

Therefore, in continuity with the work presented here, TAP performed *in planta* using light grown seedlings at different time points, under stress, in different tissues like flowers and roots, and developmental stages of *Arabidopsis thaliana*, as well as in different sub-cellular compartment, would benefit the unravelling of the complex dynamic interactions and the identification of possible other factors. *In planta*, mutant complementation test should also be completed to assess the functionality of the constructs. Reverse TAP with KHD should also be performed to confirm the presented data set.

An alternative method could also be used, such as proximity-dependent biotin identification (bioID) which labels proteins in proximity of the bait and allows purification of labelled proteins under denaturing condition (less background).

In conclusion, the low number of interactors detected so far might be because interacting proteins are not part of this complex all at the same time but are recruited to the core components at specific moments of the plant life cycle. Moreover, sensitivity limitations of the protein-protein interaction techniques such as TAP and Y2H could be a limiting factor for the discovery of other HUB1 interactors. For example, it has been shown by means of Y2H that the SPOC domain of SPEN does not participate in the binding of HUB1 and therefore it is free to interact with other proteins, moreover, there must be other proteins connecting KHD to the complex since none of the proteins tested showed direct interaction with it.

4.3   HUB1, SPEN and KHD functional analysis

We hypothesize that SPEN might help in the recruitment of HUB1/2 at the CCA1 gene, this could be tested with ChIP using HUB1/2 antibodies in *spen-1* mutants to verify the accumulation of HUB1/2 along the CCA1 gene.

Analysis of double mutant may help to show genetic interaction, it is expected to confirm the dependent or independent SPEN activity from HUB1 with respect to biomass (CCA1) or flowering time (FLC) phenotypes. RNA-seq analysis including splicing variants on the single and double mutant might uncover new common targets like *CCA1*. The RNA-seq was performed on shoot apex because of the coexpression of *HUB*, *SPEN* and *KHD* in the shoot meristem. For consistency it should have been performed on whole seedlings. In summary, RNA-seq could be repeated with paired-end reads and higher sequencing depth for the detection of alternative splicing and long non-coding RNA (Conesa *et al.,* 2016), this may allow to identify other targets of the SPEN activity. Furthermore, in yeast, the homolog of HUB1, Bre1 has been shown to have a mild but reproducible defect in splicing that has not been shown in plants yet and that we may see with this type of sequencing (Moehle *et al.,* 2012).

The analysis of a knock-out mutant of KHD should be added. We could see significant phenotypes in the knock-down mutant *khd-1* but it is likely that a knock-out mutant would show more clear phenotypes in flowering time and *FLC* analysis as well as in biomass and *CCA1* analysis and give more clues on the function of KHD.

Genome wide techniques such as ChIP-seq could be used for the identification of targets of H2Bub by HUB1. The use of different RNA deep sequencing immunoprecipitation methods would allow for the quantitative analysis of all types of RNA such as alternative splicing and lncRNA for SPEN and HUB1, to understand their specificity and targeting abilities.

In this study we mention and use HUB1 as representation of the HUB complex because HUB1 and HUB2 are homologs and have similar phenotypes. They have been shown to function in heterotetramers of HUB1 and HUB2 (Chapter 1, Liu *et al.*, 2007). Therefore, HUB1 is used more in the research as HUB2. Furthermore, expression of HUB1 and HUB2 are similar in developmental stages (Figure 1) and under perturbation (data not shown), showing that what we show for HUB1 is valid for HUB2.
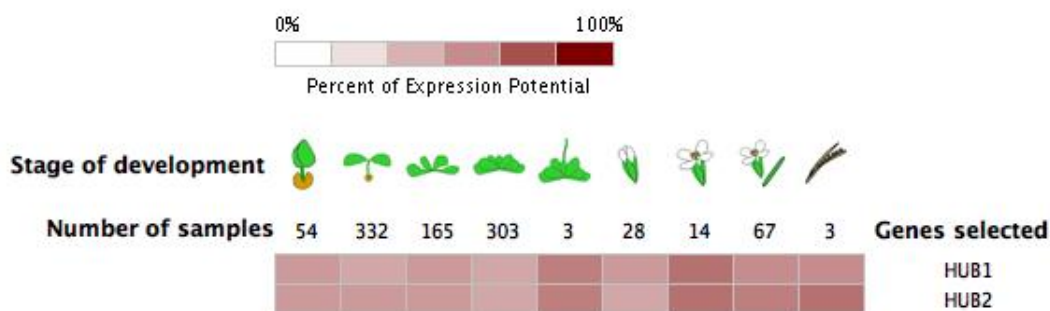

Figure 1: HUB1 and HUB2 expression in 9 developmental stages of *Arabidopsis thaliana* from mRNA sequencing data using the Genevestigator database (Hruz *et al.*, 2008).

5 Elongator has different roles in different pathways

The Elongator complex has conserved structure and enzymatic activities (Chapter 3). However, pathways regulated by Elongator have diverged in the different kingdoms. Elongator has various activities in transcription and translation that might be key to a complex regulation at different levels and enable a cross talk between transcription and translation.

In plants, Elongator regulates transcription through several regulatory processes, i.e. histone acetylation during RNAPII transcript elongation through the ELP3 HAT activity, DNA demethylation of cytosines through the ELP3 SAM activity, and microRNA

(miRNA) transcription and processing through the ELP2 interaction with DICER-LIKE1 (DCL1) and SERRATE (SE), which are components of the microprocessor complex of the siRNA machinery (Chapter 3; Woloszynska *et al.*, 2016).

Results presented in this study showed that hypocotyl elongation in darkness and photomorphogenesis are correlated with an altered transcriptome and specific genes targeted by the HAT activity of Elongator (Chapter 4, Woloszynska *et al.*, 2017); a comparison of leaf, root and hypocotyl phenotypes in *elo3* and tRNA modification mutant *grxs* distinguished between pathways targeted by the function of Elongator in tRNA modification and in transcription (Chapter 5). These findings extend the current knowledge about the function of Elongator and resulted in an improved working model, presented in Figure 4, Chapter 3 with Figure 2.

In darkness, *elo3-6* has a short hypocotyl correlated with low expression of *HYH, HY5, HFR1* and *PIF4*, decreased level of cell wall biogenesis genes and reduced expression of clock regulator (Chapter 4, Woloszynska *et al.*, 2017). We measured a reduced level of H3K14 acetylation in *LHY, HYH* and *HFR1* in *elo3-6* in darkness, but not in light condition, while their transcription level is reduced in both conditions. This may be due to the very dynamic nature of histone acetylation which could also explain the limited number of genes targeted by Elongator-mediated histone acetylation.

In conclusion, the effect on hypocotyl growth described in Chapter 4 is the result of a fine- tuned regulation pathway involving acetylation of key transcription factors in the light response, HFR1 and HYH, as well as the circadian clock LHY, thus creating responses in cell wall biogenesis, immune response and photomorphogenesis (model Figure 8 Chapter 4, Woloszynska *et al.*, 2017). H3K14 is less studied than other histone marks but appears to be very important for some genes as shown by our work.

Furthermore, we showed that hypocotyl growth in darkness is not changed in the tRNA modification mutant *grxs17-1* (Chapter 5). Therefore, changes in the hypocotyl phenotype seen in *elo* are not due to the tRNA modification pathway and support the transcriptional regulation of hypocotyl elongation as shown in Chapter 4. Furthermore, we compared primary, lateral and adventitious root development between *elo3* and *grxs* (Chapter 5). Four transcription factor genes responsible for root development,

PLETHORA1 (*PLT1*) and *PTL2, SHORT ROOT* (*SHR*), and *SCARECROW* (*SCR*) were identified as targets of the HAT activity of Elongator (Jia *et al.,* 2015). Primary root growth was reduced for *elo* and *grxs* mutants in addition to a reduced number of cortex cells in the primary root, which is in agreement with previous observations in *elo* (Nelissen *et al.*, 2010; Jia *et al.*, 2015). Lateral and adventitious root phenotypes differed between *elo* and *grxs*. Lateral root density is only reduced in *grxs17-1* and the number of adventitious roots is reduced in *elo3-6* and increased in *grxs17-1*. It suggests that adventitious root development is affected by Elongator only through its HAT activity.

Comparison of leaf development between *elo* and *grxs17-1* showed a similar leaf growth phenotype divergent from wild type, i.e. elongated shape and increased number of cells per leaf (Chapter 5).

Elongator is known to affect the auxin pathway by histone acetylation of the transmembrane auxin influx carrier gene, *LAX2*, and the auxin signalling gene, *SHY2* (Nelissen *et al.,* 2010). However, treatment of plants with zymocin, a fungal toxin that targets degradation of modified tRNA by Elongator, results in the same type of auxin related defects i.e. defects in root growth, cotyledon formation and aberration in lateral organ positioning at inflorescence axes; observed in elo and affects the post-transcriptional control of the transmembrane auxin efflux carrier *PIN1* (Leitner *et al.*, 2015). Comparison of the *elo* and *grxs17* response to topical auxin application showed a similar phenotype (Chapter 5), which is in accordance with expected results that the auxin response is affected by both the HAT and the tRNA modification activities of Elongator.
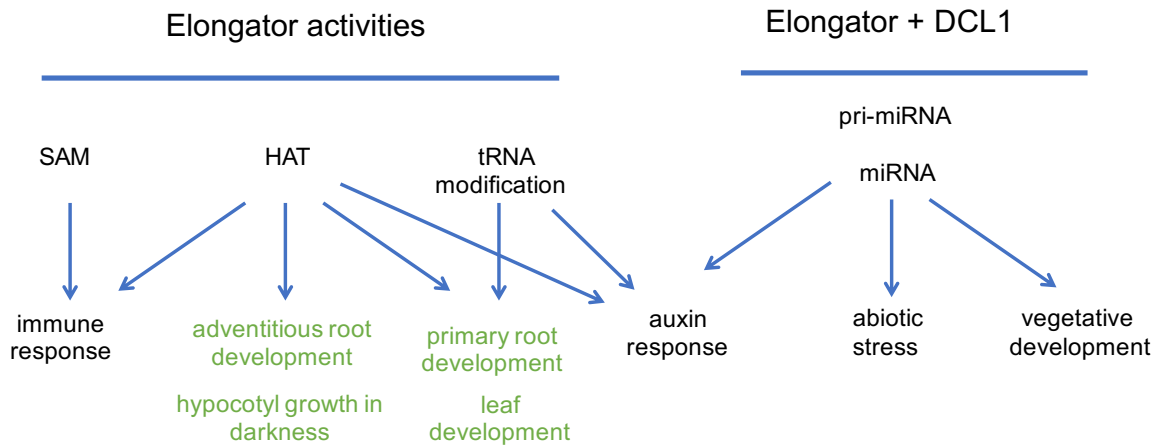
Figure 2: Plant molecular pathways targeted by Elongator activities and by the DCL1 microprocessor interaction (modified from Chapter 3). SAM, S-adenosyl methionine binding; HAT, histone acetyl transferase; pri-miRNA processing; miRNA transcription. Addition to published model in green.

In conclusion, Elongator can affect positively or negatively, directly or indirectly gene expression of various pathways allowing for a fine-tuning in time and space at the transcriptional level and also affect protein production by regulation of translation. One of the questions that remains to be resolved is the mechanism behind the specificity of the target genes, maybe similar to HUB1, an adaptor complex makes the link between the histone modifier and targeted gene. Elongator targeting could be linked to other members of the RNA pol II elongation complex such as transcript elongation factors regulating the speed of transcription. Investigation of the interaction network of Elongator inside and outside of the RNA pol II elongation complex would contribute to knowledge of the targeting processes. In addition, the role of Elongator in tRNA modification also contributes to specific developmental processes at the level of translational regulation, which might provide a fast synthesis of specific proteins upon response to specific stimuli.

6 Perspectives on Elongator research

6.1 Elongator subunits functional analysis

The Elongator mutant phenotypes are pleiotropic in plants, but a closer look shows that they are related to abiotic or biotic stress response pathways or growth processes that are inducible and part of a large network. It also shows that despite their difference the Elongator subunits are all necessary for the correct function of the complex. Mutation in the complex subunits shows similar phenotypes such as seen in hypocotyl (Chapter 4; Woloszynska *et al.*, 2017) or resistance to the necrotrophic fungal pathogens *Botrytis cinerea* and *Alternaria brassicicola* (Wang *et al.*, 2015). Unfortunately, in most studies only one or two subunits are tested together. The description of all the subunits in different situations would contribute to the discovery of the mechanisms behind the targeting by the different activities.

We also could show that expression of the subunits is mostly at similar levels during development and in different anatomical parts (Figure 3) as well as under perturbations (Chapter 3 Figure 3; Woloszynska *et al.*, 2016). Elongator subunits have different enzymatic activities such as the ELO3/HAG3 that contains the HAT and SAM activities, and forms with ELP1 and 2 the core complex, and the ELP4/5/6 forming a subcomplex with ATPase activity (Glatt and Müller, 2013). Strikingly, the ELP4/5/6 genes have a similar expression pattern as opposed to the other subunits in root tips (Fig.3B) which correlates with a role of Elongator in PIN1 regulation by tRNA modification (Leitner *et al.*, 2015). The ELP4/5/6 subcomplex is believed to be the recognition site for tRNA (Glatt and Müller, 2013). Analysis of the ELO gene expression under stress and mutant phenotypes show that the Elongator complex affects three major processes in plants, i.e. auxin signalling, immunity response, and abiotic stress response (Chapter 3 Figure 3; Woloszynska *et al.*, 2016). It is possible that the expression regulation of Elongator subunits in response to stimulus serves as a regulation mechanism for the active Elongator complex. It needs all its subunits to be functional and an holoElongator can also be formed as a large macromolecular assembly containing two of each of the six Elongator subunits (Glatt and Müller, 2013). A lower availability of one or several of the subunits would be sufficient to regulate the complex and holocomplex formation.
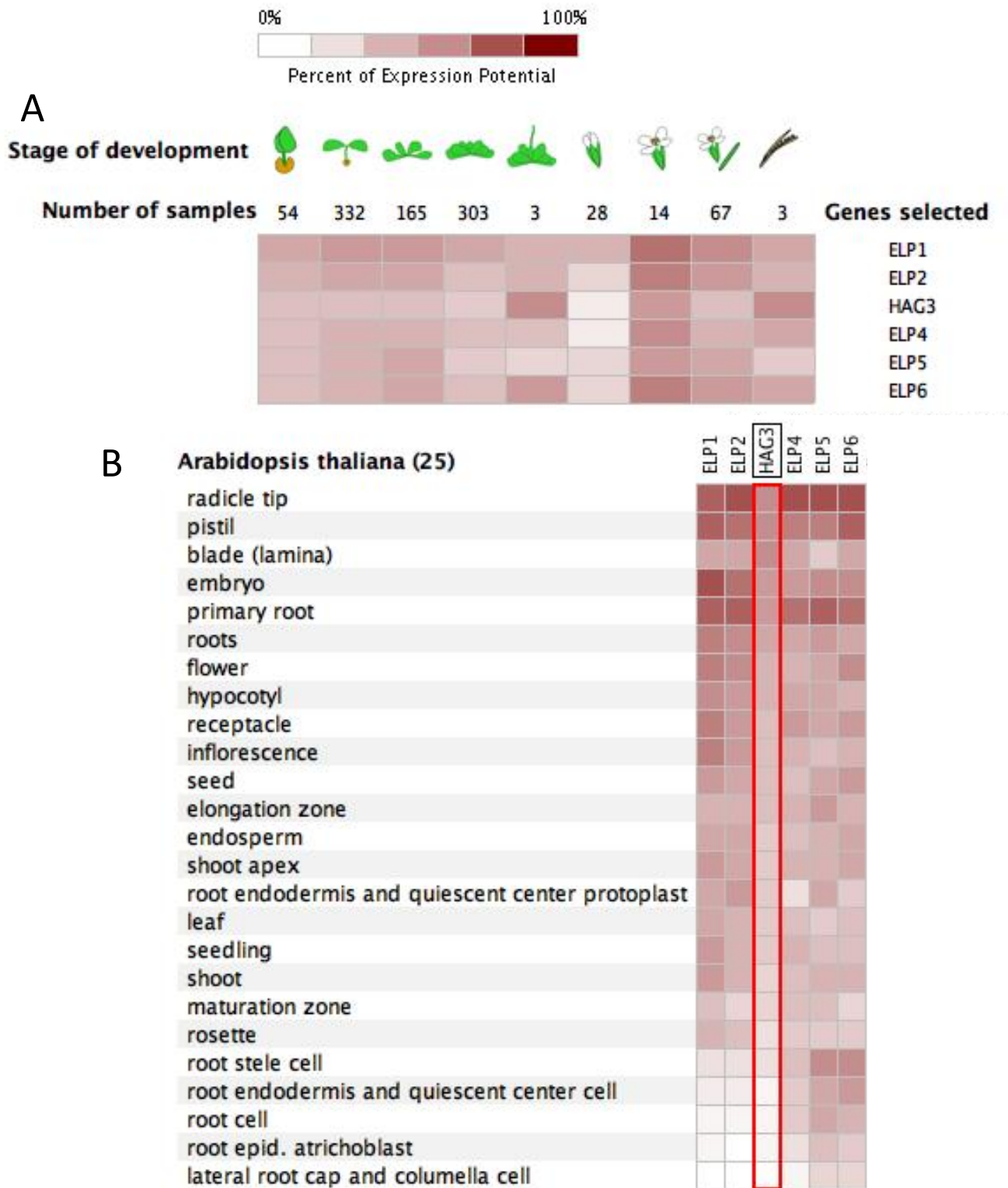
Figure 3: Elongator subunits expression in *Arabidopsis thaliana* in 9 developmental stages (A) and 25 anatomical parts (B) from mRNA sequencing data using the Genevestigator database (Hruz *et al.*, 2008). ELP1/ELO2, ELP2, HAG3/ELO3/ELP3, ELP4/ELO1, ELP5 and ELP6.

6.2 Elongator activities converges on some pathways

We hypothesize that primary root and leaf development are affected by the tRNA modification and HAT activities of Elongator. Candidate proteins and genes for these developmental pathways could be tested for histone acetylation and efficiency of translation by comparing gene expression and protein contents. tRNA modifications might have a regulatory function, because certain open reading frames (ORFs) are enriched in codons recognized by modified tRNAs.

Several pathways in parallel are probably involved and lots of changes converge on the hormonal regulation and trigger the diverging response seen in the phenotypes. Since Elongator has been shown to be involved in several processes of stress responses and development a systematic approach using high throughput methods for discovery of targets of the different activities of Elongator in development and stress would further insight into the transcriptional and translational regulation by Elongator.

It appears that the same pathway can be regulated by different Elongator activities, i.e. the auxin response is regulated by its pri-miRNA, tRNA and acetylation activities. There may be a level of cooperation between the different levels of regulation. Therefore, a combination of ChIP-seq for the HAT activity, meDIP-seq or BS-seq or RRBS for the SAM activity, RNA-seq including small RNAs for the pri-miRNA activity and tRNA profiling by labelling and specific microarray (Grelet *et al.*, 2017) for the tRNA modification activity could be used with application of topical auxin. The different levels of regulation offered by the Elongator activities are a way for the plant to fine tune the auxin levels found in a cell (Figure 4). The tRNA contents regulate the translation of the PIN transporter responsible for auxin efflux which corresponds to a cytoplasmic role of Elongator in tRNA modification (Leitner *et al.*, 2015). In the nucleus, *SHY2/IAA3* (auxin response gene) and *LAX2* (auxin efflux transporter) are targets of the Elongator HAT activity (Nelissen *et al.*, 2010). The pri-miRNAs are regulated by Elongator's interaction with DCL, targeting the negative auxin response regulator *ARF17*, the positive auxin response factor *ARF8* an and *AGO1* , which is also responsible for the regulation of *ARF17* (Fang *et al.*, 2015). Hence, the AUX/IAA-ARF loop is partially regulated by transcriptional activities of Elongator. It is likely that a balance in the regulation of all

these genes and proteins has to be reached with the help of Elongator and might allow fine-tuning of the auxin response.
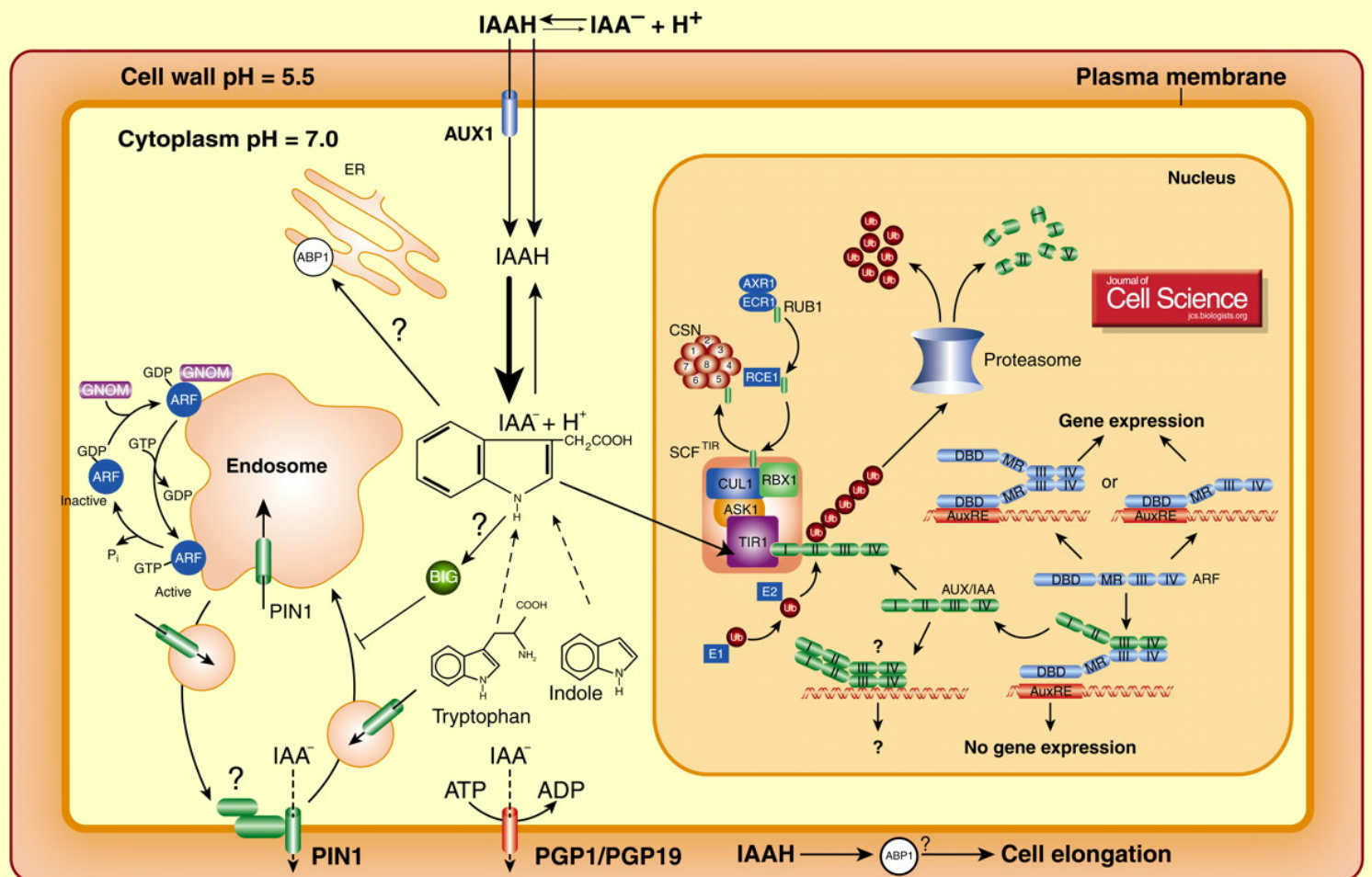

Figure 4: Auxin signalling (Paciorek and Friml, 2006).

6.3 Elongator and photomorphogenesis

Our results including light-related phenotype of the *elo* mutants and differences in transcript levels of light-related genes encourage to continue the research on the Elongator role in photomorphogenesis. The structure and the transcription related role of Elongator were confirmed many times but the genes targeted by Elongator and the exact activities involved in the control of plant physiological processes, are still elusive. The hypothesis is that via its histone acetyltransferase (HAT) or modulation of DNA methylation activities Elongator regulates transcription of light receptors or photomorphogenesis regulators or contributes directly to the massive light induced transcriptome reprogramming. ChIP-seq with antibodies against GFP on the transgenic line overexpressing the *GFP-ELO3* fusion gene and RNA-seq during early

photomorphogenesis will help to reveal genes putatively transcriptionally regulated by Elongator during photomorphogenesis. Subsequently, ChIP-qPCR and MeDIP-qPCR could verify which of the Elongator activity is involved in the regulation of those genes. The genetic interaction between Elongator and positive regulators of photomorphogenesis could be analysed for further proof of the Elongator role in light response.

6.4   Use of high throughput methods in Elongator research

In general, genome wide techniques such as ChIP-seq could be used for identification of targets of acetylation by Elongator. Very small changes in acetylation are observed in the elo mutants, less than 50% decrease making it challenging to detect. In Chapter 4, out of the 20 genes tested by ChIP only 3 were targets. ChIP-seq could be performed using ELO antibodies or using the 35S::GFP::ELO line with GFP antibodies rather than H3K14ac antibodies.

It has been shown that in plant Elongator promotes the transcription of pri-miRNA and interacts with the pri-miRNA processing factors however expression of only a few miRNA has been tested (Fang *et al.*, 2015) The use of different RNA deep sequencing immunoprecipitation methods would allow for the quantitative analysis of all types of RNA such as miRNA to understand their specificity and targeting abilities. The interaction between Elongator and DCL1 bridges the transcription elongation to the processing of pri-miRNA.

6.5   Interacting proteins of Elongator

Tandem affinity purification was already performed on ELO3 (Nelissen et al., 2010) but this was on *Arabidopsis* cell culture in the dark and since the method has progressed (Chapter 6 paragraph 4.2). In the first TAP, only the complex subunits were uncovered. Using the different subunits as baits, *in planta* and in different conditions corresponding to Elongator affected pathways, new interactors of the complex might be found that would help in targeting specificity under certain condition. Interaction between Elongator and putative interactors is likely to be transient and linked to a perturbation response.

6.6   Possible other role for Elongator in plants?

In human, *C. elegans* and drosophila Elongator has an acetylation activity in α-Tubulin (Creppe *et al.*, 2009), this has not been studied in plants. It would be interesting to perform western blots of α-Tubulin in the *elo* mutants to investigate whether they are depleted in acetylated α-Tubulin.

7   Fitting histone modification in the process of transcript elongation

This work added novel information on the interaction between transcript elongation, histone modification and their link to RNA processing. The physical and temporal proximity of these mechanisms make their interaction a valuable tool for the cell to use for regulation.

Epigenetics are a new source to broaden plant phenotype diversity (Gallusci *et al.*, 2017). Sequence variability cannot explain the full spectrum of phenotypic diversity seen in plants and there is still a portion of unexplained heritability. Understanding the mechanism that create this diverse response to the environment can enlarge the sources for heritable phenotypic variation and help improve agronomical traits, but also adaptation of crops to increasing environmental stresses due to climate change.

Histone modifiers play several types of roles in RNA post transcriptional regulation in addition to their role in histone modification. This allows for fine tuning of expression responses to environmental/developmental stimuli, specifically during the process of RNAPII transcript elongation.

During transcription, RNA pol II has to move through the nucleosomal template in a well-choreographed process while struggling to maintain the chromosomal structure. This process requires extensive modulation of chromatin structure through the remodelling and/or removal of existing nucleosomes and it is achieved through the concerted actions of chromatin remodellers, histone modifying enzymes and histone chaperones (Smolle *et al.*, 2013). Histone chaperones may facilitate elongation by disassembling nucleosomes ahead of the RNA pol II and methylation of H3K36 reduces the affinity for histone 3 of the histone chaperone Asf1 (Smolle *et al.*, 2012). When Pol II

migrates into promoter-distal regions, where the influence of activator-dependent HATs is diminishing, RNA pol II requires other HATs such as Elongator to acetylate the nucleosome in front of the transcript elongation machinery (Li *et al.*, 2007). The passage of RNA pol II causes histone displacement. Subsequently, these histones are redeposited onto the DNA behind RNA pol II via concerted actions of histone chaperones. Alternatively, the free forms of histones in the nucleus are also available for reassembly. These newly deposited nucleosomes are somehow hyperacetylated and are immediately methylated by Set2, marking them for deacetylation. It is possible that during elongation changes in the gene body of histone tails may modify their affinity to TEF such as histone chaperones, thus modifying the speed and accuracy of transcription. These changes in speed that may be modulated by histone modification allow for transcriptional control in changing the output of the transcription with alternative splicing and also allow fine tuning of the expression in a medium to short time frame. These histone modification enzymes are implicated in transcript elongation of genes responsible for developmental changes and response to stresses. The colocalization in time and space of the chromatin remodelling complexes and TEF allow for the mechanisms of transcript modification to be associated with the chromatin state and elongation speed. This transient link permits a fast regulation of the RNA transcript.

Analysis of double mutants of histone modification complexes such as HUB1/2 and Elongator complex, and transcription elongation factors might reveal genetic interactions. Some TEF have been shown to interact with these complexes (Antosz e*t al.*, 2017; Van Lijsebettens and Grasser, 2014) and we know that these complexes have specific target genes, it could be that this interaction plays a role in the target choice. In plants, mutation in some of these TEF are not lethal which argues for a redundancy in the function of these TEF.

In conclusion, the presented thesis puts in perspective the action of histone modifying complexes in the process of transcript elongation and co-processing of RNA.

8   References

Antosz, W., Pfab, A., Ehrnsberger, H.F., Holzinger, P., Köllen, K., Mortensen, S.A., Bruckmann, A., Schubert, T., Längst, G., Griesenbeck, J., Schubert, V., Grasser, M., Grasser, K.D., 2017. The

Composition of the Arabidopsis RNA Polymerase II Transcript Elongation Complex Reveals the Interplay between Elongation and mRNA Processing Factors. The Plant Cell 29, 854–870. https://doi.org/10.1105/tpc.16.00735

Berná, G., Robles, P., Micol, J.L., 1999. A mutational analysis of leaf morphogenesis in Arabidopsis thaliana. Genetics 152, 729–742. https://doi.org/PubMed 10353913

Conesa, A., Madrigal, P., Tarazona, S., Gomez-Cabrero, D., Cervera, A., McPherson, A., Szcześniak, M.W., Gaffney, D.J., Elo, L.L., Zhang, X., Mortazavi, A., 2016. A survey of best practices for RNA-seq data analysis. Genome Biology 17. https://doi.org/10.1186/s13059-016-0881-8

Creppe, C., Malinouskaya, L., Volvert, M.-L., Gillard, M., Close, P., Malaise, O., Laguesse, S., Cornez, I., Rahmouni, S., Ormenese, S., Belachew, S., Malgrange, B., Chapelle, J.-P., Siebenlist, U., Moonen, G., Chariot, A., Nguyen, L., 2009. Elongator Controls the Migration and Differentiation of Cortical Neurons through Acetylation of α-Tubulin. Cell 136, 551–564. https://doi.org/10.1016/j.cell.2008.11.043

Dolata, J., Guo, Y., Ko owerzo, A., Smolinski, D., Brzyzek, G., Jarmo owski, A., Swiezewski, S., 2015. NTR1 is required for transcription elongation checkpoints at alternative exons in Arabidopsis. The EMBO Journal 34, 544–558. https://doi.org/10.15252/embj.201489478

Elkon, R., Ugalde, A.P., Agami, R., 2013. Alternative cleavage and polyadenylation: extent, regulation and function. Nature Reviews Genetics 14, 496–506. https://doi.org/10.1038/nrg3482

Fang, X., Cui, Y., Li, Y., Qi, Y., 2015. Transcription and processing of primary microRNAs are coupled by Elongator complex in Arabidopsis. Nature Plants 1, 15075. https://doi.org/10.1038/nplants.2015.75

Fleury, D., Himanen, K., Cnops, G., Nelissen, H., Boccardi, T.M., Maere, S., Beemster, G.T.S., Neyt, P., Anami, S., Robles, P., Micol, J.L., Inze, D., Van Lijsebettens, M., 2007. The Arabidopsis thaliana Homolog of Yeast BRE1 Has a Function in Cell Cycle Regulation during Early Leaf and Root Growth. THE PLANT CELL ONLINE 19, 417–432. https://doi.org/10.1105/tpc.106.041319

Gallusci, P., Dai, Z., Génard, M., Gauffretau, A., Leblanc-Fournier, N., Richard-Molard, C., Vile, D., Brunel-Muguet, S., 2017. Epigenetics for Plant Improvement: Current Knowledge and Modeling Avenues. Trends in Plant Science 22, 610–623. https://doi.org/10.1016/j.tplants.2017.04.009

Glatt, S., Müller, C.W., 2013. Structural insights into Elongator function. Current Opinion in Structural Biology 23, 235–242. https://doi.org/10.1016/j.sbi.2013.02.009

Grelet, S., McShane, A., Hok, E., Tomberlin, J., Howe, P.H., Geslain, R., 2017. SPOt: A novel and streamlined microarray platform for observing cellular tRNA levels. PLOS ONE 12, e0177939. https://doi.org/10.1371/journal.pone.0177939

Himanen, K., Woloszynska, M., Boccardi, T.M., De Groeve, S., Nelissen, H., Bruno, L., Vuylsteke, M., Van Lijsebettens, M., 2012. Histone H2B monoubiquitination is required to reach maximal transcript levels of circadian clock genes in Arabidopsis: *HUB1 regulates transcript levels*. The Plant Journal 72, 249–260. https://doi.org/10.1111/j.1365-313X.2012.05071.x

Hruz, T., Laule, O., Szabo, G., Wessendorp, F., Bleuler, S., Oertle, L., Widmayer, P., Gruissem, W., Zimmermann, P., 2008. Genevestigator V3: A Reference Expression Database for the Meta-Analysis of Transcriptomes. Advances in Bioinformatics 2008, 1–5. https://doi.org/10.1155/2008/420747

Jankowsky, E., Harris, M.E., 2015. Specificity and nonspecificity in RNA–protein interactions. Nature Reviews Molecular Cell Biology 16, 533–544. https://doi.org/10.1038/nrm4032

Jia, Y., Tian, H., Li, H., Yu, Q., Wang, L., Friml, J., Ding, Z., 2015. The *Arabidopsis thaliana* elongator complex subunit 2 epigenetically affects root development. Journal of Experimental Botany 66, 4631–4642. https://doi.org/10.1093/jxb/erv230

Kaida, D., 2016. The reciprocal regulation between splicing and 3'-end processing: The reciprocal regulation between splicing and 3'-end processing. Wiley Interdisciplinary Reviews: RNA 7, 499–511. https://doi.org/10.1002/wrna.1348

Karaduman, R., Chanarat, S., Pfander, B., Jentsch, S., 2017. Error-Prone Splicing Controlled by the Ubiquitin Relative Hub1. Molecular Cell 67, 423–432.e4. https://doi.org/10.1016/j.molcel.2017.06.021

Kimple, M.E., Brill, A.L., Pasker, R.L., 2013. Overview of Affinity Tags for Protein Purification: Affinity Tags for Protein Purification, in: Coligan, J.E., Dunn, B.M., Speicher, D.W., Wingfield, P.T. (Eds.), Current Protocols in Protein Science. John Wiley & Sons, Inc., Hoboken, NJ, USA, p. 9.9.1-9.9.23. https://doi.org/10.1002/0471140864.ps0909s73

Köster, T., Marondedze, C., Meyer, K., Staiger, D., 2017. RNA-Binding Proteins Revisited – The Emerging Arabidopsis mRNA Interactome. Trends in Plant Science. https://doi.org/10.1016/j.tplants.2017.03.009

Lee, K., Kang, H., 2016. Emerging Roles of RNA-Binding Proteins in Plant Growth, Development, and Stress Responses. Molecules and Cells 39, 179–185. https://doi.org/10.14348/molcells.2016.2359

Leitner, J., Retzer, K., Malenica, N., Bartkeviciute, R., Lucyshyn, D., Jäger, G., Korbei, B., Byström, A., Luschnig, C., 2015. Meta-regulation of Arabidopsis Auxin Responses Depends on tRNA Maturation. Cell Reports 11, 516–526. https://doi.org/10.1016/j.celrep.2015.03.054

Li, B., Carey, M., Workman, J.L., 2007. The Role of Chromatin during Transcription. Cell 128, 707–719. https://doi.org/10.1016/j.cell.2007.01.015

Li, Y., Xia, C., Feng, J., Yang, D., Wu, F., Cao, Y., Li, L., Ma, L., 2016. The SNW Domain of SKIP Is Required for Its Integration into the Spliceosome and Its Interaction with the Paf1 Complex in Arabidopsis. Molecular Plant 9, 1040–1050. https://doi.org/10.1016/j.molp.2016.04.011

Liu, Y., Koornneef, M., Soppe, W.J.J., 2007. The Absence of Histone H2B Monoubiquitination in the Arabidopsis hub1 (rdo4) Mutant Reveals a Role for Chromatin Remodeling in Seed Dormancy. THE PLANT CELL ONLINE 19, 433–444. https://doi.org/10.1105/tpc.106.049221

Long, L., Thelen, J.P., Furgason, M., Haj-Yahya, M., Brik, A., Cheng, D., Peng, J., Yao, T., 2014. The U4/U6 Recycling Factor SART3 Has Histone Chaperone Activity and Associates with USP15

to Regulate H2B Deubiquitination. Journal of Biological Chemistry 289, 8916–8930. https://doi.org/10.1074/jbc.M114.551754

Luco, R.F., Allo, M., Schor, I.E., Kornblihtt, A.R., Misteli, T., 2011. Epigenetics in Alternative Pre-mRNA Splicing. Cell 144, 16–26. https://doi.org/10.1016/j.cell.2010.11.056

Luco, R.F., Pan, Q., Tominaga, K., Blencowe, B., Pereira-Smith, O.M., Misteli, T., 2010. Regulation of Alternative Splicing by Histone Modifications. Science 327, 996–1000. https://doi.org/10.1126/science.1184208

Misra, A., Green, M.R., 2016. From polyadenylation to splicing: Dual role for mRNA 3' end formation factors. RNA Biology 13, 259–264. https://doi.org/10.1080/15476286.2015.1112490

Moehle, E.A., Ryan, C.J., Krogan, N.J., Kress, T.L., Guthrie, C., 2012. The Yeast SR-Like Protein Npl3 Links Chromatin Modification to mRNA Processing. PLoS Genetics 8, e1003101. https://doi.org/10.1371/journal.pgen.1003101

Nagaike, T., Logan, C., Hotta, I., Rozenblatt-Rosen, O., Meyerson, M., Manley, J.L., 2011. Transcriptional Activators Enhance Polyadenylation of mRNA Precursors. Molecular Cell 41, 409–418. https://doi.org/10.1016/j.molcel.2011.01.022

Nelissen, H., De Groeve, S., Fleury, D., Neyt, P., Bruno, L., Bitonti, M.B., Vandenbussche, F., Van Der Straeten, D., Yamaguchi, T., Tsukaya, H., Witters, E., De Jaeger, G., Houben, A., Van Lijsebettens, M., 2010. Plant Elongator regulates auxin-related genes during RNA polymerase II transcription elongation. Proceedings of the National Academy of Sciences 107, 1678–1683. https://doi.org/10.1073/pnas.0913559107

Nelissen, H., Fleury, D., Bruno, L., Robles, P., De Veylder, L., Traas, J., Micol, J.L., Van Montagu, M., Inzé, D., Van Lijsebettens, M., 2005. The elongata mutants identify a functional Elongator complex in plants with a role in cell proliferation during organ growth. Proceedings of the National Academy of Sciences of the United States of America 102, 7754–7759. https://doi.org/10.1073/pnas.0502600102

Nordick, K., Hoffman, M.G., Betz, J.L., Jaehning, J.A., 2008. Direct Interactions between the Paf1 Complex and a Cleavage and Polyadenylation Factor Are Revealed by Dissociation of Paf1 from RNA Polymerase II. Eukaryotic Cell 7, 1158–1167. https://doi.org/10.1128/EC.00434-07

Paciorek, T., Friml, J., 2006. Auxin signaling. Journal of Cell Science 119, 1199–1202. https://doi.org/10.1242/jcs.02910

Perales, R., Bentley, D., 2009. "Cotranscriptionality": The Transcription Elongation Complex as a Nexus for Nuclear Transactions. Molecular Cell 36, 178–191. https://doi.org/10.1016/j.molcel.2009.09.018

Reichel, M., Liao, Y., Rettel, M., Ragan, C., Evers, M., Alleaume, A.-M., Horos, R., Hentze, M.W., Preiss, T., Millar, A.A., 2016. In Planta Determination of the mRNA-Binding Proteome of Arabidopsis Etiolated Seedlings. The Plant Cell 28, 2435–2452. https://doi.org/10.1105/tpc.16.00562

Saldi, T., Cortazar, M.A., Sheridan, R.M., Bentley, D.L., 2016. Coupling of RNA Polymerase II Transcription Elongation with Pre-mRNA Splicing. Journal of Molecular Biology 428, 2623–2635. https://doi.org/10.1016/j.jmb.2016.04.017

Sims, R.J., Millhouse, S., Chen, C.-F., Lewis, B.A., Erdjument-Bromage, H., Tempst, P., Manley, J.L., Reinberg, D., 2007. Recognition of Trimethylated Histone H3 Lysine 4 Facilitates the Recruitment of Transcription Postinitiation Factors and Pre-mRNA Splicing. Molecular Cell 28, 665–676. https://doi.org/10.1016/j.molcel.2007.11.010

Smolle, M., Venkatesh, S., Gogol, M.M., Li, H., Zhang, Y., Florens, L., Washburn, M.P., Workman, J.L., 2012. Chromatin remodelers Isw1 and Chd1 maintain chromatin structure during transcription by preventing histone exchange. Nature Structural & Molecular Biology 19, 884–892. https://doi.org/10.1038/nsmb.2312

Smolle, M., Workman, J.L., Venkatesh, S., 2013. reSETting chromatin during transcription elongation. Epigenetics 8, 10–15. https://doi.org/10.4161/epi.23333

Van Lijsebettens, M., Grasser, K.D., 2014. Transcript elongation factors: shaping transcriptomes after transcript initiation. Trends in Plant Science 19, 717–726. https://doi.org/10.1016/j.tplants.2014.07.002

Wang, C., Ding, Y., Yao, J., Zhang, Y., Sun, Y., Colee, J., Mou, Z., 2015. Arabidopsis Elongator subunit 2 positively contributes to resistance to the necrotrophic fungal pathogens *Botrytis cinerea* and *Alternaria brassicicola*. The Plant Journal 83, 1019–1033. https://doi.org/10.1111/tpj.12946

Woloszynska, M., Gagliardi, O., Vandenbussche, F., De Groeve, S., Baez, L.A., Neyt, P., Le Gall, S., Fung, J., Mas, P., Van Der Straeten, D., Van Lijsebettens, M., 2017. Elongator regulates hypocotyl growth in darkness and during photomorphogenesis. Journal of Cell Science jcs.203927. https://doi.org/10.1242/jcs.203927

Woloszynska, M., Le Gall, S., Van Lijsebettens, M., 2016. Plant Elongator-mediated transcriptional control in a chromatin and epigenetic context. Biochimica et Biophysica Acta (BBA) - Gene Regulatory Mechanisms 1859, 1025–1033. https://doi.org/10.1016/j.bbagrm.2016.06.008

Xu, L., Ménard, R., Berr, A., Fuchs, J., Cognat, V., Meyer, D., Shen, W.-H., 2009. The E2 ubiquitin-conjugating enzymes, AtUBC1 and AtUBC2, play redundant roles and are involved in activation of *FLC* expression and repression of flowering in *Arabidopsis thaliana*. The Plant Journal 57, 279–288. https://doi.org/10.1111/j.1365-313X.2008.03684.x

Acknowledgements

Firstly, I would like to express my sincere gratitude to my advisor Prof. Dr. Mieke Van Lijsebettens for the continuous support of my Ph.D. study and related research, for her patience, motivation, and immense knowledge. Her guidance helped me in all the time of research and writing of this thesis. She was there for me in good and bad times. I could not have imagined having a better advisor and mentor for my Ph.D. study.

My sincere thanks also goes to Prof. Dr. Klaus Grasser, who provided me an opportunity to join his team for a secondment, and who gave me access to his laboratory and resources. Without they precious support it would not be possible to conduct this research.

Besides my advisor, I would like to thank the rest of my thesis committee: Prof. Dr. Lieven De Veylder, Prof. Dr. Ann Depicker, Prof. Dr. Frank Van Breusegem, Prof. Dr. Koen Geuten and Dr. Hilde Nelissen, for their insightful comments and encouragement, but also for the hard question which incented me to widen my research from various perspectives.

My many thanks to Dr. Magdalena Woloszynska for guiding me through the world of Elongator and HUB. And Pia Neyt for all the technical and moral help.

I thank my fellow labmates from Gent (Stjin, Griet, Karina, Tom, Feng, Martin, Mike, Ivano, Olimpia, Liz) and Regensburg (Marion, Silvia, Wojtek, Hans, Phillip, Alex, Ines, Tina, Irene, Brian, Antje, Michael) for the stimulating discussions, for the all the advices and help, and for all the fun we have had in the last four years.

Also, thanks to all the members of the CHIP-ET network for the interesting workshops and exchanges we had over the years.

Last but not the least, I would like to thank my family, Thomas and my friends for supporting me spiritually throughout writing this thesis and my life in general. I would like to dedicate this thesis to my father who died before this thesis was finished.

Curriculum Vitae

Name: Sabine Joséphine LE GALL   **born** 25.10.1988, Brest, France

Nationality: French   **Languages:** French, English, German

e-mail: sagal@psb.vib-ugent.be / legallsj@gmail.com

Education

11/2013 – 01/2018   **Early Stage Researcher**:

12/2016 to 06/2017 PSB science fund

11/2013 to 10/2016 fellowship EC Marie Curie Research Training Network – Chromatin in Plants – European Training and Mobility (CHIP-ET) FP7-PEOPLE-2013-ITN

Ph.D. student Ghent University, Ghent, Belgium

Thesis: Chromatin modification complexes link RNA biology in the regulation of plant growth and development.

Promoter: Prof. Dr. Mieke Van Lijsebettens

01/2016 – 10/2016   Research secondment Klaus Grasser lab, Department of Cell Biology and Plant Biochemistry, University of Regensburg, Germany.

2011-2013   **Research Master Degree** in integrative plant sciences and genetics at the University of Rennes 1 and Agrocampus Ouest, Brittany, France. *Subjects studied: plant evolution and genetics, development, biotechnology and physiology.*

2nd **year thesis** at the Max Planck Institute for Plant Breeding Research (MPIPZ), Department of Plant Breeding and Genetics, research group Pecinka (Genome and epigenome maintenance), Cologne, Germany.

Thesis: « Arabidopsis epigenetic natural variation».

Promoter: Dr. Ales Pecinka.

ırst year thesis at the Center for Plant Molecular Biology (ZMBP), Plant Physiology department, research group Laubinger (MicroRNA Function and RNA Processing in Plants), University of Tübingen, Germany.

Thesis: « Plant microRNA and function in response to light ».

Promoter: Dr. Sascha Laubinger.

2010-2011   **Bachelor Degree** in plant sciences at the University of Rennes 1, Brittany, France

Subjects studied: plant biology and physiology, plant ecology, genetics, phylogenetics, biological data processing, biotechnology, microbiology, biological interaction.

Trainee at INRA of Rennes (French National Institute for Agricultural Research),UMR118, Amélioration des Plantes et Biotechnologies Végétales (Plant Improvement and Biotechnology, now IGEPP), in Ploudaniel. DsRNAguard project.

Thesis: « Production, molecular and phenotypic characterization of potato mutant resistant to late blight ».

Promoter: Murielle Philippot.

Trainee at La Ferme de Corail in Camaret-sur-Mer. Coral growing farm.

Manuscripts and peer-reviewed publications (A1)

Magdalena Woloszynska, Olimpia Gagliardi, Filip Vandenbussche, Steven De Groeve, Luis Alonso Baez, Pia Neyt, Sabine Le Gall, Jorge Fung, Paloma Mas, Dominique Van Der Straeten, Mieke Van Lijsebettens: Elongator regulates hypocotyl growth in darkness and during photomorphogenesis. Journal of Cell Science 2017; jcs.203927. doi:10.1242/jcs.203927

Sabrina Inigo, Astrid Nagels Durand, Andres Ritter, Sabine Le Gall, Martin Termathe, Roland Klassen, Takayuki Tohge, Barbara De Coninck, Jelle Van Leene, Rebecca De Clercq, Bruno Cammue, Alisdair R Fernie, Kris Gevaert, Geert De Jaeger, Sebastian A Leidel, Raffael Schaffrath, Mieke Van Lijsebettens, Laurens Pauwels, Alain Goossens: *Glutaredoxin GRXS17 Associates with the Cytosolic Iron-Sulfur Cluster Assembly Pathway*. Plant physiology 08/2016; 172(2). DOI:10.1104/pp.16.00261

Magdalena Woloszynska, Sabine Le Gall, Mieke Van Lijsebettens: *Plant Elongator-mediated transcriptional control in a chromatin and epigenetic context*. Biochimica et Biophysica Acta (BBA) - Gene Regulatory Mechanisms 06/2016; DOI:10.1016/j.bbagrm.2016.06.008

Till Bey, Suraj Jamge, Sonja Klemme, Dorota Natalia Komar, Sabine Le Gall, Pawel Mikulski, Martin Schmidt, Johan Zicola, Alexandre Berr: *Chromatin and epigenetics in all their states: Meeting report of the first conference on Epigenetic and Chromatin Regulation of Plant Traits - January 14 – 15, 2016 - Strasbourg, France.* Epigenetics 05/2016; DOI:10.1080/15592294.2016.1185580 All authors, except corresponding author Alexandre Berr, contributed equally to this work.

Magdalena Woloszynska[1], Sabine Le Gall[1], Pia Neyt, Tommasso M. Boccardi, Marion Grasser, Stijn Aesaert, Stijn Dhondt, Leonardo Bruno, Jorge Fung, Paloma Mas, Marc Van Montagu, Dirk Inzé, Geert De Jaeger, Klaus Grasser, Kristiina Himanen, and Mieke Van Lijsebettens. *RNA binding proteins link H2B monoubiquitination with m-RNA processing through interaction with the HUB1 and HUB2 E3 ubiquitin ligases.* In preparation for PNAS

1. shared first author

Research outreach

Oral presentations
CHIP-ET workshop 28-30/04/14, Gatersleben, Germany.

CHIP-ET workshop 12-13/11/14, CRAG, Barcelona, Spain.

VIB PSB cluster meeting, 05/12/2014.

CHIP-ET workshop 14-15/04/15, Regensburg University, Germany.

CHIP-ET midterm meeting and workshop 22-23/09/16, Gent.

Plant Biology Scandinavia 2015 – the 26th SPPS Congress, 9-13/08/2015, Stockholm, Sweden.

CHIP-ET meeting 13/01/16, Strasbourg, France.

Department seminar at the Cell Biology and Plant Biochemistry, 25/04/2016, Regensburg University, Germany.

CHIP-ET meeting 31/05/2107, Vienna, Austria.

RNA-protein interaction meeting, 8/06/2017, KU Leuven, Belgium.

Poster presentation

VIB seminar 2015, Blankenberge, Belgium, poster presentation, 30/03/2015

Poster and flash talk at Epigenetic & Chromatin Regulation of Plant Traits, Strasbourg, France, 14-15/01/ 2016 / Third poster price

Participation to 23rd ICAR (Vienna,2012) and satellite meeting: plant RNA symposium

Participation to 5th European Workshop on Plant Chromatin, GMI, Vienna, Austria.

Courses and training

Symposium "New Paradigms in Plant Epigenetics, Heterosis, Stress and Evolution", VIB-Gent 18 November 2013

Introduction Day for new PhD students, Cluster Research & Valorization, Ugent, 6 February 2014

Introduction to NGS data analysis, 21 February 2014

Hands-on introduction to ChIP-Seq analysis, VIB-Gent, 24 February 2014

RNA-Seq analysis for differential expression, VIB-Gent, 22 and 24 April 2014

Microscopy Workshop and Flow cytometry, IPK Gatersleben, 28 April 2014

qPCR analysis using qbase+, VIB-Gent, 27 June 2014

Workshop Luminometer Assays, Laser Microdissection and Image J Analysis: Theoretical and Practical Aspect, CRAG, Barcelona, 13 November 2014

Scientific writing from Cambridge University, VIB-Gent (Prof. Dr. Shirley Ellis, University of Oxford), 5-6 March 2015

Workshop Molecular interaction studies, Regensburg University, 15 April 2015

Workshop Hands-on transcriptome dataset analyses by PLAZA, VIB-Gent, 23 September 2015